

**QUANTITATIVE IMPACTS OF INTERACTIVE
BIOTIC AND ABIOTIC STRESSES ON PLANT
PERFORMANCE: STRESS RESPONSES, PRIMING,
AND ACCLIMATION**

**KOOSINEVATE BIOOTILISTE JA
ABIOOTILISTE STRESSIDE MÕJU TAIMEDELE:
STRESSIVASTUSTEST KOHANEMISENI**

HASSAN YUSUF SULAIMAN

A Thesis
for applying for the degree of Doctor of Philosophy
in Applied Biology

Väitekirj
filosoofiadoktori kraadi taotlemiseks
rakendusbioloogia erialal

Tartu 2023

Eesti Maaülikooli doktoritööd

**Doctoral Theses of the
Estonian University of Life Sciences**



**QUANTITATIVE IMPACTS OF
INTERACTIVE BIOTIC AND ABIOTIC
STRESSES ON PLANT PERFORMANCE:
STRESS RESPONSES, PRIMING, AND
ACCLIMATION**

**KOOSINEVATE BIOOTILISTE JA ABIOTILISTE
STRESSIDE MÕJU TAIMEDELE: STRESSIVASTUSTEST
KOHANEMISENI**

HASSAN YUSUF SULAIMAN

A Thesis
for applying for the degree of Doctor of Philosophy
in Applied Biology

Väitekirj
filosoofiadoktori kraadi taotlemiseks
rakendusbioloogia erialal

Tartu 2023

Institute of Agricultural and Environmental Sciences, Estonian University of Life Sciences

According to verdict No 6-14/1-7, the Doctoral Committee of Agricultural and Natural Science of the Estonian University of Life Sciences has accepted this thesis for the defense of the Doctor of Philosophy in Applied Biology

Opponent: **Professor Dr. Michael Staudt**
Centre d'Ecologie Fonctionnelle et Evolutive,
1919 Route de Mende,
F- 34293 Montpellier cedex 5, France

Supervisor: **Professor Dr. Ülo Niinemets**
Institute of Agricultural and Environmental Sciences,
Estonian University of Life Sciences, Tartu, Estonia.

Defense of the thesis: Estonian University of Life Sciences, Room ,
Kreutzwaldi 5-D239, Tartu, on November 16, 2023, at 14.15

The Estonian summary was translated by Tiia Kurvit and edited by Vivian Kusk

Publication of this thesis is supported by the Estonian University of Life Sciences. This research was funded by the Centre of Excellence in Environmental Adaptation (F11100PKTF), Ecology of Global Change: natural and managed ecosystems (8F160018PKTF (TK131), Ecology of Global Change: natural and managed ecosystems Analysis and Experimentation on Ecosystems (F200127PKTT (11.7-4/1076).



ISSN 2382-7076

ISBN 978-9916-719-38-1 (print)

ISBN 978-9916-719-39-8 (pdf)

Sadaukarwa ga iyaye na !

Pühendatud minu vanematele !

To my parents !



CONTENTS

LIST OF ORIGINAL PUBLICATIONS.....	9
ABBREVIATIONS.....	10
1. INTRODUCTION.....	11
2. LITERATURE REVIEW.....	15
2.1. Impacts of insect herbivory, fungal infection, and heat stress on foliage photosynthetic characteristics	15
2.2. Impact of insect herbivory, fungal infection, and heat stress on volatile emissions	16
2.3. Impact of interactive biotic and abiotic factors on plant stress responses.....	19
2.4. Stress priming.....	19
2.5. Aims and hypothesis of the study.....	20
3. MATERIALS AND METHODS	23
3.1. Plant growth under controlled conditions (Paper I-III).....	23
3.2. Plants for the field study (Paper IV).....	23
3.3. Identification of <i>Puccinia coronata</i> f. sp. <i>avenae</i> (Paper IV)	24
3.4. Application of moderate heat priming (Papers I-II)	25
3.5. <i>Trialeurodes vaporariorum</i> infestation (Paper III).....	25
3.6. Heat shock application (Papers I-III).....	26
3.7. Gas exchange measurements (Papers I-IV)	26
3.8. Volatile collection and GC-MS analysis (Paper I-IV)	27
3.9. Determination of leaf dry mass per area, and key element contents per dry mass (Paper IV).....	27
3.10. Determination of total content of phenolics and condensed tannins (Paper I).....	27
3.11. Statistical analyses (Paper I-V).....	28
4. RESULT.....	29
4.1. Effects of heat priming and heat shock stress on foliage photosynthetic characteristics	29
4.2. Effects of combined insect feeding and heat stress on photosynthetic characteristics.....	31

4.3. Effects of <i>P. coronata</i> infection on foliage photosynthetic characteristics	32
4.4. Contribution of leaf dry mass per unit area and C, N, and P contents per leaf dry mass to reductions in net assimilation rates ..	34
4.5. Effects of heat priming and heat shock stress on volatile emissions	36
4.6. Effects of heat shock on foliage phenolic content in primed and non-primed plants	40
4.7. Effects of insect infestation and heat shock on volatile emissions	41
4.8. Effects of <i>P. coronata</i> infection on volatile emissions in the two host species	43
5. DISCUSSIONS	44
5.1. Impacts of moderate heat stress on physiological responses: preparing plants for subsequent severe heat stress	44
5.2. Heat priming enhanced heat shock stress tolerance of photosynthesis	45
5.3. Impacts of priming on volatile responses and implication on heat stress tolerance	45
5.4. Whitefly infestation enhanced heat stress tolerance	46
5.5. The impact of <i>P. coronata</i> infection is more severe in the primary host than in the alternate host	48
CONCLUSION	51
REFERENCES	53
SUMMARY IN ESTONIAN	66
ACKNOWLEDGEMENT	72
ORIGINAL PUBLICATIONS	73
CURRICULUM VITAE	160
ELULOOKIRJELDUS	161
LIST OF PUBLICATIONS	162
CONFERENCE ABSTRACTS	163

LIST OF ORIGINAL PUBLICATIONS

This thesis is based on the following original publications:

- I. **Liu B, Zhang L, Rusalepp L, Kaurilind E, Sulaiman HY, Püssa T, Niinemets Ü. 2021.** Heat priming improved heat tolerance of photosynthesis, enhanced terpenoid and benzenoid emission and phenolics accumulation in *Achillea millefolium*. *Plant, Cell & Environment*, **44**: 2365-2385.
- II. **Sulaiman, HY, Liu, B, Abiola, YO, Kaurilind, E and Niinemets, Ü, 2023.** Impact of heat priming on heat shock responses in *Origanum vulgare*: Enhanced foliage photosynthetic tolerance and biphasic emissions of volatiles. *Plant Physiology and Biochemistry* **196**: 567- 579.
- III. **Sulaiman, HY, Liu B, Kaurilind E, Niinemets Ü. 2021.** Phloem-feeding insect infestation antagonizes volatile organic compound emissions and enhances heat stress recovery of photosynthesis in *Origanum vulgare*. *Environmental and Experimental Botany* **189**: 104551.
- IV. **Sulaiman, HY, Runno-Paurson, E, Kaurilind, E and Niinemets, Ü. 2023.** Differential impact of crown rust (*Puccinia coronata*) infection on photosynthesis and volatile emissions in the primary host *Avena sativa* and the alternate host *Rhamnus frangula*. *Journal of Experimental Botany* **74**: 2029-2046.
- V. **Sulaiman, HY, Runno-Paurson, E, Kaurilind, E and Niinemets, Ü. 2023.** The same boat, different storm: stress volatile emissions in response to biotrophic fungal infections in primary and alternate hosts. *Plant Signaling and Behavior* 2217030-2217030.

ABBREVIATIONS

<i>A</i>	net assimilation rate per leaf area
<i>C_i</i>	intercellular concentration of CO ₂
<i>C_M</i>	carbon content per unit dry mass
<i>D_A</i>	percentage of damaged leaf area
DOXP	1-deoxy-D-xylulose 5-phosphate
FAD	long-chain fatty acid-derived volatiles
GGDP	geranylgeranyl diphosphate
<i>g_s</i>	stomatal conductance
JA	jasmonic acid
LMA	dry mass per unit area
LOX	lipoxygenase
MeJA	methyl jasmonate
MEP	2-C-methyl-D-erythritol 4-phosphate
MeSA	methyl salicylate
MVA	mevalonate
<i>N_M</i>	nitrogen content per dry mass
<i>P_M</i>	phosphorous content per dry mass
PPFD	photosynthetic photon flux density
Rubisco	ribulose-1,5-bisphosphate carboxylase oxygenase
ROS	reactive oxygen species
SA	salicylic acid
<i>V_{cmx}</i>	maximum Rubisco carboxylase activity
VOC	volatile organic compound

QUANTITATIVE IMPACTS OF INTERACTIVE BIOTIC AND ABIOTIC STRESSES ON PLANT PERFORMANCE: STRESS RESPONSES, PRIMING, AND ACCLIMATION

1. INTRODUCTION

Plant stress refers to the broad range of abiotic and biotic external factors that negatively impact plant metabolism, growth, development, and productivity (Niinemets, 2010; Atkinson & Urwin, 2012; Ben Rejeb *et al.*, 2014; Atkinson *et al.*, 2015). Abiotic stress encompasses adverse environmental conditions, such as drought, waterlogging, salinity, air pollution, ozone, high solar radiation, heat waves, and other extreme climatic factors. On the other hand, biotic stress involves the onslaught of various herbivores and pathogens, including viruses, fungi, and bacteria. Abiotic stress and biotic stress operate differently: abiotic stresses create challenging climatic environments for plant growth, while biotic stress agents can disrupt plant hormonal balance, leading to tissue injuries and losses (Divon & Fluhr, 2007; Cramer *et al.*, 2011).

Heat stress is one of the leading abiotic stress factors that cause physiological, biochemical, and molecular changes that adversely affect the growth and development of plants (Baniwal *et al.*, 2004; Ben Rejeb *et al.*, 2014; Kask *et al.*, 2016; Turan *et al.*, 2019). In nature, plants experience single or multiple heat stress episodes sequentially or simultaneously with biotic attacks (Holopainen & Gershenson, 2010; Atkinson & Urwin, 2012; Atkinson *et al.*, 2015). Both heat stress and biotic stress individually reduce photosynthesis and activate chemical defense signaling that leads to emissions of specific volatiles and accumulation of various secondary metabolites from different synthesis pathways (Niinemets *et al.*, 2013; Niinemets, 2016; Suseela & Tharayil, 2018; Turan *et al.*, 2019). Typically, different C₅-C₆ volatile aldehydes and alcohols and their derivatives formed via the lipoxygenase (LOX) pathway (also called green leaf volatiles) are the earliest volatile organic compounds (VOC) released upon stress (Copolovici *et al.*, 2014; Jiang *et al.*, 2017; Okereke *et al.*, 2021). Shortly after the onset of the emissions of LOX volatiles, a variety of specialized volatiles are elicited, including isoprenoids (isoprene, mono- and sesquiterpenes) from the plastidial

2-C-methyl-D-erythritol 4-phosphate/1-deoxy-D -xylulose 5-phosphate (MEP/DOXP) and the cytosolic mevalonate (MVA) pathways and benzenoids from shikimate pathway in the plastid. Concurrently, stress induces the emission of long-chained saturated fatty acid-derived (FAD) compounds and carotenoid breakdown products (Chatterjee *et al.*, 2020; Okereke *et al.*, 2021), followed by the accumulation of different non-volatile secondary metabolites, such as phenolics (Dudareva *et al.*, 2005).

Whilst physiological and metabolic responses to individual biotic and abiotic stresses have been extensively studied in different plant species (Staudt and Lhoutellier 2007; Cellini *et al.*, 2016; Guidolotti *et al.*, 2019; Faiola & Taipale 2020; Birami *et al.*, 2021), responses to interactive stresses are poorly understood. Previous studies have shown that defense responses activated by one stress may interact antagonistically or synergistically with responses activated by another stress (Wu *et al.*, 2019; Kim *et al.*, 2022). In particular, pre-exposure to sublethal stresses such as insect phloem-feeding and moderately warm temperatures can increase tolerance upon subsequent severe stress episodes (Hilker & Schmülling, 2019; Liu *et al.*, 2022). In *Arabidopsis thaliana*, short-term cold stress actively regulates defense pathways that increase resistance to subsequent pathogen infections (Wu *et al.*, 2019). Pre-stressed plants acquire enhanced tolerance through a complex reprogramming of cellular and molecular mechanisms, a process termed *stress priming* or *hardening*, as sometimes used in the case of biotic stress priming (Hilker & Schmülling, 2019; Khan *et al.*, 2022). Overall, the acquired tolerance starts with a priming phase and stress memory/adaptive responses that may remain active for days to weeks and months (Sanyal *et al.*, 2018; Leuendorf *et al.*, 2020).

The vulnerability of plants to biotic stress can be influenced by the simultaneous occurrence of abiotic factors. Recent evidence showed that warmer temperatures can increase the virulence of pathogens, especially in sensitive species (Sardanyés *et al.*, 2022). For example, the development, spread, and pathogenicity of fungi such as crown rust (*Puccinia coronata*) is promoted by warm weather (Liu & Hambleton, 2013; Nazareno *et al.*, 2018); therefore, sensitive host species may experience more severe stress when infected with pathogens that thrive under warmer weather. Investigating physiological and metabolomic responses to interactive stresses is crucial in predicting plant stress responses under

a changing climate and can provide useful information in developing multiple-stress-resilient crop species.

In this thesis, we studied how interactive environmental stresses modify plant physiological traits depending on the severity of different stresses and their sequence and duration in four model species. Our study investigated the effects of different stressors on plants, specifically *Achillea millefolium* L. (Asteraceae) and *Origanum vulgare* L. (Lamiaceae). We conducted experiments exposing these plants to two distinct conditions: moderate heat stress (heat priming) and infestation by greenhouse whiteflies (*Trialeurodes vaporariorum* Westwood). Subsequently, we subjected the plants to heat shock stress and measured alterations in both leaf photosynthesis and secondary metabolite profiles over the stress recovery period. Furthermore, we determined whether elevated temperatures influence how the heteroecious biotrophic fungus *Puccinia coronata* f. sp. *avenae* regulates photosynthetic activities and volatile emissions in the primary host, common oat (*Avena sativa* L., Gramineae) and the alternate host, alder buckthorn (*Rhamnus frangula* L., syn. *Frangula alnus* P. Mill., Rhamnaceae). In the priming experiment, we investigated the influence of stress priming on volatile emissions, focusing on volatiles synthesized in the LOX, MEP/DOXP, and shikimic acid pathways. Additionally, we examined the accumulation of non-volatile protective secondary metabolites. In the fungal infection experiment, we examined the impact of warm weather on the severity of *P. coronata* infection. We assessed this impact by observing reductions in photosynthetic activity and the induction of stress volatiles.

Paper I quantified the impacts of heat priming on time-dependent modification of foliage photosynthetic characteristics and volatile emissions and the synthesis of non-volatile secondary metabolites in heat shock-stressed *A. millefolium*. **Paper II** studied the impact of mild heat stress priming on severe heat stress responses and time-dependent recovery of stomatal conductance, photosynthesis rate and Rubisco activity, and the activation of defensive volatile synthesis pathways in *O. vulgare*. **Paper III** investigated the interactive effects of combined *T. vaporariorum* infestation and heat shock on foliage photosynthesis and volatile emissions through the stress recovery period in *O. vulgare*. Finally, **Paper IV** explored *P. coronata* infection severity-dependent reductions of photosynthetic activity and inductions of volatile emissions in the primary host *A. sativa* and the alternate host *R. frangula*. **Paper V**

generalized the results of **Paper IV** and emphasized the importance of studying both primary and alternate hosts for pathogens with complex life cycles. Overall, this thesis demonstrated that pre-exposure to both biotic infestation and moderately warm weather promotes thermal tolerance, whereas warmer weather itself can increase biotic stress severity. These results contribute to the understanding of how plants cope with future warmer environments and higher pathogen and herbivore pressures. Quantitative data on VOC emission responses under complex interactive stresses provide illuminative insight into predicting plant physiological responses to contemporary climate change and aid in breeding crops with improved stress tolerance.

2. LITERATURE REVIEW

2.1. Impacts of insect herbivory, fungal infection, and heat stress on foliage photosynthetic characteristics

Herbivorous arthropod feeding is one of the key biotic stressors affecting foliage photosynthesis. The quantitative impact of insect herbivory on foliage photosynthesis and the underlying mechanisms for the reduction of photosynthesis rate are influenced by the type of herbivore feeding and the severity of infestation (Aldea *et al.*, 2006; Arimura *et al.*, 2008, 2011; Delucia *et al.*, 2012). Feeding by defoliating insects mostly results in the loss of photosynthetic tissues in the injured region of the leaf and typically leads to decreases in net assimilation rates. However, in some cases, the loss of leaf tissue results in a compensatory increase in net assimilation per unit leaf area in the remaining leaf area (Bilgin *et al.*, 2010; Hoback *et al.*, 2015; Pincebourde & Ngao, 2021). Foliage photosynthesis is also reduced remarkably by herbivory on specialized tissues, for example by phloem feeders such as aphids and whiteflies (Kucharik *et al.*, 2016). In this case, inhibition of photosynthesis occurs through increased water loss at the damaged tissue and disruption in nutrient/fluid transport, and reductions in metabolic processes throughout the leaf (Nabity *et al.*, 2009; DeLucia *et al.*, 2012). In some cases, plants respond to phloem-feeding insect herbivory by enhancing CO₂ uptake as a compensatory mechanism or due to an increase in sink demand in the leaf (Nabity *et al.*, 2009, Kucharik *et al.*, 2016).

Fungal infections typically lead to reductions in photosynthetic activities (Toome *et al.*, 2010; Jiang *et al.*, 2016; Kännaste *et al.*, 2022). Fungal-dependent reductions in photosynthesis have been demonstrated to be quantitatively associated with the severity of the infection. In this case, the reduction of photosynthetic activity can be due to stomatal and non-stomatal inhibition: for instance, reductions in ribulose-1,5-bisphosphate carboxylase-oxygenase (Rubisco) and photosynthetic electron transport activities, and reductions in mesophyll conductance and CO₂ diffusion in substomatal cavities (Aldea *et al.*, 2006; Toome *et al.*, 2010; Jiang *et al.*, 2016; Kännaste *et al.*, 2022).

Among fungal infections is oat crown rust, a devastating plant disease that primarily infects oats (*Avena* spp.), in particular the key crop common

oat (*Avena sativa* L.). In *A. sativa*, the disease is caused by the obligate biotrophic fungus *Puccinia coronata* f. sp. *avenae* P. Syd. and Syd (Liu and Hambleton, 2013). Sexual reproduction of the fungus is completed in *R. frangula*, where fertilization takes place, while karyogamy and meiosis occur in *A. sativa* (Nazareno *et al.*, 2018). *Puccinia coronata* infection has been demonstrated to reduce photosynthetic activity in plants, from the time of inoculation of the fungus to sporulation. The infection first causes reductions in photosynthesis by decreasing photosynthetic capacity in the area infected, but as the infection expands, photosynthetic activity decreases throughout the entire leaf. (Scholes & Rolfe, 1996).

Heat stress is one of the key stress elicitors that negatively impact photosynthesis in plants. Photosynthesis is highly temperature sensitive as even a transient rise in temperature to a little above optimal growth temperature (e.g. $T \geq 35$ °C for 5 min) can lead to a decrease in photosynthesis by inducing stomatal limitations and decreases in Rubisco activity (Kurek *et al.*, 2007; Barta *et al.*, 2010; Kask *et al.*, 2016; Perdomo *et al.*, 2017). Further increases in heat stress severity result in greater inhibition of photosynthesis (Kask *et al.*, 2016; Okereke *et al.*, 2022). In the case of transient moderately severe heat exposure, photosynthesis typically recovers completely in less than 24 hours after the application of the heat stress, but in lethal cases that involve direct thermal damages of photosynthesis components and denaturation of Rubisco, photosynthesis may take longer to recover completely, or not recover at all (Salvucci & Crafts-Brandner, 2004; Song *et al.*, 2014).

2.2. Impact of insect herbivory, fungal infection, and heat stress on volatile emissions

Plants synthesize a diverse array of volatile and non-volatile secondary metabolites that are involved in the interactions of plants with biotic and abiotic stresses. Some plant species are strong constitutive emitters of certain specific volatiles such as isoprene and monoterpenes, but most plant species release only a low level of volatile organic compounds (VOC) under non-stressed conditions (Geron *et al.*, 2001; Dani *et al.*, 2014; Pazouki *et al.*, 2016; Kanagendran *et al.*, 2018). Environmental stresses can trigger plants to increase the emissions of VOC and the accumulation of non-volatile secondary metabolites (Blande *et al.*, 2014; Golan *et al.*, 2017; Kanagendran *et al.*, 2018). Several stress-elicited reactive volatiles in plants act as non-enzymatic antioxidants against

oxidative stress and other impaired environmental conditions (Brilli *et al.*, 2009; Salerno *et al.*, 2017). While a part of these stress VOC emissions may emanate from the already synthesized chemicals in the storage pool of plants, others are *de novo* synthesized upon the perception of stress (induced emissions) (Brilli *et al.*, 2009; Arimura *et al.*, 2011; Lung *et al.*, 2016). Stress volatile emissions from the leaves of plants may start minutes to hours upon stress exposure. For localized abiotic stresses, emissions usually start from the sites of damage and propagate systemically throughout the leaves (Moran & Thompson, 2001; Arimura *et al.*, 2004; Niinemets, 2010).

Emissions of VOC are regulated by hormonal signalings such as jasmonic acid (JA), salicylic acid (SA), ethylene, and abscisic acid signaling. Plants typically activate distinct hormonal defense signaling in response to different stresses. Plants primarily activate JA- dependent signaling in response to abiotic stresses and biotic stressors that kill cells or defoliate tissue, e.g. necrotrophic infections and chewing herbivores (Wu & Baldwin 2010; Nabity *et al.*, 2013). SA-dependent signaling is primarily activated in response to piercing and sucking herbivory and biotrophic infections (Wu and Baldwin 2010; Kazan & Lyon 2014). The activation of either signaling pathway typically antagonizes the other (Kunkel & Brooks, 2002; Bruinsma *et al.*, 2009; Kazan & Lyon 2014). However, activation of different signaling pathways dependence on stress type is not always that clearcut, e.g. in *Oryza sativa* JA-dependent signaling regulates the defense responses to *Xanthomonas oryzae* biotrophy (Yamada *et al.*, 2012; Ullah *et al.*, 2022). It has also been demonstrated that the interaction between the JA and SA signaling pathways can be synergistic (Wei *et al.*, 2014; Li *et al.*, 2019). For example, in *Arabidopsis*, JA- and SA-dependent signalings were synergistically elicited in response to biotrophic and necrotrophic pathogens (Tsuda *et al.*, 2009). It has further been shown that both JA and SA can induce common defense responses (Tamaoki *et al.*, 2013).

Upon stress activation of defense signaling, the activity of several secondary metabolic pathways is enhanced leading to the release of a variety of volatiles (Niinemets *et al.*, 2017). Among the earliest pathways modulated are the lipoxygenase (LOX) pathway, including the 13-lipoxygenase pathway that synthesizes various short-chained C5-C6 aldehyde/alcohols and their derivatives (LOX compounds, also known as green leaf volatiles, GLV) and 9-lipoxygenase pathway that

synthesizes oxylipins such as JA (Bate & Rothstein, 1998; Copolovici *et al.*, 2011, 2012). LOX volatile emissions are ubiquitous stress indicators and are among the earliest volatile signals observed upon stress exposure (Copolovici *et al.*, 2011, 2014; Jiang *et al.*, 2016). There are several constitutively active lipoxygenases in plants that rapidly elicit LOX compound emissions contingent on the release of polyunsaturated fatty acids from membrane phospholipids upon membrane-level damage (Bate & Rothstein, 1998; Arneth & Niinemets, 2010; Copolovici *et al.*, 2012). Elicitation of LOX volatile emissions is accompanied by an oxidative burst, and LOX emissions often mark the activation of defense metabolic pathways that can prime for enhanced stress resilience and alter future stress responses (Jansen *et al.*, 2009; Niinemets *et al.*, 2013). Elicitation of LOX compounds is quantitatively associated with the intensity of stress (Copolovici *et al.*, 2012, 2014; Jiang *et al.*, 2017; Liu *et al.*, 2022).

Stress also induces emissions of volatile isoprenoids including isoprene, mono- and sesquiterpenes and their derivatives from the 2-C-methyl-D-erythritol 4-phosphate/1-deoxy-D-xylulose 5-phosphate (MEP/DOXP) pathway in the plastid and the mevalonate (MVA) pathway in the cytosol, and different phenolics/benzenoids emanating from the plastidial shikimate pathway (Dudareva *et al.*, 2005; Arneth & Niinemets, 2010; Junker & Tholl, 2013). In the plastid, both shikimate and MEX/DOXP pathways partly utilize the same substrate for the synthesis of various pathway products, leading to a certain competition or coordination at the substrate level between the two pathways (Pazouki & Niinemets, 2016; Niinemets *et al.*, 2017). Both terpenoid and benzenoid emissions can play a role in protecting photosynthetic apparatus by preserving the integrity of the thylakoid membrane and scavenging reactive oxygen species (González-Burgos & Gómez-Serranillos, 2012a; Misztal *et al.*, 2015).

In addition, stressed plants often emit other stress-associated volatiles including the emissions of long-chained saturated fatty acid-derived (FAD) alcohols and aldehydes and carotenoid breakdown products from the plastidial geranylgeranyl diphosphate (GGDP) pathway (Chatterjee *et al.*, 2020; Okereke *et al.*, 2021, 2022). Overall, the biosynthesis of volatiles involves a complex network of biochemical synthesis pathways and the kinetics of volatile emissions can vary depending on the plant species and the type of stress.

Understanding the volatile emission responses of plants to different stress types and combinations is important in understanding plant-environment chemical interactions as well as devising VOC-driven strategies for developing crop plants with improved stress tolerance.

2.3. Impact of interactive biotic and abiotic factors on plant stress responses

Several previous studies have demonstrated that plant physiological responses to the combination of abiotic and biotic stress differ from responses to single stresses (DeLucia *et al.*, 2012; Catola *et al.*, 2018; Ngumbi & Ugarte 2021). Multiple stress combinations typically result in synergistic or antagonistic effects and rarely result in an additive effect. For instance, in tomato (*Solanum lycopersicum*), herbivory by the greenhouse whitefly (*Trialeurodes vaporariorum*) antagonized volatile emissions (Darshanee *et al.*, 2017), but combined potato aphid (*Siphum euphorbiae*) and heat stress synergistically enhanced emissions of specialized volatiles (Catola *et al.*, 2018). Regardless of the responses of physiological traits, exposure to one stress can prime defense responses that are important for surviving future stresses.

2.4. Stress priming

Stress priming, also called stress hardening or training, refers to the facilitation of protection by previous stress experience upon exposure to subsequent severe stress. Moderate or sub-lethal stresses including moderately warm temperatures and piercing and sucking herbivory trigger the accumulation of defensive hormones such as SA and JA and stimulate the formation of a certain stress 'memory' (Pastor *et al.*, 2013; Hilker *et al.*, 2019). Once primed, the plants have specific biochemical adaptations or they can more rapidly induce defenses, ultimately enhancing tolerance and acclimation of plants to subsequent more severe stress(es). Thermotolerance, in particular, is induced by sub-lethal abiotic stresses and different biotic stresses (Suzuki *et al.*, 2015; Sherin *et al.*, 2022). Research on priming has received growing attention over the last decades as priming techniques have proven effective in improving adaptability and tolerance to diverse stresses (Balmer *et al.*, 2015; Martinez-Medina *et al.*, 2016). Recent studies have expatiated the underlying mechanisms that result in stress priming. For example, transcriptome and proteome analyses showed that in heat-primed plants,

the expressions of the genes encoding enzymes involved in primary metabolism were reduced, whereas the expression of genes encoding cellular receptors, signal transducers, chaperones, transcription factors, heat shock proteins, and sucrose synthase were enhanced (Khan *et al.*, 2022). Similarly, (Suzuki *et al.*, 2015) reported that light stress induced the rapid (within seconds after stress exposure) accumulation of transcripts that can enhance heat stress acclimation. Waterlogging priming enhances waterlogging resistance via increasing ethylene biosynthesis and the activity of antioxidant enzymes (Feng *et al.*, 2022). On the other hand, priming with biotic stressors increases primary metabolism, pattern recognition, and chromatin modification (Khan *et al.*, 2022). Priming is important for the survival and acclimation of plants during subsequent severe abiotic stress episodes (Leuendorf *et al.*, 2020; Sherin *et al.*, 2022).

2.5. Aims and hypothesis of the study

This thesis was designed to study the impact of pre-exposure to sublethal biotic and abiotic factors on subsequent severe stress responses in plants, in particular, the impacts of pre-exposure to the greenhouse whitefly (*Trialeurodes vaporariorum*) infestation on heat shock responses, moderate heat priming on heat shock responses and warm temperatures on the severity of fungal infection. We tested stress responses of physiological traits including foliage photosynthetic characteristics (net assimilation rate, stomatal conductance, intercellular concentration of CO₂ and maximum Rubisco carboxylase activity, V_{cmax}), and volatile and non-volatile secondary metabolites.

The specific aims of this thesis were to:

1. a. Study modifications in photosynthetic characteristics and volatile emissions in response to moderate and severe heat stresses in different plant species through the stress recovery period (**Papers I-III**).
- b. Investigate the impact of pre-exposure to moderate heat stress (heat priming) on time-dependent recovery in photosynthetic characteristics and volatile emissions in severely heat-stressed plants (**Papers I-II**).

- c. Investigate the impact of heat priming on the accumulation of total contents of phenolic and condensed tanning in heat-stressed plants (**Paper I**).
2. a. Quantify the impact of pre-exposure to *T. vaporariorum* herbivory on heat shock-induced time-dependent responses of photosynthetic characteristics and volatile emissions (**Paper III**).
 - b. Determine the role of stomatal conductance and biochemical capacity of photosynthesis in time-dependent modification in photosynthesis in heat-stressed plants (**Papers I-III**).
 3. a. Quantify oat crown rust (*Puccinia coronata*) infection severity-dependent reductions in photosynthesis and enhancement of stress volatile emissions in different host species of varying sensitivity to crown rust (**Papers IV-V**).
 - b. Investigate the impact of photosynthetic reductions on emissions of stress volatiles (**Papers IV-V**).
 - c. Assess the contributions of stomatal limitations, and factors determining leaf biochemical photosynthesis capacity (photosynthetic biomass per unit leaf area, key limiting element content) to infection severity-dependent reductions in photosynthesis rate (**Papers IV-V**).

The hypotheses of this study were:

1. Heat shock stress in *Achillea millefolium* and *Origanum vulgare* will greatly reduce photosynthetic activity and increase the emissions of volatiles through the stress recovery period (**Papers I-III**)
2. moderate heat stress (priming) decreases photosynthetic activities and modifies secondary metabolite synthesis pathways, as reflected in the increased emissions of LOX volatiles and terpenoids, and primed plants will have higher heat shock tolerance of photosynthetic apparatus, such that reduction of photosynthesis is lower and recovery is faster, and enhanced emissions of antioxidant volatiles and accumulation of protective secondary metabolites (**Papers I-II**)

3. *T. vaporariorum* infestation will reduce photosynthesis rates and operate primarily through the salicylic acid (SA)-dependent pathways, resulting in elicitation of benzenoid emissions and minor emissions of LOX volatiles and monoterpenes; and combined *T. vaporariorum* and heat shock stresses will exert antagonistic effects on VOC emissions and gas exchange characteristics during stress recovery (**Paper III**)
4. *P. coronata* infection will reduce photosynthesis and induce stress volatile emissions in a stress severity-dependent manner, and exposure to warm weather will increase the performance of fungi resulting in the depletion of defense and eventually escalated tissue damage, particularly in the sensitive host *A. sativa* (**Papers IV-V**).
5. Responses to *P. coronata* infection will vary in the primary host and the alternate host (**Papers IV-V**).

3. MATERIALS AND METHODS

3.1. Plant growth under controlled conditions (Paper I-III)

For *Achillea millefolium* (Paper I) and *Origanum vulgare* (Paper II) in the study of heat stress priming and for *O. vulgare* in the study of combined insect infestation and heat stress (Paper III), seeds (source: Nordic Botanical Ltd, Tartu, Estonia) were sown in plastic pots (2 L for *A. millefolium* and 0.5 L for *O. vulgare*) filled with a 1:1 mixture of quartz and commercial potting soil containing slow-release micro- and macronutrients (Biolan Oy, Kekkilä group, Finland). *Achillea millefolium* were cultivated in a plant growth chamber (FITOCLIMA S600PLLH, Aralab, Lisbon, Portugal) and *O. vulgare* in a growth room under similar conditions. The conditions in the growth environment of the plants were set as follows: ambient CO₂ concentration of 380–400 μmol mol⁻¹ and relative humidity of 60–70%, photosynthetic photon flux density (PPFD) at 600 μmol m⁻² s⁻¹ at plant level, day/night temperatures 25/20 °C (Papers I-III). For *A. millefolium* (Paper I), light was supplied for a 16 h photoperiod, and for *O. vulgare* (Papers II and III), for a 2 h period. All the plants (Papers I-III) were watered to soil field capacity every day. At the time of the experiments, the plants were three-month-old. Fully mature upper canopy leaves were used in the experiments.

3.2. Plants for the field study (Paper IV)

This study investigated the quantitative changes in physiological characteristics with the severity of *Puccinia coronata* infection in the primary host *Avena sativa* and alternate host *Rhamnus frangula*. The sampling site was located in Põlva County, Estonia (58.6°N, 26.5°E, elevation 61 m) in the summer of 2018. The summer (June-August) was warm with a monthly average (±SE) air temperature of 19.5 ± 1.4 °C, monthly precipitation of 56 ± 17 mm, and relative air humidity of 68.2 ± 2.8% (data from the Laboratory of Environmental Physics, Institute of Physics, University of Tartu, <http://meteo.physic.ut.ee>). Air temperatures were considerably higher than the corresponding long-term average recorded for 1991-2020 (16.7 °C; the Estonian Environment Agency, <http://www.emhi.ee>). Warm weather favors the growth and dispersal of *P. coronata* as well as its virulence (Liu & Hambleton, 2013; Nazareno *et al.*, 2018).

Rhamnus frangula was sampled in a mixed Norway spruce (*Picea abies* L.) and Scots pine (*Pinus sylvestris* L.) forest near Veski village, Põlva County, Estonia (58.6°N, 26.48°E, elevation 61 m) in mid-June. At this time, >90% of the leaves on nearly all the *R. frangula* shrubs in the forest were infected and had developed visible rust lesions. Leaves with varying degrees of visible signs of *P. coronata* infection were collected from seven infected shrubs and leaves with no visible signs of infection from three non-infected shrubs. *Rhamnus frangula* shrubs were ~3 m tall with a stem diameter of ~4 cm. Twigs ~20 cm long with multiple leaves were harvested underwater, the cut end was retained in water, and the twigs were immediately taken to the laboratory for measurements. Altogether, 15 leaves (three non-infected control and 12 infected leaves) with varying degrees of infection were selected for physiological trait measurements (Fig. 4A for representative images of leaves).

By the end of July, almost all *A. sativa* plants growing in the organic oat field at Veski village (58.65°N, 26.47°E, elevation 61 m) were infected and had visible uredinia and telia spots. In early August, ~2-month-old *A. sativa* cv. 'Kalle' plants with leaves with varying degrees of infection were collected by carefully uprooting the plants with the whole root ball and attached soil. The plants were ~90 cm tall and in a vegetative state. Each plant was immediately potted in a 1 L plastic pot. The pots were filled with field soil, irrigated, and transported to a growth room with day/night temperatures of 25/18 °C, relative humidity of 60–70%, and ambient CO₂ concentration of 380–400 μmol mol⁻¹. Light (800 μmol m⁻² s⁻¹ at plant level) was provided for 12 h a day and plants were watered to field capacity every 48 h. The plants were acclimated in the growth room for four days. Three non-infected control and 20 infected leaves with varying severity of infections from independent plants were measured. The severity of infection was quantified as the percentage of the total leaf area covered by visible chlorotic and necrotic spots (total damaged leaf area, DA). Mature topmost leaves of the same age were selected for physiological measurements (Fig. 4A for images of representative leaves).

3.3. Identification of *Puccinia coronata* f. sp. *avenae* (Paper IV)

The morphology of the aeciospores, urediniospores, and teliospores in *P. coronata*-infected leaves was examined with an SEM (Zeiss LS15, Carl Zeiss AG, Jena, Germany). The spores were imaged with the detector

SE1 set at a working distance of 8.5–9 mm between the lens and sample surfaces and with extra high tension voltages of 14.27, 15.0, or 17.6 kV. The surface characteristics of the fungus were distinctly recognized in the images (**Fig. 4C**) and based on the morphological features and the host species, the pathogen was identified as *Puccinia coronata* f. sp. *avenae*.

3.4. Application of moderate heat priming (Papers I-II)

For heat priming in **Paper I**, seven plants were carefully moved to another growth chamber similar to the chamber where the plants were cultivated. In **Paper II**, the priming treatment was applied to six plants by enclosing the leaves of individual plants in a temperature-controlled glass chamber of a customized gas-exchange measurement system (section 3.7 here for details of the system and glass chamber). For all the experiments (**Papers I-II**), the environmental conditions in the priming chamber were similar to the growth conditions of the plants except for the temperature that was set at 35 °C for 1 hr. The temperature of the priming chamber was reset to 25 °C immediately after the priming treatment. For **Paper I**, three primed plants were further subjected to heat shock treatment, while foliage gas exchange and volatile emission rates were measured in the remaining four primed plants to test whether the responses of primed plants to heat shock were due to heat shock stress or heat priming. For **Paper II**, the gas exchange and volatile emission characteristics were measured in three primed plants and the remaining three primed plants were returned to the growth conditions for 72 h and then subjected to heat shock treatment.

3.5. *Trialeurodes vaporariorum* infestation (Paper III)

Mature *O. vulgare* were infested with *T. vaporariorum* by exposing the non-infested plants to heavily-infested *O. vulgare* in the growth room for one day. Four infested plants were placed at the edges of the growth chamber and the non-infested plants were in the middle of the chamber. Gas exchange and volatile measurements were conducted after 14 days of infestation when there were only a few first-instar larvae on the lower leaf surface. Six independent infested plants with upper canopy leaves that hosted a flock of six to eight *T. vaporariorum* per leaf were sampled for the measurements. Measurements were conducted in three infested plants, and the remaining three infested plants were further subjected to heat shock treatment.

3.6. Heat shock application (Papers I-III)

Heat shock was applied using the standard procedure described by Liu *et al.* (2022). Experimental leaves were enclosed in a chemically inert polyester bag and immediately submerged in water heated to a stable temperature of 45 °C in a temperature-controlled water bath (VWR International, Radnor, PN, USA). The immersed leaves were kept in the medium for 5.5 min (heat exposure of 5 min, considering that 30 s was needed to reach the desired temperature due to the finite thermal conductivity of the polyester bag). Additionally, non-stressed control plants (six in **Paper I**, and three in **Papers II** and **III**) and three infested plants (infested control **Paper III**) were treated similarly, except that the water temperature was 25 °C. In each study, a total of six heat shock-treated plants were measured, three primed and three non-primed in **Papers I** and **II**, and three non-infested and three infested plants in **Paper III**. Control plants were measured analogously to the heat shock-stressed plants. For **Papers, I** and **II**, gas exchange data and VOC samples were collected at 0.5, 5, 10, 24, 48, and 72 h, and for **Paper III**, at 0.5, 2.5, 5, 24, and 48 h after the treatment.

3.7. Gas exchange measurements (Papers I-IV)

Gas exchange measurements were conducted in a temperature-controlled double-layered glass chamber (Copolovici & Niinemets, 2010 for a detailed description of the chamber). Concentrations of CO₂ and H₂O at the inlet and outlets of the chamber were measured using a dual-channel infrared gas analyzer (LI-7000, LI-COR Biosciences, Lincoln, NE for **Paper I** and CIRAS III, PP-systems, Amesbury, MA, USA for **Paper II-IV**). Gas exchange and volatile measurements in enclosed leaves were conducted immediately after gas exchange rates had attained a steady-state rate, *in ca.* 15–20 min after enclosure. Measurements were conducted under the standard measurement conditions as follows: leaf temperature of 25 °C, leaf-to-air vapor pressure deficit of 1.7 kPa, PPFD of 800 μmol m⁻² s⁻¹, and CO₂ concentrations of 380–400 μmol mol⁻¹. Foliage photosynthetic characteristics were calculated according to von Caemmerer and Farquhar (1981).

3.8. Volatile collection and GC-MS analysis (Paper I-IV)

Volatiles were collected during gas exchange measurements onto stainless steel cartridges filled with graphitized carbon adsorbents for maximum adsorption of C_3 – C_{17} volatiles (Kännaste *et al.*, 2014 for a detailed description of the adsorbent cartridges). Background volatile concentrations from empty chambers were collected before and after measurements. The cartridges were analyzed using a Shimadzu TD20 automated cartridge desorber and Shimadzu 2010 GC-MS system (Shimadzu Corporation, Kyoto, Japan) as detailed in Kännaste *et al.* (2014). Pure chemical standards (Sigma-Aldrich, St. Louis, MO, USA) and NIST library ver. 2.2 (2014) were used to identify the volatiles. Volatile emission rates were calculated according to Niinemets *et al.* (2011).

3.9. Determination of leaf dry mass per area, and key element contents per dry mass (Paper IV)

Both leaf sides of the measured leaves were photographed. The total leaf area and infected leaf area on both sides were calculated from the pictures using ImageJ 1.8.0 (NIH, Bethesda, MD, USA), and D_A values for both leaf surfaces were estimated. The leaves were oven-dried at 70 °C for 72 h and weighed. Dried leaves of an approximately similar severity of infection were ground together for elemental analysis. Dry mass per unit area (LMA) was computed by dividing leaf dry mass by leaf area. Nitrogen (N_M) and carbon (C_M) contents per unit dry mass were determined by the dry combustion method (Vario MAX CNS analyzer, Elementar, Langenselbold, Germany). Phosphorus content per dry mass (P_M) was determined using an Agilent 4200 microwave plasma-atomic emission spectrometer (Agilent Technologies, Inc., Santa Clara, CA, USA) after digesting the sample in sulphuric acid.

3.10. Determination of total content of phenolics and condensed tannins (Paper I)

The extraction of total phenolics and condensed tannins was carried out according to the protocol detailed in Liu *et al.* (2019). Total phenolic contents were determined by Folin–Ciocalteu assay by Liu *et al.* (2019). Total phenolic contents were expressed as gallic acid equivalents (mg of GAE g^{-1} DM) using the standard curve of gallic acid. Total condensed

tannins were measured according to the method described by Xu & Chang (2007) with some modifications as explained here. In summary, Aliquots of 100 μ l leaf extract or (+)-catechin standard solution were mixed with 1.5 ml of concentrated hydrochloric acid and 3 ml of 4% (mass/vol in methanol) vanillin solution, and the mixture was incubated for 15 min at 23 °C.

The absorbent was measured at 500 nm using methanol solvent. Total condensed tannins were expressed as (+)-catechin equivalents (mg of CAE g^{-1} DM) using the standard curve with (+)-catechin. The chemicals used in this analysis were from Sigma-Aldrich Chemie GmbH.

3.11. Statistical analyses (Paper I-V)

For the heat stress study (**Papers I-III**), differences in averages of photosynthetic characteristics and volatile emissions among different treatment groups at each recovery point were tested using single-factor ANOVA. Averages among the treatment groups were pairwise compared by the least significant difference (LSD) test (**Papers I-III**). In **Paper III**, Tukey's post hoc test following one-way ANOVA was used to test for differences in averages of total phenolic contents and condensed tannins among the different treatment groups. In **Paper IV**, a paired-sample *t*-test was used to test for the differences in damaged leaf areas of lower and upper leaf surfaces. Quantitative relationships between the severity of *P. coronata* infections and photosynthetic characteristics, LMA, N_{M^P} , P_{M^P} , C_{M^P} and VOC emission rates were explored using linear and non-linear regressions. In all the studies (**Paper I-IV**), where required, the data used for testing the difference between averages of treatment groups were log-transformed to satisfy the assumption of homoscedasticity. In **Paper I**, all the statistical tests were conducted using SPSS 22.0 (Chicago, IL). Data were visualized with OriginLab 8.0 (OriginLab Corporation, Northampton, MA). In **Paper IV**, all statistical tests and data visualization were conducted with R ver. 4.2.0 statistical software (R Core Team, 2021). All the statistical tests (**Paper I-IV**) were considered significant at $P < 0.05$.

4. RESULT

4.1. Effects of heat priming and heat shock stress on foliage photosynthetic characteristics

In *A. millefolium* (Paper I), the net assimilation rate (A) was not affected by heat priming (35 °C for 1 h) (Fig. 1A). Priming uncoupled the association between A and stomatal conductance to water vapor (g_s ; Fig. 1). Heat shock resulted in immediate decreases in A in both primed and non-primed *A. millefolium*; in non-primed plants, A remained lower than in control plants throughout the recovery period, whereas, in primed plants, A recovered to control level at 24 and 72 h after stress application (Fig. 1D). In non-primed plants, g_s decreased at 5-24 h after

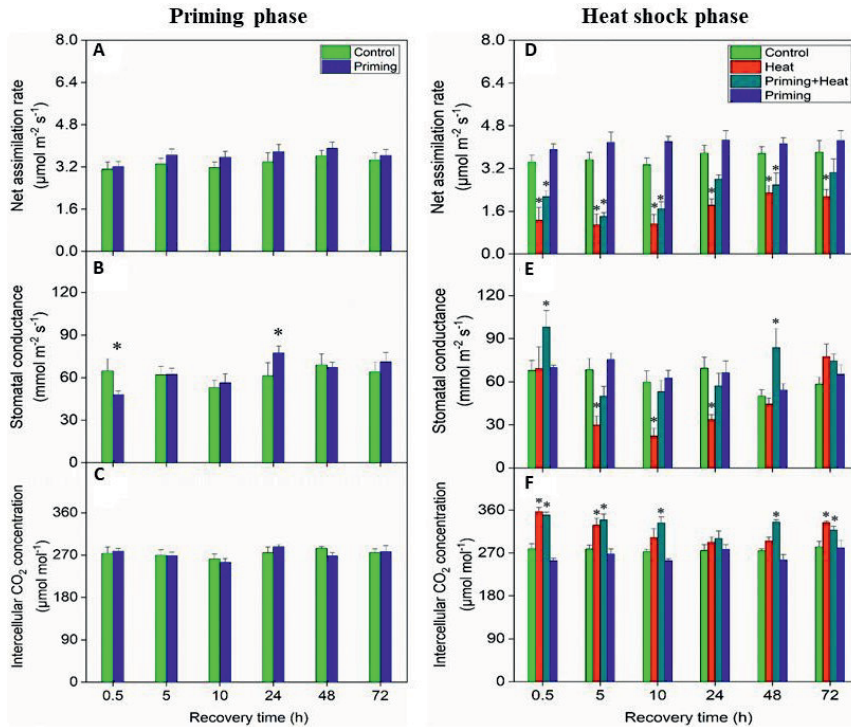


Fig. 1. Time-dependent changes in average \pm SE net assimilation rate (after priming, A; after heat shock, D), stomatal conductance (after priming, C; after heat shock, E), and intercellular CO₂ concentration (after priming, E; after heat shock, F) of unstressed control, heat-stressed non-primed (Heat), primed and heat-stressed (Priming+Heat) and primed non-heat-stressed (Priming) leaves of *Achillea millefolium*. Asterisks refer to the significant differences between control and different treatments at each recovery time point ($p \leq .05$) (reproduced from Paper I).

heat shock treatment, whereas, in primed plants, g_s was increased at 0.5 h and 48 h after heat shock (**Fig. 1E**). Intercellular concentration of CO_2 (C_i) was increased in all the heat shock-treated plants (**Fig. 1F**).

In *O. vulgare*, priming decreased A by 50% throughout the recovery period (**Fig. 2A** and **Fig. 1A** in **Paper II**). Heat shock application resulted in immediate decreases in A in primed and non-primed *O. vulgare*, but the reductions were ten times greater in non-primed plants than in primed plants (**Fig. 2A** and **Fig. 1A** in **Paper II**). At 24 h after the application of heat shock in primed *O. vulgare*, A recovered to the level observed during priming recovery and remained at that level throughout the experiments (**Fig. 2A** and **Fig. 1A** in **Paper II**). In non-primed plants, A recovered to the levels observed in primed plants at 48 h after treatment, and at the end of the experiment, A recovered fully to the level in control plants (**Fig. 2A**). Overall, all the heat stress treatments uncoupled A from g_s (**Fig. 2A, B** and **Fig. 1A** in **Paper II**). However, in all the heat treatments in *O. vulgare* (**Paper II**), we observed increases in C_i parallel to reductions in A (cf. **Fig. 2A, C**). Heat stress treatments reduced the apparent Rubisco carboxylase activity (V_{cmax}) (**Fig. 2D** and **Fig. 1D** in **Paper II**). Time-dependent modification of V_{cmax} reflected the changes in A , and V_{cmax} was positively correlated with A (cf. **Fig. 2A, D** and **Fig. 2** in **Paper II**).

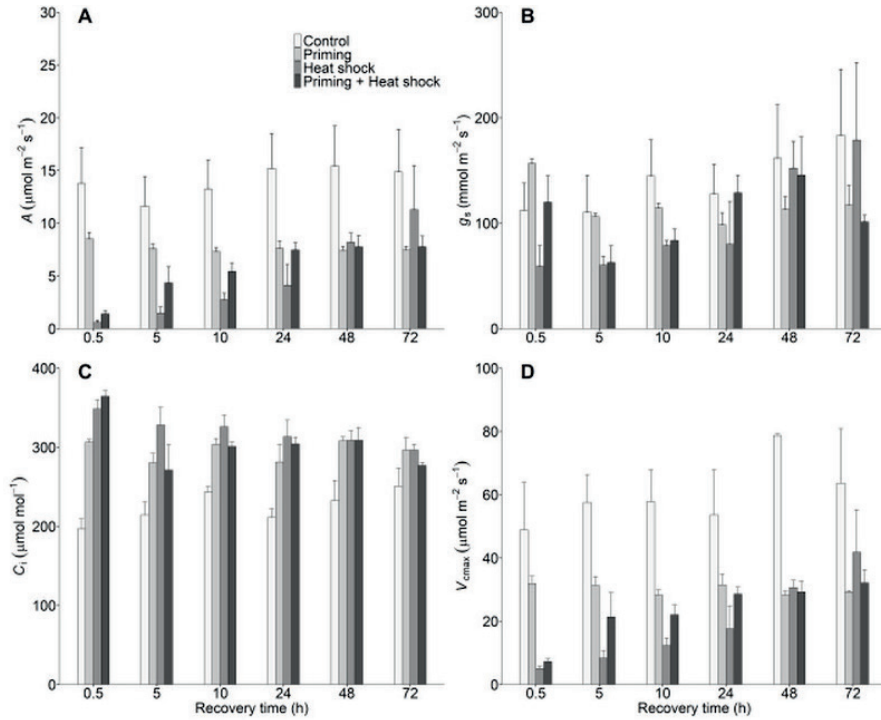


Fig. 2. Changes in net assimilation rate (A , **A**), stomatal conductance (g_s , **B**), the intercellular CO_2 concentration (C_i ; **C**), and maximum carboxylase activity of Rubisco (V_{cmax} , **D**) in non-stressed (control), heat-primed (priming), heat shock-stressed non-primed (Heat shock) and heat shock-stressed primed (Priming + Heat shock) leaves of *Origanum vulgare* (reproduced from **Paper II**).

4.2. Effects of combined insect feeding and heat stress on photosynthetic characteristics

At 2.5 h after heat stress treatment, A in non-infested *O. vulgare* (**Paper III**) decreased by 25% and remained at that level throughout the experiment (**Fig. 3A**). However, g_s in the non-infested plants was increased (**Fig. 3B**). Through the initial 5 h stress recovery period, A decreased by 64% in whitefly-treated plants and by 70% in combined whitefly and heat shock stress-treated plants in comparison to the control treatment (**Fig. 3A**). In all the infested plants, A had recovered fully at the end of the experiment and the recovery was accompanied by increases in g_s (**Fig. 3A**).

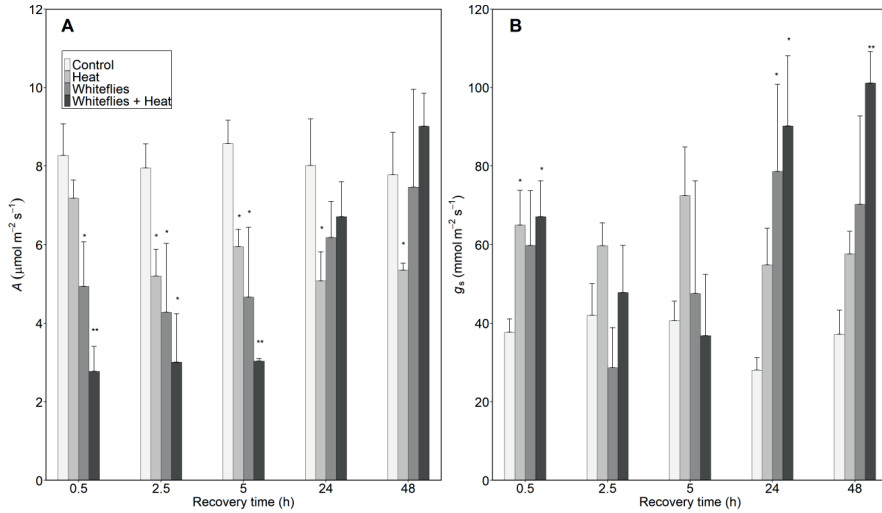


Fig. 3. Changes in net assimilation rate (A) and stomatal conductance to water vapor (B) in non-stressed (control), heat shock-stressed (heat), *Trialeurodes vaporariorum*-infested (greenhouse whitefly) and infested heat shock-treated leaves of *Origanum vulgare*. Means were compared by least significant difference (LSD) test following one-way ANOVA test. Asterisks refer to the significant differences between control and different treatments at each recovery time point ($p \leq .05$) (reproduced from **Paper III**).

4.3. Effects of *P. coronata* infection on foliage photosynthetic characteristics

In the primary host *Avena sativa* (**Paper IV-V**), percentages of the damaged area (DA) of upper and lower surfaces of infected *A. sativa* leaves were similar ($P=0.26$, data not shown). In the alternate host *R. frangula*, visual leaf damage was greater for the upper leaf surface than for the lower surface (average \pm SE of upper surface versus lower surface = $29 \pm 7\%$ versus $1.24 \pm 0.16\%$, $P < 0.001$; see **Fig. 4B** for representative sample leaves). The quantitative changes between damaged leaf area and leaf physiological characteristics were stronger with D_A for the upper leaf surfaces than with DA for the lower surfaces or with the average of the D_A of both leaf surfaces. Thus, for this study, we present only analyses performed with the D_A for the upper leaf surface.

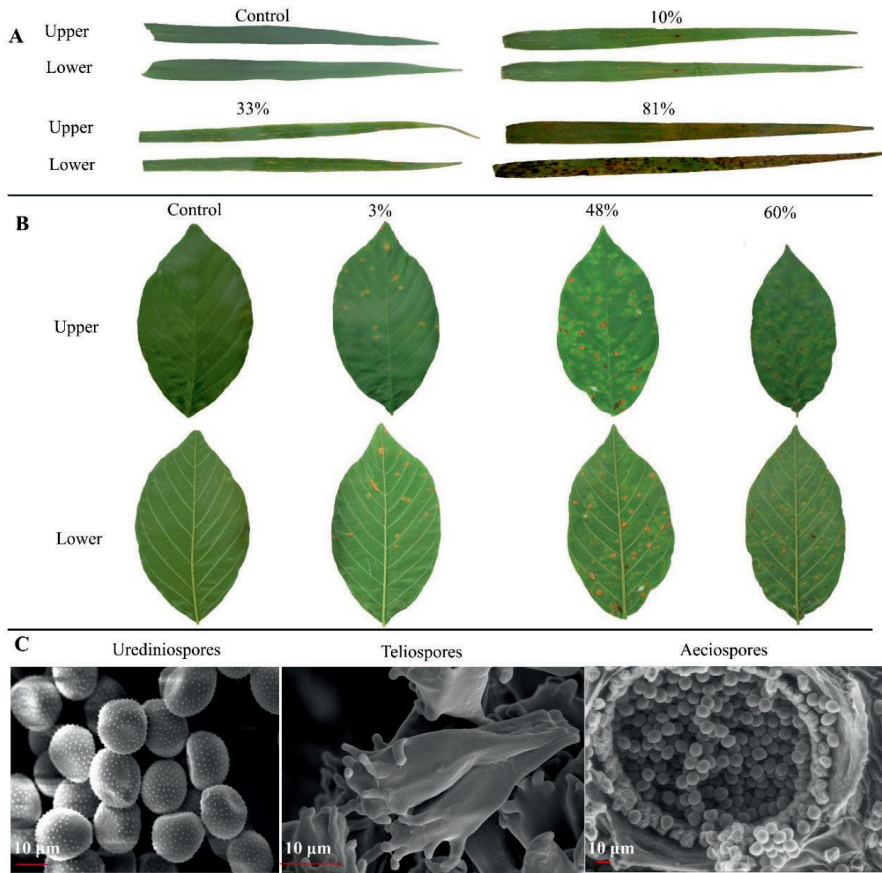


Fig. 4. Characteristic images of upper and lower leaf surfaces of the leaves of *Avena sativa* (A) and *Rhamnus frangula* (B) showing different severities of crown rust fungus (*Puccinia coronata* f. sp. *avenae*) infection, and SEM micrographs of the urediniospores, teliospores, and aeciospores (from left to right) of *P. coronata* (C) (reproduced from Paper IV).

In *A. sativa* leaves, A decreased exponentially with increasing the severity of *P. coronata* infection (Fig. 5A). A decreased to almost zero level (107-fold reduction in comparison to control) in the case of extreme infection. Stomatal conductance decreased in the leaves with the reduced rates of photosynthesis, but the reductions were less than reductions in A (Fig. 5A, B). As a result of reductions of g_s , C_i was also reduced as the infection severity increased, but the reduction was stronger during the initial stages of infection (Fig. 5B, C). In *R. frangula* leaves, A correlated negatively with the severity of infection, but the reductions in A were less than that observed in *A. sativa* (Fig. 5A, B). In *R. frangula*, g_s was unaffected, but C_i increased slightly with increasing the severity of infection (Fig. 5B, C).

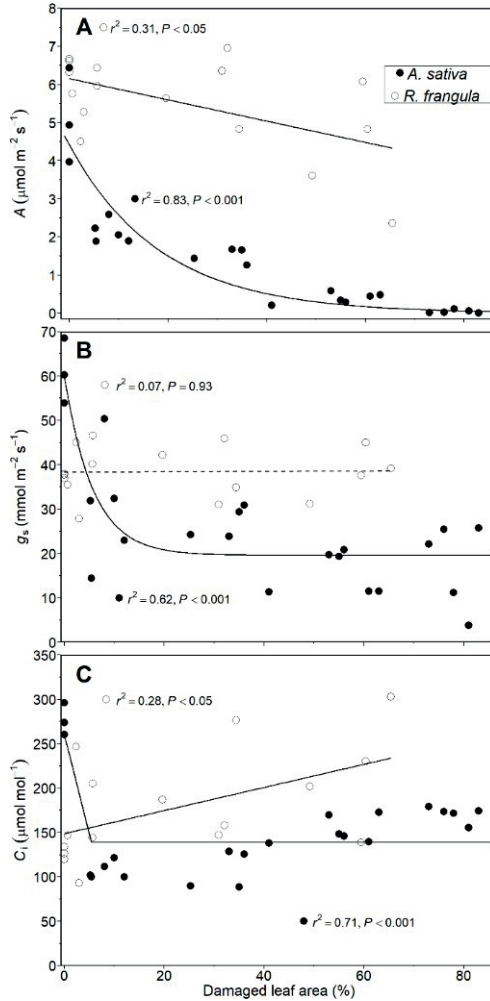


Fig. 5. Relationships of leaf net assimilation rate (A , **A**), stomatal conductance to water vapor (g_s , **B**), and intercellular CO_2 concentration (C_i , **C**) with the severity of oat crown rust (*Puccinia coronata*) infection in the primary host *Avena sativa* (filled circles) and the alternate host *Rhamnus frangula* (open circles). The degree of leaf infection was characterized by the percentage of the infected area (DA) of the lower leaf surface for *A. sativa* and the upper surface for *R. frangula*. Data were fitted by non-linear regressions for *A. sativa* and by linear regressions for *R. frangula* (reproduced from **Paper IV**).

4.4. Contribution of leaf dry mass per unit area and C, N, and P contents per leaf dry mass to reductions in net assimilation rates

In *A. sativa* (**Papers IV-V**), leaf dry mass per area (LMA) decreased with increasing severity of infection (**Fig. 6A**). Reductions in LMA were 1.6-fold throughout the severity of infection (**Fig. 6A**). Net assimilation rate

per dry mass ($A_M = A/LMA$) decreased with the severity of infection ($r^2=0.76$, $P<0.001$) and reached 54-fold reduction during extreme infections (data not shown). Thus, taking into account the reductions in A per unit area (107-fold, the contribution of infection-dependent reductions in LMA to decreases in A was relatively small, implying that reductions in net assimilation rates were primarily due to reductions in

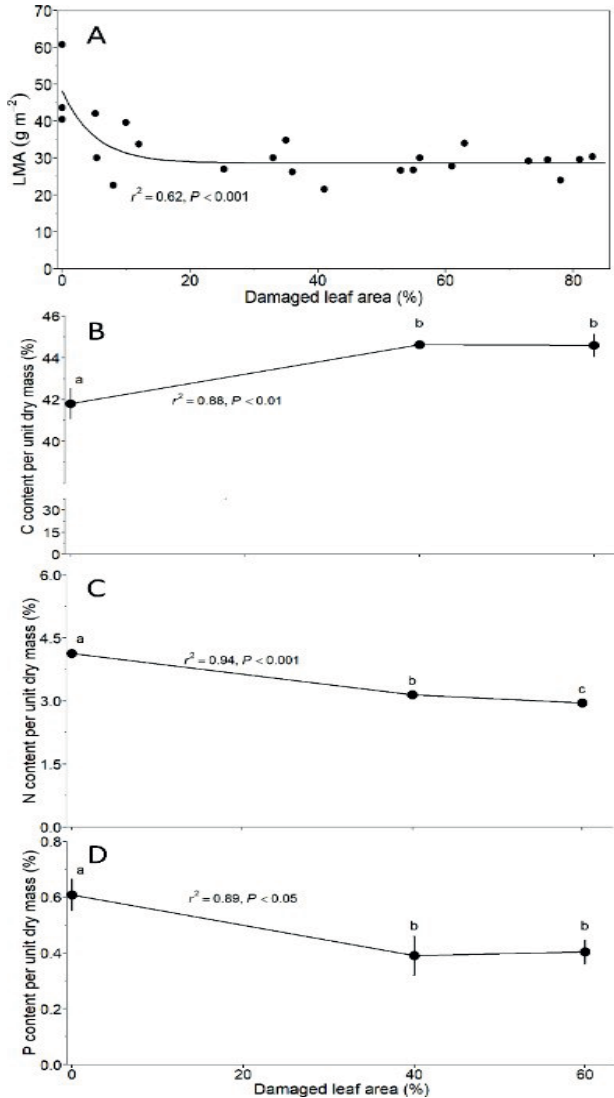


Fig. 6. Leaf dry mass per unit area (LMA; **A**), and carbon (**B**), nitrogen (**C**), and phosphorus (**D**) contents per dry mass in leaves of *A. sativa* with different severity of *P. coronata* infection. Data in *A* were fitted by non-linear regression. Different lowercase letters in B-D indicate significant differences among infected leaves with different degrees of infection (reproduced from **Paper IV**).

A_M . Additionally, in infected *A. sativa* leaves, limiting mineral nutrients (N_M and P_M) decreased with increasing the severity of infections and C_M increased in comparison to the non-infected control level (**Fig. 6A, B**). In infected *R. frangula*, LMA, C_M , N_M , and P_M were not affected (**Paper IV**).

4.5. Effects of heat priming and heat shock stress on volatile emissions

In *A. millefolium*, emissions of LOX compounds and isoprene were enhanced at 0.5 h after priming application (**Fig. 7A** and **Fig. 2A-B** in **Paper I**). LOX emissions recovered to the level in control plants at 2.5 h, whereas isoprene emissions recovered at 5 h after priming, but the emissions of LOX compounds tended to increase through 24-72 h priming recovery period (**Fig. 7A** and **Fig. 2A, B** in **Paper I**). Emissions of monoterpenes and benzenoids decreased at 5 h after priming, but increased significantly at the end of the experiment (**Fig. 7C, D** and **Fig. 2D** in **Paper I**). Monoterpenes were quantitatively the most important volatile group emitted in both control and priming-treated plants (**Fig. 7** and **Fig. 2** in **Paper I**). Total emissions of VOC were also enhanced after priming; and changes in total emissions mirrored enhanced emissions of monoterpenes (**Fig. 7C, E** and **Fig. 2C, E** in **Paper I**).

Upon heat shock treatment (**Paper I**), emissions of LOX compounds, isoprene, mono- and sesquiterpenes were enhanced in primed *A. millefolium*, whereas, emissions of LOX compounds, mono- and sesquiterpenes and benzaldehyde were enhanced in non-primed plants (**Fig. 8A** and **Fig. 4A-D** in **Paper I**). The elicitation of LOX emissions was greater in non-primed plants (**Fig. 8A** and **Fig. 4A** in **Paper I**). By 24 h after treatment, emissions of all volatile groups in all the heat-stressed plants (**Paper I**) had recovered to the level in control plants (**Fig. 8A-F**). However, emissions of LOX compounds and benzenoids increased at 48 h in primed plants and at 72 h in non-primed plants, and monoterpene emissions increased at 72 h in all the heat shock-stressed plants (**Fig. 8A, C, F** and **Fig. 4A, C, F** in **Paper I**).

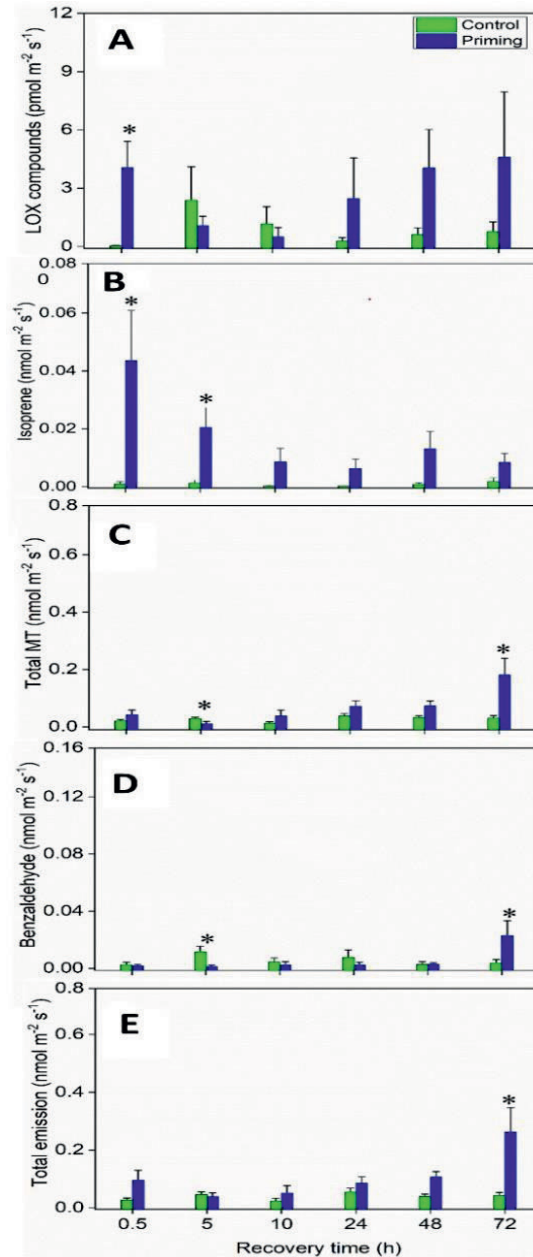


Fig. 7. Effects of heat priming treatment on emission rates of lipoxygenase pathway compounds (LOX, **A**), isoprene (**B**), total monoterpenes (MT, **C**), benzaldehyde (**D**), and total VOC (**E**) in *A. millefolium* leaves at different times after the priming treatment. Asterisks refer to the significant differences between the control and the priming treatment at each recovery time point ($p \leq .05$) (reproduced from **Paper I**).

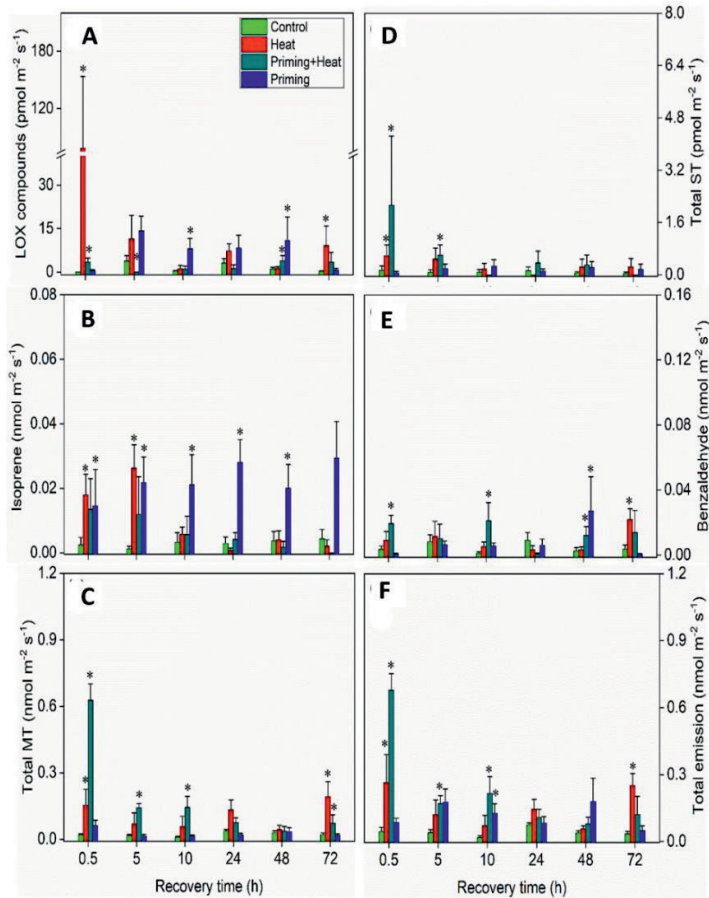


Fig. 8. Time-dependent changes in emission rates of LOX compounds (A), isoprene (B), total monoterpenes (MT, C), total sesquiterpenes (ST, D), benzaldehyde (E) and total VOC (F) in control, non-primed heat-stressed (Heat), primed and heat-stressed (Priming + Heat) and primed non-heat-stressed (Priming) *A. millefolium* leaves at different times through the recovery. Asterisks refer to the significant differences between control and specific treatments at each recovery time point ($p \leq .05$) (reproduced from **Paper I**).

In *O. vulgare*, priming enhanced LOX compound emissions at 0.5 h after application (**Fig. 9A**), and the enhanced LOX emissions were higher than those observed in *A. millefolium* (cf. **Fig. 8A** and **9A**). LOX volatile emissions in *O. vulgare* recovered to the level in control at 10 h but rose again after 24 h recovery (**Fig. 9A**). Monoterpene emissions were enhanced at 10 and 48 h after priming application (**Fig. 9C**). Despite the increases observed in the emissions of individual volatile groups, total volatile emissions in the priming-treated and control plants did not differ throughout the recovery period (**Fig. 9A-F**).

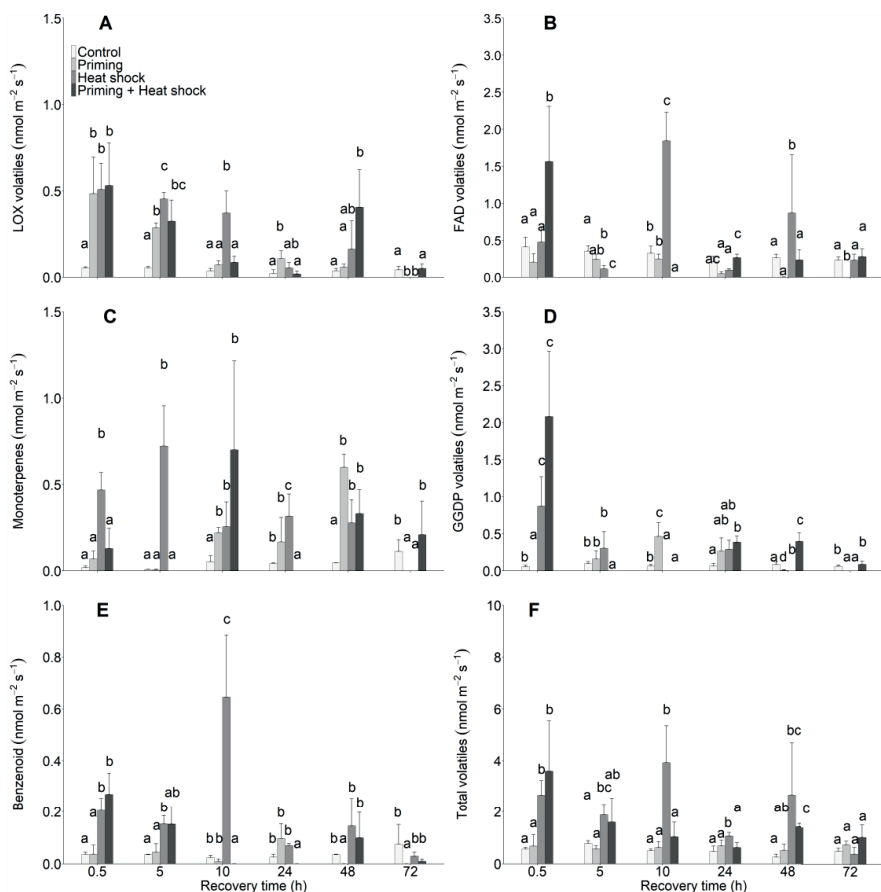


Fig. 9. Emission rates of lipoxygenase (LOX) pathway compounds (**A**), long-chained fatty acid-derived (FAD) compounds (**B**), monoterpene (**C**), geranylgeranyl (GGDP) pathway compounds (**D**), benzenoids (**E**), and total emission of volatile organic compounds (**F**) in control, moderate heat-stressed (Priming), heat shock-stressed non-primed (Heat shock), and heat shock-stressed primed (Priming + Heat shock) *Origanum vulgare* during 72 h recovery period. Different lowercase letters denote significant differences ($P < 0.05$) among the treatment groups (reproduced from **Paper II**).

Heat shock stress (**Paper II**) resulted in rapid enhancements of emissions of LOX compounds, benzenoids, GGDP volatiles, and total VOC in *O. vulgare*, irrespective of priming treatment (**Fig. 9** and **Fig. 3** in **Paper II**). In addition, we observed rapid emissions of terpenoids (isoprene, mono- and sesquiterpenes) in non-primed plants and FAD compound emissions in primed plants (**Fig. 9A-F** and **Table 1** in **Paper II**). In non-primed plants, emissions of LOX compounds and monoterpenes decreased to below the level of control at the end of the experiment (**Fig. 9A**). In primed *O. vulgare*, overall emissions of volatiles recovered at 10 h after heat

shock application, except monoterpene emissions that were enhanced at that recovery time point (Fig. 9A-F). However, secondary emission bursts were observed for most volatiles including LOX compounds, monoterpenes, and GGDP pathway compounds at 24-48 h after heat shock application, and as the result, total VOC emissions also increased at 48 h. At the end of the experiment, volatile emissions in the primed plants recovered to the level in control plants (Fig. 9A-F).

4.6. Effects of heat shock on foliage phenolic content in primed and non-primed plants

All the heat stress treatments applied induced the accumulation of total condensed tannins relative to the control treatment, but the concentration was the highest in heat shock-stressed primed plants (Fig. 10A and Fig. 7B in Paper I). Total phenolic content only increased in heat shock-stressed priming treatment (Fig. 10B and Fig. 7C in Paper I).

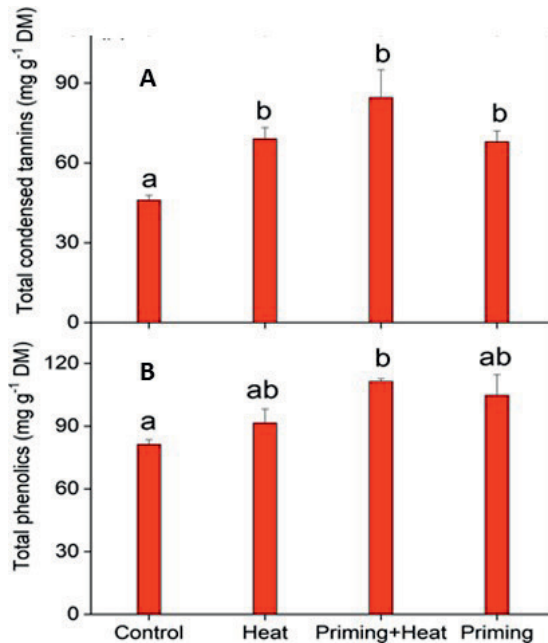


Fig. 10. Concentrations of total condensed tannins (A) and total phenolics (B) in control, non-primed heat shock stressed (Heat) and primed heat shock-stressed (Priming+Heat) leaves and priming-treated (Priming) *A. millefolium* leaves at 72h after the application of stress treatment. Different lowercase letters denote significant differences ($P < 0.05$) among the treatment groups (reproduced from Paper I).

4.7. Effects of insect infestation and heat shock on volatile emissions

Non-stressed control *O. vulgare* emitted different volatile classes including LOX pathway compounds, FAD compounds, monoterpenes, benzenoids and GGDP pathway volatiles (Fig. 11A-F). Whitefly feeding applied alone decreased the emissions of LOX compounds and benzenoids to below the level of detection (Fig. 11A, D). Whitefly infestation enhanced the emission of monoterpenes moderately throughout the recovery period (Fig. 11C). In addition, emission bursts of FAD compounds were observed at 5 h, and GGDP volatiles through 2.5–24 h whitefly-stress treatment recovery period (Fig. 11A, E).

The application of heat shock alone in *O. vulgare* resulted in a rapid enhancement of emissions of the volatile classes detected under non-stressed control conditions (Fig. 11A-F). The emissions of these volatile classes remained high throughout the experiment, except for the emissions of FAD compounds that decreased at 5–24 h after heat shock treatment (Fig. 11A-F). Overall, the increases in the emissions of volatiles in the non-infested plants were more pronounced during the first 5 h after heat stress treatment (Fig. 11A-F). In addition, we observed the induction of sesquiterpene emissions at an average level of $0.040 \pm 0.01 \text{ nmol m}^{-2} \text{ s}^{-1}$ through 0.5–5 h after heat stress treatment (Table 1 in Paper III).

Benzenoids were the only volatile class that was enhanced significantly upon heat shock application in infested plants; benzenoid emissions were enhanced through 0.5–2.5 h (Fig. 11A-F). At 24 h after applying heat stress in infested plants, emissions of LOX and benzenoids decreased to below the level of detection (Fig. 11A, D). However, emission bursts of benzenoids were observed at the end of the experiment (Fig. 11D).

In addition, all the stress treatments induced the emissions of the stress marker compound (*E*)- β -ocimene (Fig. 11F). Single stress treatments elicited (*E*)- β -ocimene emission to a larger degree in the first 5 h after treatment (Fig. 11F). As (*E*)- β -ocimene was quantitatively the most important monoterpene emitted in the stressed plants, changes in total VOC in the stressed plants reflected changes in the induction of (*E*)- β -ocimene (Fig. 11F). At the end of the stress recovery period, (*E*)- β -ocimene emissions were only detected in the plants treated with heat shock alone (Fig. 11F).

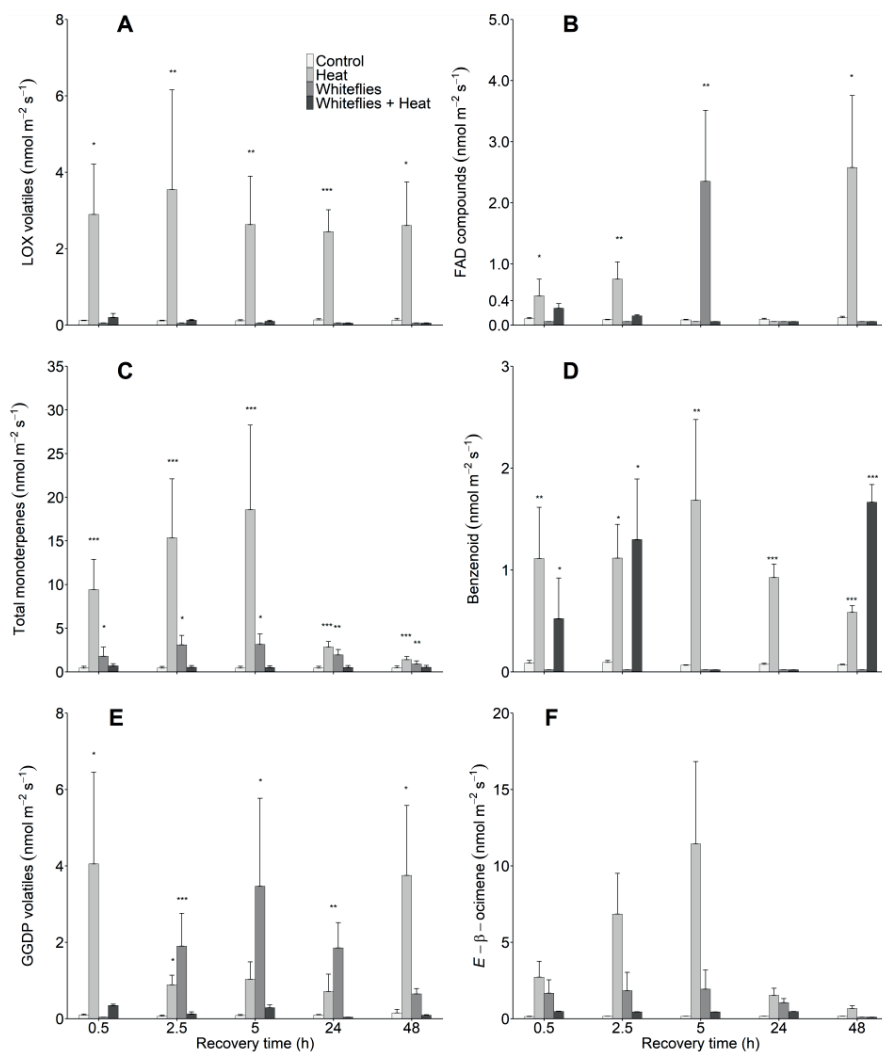


Fig. 11. Emission of total lipoxygenase pathway compounds (LOX, **A**) and long-chained fatty acid-derived compounds (FAD, **B**), total monoterpenes (**C**), benzenoids (**D**), geranylgeranyl (GGDP) pathway compounds (**E**), and (*E*)- β -ocimene (**F**) from leaves of non-treated (control), heat shock-treated (heat), *Trialeurodes vaporariorum*-infested (greenhouse whitefly), and combined heat shock-treated and *T. vaporariorum*-infested (whiteflies + heat) plants during recovery. Asterisks refer to significant differences between control and specific treatments at each recovery time point ($p \leq .05$) (reproduced from **Paper III**).

4.8. Effects of *P. coronata* infection on volatile emissions in the two host species

In *A. sativa* (Papers IV-V), *P. coronata* infection enhanced the emissions of LOX compounds, MeJA, FAD compounds, terpenoids (mono- and sesquiterpenes), GGDP compounds, and benzenoids (Fig. 12 and Table 1 in Paper IV). The emissions of volatile reached the highest level during moderate infection (Fig. 12). Emissions of all the volatile classes scaled positively with the severity of infection from 0–40%, but decreased with increasing the severity of infection from 40–80% (Fig. 12 and Fig. 5A-F in Paper IV).

In *R. frangula* (Papers IV-V), volatile emissions were moderately impacted by *P. coronata* infection (Table 2 in Paper IV). The most evident responses were the enhancement of LOX emissions in mildly infected leaves and the enhancement of constitutive isoprene emissions (Fig. 12 and Table 2 in Paper IV). The volatile emissions responses were stronger in the primary host *A. sativa* than in the alternate host *R. frangula*, except isoprene emissions that were much higher in the constitutive emitter *R. frangula* (Fig. 12 and Table 1-2 in Paper IV).

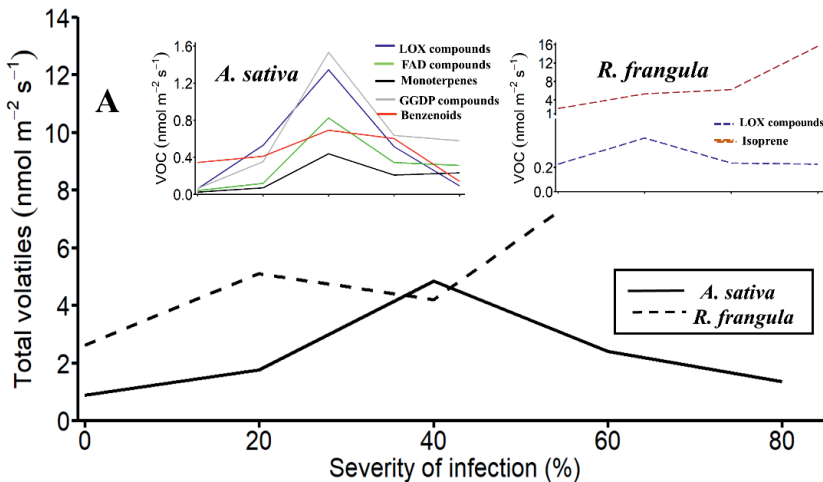


Fig. 12. Changes in total volatile emission in the primary host, the annual grass *Avena sativa*, and the alternate host, the shrub *R. frangula*, under different severity of the crown rust *Puccinia coronata* infection. The insets show the severity-dependent emissions of different volatile groups including short-chained lipoxygenase (LOX) pathway compounds, long-chained saturated fatty acid-derived (FAD) compounds, monoterpenes, geranylgeranyl diphosphate pathway (GGDP) compounds and benzenoids in the two host species (reproduced from Paper V).

5. DISCUSSIONS

5.1. Impacts of moderate heat stress on physiological responses: preparing plants for subsequent severe heat stress

In *Achillea millefolium* (**Paper I**), priming application somewhat enhanced A despite reductions in g_s (**Fig. 1A, B**), suggesting that priming stimulated photosynthetic electron flow and, and/or increased sink activity and/or increased the synthesis of rate-limiting enzymes of photosynthetic apparatus (Salvucci & Crafts-Brandner, 2004; Schrader *et al.*, 2004). In *O. vulgare* (**Paper II**), A was moderately reduced despite g_s being stable (**Fig. 2A, B**), and the reductions in A were associated with reductions in maximum Rubisco activity (**Fig. 2A, C**). This is consistent with the relatively low-temperature optimum of Rubisco activase as observed in several studies (Schrader *et al.*, 2004; Kurek *et al.*, 2007; Barta *et al.*, 2010). In *A. millefolium*, decreases in g_s reflect stomatal closure to minimize water loss due to high vapor pressure deficits (Grossiord *et al.*, 2020).

In priming-treated *A. millefolium*, the stability of A was likely fortified by emissions of isoprene (**Fig. 1A and 7B**). Several previous studies have elucidated that isoprene-emitting species have a greater thermal tolerance of photosynthetic capacity than non-emitter species (Sharkey, 2005; Monson *et al.*, 2021). The low-level elicitation of LOX volatiles in *A. millefolium* (**Fig. 7A**) reflects only minor cell membrane damage, and this is consistent with stable A (**Fig. 1A**). The delay in the enhancement of monoterpene emissions in priming-treated plants (**Fig. 7C and 9A**) reflects a delayed change of substrate availability or limited monoterpene synthase activity. Alternatively, it might be that the plants prioritized other chloroplastic metabolic pathways, e.g. synthesis of GGDP pathways volatiles over monoterpenes as observed in *O. vulgare* in **Paper II**. The emissions burst of monoterpenes observed at the later stages of priming recovery might indicate increased activity of rate-limiting enzymes or the availability of substrate for monoterpene synthesis. Altogether, the priming treatment exerted stronger stress on *O. vulgare* than on *A. millefolium*. In all cases, the responses of physiological processes observed suggest that the moderate heat stress treatment was sufficient to trigger priming defense responses.

5.2. Heat priming enhanced heat shock stress tolerance of photosynthesis

Reductions in photosynthesis upon heat shock treatment were smaller in primed plants reflecting enhanced heat resistance in the plants (**Fig. 1A and 2A**). As demonstrated in **Paper II**, reductions in maximum Rubisco activity were also relatively lower in primed plants. Priming increased the heat tolerance of Rubisco activity possibly by enhancing the expression of more heat stress-resistant Rubisco smaller subunit genes or the production of thermal-stable isoforms of Rubisco activase (Pastor *et al.*, 2013; Khan *et al.*, 2022; Cavanagh *et al.*, 2023). In addition, priming can increase thermal tolerance of photosynthesis by increasing the accumulation of protective chemicals including heat shock proteins, antioxidants, osmotica, and secondary metabolites that otherwise could be barely synthesized upon sudden exposure to severe heat stress (Teskey *et al.*, 2015; Abid *et al.*, 2016; Guihur *et al.*, 2022). Thus, the enhanced accumulation of condensed tannin and total phenolics observed in *A. millefolium* (**Fig. 10B, C**) might have played a role in protecting the photosynthetic apparatus by scavenging heat-stress-induced formation of reactive oxygen species (ROS).

In all the heat shock-stressed plants (**Papers I-II**), including non-primed *A. millefolium*, heat stress was not lethal, as *A* recovered upon cooling (**Fig. 1A, D, and 2A**). Heat shock might have resulted in irreversible damage to the photosynthetic apparatus or denaturation of Rubisco into non-soluble aggregates in the non-primed plants where *A* did not recover (**Fig. 1A**). In primed *O. vulgare*, there was no complete recovery of *A* to pre-stress levels, suggesting thermal acclimation responses that involved sustained phenotypic changes, e.g. channeling of resources from primary to secondary metabolism (Dumschott *et al.*, 2017).

5.3. Impacts of priming on volatile responses and implication on heat stress tolerance

Our study (**Papers I-II**) demonstrated that heat shock elicited volatile emissions differently in primed and non-primed plants. We observed higher LOX emissions in non-primed plants (**Fig. 8A and 9A**), suggesting severe cellular damage; greater damage can explain the greater decreases in *A*. The strong emissions of long-chained saturated fatty acid-derived (FAD) compounds (**Fig. 9B**) further indicate oxidative stress in non-

primed plants (Okereke *et al.*, 2021, 2022). In the case of primed plants, LOX emissions initially recovered, indicating a direct effect of heat shock on LOX substrate availability, but they rose at later recovery periods (**Fig. 8A** and **9A**), reflecting the activation of signaling pathways that lead to the synthesis of protective metabolites and lipids essential for membrane stability and thermal protection (Jiang *et al.*, 2017; Niu & Xiang, 2018; Guihur *et al.*, 2022). Indeed, in primed *O. vulgare* (**Paper II**), secondary emissions were observed for most volatiles indicating the activation of different defense pathways.

The decreases in isoprene emissions in heat shock-stressed primed *A. millefolium* (**Paper I**) reflect lower oxidative stress in comparison to non-primed plants; alternatively, it might reflect changes in the proportion of carbon allocation among terpenoid synthesis pathways, as the emissions of mono- and sesquiterpenes were strongly elicited (**Fig. 8B-D**). In **Paper II**, we observed that terpenoid emissions were elicited much earlier in non-primed *O. vulgare* (**Fig. 9C**), indicating a quick channeling of MEP/DOXP pathway metabolites from essential isoprenoid synthesis towards *de novo* volatile isoprenoid synthesis. Thus, this suggested strong oxidative stress that prompted rapid and high terpenoid synthesis for radical scavenging and enhancement of antioxidant status (González-Burgos & Gómez-Serranillos, 2012b).

In primed plants (**Papers I and II**), we observed relatively stronger emissions of benzenoids indicating that the enhanced stress tolerance in the plants was associated with the activities of shikimate/phenylpropanoid pathways (**Fig. 8E** and **9E**). At the end of the heat shock recovery period, primed plants (**Paper I**) accumulated higher amounts of phenolics and total condensed tannins (**Fig. 10A, B**), further indicating increases in activities of biosynthesis pathways of phenolic compounds (Suseela & Tharayil, 2018). Overall, our study (**Papers I-II**) showed that heat tolerance and acclimation in primed plants involve the adjustment of the relative activity of primary and secondary metabolic pathways.

5.4. Whitefly infestation enhanced heat stress tolerance

Our study showed that *A* recovered 24 h after the removal of insect infestation, and the recovery was supported by enhancement of g_s (**Fig. 3A, B** and **Fig. 1A, B** in **Paper III**). This suggested that this recovery

period time was sufficient to seal phloem wounds and start the repair of conductive networks. Whitefly feeding is specific to damaged/infested sites, thus overall stress-related responses including reductions in A and volatile emissions might be expected to be low (Appel & Cocroft, 2014; Darshanee *et al.*, 2017), as observed in this study (**Fig. 3A, B** and **Fig. 11A-F** in **Paper III**). Previous studies have demonstrated that *T. vaporariorum* infestation enhances volatile emissions differently in host species, for example, *T. vaporariorum* feeding enhanced emissions of LOX volatiles and monoterpenes in *Solanum melongena* (Darshanee *et al.*, 2017), but in *Melilotus albus*, the insect enhanced the emissions of monoterpenes and benzenoids (Liu *et al.*, 2022). In our study, *T. vaporariorum* infestation suppressed the emissions of LOX volatiles and enhanced monoterpene emissions (**Fig. 11A, C**), similar to *T. vaporariorum*-infested *Solanum lycopersicum* (Darshanee *et al.*, 2017).

Additionally, in *O. vulgare*, *T. vaporariorum* infestation suppressed the constitutive benzenoid emissions (**Fig. 11D** and **Fig. 4** in **Paper III**). It is unclear how emissions of LOX volatiles and benzenoids were suppressed in the infested plants (**Paper III**), but we suggest it might be a volatile-mediated mechanism to prevent volatile cues that can further attract whiteflies to the damaged leaves (Darshanee *et al.*, 2017). Low terpenoid emissions in the infested plants likely indicated low oxidative stress-associated demand for volatile isoprenoids (**Fig. 9C**) as well as the overall suppression of JA-dependent defenses by whitefly (Zarate *et al.*, 2007; Wang *et al.*, 2017). Nevertheless, despite low emission rates, terpenoid emissions possibly played a role in the repair of conductive networks by alleviating wounding-generated ROS as reflected in the negative correlation between A and monoterpenes (**Fig. 7C** in **Paper III**). Further investigations at gene expression level and hormonal signaling are required to elucidate how *T. vaporariorum* alters volatile emission profiles.

In all the heat-stressed plants (**Paper III**), A was reduced, whereas, g_s was increased (**Fig. 3A, B**), thus the reductions of A were due to non-stomatal factors. The greater decrease in A observed immediately after applying heat shock in pre-infested plants indicates the additive effect of the interaction of heat stress with the already-reduced A . In heat-stressed pre-infested plants, A recovered completely, suggesting that pre-infestation improved the recovery capacity (**Fig. 3A, B**), possibly through a certain convergence in stress response pathways (Kerchev

et al., 2011; Peschiutta *et al.*, 2018; Liu *et al.*, 2022). The recovery was also aided by increases in g_s that improved CO₂ availability for Rubisco and the elimination of non-stomatal limitations of photosynthesis. Through the experimental period, A in heat-stressed non-infested plants decreased progressively (**Paper III**), indicating chemical limitations of photosynthesis, however, the plants maintained a certain level of physiological activity, suggesting the applied stress was not lethal.

Persistent release of LOX compounds and FAD volatiles in non-infested plants (**Paper III**) reflects severe membrane-level damage and sustained oxidative stress and can explain the progressive decline of photosynthesis (**Fig. 9A, B**). In infested plants, emissions of LOX compounds and monoterpenes, including the characteristic stress marker monoterpene (*E*)- β -ocimene, were very low, implying a lower heat stress impact (**Fig. 9A, C**). The plastidial synthesis of both monoterpenes and benzenoids uses phosphoenolpyruvate as one of the substrates, thus giving rise to competition or cooperation at the substrate level between MEX/DOXP and shikimate pathways (Niinemets *et al.*, 2013). In our study (**Paper III**), we observed similarities in the emission kinetics of benzenoid and monoterpene emissions in non-infested heat-stressed plants (cf. **Fig. 9C, D**), suggesting coordination at substrate levels in the synthesis of different volatile classes. In infested heat-stressed plants, monoterpene emissions were less enhanced than benzenoid emissions (cf. **Fig. 9C, D**), indicating limiting enzyme activity-driven preferential activation of the shikimate pathway over the MEX/DOXP pathways (Niinemets, 2007; Niinemets *et al.*, 2010). At the end of heat stress recovery, we observed bursts in emissions of benzenoids in infested plants, indicating increases in the activity of the shikimate pathway and/or accumulation of substrates for benzenoid synthesis. Altogether, our gas exchange and volatile emissions data (**Paper III**) demonstrated that whitefly infestation improved heat stress resistance and acclimation.

5.5. The impact of *P. coronata* infection is more severe in the primary host than in the alternate host

Our results (**Papers IV-V**) showed that at the highest levels of infection, the total damaged area on leaf surfaces was quantitatively higher in the monocot primary host *Avena sativa* than in the alternate dicot host *R. frangula*, underscoring the greater infection vulnerability of the primary host. Fungal penetration of leaf surfaces is increased by

warmer temperatures and increased availability of light (Solanki *et al.*, 2019; Bebber, 2022). In dicots, the upper leaf surface is directly exposed to light, possibly explaining the higher damaged leaf area observed for upper leaf surfaces in *R. frangula* (**Papers IV-V**). In addition, aeciospores are formed on the lower leaf surface, and pycniospores on the upper leaf surface (Nazareno *et al.*, 2018), and it might be that at the given severity of infection, the developmental stage of aeciospores lags behind the development of pycniospores.

In infected *R. frangula* leaves, A decreased moderately with increasing infection severity, whereas in *A. sativa*, A was almost completely inhibited in severe stages of infection due to the spread of necrosis (**Fig. 5** and **Fig. 2A** in **Paper IV**). As demonstrated in previous studies, reductions of photosynthesis in fungal-infected leaves quantitatively describe the severity of the infection (Copolovici *et al.*, 2014; Jiang *et al.*, 2016). The strong variations in reductions of A in the host species emerged due to differences in physiological, structural, and chemical responses to the pathogen (**Papers IV** and **V**). In *A. sativa*, reductions in A were associated with stomatal limitations (**Fig. 5A-C** and **Fig. 2A-C** in **Paper IV**), consistent with previous studies, e.g. *Salix burjatica* \times *S. dasyclados* infected with *Melampsora epitea* (Toome *et al.*, 2010) and *Populus deltoides* infected with *Melampsora medusa* (Gortari *et al.*, 2018). The negative scaling of g_s with the severity of *P. coronata* infection is associated with the overall decline in physiological activities. Decreases in g_s in *A. sativa* were paralleled by increases in C_p , indicating that the reduction in photosynthetic capacity contributed to the decrease in A . Decreases in the content of nutrients limiting photosynthetic capacity (N and P; **Fig. 5B, C**) suggest that reductions in A were paralleled by the reductions in the content of rate-limiting enzymes, including Rubisco content in infected *A. sativa*.

Decreases in nutrient contents reflect fungal absorption of nutrients from the mesophyll cells of leaves or resorption of nutrients from damaged sites of leaves (Divon & Fluhr, 2007; Tavernier *et al.*, 2007). Reduction in photosynthesis is further escalated by loss of photosynthetic biomass reflected in the infection-severity dependent decreases in LMA (**Fig. 5A** and **Fig. 3** in **Paper IV**). In *R. frangula*, leaf nutrient content and LMA were not affected by *P. coronata* infection, suggesting that this species was less sensitive to the infection (**Papers IV** and **V**).

In the sensitive host *A. sativa*, emissions of stress volatiles including LOX compounds, FAD compounds, monoterpenes, benzenoids, and GGDP compounds increased with increasing the severity of infection from 0 to 40% (**Fig. 12** and **Fig. 5** in **Paper IV**). Scaling of volatile emissions with increasing severity of infections in primary hosts has been reported in other studies (e.g. Copolovici *et al.*, 2014; Jiang *et al.*, 2016). However, in *A. sativa*, emissions of stress volatiles reduced during the late stages of *P. coronata* infection, reflecting the shortage of substrate due to the decline in overall leaf physiological activity (**Papers IV** and **V**). Previously, such a decline in the stress volatile release has only been observed in leaves infected by necrotrophic fungi (Huang *et al.*, 2003; Hammond-Kosack & Rudd, 2008; Vandendriessche *et al.*, 2012).

In the alternate host *R. frangula*, LOX volatiles were enhanced to a much lower degree than in *A. sativa*, suggesting a much lower oxidative stress and damage in the alternate host (**Paper IV**). Analogous to primary isoprene-emitting hosts infected by *Melampsora* spp. (Toome *et al.*, 2010; Copolovici *et al.*, 2014; Jiang *et al.*, 2016), *P. coronata* elicited the emissions of mono- and sesquiterpenes and suppressed the emissions of isoprene (**Papers IV** and **V**). In *R. frangula*, we observed a low-level elicitation of volatiles, but surprisingly, emissions of isoprene were enhanced (**Fig. 1B**). This might indicate the upregulation of isoprene synthase activity or overall isoprenoid synthesis in the MEP pathway (Sharkey *et al.*, 2008; Rasulov *et al.*, 2014; Niinemets *et al.*, 2021). The stress threshold for the elicitation of mono- and sesquiterpenes was not exceeded in *R. frangula*, suggesting a lower sensitivity of this species to the pathogen stress. Overall, our study (**Papers IV-V**) showed that changes in photosynthetic traits and volatile emissions were stronger in the primary host than in the alternate host, collectively emphasizing variations in the stress sensitivity among the host species.

CONCLUSION

This thesis provides quantitative insight into how pre-exposure to biotic and abiotic stress factors alters subsequent stress responses of key plant physiological traits and induces priming and acclimation responses. Based on the results, it can be concluded that:

1. Heat-primed plants demonstrated higher heat shock tolerance of photosynthetic activities to heat shock, evident in smaller reductions in the rates of photosynthesis and faster recovery (**Papers I-II**). In primed *Origanum vulgare*, a certain decrease in photosynthetic activity remained, suggesting a sustained priming effect (**Papers II**). Heat shock stress resulted in the induction of emissions of stress volatile organic compounds (VOC) including lipoxygenase (LOX) pathway volatiles, long-chain saturated fatty acid-derived aldehydes, mono- and sesquiterpenes, geranylgeranyl diphosphate (GGDP) pathway compounds (carotenoid breakdown products) and benzenoids (**Papers I-III**). Emissions of LOX pathway volatiles were lower in primed plants, indicating lower oxidative stress. Upon heat shock, primed plants prioritized certain metabolic pathways (monoterpene versus LOX compound syntheses and benzenoids versus monoterpenes) or classes of metabolites (monoterpenes vs. isoprene). The rapid enhancement of benzenoid emissions in primed *O. vulgare* (**Paper I**) and the greater accumulation of total phenolic compounds in primed *A. millefolium* (**Paper II**) suggests the involvement of the shikimate/phenylpropanoid pathway in enhancing heat shock tolerance in primed plants. In comparison to non-primed *O. vulgare*, emissions of volatiles recovered earlier in primed *O. vulgare*, but rose again in subsequent phases of recovery, indicating sustained activation of biochemical defense pathways. Collectively (**Papers I-II**), these data suggest that moderate heat stress leads to a sustained physiological stress memory that improves plant resistance to subsequent severe heat stress episodes.
2. Greenhouse whitefly (*Trialeurodes vaporariorum*)-infestation altered plant photosynthetic and volatile emissions responses to severe transient heat stress (**Paper III**). Heat shock decreased the net assimilation rate (A) in both infested and non-infested plants, but infested plants fully recovered, indicating either a greater thermal

tolerance or a greater photosynthetic recovery capacity in the infested plants. Under heat stress, volatile emissions, particularly LOX, terpene, and benzenoid emissions were much lower in infested plants than in non-infested plants. Emissions of most VOC in non-infested heat-treated plants had not recovered to pre-stress level at the end of the 48 h stress recovery period. These results suggest that diffuse interactions with sap-sucking insects can decrease stress VOC emissions responses to heat stress and enhance the thermal acclimation of photosynthetic activities. The priming effect of biotic and abiotic stresses on thermal tolerance might reduce the devastating impacts of extreme climate events on agricultural and natural ecosystems.

3. Crown rust (*Puccinia coronata*) infection resulted in decreases in foliage photosynthesis with increasing the severity of infection in the primary host *Avena sativa* and the alternate host *Rhamnus frangula* (**Papers IV-V**). Decreases in photosynthesis were much greater in *A. sativa*, indicating a greater plant infection sensitivity. In *A. sativa*, but not in *R. frangula*, fungal infection led to reductions in nutrient contents and loss of photosynthetic biomass. In the sensitive host *A. sativa*, *P. coronata* infection induced strong emissions of stress VOC with increasing the severity of infection, but the emissions decreased at most severe infection, indicating an overall inhibition of leaf physiological activity. In *R. frangula*, the infection enhanced VOC emissions to a much smaller degree, but the emissions of constitutive isoprene were strongly enhanced. These results suggest that the infection elicited varying biochemical responses in the two hosts and highlight major differences in the fungal stress sensitivity of the different host species. We suggest that the severe stress responses in *A. sativa* were due to fungal interaction with warm weather that might have enhanced the fungal virulence.

REFERENCES

- Abid M, Tian Z, Ata-Ul-Karim ST, Liu Y, Cui Y, Zahoor R, Jiang D, Dai T. 2016.** Improved tolerance to post-anthesis drought stress by pre-drought priming at vegetative stages in drought-tolerant and -sensitive wheat cultivars. *Plant Physiology and Biochemistry* **106**: 218–227.
- Aldea M, Hamilton JG, Resti JP, Zangerl AR, Berenbaum MR, Frank TD, DeLucia EH. 2006.** Comparison of photosynthetic damage from arthropod herbivory and pathogen infection in understory hardwood saplings. *Oecologia*, **149**: 221–232.
- Appel HM, Cocroft RB. 2014.** Plants respond to leaf vibrations caused by insect herbivore chewing. *Oecologia* **175**: 1257–1266.
- Arimura G, Garms S, Maffei M, Bossi S, Schulze B, Leitner M, Mithöfer A, Boland W. 2008.** Herbivore-induced terpenoid emission in *Medicago truncatula*: concerted action of jasmonate, ethylene and calcium signaling. *Planta* **227**: 453–464.
- Arimura G, Huber DPW, Bohlmann J. 2004.** Forest tent caterpillars (*Malacosoma disstria*) induce local and systemic diurnal emissions of terpenoid volatiles in hybrid poplar (*Populus trichocarpa* × *deltoides*): cDNA cloning, functional characterization, and patterns of gene expression of (–)-germacrene D synthase, PtdTPS1. *The Plant Journal* **37**: 603–616.
- Arimura G-I, Ozawa R, Maffei ME. 2011.** Recent advances in plant early signaling in response to herbivory. *International Journal of Molecular Sciences* **12**: 3723–3739.
- Arneth A, Niinemets Ü. 2010.** Induced BVOCs: how to bug our models? *Trends in Plant Science* **15**: 118–125.
- Atkinson NJ, Jain R, Urwin PE. 2015.** The Response of plants to simultaneous biotic and abiotic stress. In: Mahalingam R, ed. combined stresses in plants: physiological, molecular, and biochemical aspects. Cham: *Springer International Publishing* 181–201.
- Atkinson NJ, Urwin PE. 2012.** The interaction of plant biotic and abiotic stresses: from genes to the field. *Journal of Experimental Botany* **63**: 3523–3543.

- Balmer A, Pastor V, Gamir J, Flors V, Mauch-Mani B. 2015.** The ‘prime-ome’: towards a holistic approach to priming. *Trends in Plant Science* **20**: 443–452.
- Baniwal SK, Bharti K, Chan KY, Fauth M, Ganguli A, Kotak S, Mishra SK, Nover L, Port M, Scharf K-D, et al. 2004.** Heat stress response in plants: a complex game with chaperones and more than twenty heat stress transcription factors. *Journal of Biosciences* **29**: 471–487.
- Barta C, Dunkle AM, Wachter RM, Salvucci ME. 2010.** Structural changes associated with the acute thermal instability of Rubisco activase. *Archives of Biochemistry and Biophysics* **499**: 17–25.
- Bate NJ, Rothstein SJ. 1998.** C6-volatiles derived from the lipoxygenase pathway induce a subset of defense-related genes. *The Plant Journal: For Cell and Molecular Biology* **16**: 561–569.
- Bebber DP. 2022.** Weather does influence fungal and oomycete crop disease outbreaks, but ProMED-mail reports don’t prove it. *New Phytologist* **234**: 1557–1558.
- Ben Rejeb I, Pastor V, Mauch-Mani B. 2014.** Plant responses to simultaneous biotic and abiotic stress: molecular mechanisms. *Plants* **3**: 458–475.
- Bilgin DD, Zavala JA, Zhu JI, Clough SJ, Ort DR, DeLUCIA EH, 2010.** Biotic stress globally downregulates photosynthesis genes. *Plant, cell & environment* **33**:1597-613.
- Birami B, Bamberger I, Ghirardo A, Grote R, Arneith A, Gaona-Colmán E, Nadal-Sala D, Ruehr NK. 2021.** Heatwave frequency and seedling death alter stress-specific emissions of volatile organic compounds in Aleppo pine. *Oecologia* **197**: 939–956.
- Blande JD, Holopainen JK, Niinemets U. 2014.** Plant volatiles in polluted atmospheres: stress responses and signal degradation. *Plant, Cell & Environment* **37**: 1892–1904.
- Brilli F, Ciccioli P, Frattoni M, Prestininzi M, Spanedda AF, Loreto F. 2009.** Constitutive and herbivore-induced monoterpenes emitted by *Populus × euroamericana* leaves are key volatiles that orient *Chrysomela populi* beetles. *Plant, Cell & Environment* **32**: 542–552.
- Bruinsma M, Posthumus MA, Mumm R, Mueller MJ, van Loon JJA, Dicke M. 2009.** Jasmonic acid-induced volatiles of *Brassica*

oleracea attract parasitoids: effects of time and dose, and comparison with induction by herbivores. *Journal of Experimental Botany* **60**: 2575–2587.

- Catola S, Centritto M, Cascone P, Ranieri A, Loreto F, Calamai L, Balestrini R, Guerrieri E. 2018.** Effects of single or combined water deficit and aphid attack on tomato volatile organic compound (VOC) emission and plant-plant communication. *Environmental and Experimental Botany* **153**: 54–62.
- Cavanagh AP, Slattery R, Kubien DS. 2023.** Temperature-induced changes in *Arabidopsis* Rubisco activity and isoform expression. *Journal of Experimental Botany* **74**: 651–663.
- Cellini A, Biondi E, Blasioli S, Rocchi L, Farneti B, Braschi I, Savioli S, Rodriguez-Estrada MT, Biasioli F, Spinelli F. 2016.** Early detection of bacterial diseases in apple plants by analysis of volatile organic compounds profiles and use of electronic nose. *Annals of applied biology* **168**: 409–20.
- Chatterjee P, Kanagendran A, Samaddar S, Pazouki L, Sa T-M, Niinemets Ü. 2020.** Influence of *Brevibacterium linens* RS16 on foliage photosynthetic and volatile emission characteristics upon heat stress in *Eucalyptus grandis*. *Science of The Total Environment* **700**: 134453.
- Coplovici L, Kännaste A, Pazouki L, Niinemets Ü. 2012.** Emissions of green leaf volatiles and terpenoids from *Solanum lycopersicum* are quantitatively related to the severity of cold and heat shock treatments. *Journal of Plant Physiology* **169**: 664–672.
- Coplovici L, Kännaste A, Rimmel T, Niinemets Ü. 2014.** Volatile organic compound emissions from *Alnus glutinosa* under interacting drought and herbivory stresses. *Environmental and Experimental Botany* **100**: 55–63.
- Coplovici L, Kännaste A, Rimmel T, Vislap V, Niinemets U. 2011.** Volatile emissions from *Alnus glutinosa* induced by herbivory are quantitatively related to the extent of damage. *Journal of Chemical Ecology* **37**: 18–28.
- Coplovici L, Niinemets Ü. 2010.** Flooding induced emissions of volatile signalling compounds in three tree species with differing waterlogging tolerance. *Plant, Cell & Environment* **33**: 1582–1594.

- Copolovici L, Väärtnõu F, Estrada MP, Niinemets Ü. 2014.** Oak powdery mildew (*Erysiphe alphitoides*) induced volatile emissions scale with the degree of infection in *Quercus robur*. *Tree Physiology* **34**: 1399.
- Cramer GR, Urano K, Delrot S, Pezzotti M, Shinozaki K. 2011.** Effects of abiotic stress on plants: a systems biology perspective. *BMC Plant Biology* **11**: 163.
- Dani KS, Jamie IM, Prentice IC, Atwell BJ. 2014.** Evolution of isoprene emission capacity in plants. *Trends in Plant Science* **19**: 439-46.
- Darshanee HLC, Ren H, Ahmed N, Zhang Z-F, Liu Y-H, Liu T-X. 2017.** Volatile-mediated attraction of greenhouse whitefly *Trialeurodes vaporariorum* to tomato and eggplant. *Frontiers in Plant Science* **8**: 1285.
- DeLucia EH, Nabity PD, Zavala JA, Berenbaum MR. 2012.** Climate change: resetting plant-insect interactions. *Plant physiology* **160**:1677-85.
- Demirevska-Kepova K, Holzer R, Simova-Stoilova L, Feller U. 2005.** Heat stress effects on ribulose-1,5-bisphosphate carboxylase/oxygenase, Rubisco binding protein and Rubisco activase in wheat leaves. *Biologia Plantarum* **49**: 521–525.
- Divon HH, Fluhr R. 2007.** Nutrition acquisition strategies during fungal infection of plants. *FEMS Microbiology Letters* **266**: 65–74.
- Dudareva N, Andersson S, Orlova I, Gatto N, Reichelt M, Rhodes D, Boland W, Gershenzon J. 2005.** The nonmevalonate pathway supports both monoterpene and sesquiterpene formation in snapdragon flowers. *Proceedings of the National Academy of Sciences of the United States of America* **102**: 933–938.
- Dumschott K, Richter A, Loescher W, Merchant A. 2017.** Post photosynthetic carbon partitioning to sugar alcohols and consequences for plant growth. *Phytochemistry* **144**: 243– 252.
- Faiola C, Taipale D. 2020.** Impact of insect herbivory on plant stress volatile emissions from trees: A synthesis of quantitative measurements and recommendations for future research. *Atmospheric Environment* **5**: 100060.
- Feng K, Wang X, Zhou Q, Dai T, Cao W, Jiang D, Cai J. 2022.** waterlogging priming enhances hypoxia stress tolerance of wheat offspring plants by regulating root phenotypic and physiological adaption. *Plants* **11**: 1969.

- Geron C, Harley P, Guenther A. 2001.** Isoprene emission capacity for US tree species. *Atmospheric Environment* **35**:3341-52.
- Golan K, Sempruch C, Górska-Drabik E, Czerniewicz P, Łagowska B, Kot I, Kmieć K, Magierowicz K, Leszczyński B. 2017.** Accumulation of amino acids and phenolic compounds in biochemical plant responses to feeding of two different herbivorous arthropod pests. *Arthropod-Plant Interactions* **11**: 675–682.
- González-Burgos E, Gómez-Serranillos MP. 2012a.** Terpene compounds in nature: a review of their potential antioxidant activity. *Current Medicinal Chemistry* **19**: 5319–5341.
- González-Burgos E, Gómez-Serranillos MP. 2012b.** Terpene compounds in nature: a review of their potential antioxidant activity. *Current Medicinal Chemistry* **19**: 5319–5341.
- Gortari F, Guiamet JJ, Graciano C. 2018.** Plant–pathogen interactions: leaf physiology alterations in poplars infected with rust (*Melampsora medusae*). *Tree Physiology* **38**: 925– 935.
- Grossiord C, Buckley TN, Cernusak LA, Novick KA, Poulter B, Siegwolf RTW, Sperry JS, McDowell NG. 2020.** Plant responses to rising vapor pressure deficit. *New Phytologist* **226**: 1550–1566.
- Guidolotti G, Pallozzi E, Gavrichkova O, Scartazza A, Mattioni M, Loreto F, Calfapietra C. 2019.** Emission of constitutive isoprene, induced monoterpenes, and other volatiles under high temperatures in *Eucalyptus camaldulensis*: A 13C labelling study. *Plant, cell & environment* **42**: 1929-38.
- Guihur A, Rebeaud ME, Goloubinoff P. 2022.** How do plants feel the heat and survive? *Trends in Biochemical Sciences* **47**: 824–838.
- Hammond-Kosack KE, Rudd JJ. 2008.** Plant resistance signalling hijacked by a necrotrophic fungal pathogen. *Plant Signaling & Behavior* **3**: 993–995.
- Hilker M, Schmülling T. 2019.** Stress priming, memory, and signalling in plants. *Plant, Cell & Environment* **42**: 753–761.
- Hoback WW, de Freitas BA, Martinez CA, Higley LG, Fernandes OA. 2015.** Photosynthetic responses of potato to Colorado potato beetle injury and differences in injury between adult males and females. *Entomologia Experimentalis et Applicata* **157**: 181–187.

- Holopainen JK, Gershenzon J. 2010.** Multiple stress factors and the emission of plant VOCs. *Trends in Plant Science* **15**: 176–184.
- Huang J, Cardoza YJ, Schmelz EA, Raina R, Engelberth J, Tumlinson JH. 2003.** Differential volatile emissions and salicylic acid levels from tobacco plants in response to different strains of *Pseudomonas syringae*. *Planta* **217**: 767–775.
- Jansen RMC, Miebach M, Kleist E, Henten EJV, Wildt J. 2009.** Release of lipoxygenase products and monoterpenes by tomato plants as an indicator of *Botrytis cinerea*-induced stress. *Plant Biology* **11**: 859–868.
- Jiang Y, Ye J, Li S, Niinemets Ü. 2017.** Methyl jasmonate-induced emission of biogenic volatiles is biphasic in cucumber: a high-resolution analysis of dose dependence. *Journal of Experimental Botany* **68**: 4679–4694.
- Jiang Y, Ye J, Veromann L-L, Niinemets Ü. 2016.** Scaling of photosynthesis and constitutive and induced volatile emissions with severity of leaf infection by rust fungus (*Melampsora larici-populina*) in *Populus balsamifera* var. *suaveolens*. *Tree Physiology* **36**: 856–872.
- Junker RR, Tholl D. 2013.** Volatile organic compound mediated interactions at the plant-microbe interface. *Journal of Chemical Ecology* **39**: 810–825.
- Kanagendran A, Pazouki L, Niinemets Ü. 2018.** Differential regulation of volatile emission from *Eucalyptus globulus* leaves upon single and combined ozone and wounding treatments through recovery and relationships with ozone uptake. *Environmental and Experimental Botany* **145**: 21–38.
- Kanagendran A, Pazouki L, Niinemets Ü. 2018.** Differential regulation of volatile emission from *Eucalyptus globulus* leaves upon single and combined ozone and wounding treatments through recovery and relationships with ozone uptake. *Environmental and Experimental Botany* **145**: 21–38.
- Kännaste A, Copolovici L, Niinemets Ü. 2014.** Gas chromatography-mass spectrometry method for determination of biogenic volatile organic compounds emitted by plants. *Methods in Molecular Biology (Clifton, N.J.)* **1153**: 161–169.
- Kask K, Kännaste A, Talts E, Copolovici L, Niinemets Ü. 2016.** How specialized volatiles respond to chronic, and short-term physiological

- and shock heat stress in *Brassica nigra*. *Plant, Cell & Environment* **39**: 2027–2042.
- Kazan K, Lyons R. 2014.** Intervention of phytohormone pathways by pathogen effectors. *The Plant Cell* **26**: 2285–2309.
- Kerchev PI, Fenton B, Foyer CH, Hancock RD. 2012.** Plant responses to insect herbivory: interactions between photosynthesis, reactive oxygen species and hormonal signalling pathways. *Plant, cell & environment* **35**: 441–53.
- Khan A, Khan V, Pandey K, Sopory SK, Sanan-Mishra N. 2022.** Thermo-priming mediated cellular networks for abiotic stress management in plants. *Frontiers in Plant Science* **13**: 866409.
- Kim JH, Castroverde CDM, Huang S, Li C, Hilleary R, Seroka A, Sohrabi R, Medina- Yerena D, Huot B, Wang J, et al. 2022.** Increasing the resilience of plant immunity to a warming climate. *Nature* **607**: 339–344.
- Kucharik CJ, Mork AC, Meehan TD, Serbin SP, Singh A, Townsend PA, Stack Whitney K, Gratton C. 2016.** Evidence for compensatory photosynthetic and yield response of soybeans to aphid herbivory. *Journal of Economic Entomology* **109**: 1177–1187.
- Kunkel BN, Brooks DM. 2002.** Cross talk between signaling pathways in pathogen defense. *Current Opinion in Plant Biology* **5**: 325–331.
- Kurek I, Chang TK, Bertain SM, Madrigal A, Liu L, Lassner MW, Zhu G. 2007.** Enhanced thermostability of arabidopsis rubisco activase improves photosynthesis and growth rates under moderate heat stress. *The Plant Cell* **19**: 3230–3241.
- Leuendorf JE, Frank M, Schmölling T. 2020.** Acclimation, priming and memory in the response of *Arabidopsis thaliana* seedlings to cold stress. *Scientific Reports* **10**: 689.
- Li N, Han X, Feng D, Yuan D, Huang L-J. 2019.** Signaling crosstalk between salicylic acid and ethylene/jasmonate in plant defense: do we understand what they are whispering? *International Journal of Molecular Sciences* **20**: E671.
- Liu B, Kaurilind E, Zhang L, Okereke CN, Rimmel T, Niinemets Ü. 2022.** Improved plant heat shock resistance is introduced differently by heat and insect infestation: the role of volatile emission traits. *Oecologia* **199**: 53–68.

- Liu B, Marques dos Santos B, Kanagendran A, Neilson EHJ, Niinemets Ü. 2019.** Ozone and wounding stresses differently alter the temporal variation in formylated phloroglucinols in *Eucalyptus globulus* leaves. *Metabolites* **9**: 46.
- Liu M, Hambleton S. 2013.** Laying the foundation for a taxonomic review of *Puccinia coronata* s.l. in a phylogenetic context. *Mycological Progress* **12**: 63–89.
- Lung I, Soran M-L, Opreș O, Trușcă MRC, Niinemets Ü, Copolovici L. 2016.** Induction of stress volatiles and changes in essential oil content and composition upon microwave exposure in the aromatic plant *Ocimum basilicum*. *Science of the Total Environment* **569–570**: 489–495.
- Martinez-Medina A, Flors V, Heil M, Mauch-Mani B, Pieterse CMJ, Pozo MJ, Ton J, van Dam NM, Conrath U. 2016.** Recognizing plant defense priming. *Trends in Plant Science* **21**: 818–822.
- Misztal PK, Hewitt CN, Wildt J, Blande JD, Eller ASD, Fares S, Gentner DR, Gilman JB, Graus M, Greenberg J, et al. 2015.** Atmospheric benzenoid emissions from plants rival those from fossil fuels. *Scientific Reports* **5**: 12064.
- Monson RK, Weraduwage SM, Rosenkranz M, Schnitzler J-P, Sharkey TD. 2021.** Leaf isoprene emission as a trait that mediates the growth-defense tradeoff in the face of climate stress. *Oecologia* **197**: 885–902.
- Moran PJ, Thompson GA. 2001.** Molecular responses to aphid feeding in arabidopsis in relation to plant defense pathways. *Plant Physiology* **125**: 1074–1085.
- Nabity PD, Zavala JA, DeLucia EH 2013.** Herbivore induction of jasmonic acid and chemical defences reduce photosynthesis in *Nicotiana attenuata*. *Journal of experimental botany*. **64**: 685-94.
- Nabity PD, Zavala JA, DeLucia EH. 2009.** Indirect suppression of photosynthesis on individual leaves by arthropod herbivory. *Annals of Botany* **103**: 655.
- Nazareno ES, Li F, Smith M, Park RF, Kianian SF, Figueroa M. 2018.** *Puccinia coronata* f. sp. *avenae*: a threat to global oat production. *Molecular Plant Pathology* **19**: 1047–1060.

- Ngumbi EN, Ugarte CM 2021.** Flooding and herbivory interact to alter volatile organic compound emissions in two maize hybrids. *J Chem Ecol* **47**: 707–718.
- Niinemets Ü, Arneth A, Kuhn U, Monson RK, Peñuelas J, Staudt M. 2010.** The emission factor of volatile isoprenoids: stress, acclimation, and developmental responses. *Biogeosciences* **7**: 2203–2223.
- Niinemets Ü, Kahru A, Mander Ü, Nõges P, Nõges T, Tuvikene A, Vasemägi A. 2017.** Interacting environmental and chemical stresses under global change in temperate aquatic ecosystems: stress responses, adaptation, and scaling. *Regional Environmental Change* **17**: 2061–2077.
- Niinemets Ü, Kännaste A, Copolovici L. 2013.** Quantitative patterns between plant volatile emissions induced by biotic stresses and the degree of damage. *Frontiers in Plant Science* **4**.
- Niinemets Ü, Kuhn U, Harley PC, Staudt M, Arneth A, Cescatti A, Ciccioli P, Copolovici L, Geron C, Guenther A, et al. 2011.** Estimations of isoprenoid emission capacity from enclosure studies: measurements, data processing, quality and standardized measurement protocols. *Biogeosciences* **8**: 2209–2246.
- Niinemets Ü, Rasulov B, Talts E. 2021.** CO₂-responsiveness of leaf isoprene emission: Why do species differ? *Plant, Cell & Environment* **44**: 3049–3063.
- Niinemets Ü. 2007.** Photosynthesis and resource distribution through plant canopies. *Plant, Cell & Environment* **30**: 1052–1071.
- Niinemets Ü. 2010.** Mild versus severe stress and BVOCs: thresholds, priming and consequences. *Trends in Plant Science* **15**: 145–153.
- Niinemets Ü. 2016.** Uncovering the hidden facets of drought stress: secondary metabolites make the difference. *Tree Physiology* **36**: 129–132.
- Niu Y, Xiang Y. 2018.** An overview of biomembrane functions in plant responses to high- temperature stress. *Frontiers in Plant Science* **9**.
- Okereke CN, Kaurilind E, Liu B, Kanagendran A, Pazouki L, Niinemets Ü. 2022.** Impact of heat stress of varying severity on papaya (*Carica papaya*) leaves: major changes in stress volatile signatures, but surprisingly small enhancements of total emissions. *Environmental and Experimental Botany* **195**: 104777.

- Okereke CN, Liu B, Kaurilind E, Niinemets Ü. 2021.** Heat stress resistance drives coordination of emissions of suites of volatiles after severe heat stress and during recovery in five tropical crops. *Environmental and Experimental Botany* **184**: 104375.
- Pastor V, Luna E, Mauch-Mani B, Ton J, Flors V. 2013.** Primed plants do not forget. *Environmental and experimental botany* **94**: 46-56.
- Pazouki L, Kanagendran A, Li S, Kännaste A, Memari HR, Bichele R, Niinemets Ü. 2016.** Mono- and sesquiterpene release from tomato (*Solanum lycopersicum*) leaves upon mild and severe heat stress and through recovery: from gene expression to emission responses. *Environmental and Experimental Botany* **132**: 1–15.
- Pazouki L, Niinemets Ü. 2016.** Multi-substrate terpene synthases: their occurrence and physiological significance. *Frontiers in Plant Science* **7**.
- Perdomo JA, Capó-Bauçà S, Carmo-Silva E, Galmés J. 2017.** Rubisco and rubisco activase play an important role in the biochemical limitations of photosynthesis in rice, wheat, and maize under high temperature and water deficit. *Frontiers in Plant Science* **8**.
- Pincebourde S, Ngao J. 2021.** The impact of phloem-feeding insects on leaf ecophysiology varies with leaf age. *Frontiers in Plant Science* **12**.
- Rasulov B, Bichele I, Laisk A, Niinemets Ü. 2014.** Competition between isoprene emission and pigment synthesis during leaf development in aspen. *Plant, Cell & Environment* **37**: 724– 741.
- Salerno G, Frati F, Marino G, Ederli L, Pasqualini S, Loreto F, Colazza S, Centritto M. 2017.** Effects of water stress on emission of volatile organic compounds by *Vicia faba*, and consequences for attraction of the egg parasitoid *Trissolcus basal*s. *Journal of Pest Science* **90**: 635–647.
- Sallaud C, Rontein D, Onillon S, Jabès F, Duffé P, Giacalone C, Thoraval S, Escoffier C, Herbette G, Leonhardt N, et al. 2009.** a novel pathway for sesquiterpene biosynthesis from z,z-farnesyl pyrophosphate in the wild tomato *Solanum habrochaites*. *The Plant Cell* **21**: 301–317.
- Salvucci ME, Crafts-Brandner SJ. 2004.** Inhibition of photosynthesis by heat stress: the activation state of Rubisco as a limiting factor in photosynthesis. *Physiologia Plantarum* **120**: 179–186.

- Salvucci ME, Crafts-Brandner SJ. 2004.** Mechanism for deactivation of Rubisco under moderate heat stress. *Physiologia Plantarum* **122**: 513–519.
- Sanyal RP, Misra HS, Saini A. 2018.** Heat-stress priming and alternative splicing-linked memory. *Journal of Experimental Botany* **69**: 2431–2434.
- Sardanyés J, Alcaide C, Gómez P, Elena SF. 2022.** Modelling temperature-dependent dynamics of single and mixed infections in a plant virus. *Applied Mathematical Modelling* **102**: 694–705.
- Scholes JD, Rolfe SA. 1996.** Photosynthesis in localised regions of oat leaves infected with crown rust (*Puccinia coronata*): quantitative imaging of chlorophyll fluorescence. *Planta* **199**: 573–582.
- Schrader SM, Wise RR, Wacholtz WF, Ort DR, Sharkey TD. 2004.** Thylakoid membrane responses to moderately high leaf temperature in Pima cotton. *Plant, Cell & Environment* **27**: 725–735.
- Sharkey TD, Wiberley AE, Donohue AR. 2008.** Isoprene emission from plants: why and how. *Annals of Botany* **101**: 5–18.
- Sharkey TD. 2005.** Effects of moderate heat stress on photosynthesis: importance of thylakoid reactions, rubisco deactivation, reactive oxygen species, and thermotolerance provided by isoprene. *Plant, Cell & Environment* **28**: 269–277.
- Sherin G, Aswathi KPR, Puthur JT. 2022.** Photosynthetic functions in plants subjected to stresses are positively influenced by priming. *Plant Stress* **4**: 100079.
- Solanki S, Ameen G, Borowicz P, Brueggeman RS. 2019.** Shedding light on penetration of cereal host stomata by wheat stem rust using improved methodology. *Scientific Reports* **9**: 7939.
- Song Y, Chen Q, Ci D, Shao X, Zhang D. 2014.** Effects of high temperature on photosynthesis and related gene expression in poplar. *BMC Plant Biology* **14**: 111.
- Staudt M, Lhoutellier L. 2007.** Volatile organic compound emission from holm oak infested by gypsy moth larvae: evidence for distinct responses in damaged and undamaged leaves. *Tree physiology* **1433**–1440.
- Suseela V, Tharayil N. 2018.** Decoupling the direct and indirect effects of climate on plant litter decomposition: Accounting for stress-

induced modifications in plant chemistry. *Global Change Biology* **24**: 1428–1451.

Suzuki N, Devireddy AR, Inupakutika MA, Baxter A, Miller G, Song L, Shulaev E, Azad RK, Shulaev V, Mittler R. 2015. Ultra-fast alterations in mRNA levels uncover multiple players in light stress acclimation in plants. *The Plant Journal* **84**: 760–772.

Tamaoki D, Seo S, Yamada S, Kano A, Miyamoto A, Shishido H, Miyoshi S, Taniguchi S, Akimitsu K, Gomi K. 2013. Jasmonic acid and salicylic acid activate a common defense system in rice. *Plant Signaling & Behavior* **8**: e24260.

Tavernier V, Cadiou S, Pageau K, Laugé R, Reisdorf-Cren M, Langin T, Masclaux- Daubresse C. 2007. The plant nitrogen mobilization promoted by *Colletotrichum lindemuthianum* in Phaseolus leaves depends on fungus pathogenicity. *Journal of Experimental Botany* **58**: 3351–3360.

Teskey R, Wertin T, Bauweraerts I, Ameye M, Mcguire MA, Steppe K. 2015. Responses of tree species to heat waves and extreme heat events. *Plant, Cell & Environment* **38**: 1699– 1712.

Toome M, Randjäv P, Copolovici L, Niinemets U, Heinsoo K, Luik A, Noe SM. 2010. Leaf rust induced volatile organic compounds signalling in willow during the infection. *Planta* **232**: 235–243.

Tsuda K, Sato M, Stoddard T, Glazebrook J, Katagiri F. 2009. Network properties of robust immunity in plants. *PLOS Genetics* **5**: e1000772.

Turan S, Kask K, Kanagendran A, Li S, Anni R, Talts E, Rasulov B, Kännaste A, Niinemets Ü. 2019. Lethal heat stress-dependent volatile emissions from tobacco leaves: what happens beyond the thermal edge? *Journal of Experimental Botany* **70**: 5017–5030.

Ullah C, Schmidt A, Reichelt M, Tsai C-J, Gershenson J. 2022. Lack of antagonism between salicylic acid and jasmonate signalling pathways in poplar. *New Phytologist* **235**: 701–717.

Vandendriessche T, Keulemans J, Geeraerd A, Nicolai BM, Hertog MLATM. 2012. Evaluation of fast volatile analysis for detection of *Botrytis cinerea* infections in strawberry. *Food Microbiology* **32**: 406–414.

- von Caemmerer S, Farquhar GD. 1981.** Some relationships between the biochemistry of photosynthesis and the gas exchange of leaves. *Planta* **153**: 376–387.
- Wang XW, Li P, Liu, SS, 2017.** Whitefly interactions with plants. *Current Opinion in Insect Science* **19**: 70-75.
- Wei J, van Loon JJA, Gols R, Menzel TR, Li N, Kang L, Dicke M. 2014.** Reciprocal crosstalk between jasmonate and salicylate defence-signalling pathways modulates plant volatile emission and herbivore host-selection behaviour. *Journal of Experimental Botany* **65**: 3289–3298.
- Wu J, Baldwin IT. 2010.** New insights into plant responses to the attack from insect herbivores. *Annual review of genetics* **44**:1-24.
- Wu Z, Han S, Zhou H, Tuang ZK, Wang Y, Jin Y, Shi H, Yang W. 2019.** Cold stress activates disease resistance in *Arabidopsis thaliana* through a salicylic acid dependent pathway. *Plant, Cell & Environment* **42**: 2645–2663.
- Xu B J, Chang S. 2007.** A comparative study on phenolic profiles and antioxidant activities of legumes as affected by extraction solvents. *Journal of Food Science* **72**: S159–S166.
- Yamada S, Kano A, Tamaoki D, Miyamoto A, Shishido H, Miyoshi S, Taniguchi S, Akimitsu K, Gomi K. 2012.** Involvement of OsJAZ8 in jasmonate-induced resistance to bacterial blight in rice. *Plant and Cell Physiology* **53**: 2060–2072.
- Zarate SI, Kempema LA, Walling LL, 2007.** Silverleaf whitefly induces salicylic acid defenses and suppresses effectual jasmonic acid defenses. *Plant Physiology* **143**: 866-875.

SUMMARY IN ESTONIAN

KOKKUVÕTE EESTI KEELES

Koosesinevate biootiliste ja abiootiliste stresside mõju taimedele: stressivastustest kohanemiseni

Sissejuhatus

Taimed puutuvad looduses kokku erinevate keskkonnamõjudega, sealhulgas mitut tüüpi abiootilise stressiga nagu kõrge ja madal temperatuur, põud ja õhusaaste, ning biootilise stressiga, mille on põhjustanud näiteks nakatumine haigustekitajatega või taimtoiduliste putukate rünnak. Taimed kogevad sageli mitut üksteisele järgnevat või samaaegset stressiolukorda. Kliimamuutused on suurendanud kombineeritud stressi, eriti kuumastressi ja biootilise stressi ilmumise sagedust. Nii kuumastress kui ka erinevatest teguritest tingitud biootiline stress põhjustavad füsioloogilisi, biokeemilisi ja molekulaarseid muutusi, mis mõjutavad negatiivselt taimede kasvu ja arenguprotsesse. Stress aktiveerib taimes kaitsereaktsioone: aktiveeruvad signaalsüsteemid, mis omakorda käivitavad biogeensete lenduvate orgaaniliste ühendite eraldumise ja mittelenduvate sekundaarsete metaboliitide kuhjumise.

Lenduvate orgaaniliste ühendite hulk ja kogus näitab taimede stressi ulatust ja iseloomu nii kvalitatiivselt kui kvantitatiivselt. Stress võib põhjustada õhulõhede juhtivuse ja Rubisco fotosünteesivõime langust, mis kokkuvõttes tingib taime fotosünteesi ja füsioloogilise aktiivsuse üldise vähenemise.

Ühe stressifaktori poolt aktiveeritud kaitsereaktsioonid võivad toimida vastandlikult või koostoimeliselt samal ajal toimiva teise stressifaktori suhtes, mille käigus muutuvad ka stressist tulenevad lenduvad ühendid. Eelnev kokkupuude kerge stressiga ehk primaarne, nagu taimtoiduliste putukate mõningane rünnak ja mõõdukalt soe temperatuur, võivad suurendada stressitaluvust järgnevate, tõsiste stressiolukordade suhtes. See toimub primaarse ajal raku molekulaarsete mehhanismide keeruka ümberprogrammeerimise kaudu. Omandatud taluvus algab stressi ettevalmistuse ja stressimälu/kohanemisreaktsiooniga, mis võivad pärast stressiepisoodi jääda taimes aktiivseks mitme kuu jooksul.

Seetõttu oletatakse, et võrreldes taimedega, kes ei ole läbinud ettevalmistust ehk eelnevat kerget kokkupuudet stressiga, kaotavad ettevalmistuse läbinud taimed tulevaste tõsiste stressiolukordade ajal oma fotosünteesivõimest vähem ja kaasnev lenduvate stressiühendite eraldumine on väiksem. Taimede füsioloogiliste ja metaboolsete reaktsioonide uurimine, mida käivitavad koosinevad stressid, on stressireaktsioonide ennustamisel muutuvast kliimas ülioluline ja võib anda kasulikku teavet samaaegselt mitme stressi suhtes vastupidavate põllukultuuride aretamiseks.

Uurimistöö eesmärgid ja hüpoteesid

Doktoritöö üldised eesmärgid olid:

1. a. Uurida erinevate taimeliikide fotosünteesi näitajate ja lenduvate orgaaniliste ühendite emissioonide muutusi mõõduka ja tugeva kuumastressi puhul stressist taastumise perioodil (**I–III artikkel**).
- b. Uurida mõõduka kuumastressiga kokkupuute (kuuma praiming) mõju tugeva kuumastressi läbinud taimede fotosünteesi ja lenduvate ühendite emissiooni taastumisele sõltuvalt ajast (**I, II artikkel**).
- Uurida eelneva kuumaga kokkupuute (kuuma praiming) mõju fenool- ja kondensparkaine üldsisaldusele kuumastressis taimedes (**I artikkel**).
2. a. Määrata eelnevalt taimtoidulise putuka, kasvuhoonekarilasega (*Trialeurodes vaporariorum*), kokkupuutest tekitatud šoki mõju ulatus järgneva kuumašokist põhjustatud fotosünteesi reaktsiooni ja lenduvühendite eritumisele ajast sõltuvalt (**III artikkel**).
- b. Uurida õhulõhede juhtivuse ja fotosünteesi biokeemilise suutlikkuse rolli kuumastressis taimede fotosünteesi muutumises ajast sõltuvalt (**I–III artikkel**).
3. a. Määrata kaera kroonrooste (*Puccinia coronata*) suhtes erineva tundlikkusega peremeesliikidel nakkuse raskusastmest sõltuv fotosünteesi vähenemine ja stressi iseloomustavate lenduvühendite eraldumise suurenemise ulatus (**IV, V artikkel**).

b. Uurida stressi käigus väheneva fotosünteesi mõju lenduvühendite eraldumisele (**IV, V artikkel**).

c. Hinnata õhulõhedega seotud piirangute ja lehtede biokeemilise fotosünteesi võimet määravate tegurite (fotosünteesiline biomass lehe pindalaühiku kohta ja peamise piirava elemendi sisaldus) panust nakkuse raskusastmest sõltuvasse fotosünteesi kiiruse vähenemisse (**IV, V artikkel**).

Hüpotees:

1. Hariliku raudrohu (*Achillea millefolium*) ja hariliku pune (*Origanum vulgare*) kuumašoki stress vähendab oluliselt fotosünteesi aktiivsust ja suurendab lenduvühendite eraldumist stressist taastumise perioodi jooksul (**I–III artikkel**).
2. Mõõdukas eelnev kokkupuude kuumaga (kuuma praiming) vähendab fotosünteesi aktiivsust ja muudab sekundaarsete metaboliitide sünteesi radasid, mis kajastub lenduvate LOX-ide ja terpenoidide suurenenud emissioonis, ning kuumaga praimitud taimede fotosünteesi aparaadil on suurem kuumašokitaluvus, sest fotosüntees väheneb väiksemal määral ja taastumine on kiirem ning antioksüdantsete lenduvühendite emissioon ja kaitsvate sekundaarsete metaboliitide kogunemine on suurem (**I, II artikkel**).
3. Nakatumine kasvuhoonekarilasega (*T. vaporariorum*) vähendab fotosünteesi kiirust ja toimib peamiselt salitsüülhappes (SA) sõltuvate radade kaudu, mille tulemuseks on bensenoidide ja vähesel määral lenduvate LOX-i ja monoterpeenide emissioon; kombineeritud herbivoori (*T. vaporariorum*) ja kuumašoki stress avaldab šokist taastumise ajal antagonistlikku mõju nii lenduvate orgaaniliste ühendite emissioonile kui ka gaasivahetuse iseloomule (**III artikkel**).
4. Nakatumine kroonroostega (*P. coronata*) vähendab fotosünteesi ja indutseerib stressi raskusastmest sõltuvalt lenduvühendite emissiooni. Seente mõju suureneb sooja ilmaga. Selle tulemuseks on kaitsevõime ammendumine ja lõpuks suurenev koekahjustus, mida on eriti näha kaera (*A. sativa*) kui tundliku peremeesorganismi puhul (**IV, V artikkel**).

5. Taime vastused nakatumisele kaera-kroonroostega on esimeses ja järgnevas peremeesorganismis erinevad (**IV, V artikkel**).

Peamised tulemused

Selles töös näitame, kuidas eelnev kokkupuude biotiliste ja abiotiliste stressiteguritega muudab järgnevaid taimede peamiste füsioloogiliste tunnuste stressireaktsioone ning kutsub esile praimimis- ja aklimatiseerumisreaktsioonid neljas mudelliigis. Tulemuste põhjal võib järeldada, et:

1. Eelnevalt kuumaga kokkupuutunud taimede fotosünteesi aktiivsus ei sõltunud kuumašokist samas ulatuses kui praimimata taimedel. Praimitud taimed talusid kuumastressi paremini. See ilmnis fotosünteesi kiiruse väiksemas vähenemises ja taimede kiiremas taastumises (**I, II artikkel**). Eelnevalt stressiga kokku puutunud harilikus punes (*Origanum vulgare*) jäi teatud fotosünteesi aktiivsuse langus alles, mis viitab praimimise püsivale toimele (**I artikkel**). Kuumastress põhjustas lenduvate orgaaniliste stressiühendite eraldumise, sealhulgas lipoksügenaasi (LOX) raja lenduvate ainete, pika ahelaga küllastunud rasvhapetest pärinevate aldehüüdide, mono- ja seskviterpeenide, geranüüldifosfaadi (GDP) raja ühendite (karotenoidide laguproduktid) ja bensenoidide eraldumise (**I-III artikkel**). LOX-i radade lenduvate ainete emissioon oli praimitud taimedes madalam, mis näitab madalamat oksüdatiivset stressi. Kuumašoki korral eelistasid praimitud taimed teatud metaboolseid teid (monoterpeen versus LOX-ühendi süntees ja bensenoidid vs monoterpeenid) või metaboliitide klasse (monoterpeenid vs isopreen) (**I, II artikkel**).

Bensenoidide emissiooni kiire suurenemine praimitud harilikus raudrohus (*A. millefolium*) (**I artikkel**) ja fenoolsete ühendite koguhulga suurem kogunemine praimitud harilikus raudrohus (**II artikkel**) viitab šikimaadi/fenüülpropanoidi raja osalemisele praimitud taimede kuumašokitaluvuse suurendamisel. Võrreldes praimimata hariliku punega ehk taimega, kellel puudus eelnev kokkupuude kerge stressiga, taastus lenduvate ainete eraldumine praimitud taimes varem, kuid see suurenes taas taastumise järgnevas faasis, mis näitab biokeemiliste kaitseteede püsivat aktiveerumist. Kokkuvõttes (**I, II artikkel**) näitavad need andmed,

et taime kokkupuude mõõduka kuumastressiga põhjustab püsivat füsioloogilist stressimälu, mis parandab taime vastupidavust järgnevatele tõsistele kuumastressi olukordadele.

2. Nakatumine kasvuhoonekarilasega (*Trialeurodes vaporariorum*) muutis taime fotosünteesi ja lenduvühendite emissiooni reaktsiooni vastuseks tõsisele mõõduvale kuumastressile (**III artikkel**). Kuumašokk vähendas netoassimilatsioonikiirust (A) nii nakatunud kui ka nakatumata taimedes, kuid nakatunud taimed taastusid peaaegu täielikult. See näitab kas suuremat termilist taluvust või suuremat fotosünteesi taastumisvõimet nakatunud taimedes. Kuumusestressi korral oli nakatunud taimedes lenduvühendite emissioon, eriti LOX-i, terpeeni ja bensenoidi eraldumine palju väiksem kui nakatumata taimedes. Enamiku lenduvate orgaaniliste ühendite emissioon nakatumata kuumaga praimitud taimedes ei olnud 48-tunnise stressist taastumise aja lõpuks saavutanud stressieelset taset. Need tulemused viitavad sellele, et hajus vastastikkune mõju taimetoidulistest putukatest põhjustatud stressi ja kuumastressi vahel võib vähendada lenduvate orgaaniliste stressiühendite emissiooni vastuseks kuumastressile ja suurendada fotosünteesi kohanemist kuumaga. Taimede eelnev kokkupuude biotilise ja abiootilise stressiolukordadega võib avaldada soodsat mõju taime termilisele taluvusele ja seeläbi vähendada äärmuslike kliimasündmuste laastavat mõju põllumajanduskultuuridele ja looduslikele ökosüsteemidele.
3. Kaera kroonrooste (*Puccinia coronata*) nakkus põhjustas lehestiku fotosünteesi vähenemise, suurendades infektsiooni raskust peremeestaimel, harilikul kaeral (*Avena sativa*) ja ka vaheperemehel, harilikul paakspuul (*Rhamnus frangula*) (**IV,V artikkel**). Kaera fotosünteesivõime vähenes suuremal määral, mis viitab nende taime suuremale nakkustundlikkusele. Kaeral põhjustas seeninfektsioon toitainete sisalduse vähenemise ja fotosünteesilise biomassi kadumise, kuid selline negatiivne mõju puudus paakspuul. Tundlikul peremeestaimel (*A. sativa*) kutsus kroonrooste esile suure lenduvate orgaaniliste stressiühendite eraldumise, mis suurenes koos nakkuse raskusastmega. Emissioon vähenes kõige raskema infektsiooni korral, mis viitab lehtede füsioloogilise aktiivsuse üldisele pärssimisele.

Võrreldes kaeraga suurenes roostenakkuse tõttu lenduvate orgaaniliste ühendite emissioon harilikul paakspuul palju väiksemas ulatuses, kuid oluliselt suurenes konstitutiivse isopreeni emissioon. Need tulemused viitavad sellele, et nakkus kutsus kahes peremeesorganismis esile erinevad biokeemilised vastused. Tulemused näitavad suuri erinevusi vaheperemees- ja peremeestaime liikide vastuses roosteseenega nakatumisele. Tulemuste põhjal saab järeldada, et kaera taimede tugevamad stressireaktsioonid olid tingitud seente koostoimest sooja ilmaga, mis võis omakorda suurendada seente virulentsust.

Uuringu tulemused näitavad, et kvantitatiivsed andmed taimedest lenduvate orgaaniliste ühendite eraldumise kohta keeruliste koosinevate stressijuhtude korral annavad hea ülevaate taimede füsioloogilise käitumise ennustamiseks kliimamuutuste tingimustes ja aitavad aretada parema stressitaluvusega põllukultuure.

ACKNOWLEDGEMENT

I am extremely grateful to my supervisor Professor Dr. Ülo Niinemets, a super mentor and an extraordinary scientist, for his immense support, insightful guidance, motivation, and contribution throughout my doctoral journey. No metric can express or gauge his contribution to my scientific knowledge and academic career development. Extreme gratitude to Dr. Eve Kaurilind and Dr. Bin Liu for their guidance and continuous support. A special gratitude to Professor Dr. Eve Runno-Paurson for her continuous support and encouragement. My gratitude also goes to Tiia Kurvit for her academic and administrative support. I can't forget to thank you, Tiia, for the Estonian translation of the summary of this thesis, and Vivian Kuusk, for editing the translated summary. I owe Dr. Vinícius de Souza a debt of gratitude for reviewing my thesis and providing powerful suggestions. I appreciate **all my current and former co-workers** at the Institute of Agricultural and Environmental Sciences, big names like Dr. Arooran Kanagendran, Dr. Kaia Kask, Dr. Chikodinaka Okereke, Dr. Keyvan Selastani, Evi Vaino, Yusuph Abiola, and **any other person**, experimental plant or insect that have contributed in one way or other to the success of my doctoral journey. This study was funded by the Centre of Excellence in Environmental Adaptation (F11100PKTF), Ecology of Global Change: natural and managed ecosystems (8F160018PKTF (TK131), Ecology of Global Change: natural and managed ecosystems Analysis and Experimentation on Ecosystems (F200127PKTF (11.74/1076). My doctoral allowance was provided by the DoRa Plus Scholarship, funded by the EU Regional Development Fund through the Archimedes Foundation.

Liu B, Zhang L, Rusalepp L, Kaurilind E, **Sulaiman HY**, Püssa T, Niinemets Ü. 2021. Heat priming improved heat tolerance of photosynthesis, enhanced terpenoid and benzenoid emission and phenolics accumulation in *Achillea millefolium*. *Plant, Cell & Environment*, 44: 2365-2385.

Heat priming improved heat tolerance of photosynthesis, enhanced terpenoid and benzenoid emission and phenolics accumulation in *Achillea millefolium*

Bin Liu¹ | Lu Zhang² | Linda Rusalepp³ | Eve Kaurilind¹ | Hassan Yusuf Sulaiman¹ | Tõnu Püssa³ | Ülo Niinemets^{1,4,5}

¹Chair of Crop Science and Plant Biology, Estonian University of Life Sciences, Tartu, Estonia

²College of Horticulture and Landscape Architecture, Northeast Agricultural University, Harbin, China

³Chair of Food Hygiene and Veterinary Public Health, Estonian University of Life Sciences, Tartu, Estonia

⁴Estonian Academy of Sciences, Tallinn, Estonia

⁵School of Forestry and Bio-Technology, Zhejiang Agriculture and Forestry University, Hangzhou, China

Correspondence

Bin Liu, Chair of Crop Science and Plant Biology, Estonian University of Life Sciences, Kreutzwaldi 5, 51006 Tartu, Estonia.
Email: bin.liu@emu.ee

Funding information

Archimedes Foundation; Estonian University of Life Sciences, Grant/Award Number: P190252PKTT; European Regional Development Fund; Centre of Excellence EcolChange; European Research Council, Grant/Award Numbers: 322603, SIP-VOL+; National Natural Science Foundation of China, Grant/Award Number: 31711530648; Northeast Agricultural University, Grant/Award Number: 18XG07; Estonian Research Council, Grant/Award Number: PRG947

Abstract

The mechanism of heat priming, triggering alteration of secondary metabolite pathway fluxes and pools to enhance heat tolerance is not well understood. *Achillea millefolium* is an important medicinal herbal plant, rich in terpenoids and phenolics. In this study, the potential of heat priming treatment (35°C for 1 hr) to enhance tolerance of *Achillea* plants upon subsequent heat shock (45°C for 5 min) stress was investigated through recovery (0.5–72 hr). The priming treatment itself had minor impacts on photosynthesis, led to moderate increases in the emission of lipoxygenase (LOX) pathway volatiles and isoprene, and to major elicitation of monoterpene and benzaldehyde emissions in late stages of recovery. Upon subsequent heat shock, in primed plants, the rise in LOX and reduction in photosynthetic rate (A) was much less, stomatal conductance (g_s) was initially enhanced, terpene emissions were greater and recovery of A occurred faster, indicating enhanced heat tolerance. Additionally, primed plants accumulated higher contents of total phenolics and condensed tannins at the end of the recovery. These results collectively indicate that heat priming improved photosynthesis upon subsequent heat shock by enhancing g_s and synthesis of volatile and non-volatile secondary compounds with antioxidative characteristics, thereby maintaining the integrity of leaf membranes under stress.

KEYWORDS

heat shock, secondary metabolites, volatile organic compounds

1 | INTRODUCTION

Supra-optimal temperatures exceeding the optimal environmental temperature for plant growth and development constitute a particularly significant environmental hazard for sessile organisms such as plants. As global warming proceeds, extreme atmospheric heat events are expected to occur more frequently (IPCC, 2018), and thus, heat stress is becoming one of the most frequent abiotic stresses confronted by plants in nature (Perkins, Alexander, & Nairn, 2012). The effects of heat stress on plants will depend on

the severity of the stress (Niinemets, 2018; Pazouki et al., 2016; Zhu et al., 2018). Even short-term sudden exposure to a temperature strongly exceeding the optimal range such that can occur during lightflecks in natural environments (Hüve et al., 2019; Singaas et al., 1999) will immediately result in suppressed foliage photosynthesis, formation of reactive oxygen species (ROS), elicitation of lipoxygenase pathway (LOX) volatile emissions, and it might eventually trigger programmed cell death-like processes in stressed plant tissues (Bita & Gerats, 2013; Hüve et al., 2019; Vacca et al., 2004).

In the case of moderate heat stress, when plant temperatures exceed the optimum temperature by 5–10°C, the resulting damage is absent or when present, it is usually reversible upon return to lower temperatures (Luo et al., 2011; Pazouki et al., 2016). Plant responses to a moderate heat stress include immediate stress reactions such as changing the leaf orientation and enhancing transpiration to cool down the leaf (Hasanuzzaman, Nahar, Alam, Roychowdhury, & Fujita, 2013). The effects of heat stress are also reflected in changes in different secondary metabolite levels including direct changes in emission rate of constitutively emitted volatile organic compounds (VOCs), but also after-stress effects including synthesis of phenolic compounds, induction of stress-induced volatiles and modifications in antioxidative capacity of plants (Kask, Kännaste, Talts, Copolovici, & Niinemets, 2016; Panchuk, Volkov, & Schöffl, 2002; Rivero et al., 2001). The adaptive traits activated by plants when exposed to a certain moderate stress stimulus are referred to as defence priming, and serve to enhance plant tolerance to subsequent severe stress (Martinez-Medina et al., 2016). Contrary to heat shock stress that can be lethal, defence priming activates a low-cost adaptive and defensive response at the same time without threatening the normal survival of the plant (Martinez-Medina et al., 2016). Priming triggers synthesis and accumulation of a wide range of secondary metabolites, mainly plant defensive compounds, which include volatile compounds such as volatile isoprenoids as well as non-volatile compounds such as salicylic acid (Conrath et al., 2006; Frost, Mescher, Carlson, & De Moraes, 2008; Niinemets, 2010). The physiological adjustments and the stored secondary metabolites form the “stress memory” that stimulates quicker responses to subsequent exposures to severe stresses (Martinez-Medina et al., 2016; Niinemets, 2010).

Secondary metabolites including terpenoids and phenolics have been demonstrated to play an important role in facilitating plant resistance and acclimation to extreme heat stresses by potentially directly improving heat tolerance or serving as antioxidants reducing the extent of lesion development after heat stress (Holopainen & Gershenzon, 2010; Loreto & Schnitzler, 2010; Possell & Loreto, 2013). Heat stress-dependent damage can lead to immediate emissions of LOX and terpenoids that are either stored or de novo synthesized (Kask et al., 2016; Pazouki et al., 2016; Turan et al., 2019) and a longer-term accumulation of phenolics continuing for hours to days after stress exposure (Sgarbi, Fornasiero, Lins, & Bonatti, 2003; Yoshikawa et al., 2018). Such response patterns involving progressive syntheses of terpenoids and phenolics provides an efficient means to cope with enhanced plant oxidative status in stressed plants (Liu, Marques dos Santos, Kanagendran, Neilson, & Niinemets, 2019). To the best of our knowledge, there is very limited information of whether the heat priming can enhance the synthesis potential of key secondary metabolites such as terpenoids and phenolics in primed plants, and how priming alters the synthesis of these metabolites upon exposure to a subsequent severe stress.

It is well established that 2-C-methyl-D-erythritol-4-phosphate/1-deoxy-D-xylulose-5-phosphate (MEP/DOXP) and mevalonate (MVA) pathways are the two pathways responsible for terpenoid synthesis in plants, while shikimate and phenylpropanoid pathways are the core

pathways for the biosynthesis of the various phenolic compounds (Hermann & Weaver, 1999; Niinemets, Kännaste, & Copolovici, 2013; Vogt, 2010). These pathways are altered during the priming phase to produce defensive metabolites and increase resistance to eventual heat shock (Serrano, Ling, Bahieldin, & Mahfouz, 2019). Although MEP/DOXP pathway and shikimate pathways synthesize different biochemical metabolites, the two pathways are both located in plastids and use the same photosynthetic intermediates. This can result in a competition between terpenoid and phenolic synthesis pathways, especially when both are needed in large quantities and carbon input is limited due to stress. Such a possible competition complicates prediction of changes in metabolite profiles upon heat priming and heat shock stress.

The plant response and adaptation mechanisms under severe environmental stresses associated with priming treatment have extensively been investigated for biotic stresses, for example, using pathogens and herbivores as priming stimuli (Dicke & Baldwin, 2010; Frost et al., 2008; Pastor et al., 2013). In the case of abiotic stresses, there is evidence of positive effects of early heat priming on subsequent abiotic stress tolerance (such as heat and drought) (Havaux, 1993; Wang et al., 2011, 2014; Wang et al., 2012). Most of these previous investigations were either excessively concentrated on biotic stimuli such as pathogens, microbes and natural/synthetic chemicals, or focused on crops such as wheat or potato (Havaux, 1993; Mauch-Mani, Baccelli, Luna, & Flors, 2017; Wang et al., 2014). In the context of global warming, a stronger emphasis on priming by abiotic stresses in different species, in particular, by heat priming is needed to generalize from case studies to responses of ecosystems to heat waves (Fan et al., 2018; Wang, Heckathorn, Mainali, & Tripathee, 2016; Wang, Liu, & Jiang, 2017).

Achillea millefolium L. is a perennial herb that has been used as an important medicinal plant since the antiquity (Saeidnia, Gohari, Mokhter-Dezfuli, & Kiuchi, 2011). Due to a high constitutive defence capacity, the foliage of *A. millefolium* grown under ambient non-stressed conditions contains a large number of secondary metabolites, in particular, volatile and non-volatile terpenoids including monoterpenes, sesquiterpenes and their derivatives, and various phenolics such as chlorogenic acids and flavonoids having antioxidative, antimicrobial and anti-feedant activities (Pazouki, Memari, Kännaste, Bichele, & Niinemets, 2015; Vitalini et al., 2011). Thus, *A. millefolium* is an ideal species to investigate simultaneous modifications in rate of synthesis and compound profiles of both terpenoids and phenolics under stresses. The main aim of this study was to investigate whether heat priming treatment enhances tolerance to subsequent heat shock stress in the foliage of *A. millefolium* and understand how priming alters secondary metabolite profiles without and with subsequent severe heat stress. We examined how priming treatment impacted the emission of VOCs, particularly those synthesized in MEP/DOXP and LOX pathways, and also by comparing the accumulation of phenolics as induced by heat shock in primed and non-primed *A. millefolium* plants. We hypothesized that under heat shock stress: (a) heat-primed *A. millefolium* leaves emit more VOCs, particularly terpenoids; (b) primed *A. millefolium* leaves accumulate more phenolics than non-primed plants and (c) primed *A. millefolium* leaves have higher heat resistance of photosynthetic apparatus such that the

photosynthetic rate is reduced to a lower degree and recovers faster upon exposure to severe heat stress.

2 | MATERIALS AND METHODS

2.1 | Plant materials

The plants of *A. millefolium* were grown from seed purchased from Nordic Botanical Ltd. (Tartu, Estonia). The seeds were sown in 2 L plastic pots filled with an 1:1:1 mixture of commercial garden soil with added fertilizers (N:P:K = 10:8:16, Kekkilä Group, Vantaa, Finland), sand (AS Siilikaat, Tallinn, Estonia) and vermiculite (Schetelig Group, Vantaa, Finland). The plants were grown in a plant growth chamber (FITOCLIMA S600PLLH, Aralab, Lisbon, Portugal) at day/night temperatures of 25/20°C under 16 hr light period with relative humidity of 60% and light intensity of 600 $\mu\text{mol m}^{-2} \text{s}^{-1}$ at the plant level. The plants were watered every other day to soil field capacity. At the time of the experiments, the plants were 3 months old.

2.2 | Priming treatment

To apply the priming treatment, seven plants were carefully moved to another identical growth chamber where the same growth conditions were maintained except that the temperature was raised to 35°C for 1 hr under light. The temperature of the growth chamber was changed to 25°C immediately after the priming treatment and the plants were allowed to recover for 72 hr. Gas exchange data and VOC samples were collected at 0.5, 5, 10, 24, 48 and 72 hr after the priming treatment.

2.3 | Heat shock treatment

The heat shock treatment started in the morning after the plants had been exposed to light for 1 hr. The heat shock treatment protocol followed that in Copolovici, Kännaste, Pazouki, and Niinemets (2012) with some modifications detailed here. A circulating water bath (VWR, Westchester, NY) was filled with distilled water and the temperature was set to 45°C. To prevent any possible effects caused by direct plant contact with the hot water or by blotting the leaves dry after the treatment, the plant uppermost part was carefully enclosed in a chemically inert polyester bag before immersion in the heated water. Separate tests where the temperature was measured by an infrared thermometer demonstrated that the temperature in the bag reached the water temperature in about 30 s. Application of heat resistant polyester bags ("cooking bags") has been advocated by previous studies as these bags are heat stable and have minimum emission and storage of volatile organics (Niinemets et al., 2011; Stewart-Jones & Poppy, 2006). The immersed plant was carefully removed from the warm water after 5 min, removed from the plastic bag and immediately transferred to the measurement chamber system

(described below) for collection of VOCs and gas exchange measurements at 0.5, 5, 10, 24, 48 and 72 hr.

A total of six plants were used for the heat shock experiment, three primed and three non-primed plants. To test, whether the response of primed plants to heat shock was due to the heat shock or priming treatment itself, the other four primed plants not subjected to heat shock treatment were measured in parallel with the heat shocked plants. Additionally, six non-heat-shock-treated plants (without priming and treated by immersion in 25°C water) were used as controls and measured analogously as the other plants. After 72 hr, the leaves from four treatments, that is, control, non-primed + heat shock, primed + heat shock and primed without heat shock were harvested, weighed and scanned for leaf area measurement. A part of collected foliage was immediately weighed, dried at 70°C in a drying-oven for 48 hr and leaf dry to fresh mass ratio was estimated. Another fresh leaf sample was immediately frozen in liquid nitrogen and stored at -80°C for further analysis.

2.4 | Gas exchange measurements

A custom-made eight-chamber open gas exchange system (Copolovici, Kännaste, Rimmel, & Niinemets, 2014) was used to measure plant photosynthesis and collect VOC samples (for design principle, see Copolovici and Niinemets (2010)). The system was equipped with eight 2 L glass chambers whose stainless steel bottoms were fixed on a wooden platform. A narrow slot was made through the cap and wooden platform so the plants could be installed and air-tightly sealed in the individual glass chambers. The ambient air was pumped through a 10 L buffer volume and an HCl-activated copper tubing to scrub ozone and humidified to about 60% before passing into the glass chambers. The flow rate through each chamber was maintained at 0.036 L s^{-1} . In the chambers, the CO_2 concentration was between 380 and 400 $\mu\text{mol mol}^{-1}$ and the air temperature was kept at 23°C (room temperature). The light intensity at the leaf surface was 600 $\mu\text{mol m}^{-2} \text{s}^{-1}$ provided by a Heliospectra LX60 LED plant growth lamp (Heliospectra AB, Göteborg, Sweden). A LI-7000 $\text{CO}_2/\text{H}_2\text{O}$ analyser (LI-COR Biosciences, Lincoln, NE) was used to measure CO_2 and H_2O concentrations at the in- and outlets of each individual chamber in sequence. Values of net assimilation rate (A) and stomatal conductance (g_s) were recorded after the gas flows stabilized and leaf gas exchange rate reached a steady state, which typically took 10–20 min after plant enclosure.

2.5 | VOC collection and analysis by GC-MS

The VOC samples were collected simultaneously with the gas exchange measurements as described by Liu, Kaurilind, Jiang, and Niinemets (2018). An air sample pump (210-1003MTX, SKC Inc., Houston, TX) was used to collect the volatiles at a constant flow rate of 0.2 L min^{-1} for 25 min. The volatiles were collected onto stainless steel cartridges filled with three different carbon-based adsorbents (Carbotrap, Supelco, Bellefonte, PA) to trap all VOCs between C3-C17

(Kännaste, Copolovici, & Niinemets, 2014). The volatile samples in the cartridges were desorbed by a Shimadzu TD20 automated cartridge desorber and analysed with a Shimadzu 2010 Plus gas chromatography–mass spectrometer (GC–MS; Shimadzu, Kyoto, Japan) with a Zebron ZB-624 fused silica capillary column (0.32 mm i.d., 60 m length, 1.8 μ m film thickness, Phenomenex, Torrance, CA). Individual VOCs were identified using authentic standards (Sigma-Aldrich, St. Louis, MO) and by comparison of mass spectra in the National Institute of Standards of Technology library (NIST 05). The GC–MS system was calibrated by authentic standards (Kännaste et al., 2014). Background VOC concentrations (blanks) from empty chambers were subtracted from measurements with leaf samples.

2.6 | HPLC-Q-TOF-MS/MS analysis of individual phenolic compounds

The extraction, detection and quantification of individual phenolic compounds were performed according to Raal, Boikova, and Püssa (2015). In brief, 100 mg frozen and homogenized leaf material was extracted with 1.5 mL 60% (vol/vol) aqueous ethanol solution. The mixture was shortly vortexed and extracted in an ultrasonic bath for 15 min. After repeating the last step twice, the extraction was continued in a tube rotator (Multi RS-60, BIOSAN, Riga, Latvia) at room temperature for 2 hr. Afterwards, the mixtures were centrifuged at 10,000g for 10 min with an Eppendorf MiniSpin (Eppendorf AG, Hamburg, Germany) at room temperature. The obtained supernatants were transferred to glass vials and LC analysis was conducted with a 1290 Infinity LC (Agilent Technologies) using a Zorbax 300SB-C18 column (2.1 \times 150 mm; 5 μ m film thickness; Agilent Technologies) kept at 40°C. For the elution of the samples, a gradient of 0.1% formic acid in water (A) and acetonitrile (B) was used as follows: 0.0 min 1% B, 45.0 min 40% B, 47.0 min 99% B, 57.0 min 99% B, 57.1 min 1% B, regeneration time 8 min. The eluent flow rate was set to 0.3 mL min⁻¹. The compounds were detected by a mass-spectrometer (6540 UHD Accurate-Mass Q-ToF LC/MS, Agilent Technologies) working in negative ionization mode in the mass to charge ratio (*m/z*) range of 100–1,000 amu. Data acquisition and initial data processing were carried out by MassHunter software (Version B.08.00, Agilent Technologies).

The phenolic compounds detected in the extracts of *A. millefolium* leaves including caffeoylquinic acids (CQAs), dicaffeoylquinic acids (diCQAs), luteolin and apigenin derivatives were identified and quantified using five-point calibration curves ($r^2 > .99$) with chlorogenic acid, luteolin and apigenin (Sigma Aldrich, Darmstadt, Germany), respectively. MS extracted ion chromatograms for specific [M–H][–] ions were used to locate and quantify compounds.

2.7 | Estimation of total contents of phenolics, flavonoids and condensed tannins

For extraction of total phenolics, flavonoids and condensed tannins, 1 mL 50% (vol/vol) aqueous acetone was added to 50 mg

frozen, homogenized leaf powder on ice and vortexed. After incubating the extraction mixture at room temperature with shaking for 15 min, the mixture was vortexed again and centrifuged at 10,000g for 5 min with a vortex mixer (Vortex Genie-2, Scientific Industries, Bohemia, NY). The supernatant was transferred to new tubes, 1 mL 50% acetone was added to the pellet and the extraction procedure was repeated twice. The supernatants of the three extractions were combined and stored on ice in darkness for further analyses.

Total phenolic contents were determined by Folin–Ciocalteu assay (Singleton & Rossi, 1965; Xu & Chang, 2007) with modifications. For the Folin–Ciocalteu assay, gallic acid (Sigma-Aldrich GmbH, Germany) was used as the standard. The reaction mixture containing 40 μ L standard solution/sample extracts, 1,560 μ L deionized H₂O and 100 μ L Folin–Ciocalteu reagent (Sigma-Aldrich GmbH) was incubated for 8 min at room temperature and 300 μ L of 20% Na₂CO₃ (wt/vol in distilled H₂O) was added to each tube and vortexed. After incubation for 2 hr at room temperature, the absorbance was determined at 765 nm with a Shimadzu UV2550PC spectrophotometer (Shimadzu). Total phenolic contents were expressed as gallic acid equivalents (mg of GAE g⁻¹ DM) using the standard curve of gallic acid.

Total flavonoid content was determined using a colorimetric method as described by Xu and Chang (2007). Aliquots of 250 μ L leaf extract or (+)-catechin standard solution were mixed with 1.25 mL distilled H₂O and 75 μ L 5% NaNO₂ (wt/vol in distilled H₂O) solution. After 6 min of incubation, 150 μ L of 10% (wt/vol in distilled H₂O) AlCl₃·6H₂O solution was added to the mixture and incubated for another 5 min at room temperature. After adding 0.5 mL of 1 M NaOH solution, the mixture was brought to 2.5 mL with distilled H₂O and mixed well. The solution absorbance was determined immediately at 510 nm. Total flavonoids were expressed as (+)-catechin equivalents (mg of CAE g⁻¹ DM) using the standard curve with (+)-catechin.

Total condensed tannins were measured according to the method described by Xu and Chang (2007) with the modifications explained here. Aliquots of 100 μ L leaf extract or (+)-catechin standard solution were added to 3 mL of 4% (wt/vol in methanol) vanillin solution and 1.5 mL of concentrated hydrochloric acid. After incubating the mixture for 15 min at room temperature, the absorbance was measured at 500 nm using methanol as a blank. Total condensed tannins were expressed as (+)-catechin equivalents (mg of CAE g⁻¹ DM) using the standard curve with (+)-catechin. All chemicals for these analyses were from Sigma-Aldrich Chemie GmbH.

2.8 | Data analysis

Foliar photosynthetic characteristics *A* and *g_s* were calculated according to von Caemmerer and Farquhar (1981), and volatile emission rates according to Niinemets et al., (2011). In the priming phase, the effects of priming treatment on gas exchange characteristics and VOC emissions of *A. millefolium* foliage were tested by linear mixed models (LMMs; SPSS 22.0, Chicago, IL) with the treatment (priming)

and recovery time as fixed effects. In the subsequent heat shock experiment, the impacts of heat shock, priming + heat shock and priming treatments on time-dependent changes of gas exchange characteristics, total and individual VOC emissions of *A. millefolium* foliage were tested by using LMMs with the treatments (non-primed + heat shock; primed + heat shock and primed without heat shock) and recovery time as fixed effects. Paired comparisons among the levels of the same factor were tested for significance by comparing differences of least squares means. Assumptions of constant variance and normality were checked by examining residual and quantile-quantile plots and Log10-transformation was applied to satisfy the requirements for LMMs when required (Marías, Meinzer, & Still, 2017). In addition, linear and non-linear regression analyses were performed to explore the relationships among gas exchange characteristics and different VOC groups in different treatments (SigmaPlot 11.0, Systat Software GmbH, Germany). Principal component analysis (PCA) was used to evaluate the effects of different treatments on the VOC compositions. Loading and score plots were initially derived after mean-centring and cube root transformation by MetaboAnalyst version 3.0 (Xia, Sinelnikov, Han, & Wishart, 2015; Xia & Wishart, 2016) and then redrawn in OriginLab 8.0 (OriginLab Corporation, Northampton, MA). For the individual and total phenolic compounds, one-way analysis of variance (ANOVA) followed by Tukey's post hoc test was used to compare the concentration differences among differently treated groups. All statistical tests were considered significant at $p \leq .05$.

3 | RESULTS

3.1 | Effects of heat priming treatment on photosynthetic characteristics and VOC emissions from *A. millefolium* plants

The heat priming treatment (35°C for 1 hr) did not affect *A. millefolium* plants (Figure 1a; Table 1). However, an immediate decrease in g_s was observed after the priming treatment, followed by recovery, during which g_s increased at 24 hr and reached 126% of that in control leaves (Figure 1b; $p = .04$ for the time \times treatment interaction). No significant changes in g_s were observed with further recovery at 48 and 72 hr time points. Priming treatment had minor impacts on intercellular CO₂ concentration (C_i), which mainly showed time-dependent changes (Figure 1c; Table 1).

Although *A* was not affected, heat priming induced emissions of different VOC groups in *A. millefolium* foliage. A significant increase of LOX compound emissions and isoprene occurred already at 0.5 hr after the priming treatment (Figure 2a,b; Table 1). Priming-induced LOX emissions showed a time-dependent increase starting from 24 hr, while isoprene emission decreased with the time of recovery (Figure 2a,b). On the other hand, emissions of monoterpenes and the only benzenoid observed in the emission blend, benzaldehyde, decreased at 5 hr after the priming treatment but significantly increased by the end of the priming treatment (Figure 2c,d; Table 1).

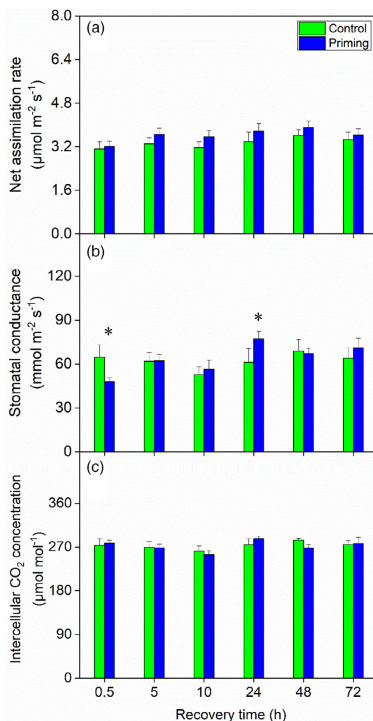


FIGURE 1 Effects of heat priming treatment (35°C for 1 hr) on average \pm SE net assimilation rate (a), stomatal conductance (b) and intercellular CO₂ concentration (c) of leaves of *A. millefolium*. The priming treatment was applied by transferring seven plants from one growth chamber at 25°C to another at 35°C. All other environmental conditions were identical in the two growth chambers. The priming treatment continued for 1 hr. After the priming treatment, the plants were transferred again to 25°C and allowed to recover for 72 hr before applying the heat shock treatments. The gas exchange characteristics and VOC emissions were measured at 0.5, 5, 10, 25, 48 and 72 hr after the priming treatment. Linear mixed models were applied to test for the effects of the treatment (priming) and the time of recovery. The summary of linear mixed models is shown in Table 1. Asterisks refer to the significant differences between control and different treatments at each recovery time point ($p \leq .05$) [Colour figure can be viewed at wileyonlinelibrary.com]

Total VOC emission was also enhanced in the primed plants at 72 hr, mainly reflecting enhanced monoterpene emissions (Figure 2e; Table 1).

TABLE 1 Summary of linear mixed model analyses of the effects of priming treatment (control, $n = 6$ vs. priming, $n = 7$) and recovery time on gas exchange characteristics (net assimilation rate, A ; stomatal conductance to water vapour, g_s ; and intercellular CO_2 concentrations, C_i) and VOC (lipoxygenase pathway compounds LOX; isoprene, ISO; monoterpene, MT; and benzenoid, BZ) emission rates in *A. millefolium* leaves

		Priming	Time	Priming x time
A	F	1.16	3.98	0.30
	P	0.30	<.01	0.91
g_s	F	0.18	3.71	2.49
	P	0.67	<.01	.04
C_i	F	0.01	4.84	2.70
	P	0.94	<.01	.03
LOX	F	4.55	2.90	1.84
	P	.04	.02	0.12
ISO	F	23.87	0.63	0.65
	P	<.01	0.68	0.66
MT	F	0.02	5.65	3.10
	P	0.88	<.01	.02
BZ	F	0.10	0.56	3.62
	P	0.76	0.73	.01
Total VOC	F	2.00	4.11	1.72
	P	0.17	<.01	0.15

Note: Significant values are shown in bold and italic ($p \leq .05$).
Abbreviation: VOCs, volatile organic compounds.

3.2 | Photosynthetic characteristics of primed and non-primed *A. millefolium* plants under heat shock stress

Primed and non-primed *A. millefolium* plants responded somewhat differently to heat shock treatment. Heat shock resulted in an immediate decrease of A in both non-primed and primed plants at 0.5 hr after the treatment, but the impacts on A were less in primed plants (Figure 3a; Table 2). Although A in both primed and non-primed plants fell onto the same level at 5 hr after the heat shock, in primed plants, the recovery in A started earlier and it returned to the control level by 24 hr after the heat shock. While in non-primed *A. millefolium* plants, A did not recover to the control level during the whole recovery period (Figure 3a; Table 2).

In primed *A. millefolium* plants, heat shock caused two transient enhancements in g_s , at 0.5 and 48 hr after application of heat shock stress, but g_s remained similar to that in control plants through the rest of the recovery period (Figure 3b; Table 2). In contrast, g_s in non-primed plants was reduced between 5 and 24 hr after the heat shock (Figure 3b; Table 2). Heat shock treatment resulted in significant increases in C_i in both primed and non-primed plants (Figure 3c; Table 2). Different from primed plants maintaining relatively high C_i values, the C_i in non-primed plants followed similar changing patterns to the g_s (Figure 3c). For the primed plants not subjected to the heat shock, all photosynthetic characteristics were maintained at the same level as those in the control plants (Figure 3; Table 2).

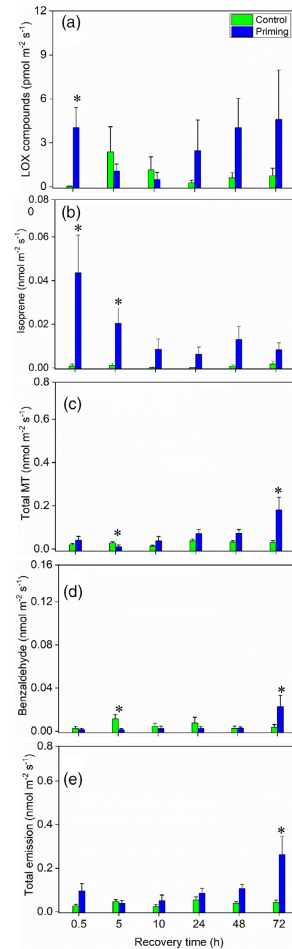


FIGURE 2 Effects of heat priming treatment (35°C for 1 hr) on average \pm SE emission rates of lipoxygenase pathway compounds (LOX, a), isoprene (b), total monoterpenes (MT, c), benzaldehyde (d) and total VOC emission rates (e) of *A. millefolium* leaves at different times after the priming treatment. Application of priming treatment is described in Figure 1. Linear mixed models were applied to test for the effects of the treatment (priming) and the time of recovery. The summary of linear mixed models is shown in Table 1. Asterisks refer to the significant differences between control and different treatments at each recovery time point ($p \leq .05$) [Colour figure can be viewed at wileyonlinelibrary.com]

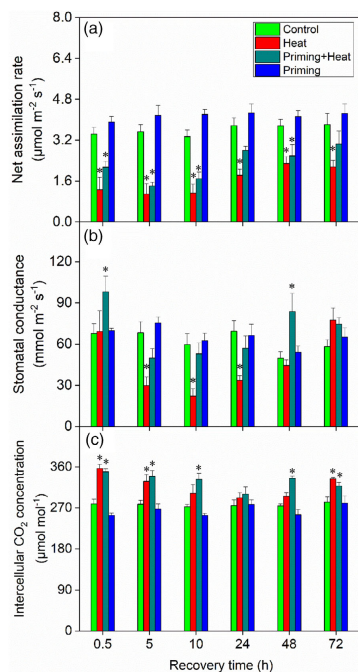


FIGURE 3 Time-dependent changes in average \pm SE net assimilation rate (a), stomatal conductance (b) and intercellular CO_2 concentration (c) of control (green bars), heat-stressed non-primed (Heat, red bars), primed and heat-stressed (Priming + Heat, cyan bars) and primed non-heat-stressed (Priming, blue bars) leaves of *A. millefolium*. Heat shock treatment consisted of plant exposure to 45°C for 5 min. The plants were measured at 0.5, 5, 10, 25, 48 and 72 hr recovery at 25°C . Untreated plants measured at 25°C for 72 hr were used as controls. Linear mixed models were applied to test for the effects of the treatments (heat, priming + heat and priming) and the time of recovery. The summary of linear mixed models is shown in Table 2. Asterisks refer to the significant differences between control and different treatments at each recovery time point ($p < .05$)

3.3 | VOC emissions in primed and non-primed *A. millefolium* plants under heat shock stress

In total, 29 VOCs were detected in the emissions of primed and non-primed *A. millefolium* leaves after the heat shock treatment (Table 3). The emission rates of different VOC groups kept low in the control plants as in the priming phase. For example, in the control plants, the emission of LOX pathway compounds was close to the detection limit

and mostly consisted of hexanal (Figure 4a; Table 3). Similarly, isoprene emission rate was also very low, up to $0.0043 \pm 0.0029 \text{ nmol m}^{-2} \text{ s}^{-1}$ (Figure 4b). Monoterpenes were quantitatively the largest emitted VOC group in *A. millefolium* (Figure 4c; Table 3). A total of 11 distinct monoterpene compounds were detected in the control plants, but only one sesquiterpene, longifolene, was detected (Figure 4c; Table 3).

Heat shock significantly altered VOC emission patterns in both primed and non-primed plants (Figure 4; Tables 2 and 3). A strong enhancement of LOX compound emissions in response to the heat shock stress was observed at 0.5 hr in the stressed plants (Figure 4a), and the emission rates of major individual LOX compounds ((E)-3-hexen-1-ol, 1-hexanol and (Z)-3-hexen-1-ol) reached the maximum values at this moment of time (Table 3). The initial LOX emission burst was remarkably lower in the primed than in non-primed plants (Figure 4a). A secondary rise in LOX emissions was observed in non-primed plants at 72 hr, but not in the primed plants (Figure 4a). Similar to LOX emissions, emission rates of long-chained saturated aldehydes (heptanal, 2-ethyl-hexanal and decanal) and the alcohol 1-octanol were also elevated in both primed and non-primed plants during the recovery period (Tables 3 and S1). In comparison with the primed plants subjected to heat shock, non-stressed primed plants demonstrated continuously higher LOX emissions during the recovery period (Figure 4a and Table 3). These emissions were dominated by hexanal that comprised up to 100% of the total LOX emissions (Figure 4a and Table 3). The long-chained saturated aldehydes and alcohols, particularly heptanal and 1-octanol had significantly higher emission rates in non-stressed primed plants similarly to heat shock stressed primed plants (Tables 3 and S1).

Heat shock treatment led to immediate increases in isoprene emissions in both primed and non-primed plants although such an increase was only statistically significant in non-primed plants (Figure 4b; Table 2). In non-primed plants, enhanced isoprene emissions continued till 10 hr after heat shock and isoprene emission rates decreased with the time of recovery (Figure 4b). Differently from the heat shock stressed primed plants in which isoprene emission did not show significant increases through the recovery period, non-stressed primed plants maintained significantly higher isoprene emissions through the 72 hr recovery time (Figure 4b; Table 2).

Heat shock elicited strong monoterpene emissions with particularly high emissions observed in primed plants at 0.5 hr after the treatment when monoterpene emissions reached a maximum of $0.63 \pm 0.07 \text{ nmol m}^{-2} \text{ s}^{-1}$ (Figure 4c) corresponding to 90% of total VOC emission (Figure 4f). In non-primed plants, the maximum monoterpene emission rate was only 25% of that in the primed plants and monoterpenes contributed 59% of total VOC emission (Figure 4c,f). At 0.5 hr, four individual monoterpenes (α -pinene, β -pinene, limonene and *p*-cymene) together contributed more than 80% of total monoterpene emissions in both primed and non-primed plants (Table 3). In the primed plants, total monoterpene emission rates were maintained at a considerably higher level than those in the control and non-primed plants for 10 hr after the heat shock treatment (Figure 4c). In contrast, monoterpene emissions in non-primed plants fell to the level observed in control plants at 5 hr with a secondary increase at 72 hr when the maximum emission rate reached $0.19 \pm 0.07 \text{ nmol m}^{-2} \text{ s}^{-1}$ (Figure 4c). Due to the large share of monoterpene emission, total

TABLE 2 Summary of linear mixed model analyses of the effects of treatments (Control, $n = 6$; Heat, $n = 3$; Priming + Heat, $n = 3$; and Priming, $n = 4$) and recovery time on photosynthetic characteristics and VOC emission rates of *A. millefolium* leaves. ST stands for sesquiterpene and other abbreviations are as in Table 1

		Heat	Time	Heat × time	Priming + Heat	Time	(Priming + Heat) × time	Priming	Time	Priming × time
A	F	19.29	18.13	9.80	15.65	14.84	10.89	1.95	1.67	1.33
	P	<.01	<.01	<.01	<.01	<.01	<.01	0.19	0.16	0.27
g_s	F	7.88	28.26	21.60	0.65	6.55	12.45	0.54	8.37	0.55
	P	.02	<.01	<.01	0.43	<.01	<.01	0.47	<.01	0.74
C_i	F	12.62	5.27	2.97	28.75	2.12	2.45	1.31	4.86	2.97
	P	<.01	<.01	.02	<.01	0.08	.05	0.28	<.01	.02
LOX	F	31.53	2.63	2.46	2.36	1.36	4.85	11.30	6.01	1.19
	P	<.01	.04	.05	0.14	0.26	<.01	<.01	<.01	0.33
ISO	F	4.82	2.28	3.84	0.20	0.57	1.82	13.79	1.25	0.85
	P	.05	0.07	.01	0.66	0.72	0.13	<.01	0.30	0.52
MT	F	10.92	3.50	0.89	14.81	3.71	3.15	0.31	2.43	1.68
	P	<.01	<.01	0.50	<.01	<.01	.02	0.59	.05	0.16
ST	F	6.00	1.15	1.09	5.02	1.52	1.18	1.07	0.20	0.47
	P	.02	0.36	0.39	.04	0.21	0.34	0.32	0.96	0.80
BZ	F	4.59	1.24	2.39	3.53	1.10	6.40	0.34	2.81	3.38
	P	.04	0.31	0.06	0.08	0.38	<.01	0.57	.03	.01
Total VOC	F	12.72	3.95	1.21	15.59	2.79	3.99	3.95	2.19	2.23
	P	<.01	<.01	0.33	<.01	.03	<.01	0.07	0.07	0.07

Note: Significant values are shown in bold and italic ($p \leq .05$).
Abbreviation: VOCs, volatile organic compounds.

VOC emissions in both primed and non-primed plants followed the emission pattern of total monoterpenes (Figure 4c,f). For non-stressed primed plants, total monoterpene emission rates remained at the control level and the proportion of monoterpenes contributed less than 35% of total VOC emissions except at 0.5 hr, when monoterpene contribution reached to 72% of the total emissions (Figure 4c,f). Similar to the plants under heat shock, total VOC emissions in non-stressed primed plants increased considerably, but this increase was significant only at 10 hr after the start of the recovery (Figure 4f; Table 2).

Once exposed to the heat shock, elicitation of sesquiterpene emissions was observed in both primed and non-primed plants immediately after the start of recovery (Figure 4d). Four sesquiterpene compounds were detected in the sesquiterpene emission blends, albeit the emission rates were low and total sesquiterpene emissions did not exceed $0.01 \text{ nmol m}^{-2} \text{ s}^{-1}$ (Figure 4d; Table 3). At 0.5 hr after the heat shock, sesquiterpene emissions of primed plants were slightly higher than those in non-primed plants, reflecting greater emissions of longifolene and β -caryophyllene in primed plants (Figure 4d; Table 3). During the whole recovery period, total sesquiterpene emissions in non-stressed primed plants stayed at the control level (Figure 4d).

In addition to induction of sesquiterpenes, emissions of benzaldehyde, the only benzenoid detected in the VOC blend from heat shock stressed *A. millefolium* plants, and two geranylgeranyl diphosphate (GGDP) pathway compounds (6-methyl-5-heptene-2-one and geranylacetone) were observed in heat-stressed plants (Tables 3). Heat shock effects on benzaldehyde emission were moderate. In primed plants, significant

increases of benzaldehyde emission were observed through recovery (Figure 4e; Table 2). In non-primed plants, significant benzaldehyde emissions occurred at 72 hr (Figure 4e). The emission of 6-methyl-5-heptene-2-one and geranylacetone generally decreased at 0.5 hr but recovered and increased at the end of the recovery period in both non-primed and primed plants (Tables 3 and S1). For non-stressed primed plants, benzaldehyde emission followed an increasing pattern and peaked at 48 hr of recovery phase when that was also found significantly increased in heat shock stressed primed plants (Figure 4e). Notably, in non-stressed primed plants at 5 hr of recovery, the emission rate of 6-methyl-5-heptene-2-one had increased to a more than 12-fold higher value than that in stressed primed plants (Table 3).

According to the results of PCA, the variation in emission blends at different times through recovery in plants of different treatment groups was most strongly influenced by isoprene, LOX volatiles, monoterpenes and benzaldehyde (Figure 5a). PCA demonstrated that heat shock stressed plants, regardless of whether earlier primed or not, were clearly distinguished from controls due to changes in the emission rates of detected VOCs, and furthermore, primed and non-primed heat-stressed plants were also clearly differentiated (Figure 5b). Emissions of all the LOX compounds were associated with non-primed stressed plants, whereas isoprene and benzaldehyde were only associated with non-stressed and heat shock stressed primed plants. Monoterpenes including tricyclene, α -pinene and limonene constituted the characteristic VOCs that separated the heat shock stressed plants from control and non-stressed primed plants (Figure 5a).

TABLE 3 Average \pm SE emission rates ($\text{pmol m}^{-2} \text{s}^{-1}$) of VOCs emitted from non-primed (Heat) and primed (Priming + Heat) *A. millefolium* leaves subjected to heat shock treatment and from non-stressed primed (Priming) and control plants during 72 hr recovery period. The replicate number for each treatment is as in Table 2

LOV pathway compounds	0.5 hr				5 hr				10 hr			
	Control		Priming + Heat		Control		Priming + Heat		Control		Priming + Heat	
	Control	Heat	Priming + Heat	Priming	Control	Heat	Priming + Heat	Priming	Control	Heat	Priming + Heat	Priming
1 Hexanal	0.026 \pm 0.022	4.9 \pm 4.7	N.D.	0.41 \pm 0.41	1.4 \pm 1.4	0.39 \pm 0.39	N.D.	18.9 \pm 5.2	0.25 \pm 0.25	N.D.	N.D.	7.6 \pm 3.4
2 (Z)-3-Hexen-1-ol	N.D.	64 \pm 64	3.0 \pm 1.8	N.D.	N.D.	5.5 \pm 3.9	N.D.	N.D.	N.D.	1.2 \pm 1.2	1.0 \pm 1.0	N.D.
3 1-Hexanol	N.D.	3.2 \pm 3.2	0.37 \pm 0.37	N.D.	N.D.	N.D.	N.D.	0.28 \pm 0.28	N.D.	N.D.	0.43 \pm 0.43	N.D.
4 (E)-3-Hexen-1-ol	N.D.	5.7 \pm 2.3	N.D.	N.D.	N.D.	5.5 \pm 3.9	N.D.	N.D.	N.D.	N.D.	N.D.	N.D.
<i>Long-chain aldehydes and alcohols</i>												
5 Hexanal	2.3 \pm 1.8	1.7 \pm 1.6	N.D.	0.32 \pm 0.32	0.86 \pm 0.54	0.12 \pm 0.12	N.D.	8.0 \pm 2.8	0.37 \pm 0.37	N.D.	N.D.	4.6 \pm 2.3
6 2-Ethyl-hexanal	N.D.	1.8 \pm 1.8	N.D.	N.D.	N.D.	N.D.	2.9 \pm 2.9	N.D.	N.D.	N.D.	3.6 \pm 3.6	N.D.
7 1-Octanol	N.D.	1.41 \pm 0.73	2.36 \pm 0.78	N.D.	N.D.	1.19 \pm 0.26	0.66 \pm 0.37	0.90 \pm 0.68	N.D.	0.75 \pm 0.75	4.67 \pm 0.87	0.9 \pm 0.59
8 Decanal	1.42 \pm 0.94	0.068 \pm 0.068	3.3 \pm 1.8	N.D.	1.41 \pm 0.80	N.D.	0.37 \pm 0.37	N.D.	2.0 \pm 2.0	N.D.	10.2 \pm 9.8	N.D.
<i>Terpenoids</i>												
9 Isoprene	2.4 \pm 2.4	18.0 \pm 6.4	13.5 \pm 9.6	14.5 \pm 11.3	1.24 \pm 0.82	26.3 \pm 7.3	11.8 \pm 11.8	21.7 \pm 7.9	3.2 \pm 3.0	5.5 \pm 2.3	5.7 \pm 5.7	21.1 \pm 9.3
10 α -Thujene	0.89 \pm 0.56	3.0 \pm 1.7	3.77 \pm 0.80	N.D.	0.89 \pm 0.62	1.37 \pm 0.65	N.D.	N.D.	0.21 \pm 0.21	0.035 \pm 0.035	0.39 \pm 0.20	N.D.
11 Tricyclene	0.50 \pm 0.17	0.52 \pm 0.52	5.0 \pm 1.5	0.71 \pm 0.42	1.04 \pm 0.53	0.13 \pm 0.13	3.4 \pm 1.3	0.12 \pm 0.12	0.76 \pm 0.23	1.3 \pm 1.3	4.7 \pm 1.9	N.D.
12 α -Pine	4.7 \pm 2.4	3.1 \pm 1.6	18.1 \pm 3.8	4.1 \pm 2.1	2.9 \pm 1.9	1.6 \pm 1.2	6.04 \pm 8.7	0.46 \pm 0.46	0.96 \pm 0.84	2.6 \pm 2.5	6.7 \pm 2.9	1.4 \pm 0.79
13 Camphene	2.66 \pm 0.91	2.5 \pm 1.6	20.1 \pm 7.1	3.4 \pm 2.4	1.00 \pm 0.64	0.85 \pm 0.85	12.1 \pm 5.6	N.D.	1.18 \pm 0.78	7.1 \pm 6.9	11.5 \pm 3.6	0.7 \pm 0.27
14 β -Pine	6.6 \pm 2.9	4.2 \pm 1.8	2.65 \pm 1.3	1.03 \pm 0.92	7.3 \pm 4.4	2.6 \pm 2.1	21.5 \pm 8.5	2.41 \pm 0.82	5.2 \pm 5.1	4.6 \pm 3.0	2.2 \pm 1.1	1.62 \pm 0.74
15 β -Caryophyllene	1.9 \pm 1.9	5.3 \pm 4.6	39.0 \pm 9.0	9.6 \pm 3.9	1.3 \pm 1.3	3.9 \pm 2.9	12.3 \pm 4.1	9.0 \pm 4.1	N.D.	3.4 \pm 2.3	16.3 \pm 6.6	7.1 \pm 3.4
16 β -Juncene	N.D.	1.58 \pm 0.88	9.6 \pm 4.4	N.D.	N.D.	0.60 \pm 0.60	N.D.	N.D.	N.D.	N.D.	N.D.	N.D.
17 α -Caryophyllene	N.D.	1.8 \pm 1.6	1.30 \pm 0.22	N.D.	N.D.	0.115 \pm 0.063	0.997 \pm 0.097	N.D.	N.D.	N.D.	N.D.	N.D.
18 Limonene	0.83 \pm 0.83	16.5 \pm 9.6	5.2 \pm 1.6	3.6 \pm 1.3	0.34 \pm 0.34	10.2 \pm 6.0	13.5 \pm 2.7	1.9 \pm 1.1	0.42 \pm 0.42	5.9 \pm 2.4	4.6 \pm 3.6	2.00 \pm 0.98
19 p -Cymene	0.72 \pm 0.66	4.9 \pm 3.6	30.3 \pm 5.8	2.0 \pm 1.6	1.5 \pm 1.1	5.9 \pm 3.0	16.7 \pm 5.2	N.D.	N.D.	9.0 \pm 8.5	13.0 \pm 2.2	1.38 \pm 0.94
20 β -Phellandrene	0.019 \pm 0.019	1.05 \pm 0.54	4.94 \pm 1.05	0.23 \pm 0.22	0.20 \pm 0.20	1.17 \pm 0.76	N.D.	0.36 \pm 0.24	0.048 \pm 0.048	N.D.	1.5 \pm 1.5	0.37 \pm 0.13
21 1,8-Cineole	0.19 \pm 0.19	4.4 \pm 2.9	12.3 \pm 4.2	N.D.	N.D.	4.1 \pm 3.6	2.1 \pm 2.1	0.42 \pm 0.16	N.D.	N.D.	1.82 \pm 0.91	0.38 \pm 0.15
22 Terpinolene	N.D.	1.26 \pm 0.87	3.1 \pm 1.5	N.D.	N.D.	0.24 \pm 0.12	N.D.	N.D.	N.D.	N.D.	N.D.	N.D.
23 α -Copaene	N.D.	0.23 \pm 0.13	N.D.	N.D.	N.D.	N.D.	N.D.	N.D.	N.D.	N.D.	N.D.	N.D.
24 Longifolene	0.14 \pm 0.14	N.D.	0.80 \pm 0.80	0.053 \pm 0.051	0.076 \pm 0.076	0.11 \pm 0.11	0.36 \pm 0.36	0.18 \pm 0.15	0.078 \pm 0.078	N.D.	N.D.	0.26 \pm 0.21
25 β -Caryophyllene	N.D.	N.D.	1.3 \pm 1.3	N.D.	N.D.	N.D.	N.D.	N.D.	N.D.	N.D.	N.D.	N.D.
26 γ -Selinene	N.D.	0.35 \pm 0.20	N.D.	N.D.	N.D.	0.37 \pm 0.37	0.23 \pm 0.23	N.D.	N.D.	0.17 \pm 0.17	N.D.	N.D.
<i>Benzenoid</i>												
27 Benzaldehyde	3.5 \pm 2.0	9.1 \pm 5.3	18.4 \pm 5.0	0.56 \pm 0.56	8.2 \pm 4.2	11.5 \pm 9.3	10.2 \pm 8.7	6.2 \pm 2.4	1.0 \pm 1.0	5.3 \pm 2.7	2.1 \pm 1.1	5.6 \pm 1.9

(Continues)

TABLE 3 (Continued)

	0.5 hr			5 hr			10 hr						
	Control	Heat	Priming + Heat	Control	Heat	Priming + Heat	Control	Heat	Priming + Heat				
	Control	Heat	Priming + Heat	Control	Heat	Priming + Heat	Control	Heat	Priming + Heat				
GGDP pathway compounds													
28	6-Methyl-5-hepten-2-one	10 ± 10	0.58 ± 0.58	4.9 ± 1.2	9.0 ± 5.9	8.8 ± 8.8	N.D.	1.7 ± 1.6	109 ± 42	N.D.	21 ± 13	71 ± 35	
29	Geranylacetone	2.16 ± 0.98	0.11 ± 0.11	2.1 ± 2.1	N.D.	1.54 ± 0.62	0.66 ± 0.40	N.D.	1.46 ± 0.95	1.9 ± 1.3	0.3 ± 0.3	4.0 ± 3.8	0.79 ± 0.47
24 hr													
LOX pathway compounds													
1	Hexanal	2.25 ± 0.83	1.52 ± 0.94	1.2 ± 1.2	2.4 ± 2.4	0.38 ± 0.38	0.63 ± 0.63	3.91 ± 1.79	2.8 ± 1.9	0.17 ± 0.17	6.2 ± 4.1	3.4 ± 3.4	0.60 ± 0.40
2	(Z)-3-Hexen-1-ol	0.62 ± 0.62	N.D.	N.D.	4.8 ± 1.9	0.54 ± 0.54	N.D.	N.D.	7.3 ± 5.6	N.D.	2.9 ± 2.9	N.D.	N.D.
3	1-Hexanol	0.25 ± 0.25	N.D.	N.D.	1.09 ± 0.69	0.073 ± 0.073	N.D.	N.D.	0.82 ± 0.82	N.D.	N.D.	N.D.	N.D.
4	(E)-3-Hexen-1-ol	N.D.	5.8 ± 2.3	N.D.	N.D.	N.D.	0.64 ± 0.64	N.D.	N.D.	N.D.	N.D.	N.D.	N.D.
Long-chain aldehydes and alcohols													
5	Heptanal	1.30 ± 0.49	N.D.	0.73 ± 0.37	0.92 ± 0.92	N.D.	N.D.	1.32 ± 0.56	9.5 ± 9.0	0.24 ± 0.24	2.1 ± 1.1	6.1 ± 6.1	0.26 ± 0.26
6	2-Ethylhexanal	N.D.	N.D.	0.46 ± 0.46	N.D.	N.D.	2.7 ± 1.5	N.D.	N.D.	N.D.	3.9 ± 3.9	N.D.	N.D.
7	1-Octanol	0.24 ± 0.18	0.37 ± 0.37	1.18 ± 0.12	2.5 ± 1.2	1.09 ± 0.60	0.61 ± 0.61	2.07 ± 0.67	3.7 ± 3.6	N.D.	1.3 ± 1.0	N.D.	N.D.
8	Decanal	2.4 ± 1.6	N.D.	1.4 ± 1.2	N.D.	N.D.	N.D.	7.4 ± 3.5	N.D.	1.57 ± 0.99	4.0 ± 3.1	1.2 ± 1.2	N.D.
Terpenoids													
9	Isoprene	2.9 ± 2.0	0.72 ± 0.72	4.1 ± 2.2	28.0 ± 7.2	3.6 ± 3.1	4.1 ± 2.7	1.7 ± 1.7	20.1 ± 7.3	4.3 ± 3.0	2.0 ± 2.0	N.D.	2.9 ± 1.1
10	α -Thujene	1.29 ± 0.86	3.2 ± 1.4	0.390 ± 0.040	N.D.	1.00 ± 0.58	0.71 ± 0.19	0.40 ± 0.40	N.D.	0.57 ± 0.29	2.57 ± 0.78	N.D.	N.D.
11	Tricycylene	0.27 ± 0.21	0.20 ± 0.20	N.D.	N.D.	0.158 ± 0.072	0.20 ± 0.20	N.D.	0.148 ± 0.087	0.089 ± 0.079	1.3 ± 1.1	3.67 ± 0.79	0.130 ± 0.096
12	α -Pine	12.5 ± 6.1	21.3 ± 4.3	23 ± 11	0.63 ± 0.63	3.4 ± 1.9	9.9 ± 5.0	9.9 ± 9.8	2.1 ± 1.8	3.0 ± 2.5	6.2 ± 2.9	8.5 ± 4.4	11.4 ± 4.6
13	Camphene	1.74 ± 0.77	3.8 ± 2.1	5.9 ± 3.0	N.D.	1.9 ± 1.1	2.3 ± 1.7	N.D.	0.66 ± 0.66	1.66 ± 0.94	3.3 ± 3.0	7.0 ± 2.8	0.54 ± 0.43
14	β -Pine	6.6 ± 2.5	5.4 ± 2.2	25.7 ± 8.3	3.5 ± 1.4	7.5 ± 2.8	16.5 ± 9.6	17.4 ± 4.9	5.6 ± 2.7	5.6 ± 3.3	5.8 ± 2.2	2.7 ± 2.3	1.29 ± 0.53
15	β -Caryophyllene	4.1 ± 1.3	4.3 ± 1.4	3.6 ± 1.7	9.2 ± 4.3	0.89 ± 0.63	N.D.	4.4 ± 4.4	9.2 ± 6.8	2.2 ± 1.7	1.89 ± 3.3	1.1 ± 1.0	1.5 ± 1.2
16	(Z)- β -Ocimene	1.0 ± 1.0	2.7 ± 1.6	N.D.	N.D.	1.0 ± 1.0	0.56 ± 0.56	N.D.	N.D.	1.10 ± 0.70	8.0 ± 3.9	N.D.	N.D.
17	β -Caryophyllene	N.D.	0.53 ± 0.36	N.D.	N.D.	N.D.	N.D.	N.D.	N.D.	N.D.	0.64 ± 0.52	N.D.	N.D.
18	Limonene	5.5 ± 1.1	11.5 ± 2.0	9.0 ± 6.3	3.6 ± 2.2	5.3 ± 2.9	0.89 ± 0.47	3.9 ± 3.8	15 ± 12	2.5 ± 1.2	1.96 ± 6.0	2.9 ± 2.2	1.14 ± 0.90
19	<i>p</i> -Cymene	3.7 ± 2.4	2.4 ± 1.9	5.0 ± 2.5	1.7 ± 1.5	7.4 ± 2.4	11.30 ± 10.48	N.D.	1.9 ± 1.4	3.2 ± 1.3	8.7 ± 6.1	10.4 ± 2.5	0.75 ± 0.46
20	β -Phellandrene	N.D.	1.38 ± 0.72	0.28 ± 0.28	0.50 ± 0.24	0.30 ± 0.29	0.46 ± 0.46	N.D.	0.015 ± 0.015	0.32 ± 0.19	2.27 ± 0.89	N.D.	0.13 ± 0.13
21	1,8-Cineole	1.66 ± 0.93	5.5 ± 3.1	2.16 ± 0.49	0.37 ± 0.21	1.00 ± 0.72	1.0 ± 1.0	0.76 ± 0.48	0.048 ± 0.048	0.73 ± 0.37	7.3 ± 4.0	1.8 ± 1.5	0.060 ± 0.060
22	Terpinolene	0.65 ± 0.44	0.70 ± 0.54	N.D.	N.D.	N.D.	0.09 ± 0.09	N.D.	N.D.	N.D.	0.47 ± 0.47	N.D.	N.D.
23	α -Copaene	N.D.	N.D.	N.D.	N.D.	N.D.	N.D.	N.D.	N.D.	N.D.	N.D.	N.D.	N.D.

Downloaded from https://onlinelibrary.wiley.com/doi/10.1111/1522-2675.13811 by Eastman University Library, Wiley Online Library on [08/06/2023]. See the Terms and Conditions (https://onlinelibrary.wiley.com/terms-and-conditions) on Wiley Online Library for rules of use; OA articles are governed by the applicable Creative Commons License

TABLE 3 (Continued)

	24 hr			48 hr			72 hr		
	Control	Heat	Priming + Heat	Control	Heat	Priming + Heat	Control	Heat	Priming + Heat
24 Linaldiene	0.12 ± 0.12	N.D.	N.D.	0.112 ± 0.049	N.D.	N.D.	0.22 ± 0.18	0.042 ± 0.042	N.D.
25 β-Caryophyllene	N.D.	N.D.	N.D.	N.D.	N.D.	N.D.	N.D.	N.D.	N.D.
26 γ-Selinene	N.D.	N.D.	0.36 ± 0.36	N.D.	0.237 ± 0.237	0.30 ± 0.30	N.D.	0.25 ± 0.25	N.D.
Benzoid									
27 Benzaldehyde	9.0 ± 4.9	3.2 ± 2.5	6.6 ± 0.62	6.0 ± 3.7	3.3 ± 1.8	12.1 ± 5.4	27.1 ± 2.1	3.6 ± 2.6	13 ± 13
GGPP pathway compounds									
28 6-Methyl-5-heptene-2-one	15.5 ± 5.0	N.D.	9.4 ± 9.4	11 ± 10	N.D.	12 ± 12	40 ± 40	2.0 ± 2.0	7.1 ± 7.1
29 Geranylacetone	2.9 ± 1.5	0.069 ± 0.049	0.89 ± 0.68	7.5 ± 6.9	2.1 ± 2.1	1.68 ± 0.30	33 ± 30	1.3 ± 1.3	6.8 ± 1.9
									10.5 ± 7.6
									0.25 ± 0.25

Note: N.D., not detectable. The summary of linear mixed models testing for the effects of treatments and the time of recovery on individual VOC emissions is shown in Table S1. Abbreviations: GGPP, geranylgeranyl diphosphate; VOCs, volatile organic compounds.

3.4 | Correlations among different volatile groups and photosynthetic characteristics

In heat shock stressed primed plants, both isoprene and total sesquiterpene emission rates correlated positively with total monoterpene emissions (Figure 6a,b). In non-primed plants, there was a positive correlation between benzaldehyde and monoterpene emissions (Figure 6c), and LOX compound emission rate was positively correlated with the emission rate of isoprene (Figure 6d), but similar positive correlations of LOX compound emissions with monoterpene and sesquiterpene emissions were weaker (Figure 6e,f). In non-stressed primed plants, only isoprene correlated negatively with monoterpene emissions (Figure 6a).

In general, in heat shock stressed primed plants, the emissions of isoprene, monoterpenes and sesquiterpenes were negatively correlated with A but positively correlated with g_s (Figure S1b–d,g–i), while in non-primed plants, negative correlations were found between A and the emission rates of LOX compounds and isoprene; and benzaldehyde was the only compound scaling positively with g_s (Figure S1a,b,j). In non-stressed primed plants, isoprene emission scaled positively but monoterpene emission scaled negatively with A (Figure S1b,c).

3.5 | Effects of heat shock treatment on foliage phenolic contents in primed and non-primed *A. millefolium*

Accumulation of phenolic compounds was analysed 3 days after the heat shock treatment. Heat shock did not significantly affect the total flavonoid contents in both non-stressed and stressed plants regardless of the priming treatment (Figure 7a). In contrast to control plants, all other treatments induced accumulation of total condensed tannins in *A. millefolium* foliage, whereas in heat shock stressed primed plants the concentration reached up to $85 \pm 10 \text{ mg g}^{-1}$ DM (1.8-fold of control level, Figure 7b). In addition, total phenolic contents also increased in the stressed primed plants (1.4-fold increase, Figure 7c).

In *A. millefolium* leaf extracts, 13 individual phenolic compounds including hydroxycinnamic acid derivatives (four CQA isomers and four diCQA isomers), and flavonoids (three luteolin and luteolin derivatives and two apigenin derivatives) were identified and quantified (Table 4; Figure S2). The dominant CQA detected in plants was chlorogenic acid (CQA I). Heat shock increased the concentrations of individual CQA isomers and total CQA contents similarly in primed and non-primed plants (Table 4). Heat shock also led to increases in diCQA IV and total diCQA contents, whereas these increases were stronger in non-primed plants (Table 4). In turn, by the end of the recovery, non-stressed primed plants accumulated the highest individual CQA (except CQA II) and total CQA pools, as well as the highest individual diCQA (diCQA III and IV) and total diCQA contents (Table 4). Although heat shock treatment did not affect individual flavonoid contents in all plant groups, non-stressed primed plants accumulated evidently more luteolin and apigenin derivatives than both control and stressed plants (Table 4).

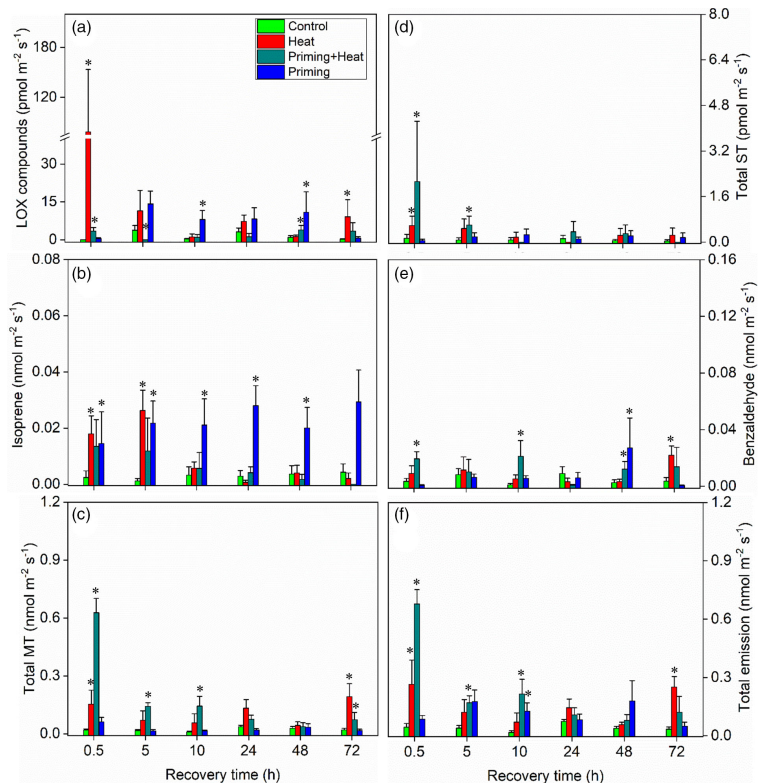


FIGURE 4 Time-dependent changes in average \pm SE emission rates of LOX compounds (a), isoprene (b), total monoterpenes (MT, c), total sesquiterpenes (ST, d), benzaldehyde (e) and total VOC emission rates (f) of control (green bars), non-primed heat-stressed (Heat, red bars), primed and heat-stressed (Priming + Heat, cyan bars) and primed non-heat-stressed (Priming, blue bars) *A. millefolium* leaves at different times through the recovery. Measurements and statistical analysis are as in Figure 3. The summary of linear mixed models is shown in Table 2. Effects of heat shock treatment on individual VOC emissions are shown in Table 3. Asterisks refer to the significant differences between control and different treatments at each recovery time point ($p \leq .05$)

4 | DISCUSSION

4.1 | How did heat priming alter VOC emission patterns to prepare *A. millefolium* for subsequent heat shock?

In plants, the photosynthetic apparatus, particularly thylakoid membranes are highly susceptible to heat stress (Sharkey, 2005). Exceeding certain temperature threshold can seriously impair the photosynthetic

apparatus (Kim & Portis Jr, 2005; Niinemets, 2018). In our study, in general, the primed plants only adjusted g_s , while *A* remained unaffected throughout the time-period following priming treatment (Figure 1). Stable values of *A* suggest that 35°C treatment is an appropriate temperature condition to trigger heat priming defence in *A. millefolium* plants. However, the heat treatment may in some cases result in high vapour pressure deficit and lead to stomata closure (Devi & Reddy, 2018; Hüve et al., 2019; Shinohara & Leskovar, 2014), which can eventually cause an immediate decrease in g_s upon the priming treatment (Figure 1b).

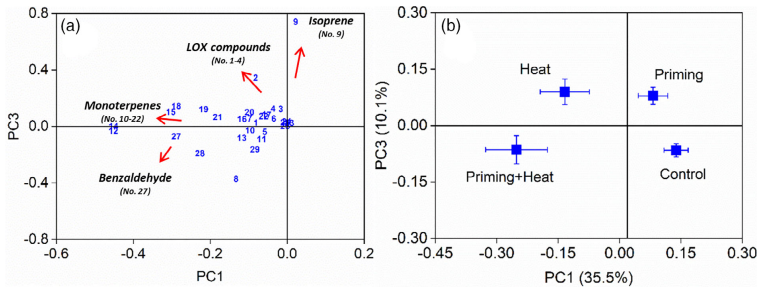


FIGURE 5 Loading plot (a) and score plot (b) of the principal component analysis (PCA) of the VOC emission profiles of heat shock stressed non-primed (Heat) and primed (Priming + Heat) plants, as well as non-stressed primed (Priming) and control *A. millefolium* plants. Emission rates of all volatiles (Table 3 for compound names and codes) collected from three or four biological replicates through 72 hr after heat shock stress together with those from non-stressed primed and control plants were used in the PCA. In the loading plot (a), the impact of volatiles increases with the distance from the origin of the co-ordinate system. In the score plot (b), the mean scores \pm SE ($n = 3$ or 4 for each treatment) of principal components (PC1 and PC3) were shown. The variation explained by the PC components is shown in both axes [Colour figure can be viewed at wileyonlinelibrary.com]

The increase in g_s at later stages of priming recovery seemed independent of A , as A remained constant after the priming treatment. This contrasts numerous findings revealing that under optimal growth environment, g_s positively correlates with A as temperature increases (Leuning, 1995; Urban, Ingwers, McGuire, & Teskey, 2017). Since environmental factors during the recovery period were stable, the priming induced decoupling of the association between g_s and A , was presumably driven by active (such as abscisic acid-mediated) rather than passive (hydraulic-mediated) mechanisms (Tombesi et al., 2015), which was further supported by less affected C_i levels in primed plants (Figure 1c).

After the priming treatment, LOX compounds, mainly hexanal emissions (data not shown), were still observed among the VOC blends in primed plants. LOX compounds are synthesized by LOXs from polyunsaturated fatty acids released from plant membranes upon different stresses (Feussner & Wasternack, 2002; Porta & Rocha-Sosa, 2002). Thus, induced emissions of LOX are normally considered as indicators of leaf damage that can result due to different severe stresses including wounding, acute ozone or heat shock (Kanagendran, Pazouki, & Niinemets, 2018; Li, Harley, & Niinemets, 2017; Pazouki & Niinemets, 2016; Rasulov, Talts, & Niinemets, 2019). However, the total amount of priming-induced LOX was less than 5% of the whole leaf VOC emissions (Figure 2a,e) and likely reflected only minor damage of cell membranes and/or originated from an existing non-specific storage pools of ready-made LOX compounds. The minor effects of the priming treatment on A further emphasizes that the damage of plastid membranes likely did not contribute to LOX compound emissions in *A. millefolium*.

In this study, significant isoprene and monoterpene emissions in primed *A. millefolium* foliage were observed (Figure 2b,c). The physiological functions of isoprene and monoterpenes have been well documented; both are protective agents that function to defend directly and

indirectly leaf photosynthesis apparatus against high temperature (Copolovici, Filella, Llusà, Niinemets, & Peñuelas, 2005; Loreto, Förster, Dürr, Csisy, & Seufert, 1998; Sharkey, Wiberley, & Donohue, 2008). The direct defence has been associated with preservation of the integrity of thylakoid membranes and indirect defence by their capacity to scavenge ROS (Copolovici et al., 2005; Loreto, Pinelli, Manes, & Kollist, 2004; Loreto & Velikova, 2001; Velikova et al., 2015). Thus, the priming-induced enhancement of emissions of isoprene and monoterpenes in *A. millefolium* might be one of the important mechanisms protecting photosynthesis from more severe heat stress. Previous studies on field grown *A. millefolium* focused on mono- and sesquiterpene emissions under ambient conditions (Pazouki et al., 2015). The current study suggests that in addition to larger isoprenoids, isoprene emissions elicited by heat priming in *A. millefolium* can be an important component of the suite of priming-induced defensive mechanisms (Figure 2b). The start of isoprene release was associated with the heat stress itself as it correlated with LOX compound emissions both under priming and under the heat shock treatments (Figures 2a,b and 6d). Isoprene might be produced non-enzymatically in stressed plants when the pool size of dimethylallyl diphosphate (DMADP) or isopentenyl diphosphate (IDP) builds up or pH rapidly changes in chloroplasts (Brilli et al., 2011; Silver & Fall, 1991; Turan et al., 2019; Velikova, Pinelli, & Loreto, 2005). Alternatively, the isoprene from heated *A. millefolium* foliage could be produced by multi-substrate terpene synthases such as myrcene synthase in *Humulus lupulus* that can synthesize both isoprene and other terpenes depending on corresponding substrate availabilities (Pazouki & Niinemets, 2016). As isoprene emissions occurred rapidly, as soon as *A. millefolium* plants were subjected to priming treatment, it is not likely that there is a specific isoprene synthase expressed instantly upon the heat priming. However, gene expression level responses might have been involved in the later stages of recovery (Figures 2b and 4b).

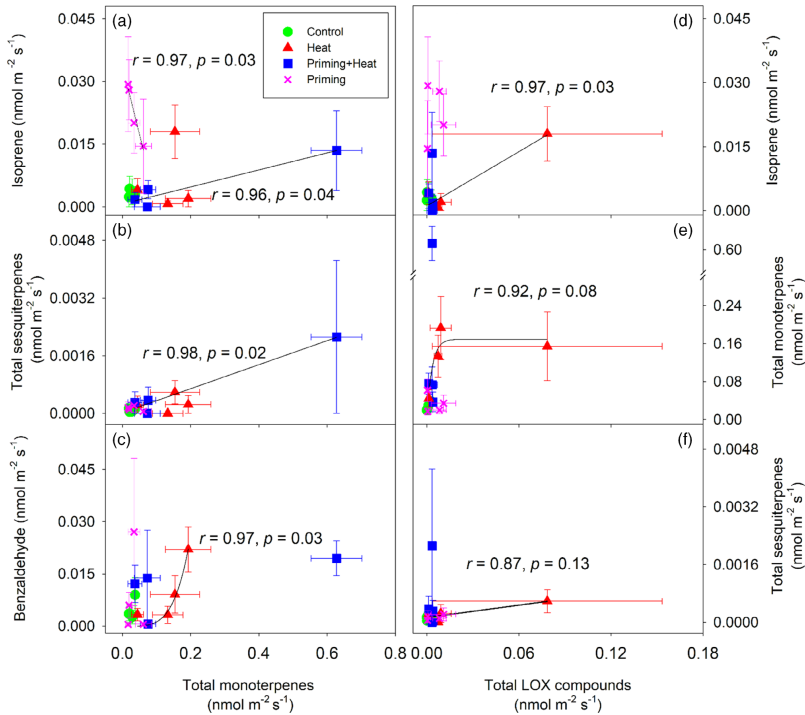


FIGURE 6 Correlations between total monoterpene emissions and emissions of isoprene (a), total sesquiterpenes (b), and benzaldehyde (c) and correlations between total LOX compound emissions and emissions of isoprene (d), total monoterpenes (e) and total sesquiterpenes (f) in control, heat shock stressed non-primed (Heat) and primed (Priming + Heat) leaves as well as non-stressed primed (Priming) *A. millefolium* leaves. Each symbol corresponds to the mean value of three or four independent biological replicates at 0.5, 24, 48 and 72 hr of plants from different treatments, and error bars show \pm SE. Linear regressions were applied to data from non-stressed primed plants (a), heat shock stressed primed plants in (a,b) and non-primed plants in (d,f) with the regression equations of $y = 0.034 - 0.329x$ (a, non-stressed primed plants); $y = 0.0007 + 0.0204x$ (a, heat shock stressed primed plants); $y = 1.92 \cdot 10^{-5} + 0.0033x$ (b); $y = 0.0011 + 0.2119x$ (d) and $y = 0.0001 + 0.0057x$ (f). Non-linear regressions were applied to the data from non-primed plants in (c) and (e) with the equations of $y = 31.3x^{4.44}$ (c) and $y = 0.169(1 - e^{-29.5x})$ (e)

Contrary to isoprene, monoterpene emissions did not show immediate increases upon priming (Figure 2c). However, increased emissions observed later during the recovery indicated that a progressive increase in monoterpene synthesis capacity has probably occurred during the recovery (Figure 2c). In plants, monoterpenes are synthesised by condensation of DMADP and IDP by monoterpene synthases (Pazouki & Niinemets, 2016), and a lack of an immediate response upon priming, differently from isoprene, might indicate shift of the substrate equilibrium to DMADP or limited monoterpene synthase

activity. Notably, a significant emission burst of monoterpenes was found at 72 hr after the priming (Figure 2c). This can reflect increase of the transcription of monoterpene synthase enzymes in the later stages of recovery (Kanagendran, Pazouki, Bichele, Külheim, & Niinemets, 2018; Pazouki et al., 2016). In addition, it can also indicate greater availability of precursors for monoterpene synthesis. If so, the enhanced pool of carbon substrates for monoterpene synthesis might not originate directly from photosynthesis as A remained unaffected during the recovery period, but from other sources, such as

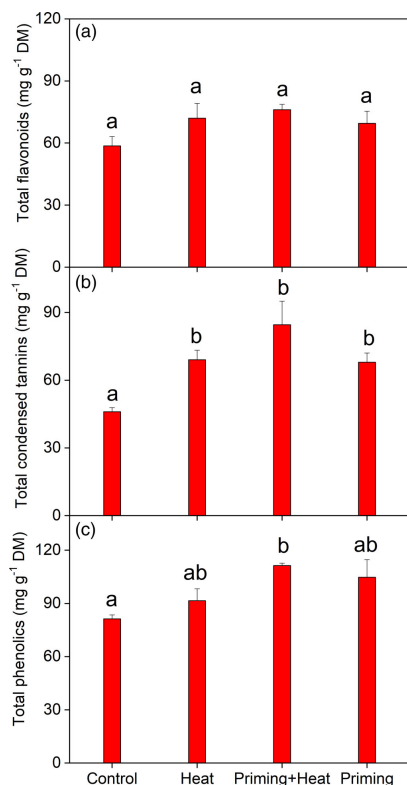


FIGURE 7 Concentrations of total flavonoids (a), total condensed tannins (b) and total phenolics (c) in control, heat shock stressed non-primed (Heat) and primed (Priming + Heat) leaves as well as non-stressed primed (Priming) *A. millefolium* leaves at 72 hr after the heat shock treatment was applied to stressed plants. The data shown are average \pm SE from three independent biological replicates. Total flavonoids and condensed tannins are expressed as mg g^{-1} DM of (+)-catechin equivalents, while total phenolic contents are expressed as mg g^{-1} DM of gallic acid equivalents. Different lowercase letters indicate significant differences between different treatments analysed by one-way analysis of variance (ANOVA) followed by Tukey's HSD post hoc tests [Colour figure can be viewed at [wileyonlinelibrary.com](https://onlinelibrary.wiley.com/doi/10.1111/pce.13810)]

starch (Ferner, Rennenberg, & Kreuzwieser, 2012; Kreuzwieser & Rennenberg, 2013; Schnitzler et al., 2004). We conclude that these concurrent events, including the increase of g_s , fast isoprene emission and progressively increased monoterpene emissions due to possible

substrate accumulation, or increased enzyme activity are involved in the defence mechanisms that primed *A. millefolium* employs to adapt to subsequent severe heat stress episodes.

4.2 | High potential VOC emissions enhanced tolerance of primed plants to severe heat stress

In agreement with previous studies (Kask et al., 2016; Pazouki et al., 2016), heat shock led to significant decreases in photosynthetic rates in *A. millefolium* plants (Figure 3a and Table 2). The primed plants had a higher tolerance to heat shock stress as photosynthetic characteristics were less affected and their recovery time was shorter (Figure 3a). A severe cellular damage reflected by long-term intense LOX compound emissions possibly explained the immediate decrease in A in non-primed plants in our study and in other studies (Hüve, Bichele, Rasulov, & Niinemets, 2011). A higher membrane-level damage in non-primed plants, moreover, is supported by a negative correlation between LOX compound emissions and A (Figure S1a). Differently from the primed plants, two LOX compound emission bursts occurred after the heat shock in non-primed plants, indicating the onset of LOX pathway gene expression level responses in the later recovery phase in non-primed plants (Jiang, Ye, Li, & Niinemets, 2017). Interestingly, the heat shock treatment could have suppressed the LOX pathway in primed plants as the LOX emissions in non-stressed primed plants actually occurred at a higher level during the whole recovery period (Figure 4a). Considering that plants during heat waves can lose up to 5% of photosynthetic carbon via VOC emissions including the release of LOX volatiles (Salomón, Rodríguez-Calcerrada, & Staudt, 2017), inhibition of LOX volatile emission can be one of the strategies of primed *A. millefolium* that allows saving resources for direct defences to cope with severe stresses, such as monoterpene synthesis in this study.

Stomatal closure might be another reason accounting for the decrease in A in heat stressed plants (Hasanuzzaman et al., 2013; Hüve et al., 2019). Given the increased C_i in both primed and non-primed plants under heat shock stress, non-stomatal rather than stomatal factors such as inactive PS II, ribulose-1,5-bisphosphate carboxylase/oxygenase, etc. were more likely to account for the reductions in A (Turan et al., 2019). Indeed, the current study found positive correlations between g_s and different VOC groups in heat shock stressed plants, mostly in primed plants (Figure S1g–j). Increased g_s cannot directly enhance emissions of most of the volatile compounds (Niinemets & Reichstein, 2003; Niinemets, Seufert, Steinbrecher, & Tenhunen, 2002). However, elevated g_s in primed plants contributes to a higher C_i and thereby to maintenance of the photosynthetic rate after the heat shock (Hasanuzzaman et al., 2013), even if heat shock did suppress leaf photosynthetic capacity. This in turn is expected to maintain the carbon flux to synthesis of key volatile groups, especially to isoprene and monoterpene synthesis.

Although isoprene emission was elicited by heat shock treatment in all plants, and in particular in non-primed plants, our results indicate that heat shock might differently affect isoprene synthesis and emission in non-primed and primed *A. millefolium* plants. Under non-stressed

TABLE 4 Average \pm SE contents (mg g⁻¹ DM) of individual phenolic compounds detected and quantified by HPLC-Q-ToF-MS/MS in non-primed (Heat) and primed (Priming + Heat) *A. millefolium* leaves subjected to heat shock stress and in non-stressed primed (Priming) and control plants after 72 hr of recovery time

Phenolic compounds	Control	Heat	Priming + Heat	Priming
<i>Caffeoylquinic acids</i>				
Caffeoylquinic acid I (Chlorogenic acid)	6.07 \pm 0.29 ^a	7.41 \pm 0.37 ^a	7.27 \pm 0.19 ^a	9.76 \pm 0.32 ^b
Caffeoylquinic acid II	0.410 \pm 0.066 ^a	0.680 \pm 0.028 ^{ab}	0.772 \pm 0.067 ^b	0.73 \pm 0.11 ^{ab}
Caffeoylquinic acid III	0.827 \pm 0.034 ^a	1.088 \pm 0.012 ^{ab}	1.184 \pm 0.036 ^{bc}	2.82 \pm 0.12 ^c
Caffeoylquinic acid IV	0.371 \pm 0.015 ^a	0.714 \pm 0.015 ^b	0.656 \pm 0.020 ^b	0.907 \pm 0.034 ^c
Total caffeoylquinic acids	7.67 \pm 0.37 ^a	9.89 \pm 0.36 ^b	9.89 \pm 0.17 ^b	14.22 \pm 0.28 ^c
<i>Dicaffeoylquinic acids</i>				
Dicaffeoylquinic acid I	0.32 \pm 0.28	1.31 \pm 0.63	0.79 \pm 0.15	0.82 \pm 0.45
Dicaffeoylquinic acid II	2.24 \pm 0.76	7.4 \pm 1.8	4.33 \pm 1.3	5.91 \pm 0.35
Dicaffeoylquinic acid III	9.8 \pm 1.0 ^a	11.48 \pm 0.19 ^a	11.93 \pm 0.37 ^a	16.25 \pm 0.67 ^b
Dicaffeoylquinic acid IV	4.53 \pm 0.21 ^a	9.51 \pm 0.27 ^c	7.87 \pm 0.10 ^b	9.57 \pm 0.45 ^c
Total dicaffeoylquinic acids	16.93 \pm 0.51 ^a	29.65 \pm 0.92 ^c	24.9 \pm 1.1 ^b	32.5 \pm 1.5 ^c
<i>Luteolin and luteolin derivatives</i>				
Luteolin glucuronide	0.44 \pm 0.13	0.31 \pm 0.12	0.56 \pm 0.14	0.808 \pm 0.051
Luteolin O-glucoside	0.038 \pm 0.026	0.0142 \pm 0.0055	0.067 \pm 0.025	0.0422 \pm 0.0059
Luteolin	0.0012 \pm 0.0012	N.D.	0.0008 \pm 0.0008	0.0007 \pm 0.0007
Total luteolin derivatives	0.47 \pm 0.16	0.33 \pm 0.12	0.63 \pm 0.16	0.851 \pm 0.050
<i>Apigenin derivatives</i>				
Apigenin C-hexoside-C-pentoside	0.0136 \pm 0.0064	0.0071 \pm 0.0016	0.0105 \pm 0.0031	0.041 \pm 0.019
Apigenin 6,8-di-C-glucoside	0.104 \pm 0.037	0.078 \pm 0.052	0.041 \pm 0.025	0.088 \pm 0.062
Total apigenin derivatives	0.117 \pm 0.044	0.085 \pm 0.052	0.052 \pm 0.028	0.129 \pm 0.060

Note: N.D., not detectable. Different letters indicate statistically significant differences ($p \leq .05$; $n = 3$) among the treatments as tested by one-way ANOVA followed by Tukey's HSD post hoc test. The roman numerals denote order of appearance for different compounds with distinct peaks on chromatograms within given compound classes.

Abbreviations: ANOVA, analysis of variance; VOCs, volatile organic compounds.

conditions, isoprene synthesis is closely connected to photosynthesis which provide carbon and energy for isoprene synthesis (Magel et al., 2006; Niinemets, Tenhunen, Harley, & Steinbrecher, 1999). However, the temperature optimum for isoprene synthesis is typically much higher, by 10°C or more than that for carbon assimilation (Rasulov, Hüve, Bichele, Laisk, & Niinemets, 2010). This could provide an explanation for the significant increase in isoprene emissions observed in non-primed plants under the heat stress (Figure 4b). Moreover, in non-primed plants, isoprene emission correlated negatively with A (Figure S1b), and accordingly the increased isoprene emission occurring at 5 hr in leaves with inhibited photosynthesis could have relied on alternative carbon sources (Kreuzwieser et al., 2002; Schnitzler et al., 2004). In the case of primed plants, heat shock treatment oppositely changed the positive correlation between isoprene emission and A, and suppression of isoprene emission after heat shock is surprising given that priming itself increased isoprene emission (Figures 4b and S1b). As discussed above, suppression of isoprene emission might reflect overall lower oxidative stress, changes in the share of carbon allocation between isoprene and monoterpene synthesis as well as enhancement of non-volatile metabolite production (see below, Table 4).

PCA results invariably underscored an essential role of monoterpenes (e.g., α - and β -pinene) in the response to heat shock stress in primed plants (Figure 5). In contrast to that found under moderate temperature (Niinemets et al., 2002; Peñuelas & Llusià, 2003; Wright et al., 2014), heat shock resulted in a negative correlation between monoterpene emission and A in primed *A. millefolium* plants (Figure S1c). Those emitted monoterpenes can originate either from specialized storage tissues such as glandular trichomes on leaf surface or from a non-specific storage in cellular membranes, or de novo synthesis (Borgen et al., 2012; Figueiredo & Pais, 1994; Niinemets, 2010; Niinemets & Reichstein, 2003). Considering the accumulated monoterpenes prior to the heat shock treatment, in primed plants the immediate rise of monoterpene emissions after the heat shock could come from the storage pool, for instance the pool in glandular trichomes. However, de novo synthesis of monoterpenes might also contribute to this emission burst in stressed primed plants as such a negative correlation between monoterpene emission and A also existed in non-stressed primed plants (Figure S1c). In contrast to stressed primed plants, correlations existing positively between monoterpene and LOX emissions but negatively between A and LOX emissions indicated increased monoterpene emissions in non-primed plants might be due to membrane damage.

Moreover, the lack of substrate could be a limiting factor for monoterpene synthesis in heat shock stressed plants (Pazouki et al., 2016). Sufficient accumulation of active metabolites (precursors) is another advantage that primed plants possess over non-primed plants when both are subjected to severe stress conditions (Ton et al., 2009). This, together with the onset of gene expression, could be the main reasons for the monoterpene burst at 72 hr priming recovery interval and immediately after the heat shock in primed *A. millefolium* plants (Figures 2c and 4c). Another factor that can contribute to changes in MEP/DOXP substrate pool size is increased rate of chloroplastic carotenoid synthesis (GGDP pathway) due to enhanced carotenoid turnover (Kask et al., 2016). However, regardless of priming treatment, both emissions of monoterpenes and the GGDP pathway compounds, 6-methyl-5-heptene-2-one and geranylacetone in stressed *A. millefolium* plants, were increased at 72 hr since the heat shock (Figure 4c; Table 3), suggesting that monoterpene synthesis was not limited by carotenoid turnover.

Heat shock in *A. millefolium* induced considerable sesquiterpene emissions, although at a relatively low level and mainly in the primed plants (Figure 4d). In agreement with the measurements in field-grown *A. millefolium* (Pazouki et al., 2015), β -caryophyllene was the dominant sesquiterpene emitted by primed *A. millefolium* foliage. Sesquiterpene synthesis normally occurs via MVA pathway in the cytosol, but sesquiterpenes can also be synthesized by multi-substrate terpene synthases in chloroplasts provided the substrate, farnesyl diphosphate, is available (Pazouki & Niinemets, 2016). MVA and MEP/DOXP pathways can exchange common precursors, typically IDP, through the plastid membranes (Laule et al., 2003), yet, this exchange occurs at a low level in non-stressed conditions (Laule et al., 2003; Rasulov, Talts, Kännaste, & Niinemets, 2015). Although the sesquiterpene emissions here might come from the glandular trichomes, heat shock induced a dramatic rise in monoterpene emissions in primed *A. millefolium* plants (Figure 4c,d), and accordingly, it cannot be ruled out that heat shock enhanced IDP transport from plastids to cytosol, leading to the enhancement of sesquiterpene emissions observed. This suggestion is supported by the positive correlation observed between monoterpene and sesquiterpene emissions in the primed *A. millefolium* plants (Figure 6b). In non-primed plants, the induced sesquiterpene emissions (Figure 4d) can be attributed to membrane damage caused by heat shock, reflected in a positive association between sesquiterpene and LOX compound emissions (Figure 6f).

4.3 | Does the accumulation of phenolic compounds contribute to the enhanced heat tolerance observed in primed *A. millefolium* plants?

In the current study, benzaldehyde is the only benzenoid found in the constitutive VOC blend in *A. millefolium* foliage (Figure 4e). The significant increase in benzenoid emissions observed during the recovery period is a robust indicator that heat shock triggered certain acclimation mechanisms, which engaged shikimate/phenylpropanoid pathway. In fact, one of the most conspicuous features of *A. millefolium* response to heat stress was that the primed *A. millefolium* plants

accumulated considerably higher phenolic contents than non-primed plants (Figure 7). Previous studies have demonstrated that flavonoids play an active role in quenching ROS in stressed plants (Di Ferdinando, Brunetti, Fini, & Tattini, 2012; Nakabayashi et al., 2014; Tattini et al., 2004). However, as the concentrations of individual flavonoids including luteolin, apigenin as well as their derivatives did not change in our study, the flavonoids were unlikely the phenolics group alleviating the heat damage during recovery in *A. millefolium* plants (Figure 7a; Table 4).

Content of condensed tannins was increased in primed *A. millefolium*, but it is not clear what is the role of this increase in heat tolerance (Figure 7b). Previous studies have associated the accumulation of condensed tannins to different environmental stresses including UV radiation, herbivory, tropospheric O₃ and so forth (Forkner, Marquis, & Lill, 2004; Lavola, Julkunen-Titto, de la Rosa, Lehto, & Aphalo, 2000; Peltonen, Vapaavuori, & Julkunen-titto, 2005). Condensed tannins also accumulate when plants are under moderate heat condition; however, the exact role of condensed tannins in heat shock tolerance is still not understood (Lees et al. 1994). Considering that the condensed tannins are stored in vacuoles, where the polymerization of condensed tannins is believed to further increase (Harding, 2019), it is possible that condensed tannins in primed *A. millefolium* plants had accumulated already during the priming phase. Although the condensed tannins are polymers of well-known antioxidant monomers, due to their strong protein coagulation activity, it is unlikely that they play a direct antioxidant role outside the vacuole (Adamczyk, Simon, Kitunen, Adamczyk, & Smolander, 2017; Sato & Matsui, 2012). Instead, given the increased total phenolic contents in primed plants (Figure 7c), increased accumulation of condensed tannins might reflect the overall increase in the activity of phenolic biosynthesis pathways due to enhanced precursor availability.

CQAs and diCQAs, both potent antioxidants, were the dominant individual phenolic compounds in *A. millefolium* foliar extracts (Table 4; Figure S2), consistent with the findings of Vitalini et al. (2011). Given the antioxidative properties of different CQA compounds (Oh, Carey, & Rajashekar, 2009), CQA accumulation might be involved in heat shock protection, especially in the primed *A. millefolium* plants that had 1.8-fold higher leaf CQA content prior to heat stress application than that in the non-primed control plants (Table 4). The decrease in the content of CQA in stressed primed *A. millefolium* plants compared to non-stressed primed plants supports the hypothesis that CQA might directly function as ROS quenchers.

Interestingly, heat shock-induced diCQA accumulation was higher in non-primed *A. millefolium* plants than in the primed plants (Table 4). Given that diesters possess higher antioxidant properties than monoesters (Mondolot et al., 2006), higher concentration of diCQAs together with CQAs suggests a stronger antioxidative potential in non-primed *A. millefolium* plants. Nevertheless, similarly to the CQA, diCQA level in stressed primed plants was lower than in non-stressed primed plants, again suggesting that diCQA participated in quenching of ROS. In comparison to primed plants, non-primed plants were predicted to suffer more from oxidative stress brought about by heat shock and the recovery was much delayed (Figure 3). Thus, although diCQA was assumed to play a similar antioxidant role, the relatively higher diCQA accumulation

in non-primed plants might be insufficient to protect from heat shock stress.

5 | CONCLUSIONS

The present study investigated the mechanisms of how heat priming treatment enhances tolerance to subsequent heat shock stresses in *A. millefolium* plants. The primed *A. millefolium* plants showed higher tolerance to heat shock, characterised by smaller reductions in photosynthesis rate and shorter recovery time. The results indicate that *A. millefolium* plants show complex response mechanisms by adjusting different secondary metabolic pathways. Under moderate heat stress (priming), isoprene and monoterpene syntheses via MEP/DOXP pathway are expected to play an important role in mitigating corresponding stress, while the stress severity increases, sesquiterpene synthesis via the MVA pathway, possibly together with intermediate contribution from MEP/DOXP pathway, is further elicited. Under heat shock, primed plants clearly prioritized certain metabolic pathways (monoterpene vs. LOX compound syntheses) and particular group of metabolites (monoterpenes vs. isoprene). Moreover, the significant accumulation of total phenolic compounds in heat shock treated plants suggests occurrence of certain adjustments in shikimate/phenylpropanoid pathway under heat stress. The increase in condensed tannins and CQAs at the end of the heat shock recovery period suggests that the two groups of phenolic compounds can be essential in coping with heat shock stress in primed *A. millefolium* plants. Although the positive correlations between monoterpenes and benzaldehyde emissions in heat shock treated *A. millefolium* plants provided evidence of the cooperation of terpenoid and aromatic compound synthesis pathways, further studies are still required to explore the nature of the time-dependent interactions between the terpenoid and phenolics synthesis pathways in stressed *A. millefolium* plants.

ACKNOWLEDGMENT

This work was supported by the grants from European Regional Development Fund (Centre of Excellence EcolChange), European Research Council (grant 322603, SIP-VOL+), Estonian Research Council (team grant project PRG947), and Estonian University of Life Sciences (baseline-funded project P190252PKTT). L. Z. was supported by Archimedes Foundation (Scholarships for International Researchers and Academic Staff), National Natural Science Foundation of China (31711530648), and Northeast Agricultural University (Academic backbone Project, 18XG07). The authors thank Lauri Laanisto, for providing the *A. millefolium* seeds used in this study, and also Ilmar-Jürgen Rammi, for growing and maintaining the plants.

CONFLICT OF INTEREST

The authors declare no conflicts of interest.

ORCID

Bin Liu  <https://orcid.org/0000-0003-4738-8690>

Ülo Niinemets  <https://orcid.org/0000-0002-3078-2192>

REFERENCES

- Adamczyk, B., Simon, J., Kitunen, V., Adamczyk, S., & Smolander, A. (2017). Tannins and their complex interaction with different organic nitrogen compounds and enzymes: Old paradigms versus recent advances. *ChemistryOpen*, 6(5), 610–614.
- Bitá, C., & Gerats, T. (2013). Plant tolerance to high temperature in a changing environment: Scientific fundamentals and production of heat stress-tolerant crops. *Frontiers in Plant Science*, 4, 273.
- Borgen, B., Ahuja, I., Thangstad, O., Honne, B., Rohloff, J., Rossiter, J., & Bones, A. (2012). 'Myrosin cells' are not a prerequisite for aphid feeding on oilseed rape (*Brassica napus*) but affect host plant preferences. *Plant Biology*, 14(6), 894–904.
- Brilli, F., Ruuskanen, T. M., Schnitzhofer, R., Müller, M., Breitenlechner, M., Bittner, V., ... Hansel, A. (2011). Detection of plant volatiles after leaf wounding and darkening by proton transfer reaction "time-of-flight" mass spectrometry (PTR-TOF). *PLoS One*, 6(5), e20419.
- Conrath, U., Beckers, G. J., Flors, V., Garcia-Agustin, P., Jakab, G., Mauch, F., & Pozo, M. J. (2006). Priming: Getting ready for battle. *Molecular Plant-Microbe Interactions*, 19(10), 1062–1071.
- Copolovici, L., Filella, I., Llusia, J., Niinemets, Ü., & Peñuelas, J. (2005). The capacity for thermal protection of photosynthetic electron transport varies for different monoterpenes in *Quercus ilex*. *Plant Physiology*, 139(1), 485–496.
- Copolovici, L., Kännaste, A., Pazouki, L., & Niinemets, Ü. (2012). Emissions of green leaf volatiles and terpenoids from *Solanum lycopersicum* are quantitatively related to the severity of cold and heat shock treatments. *Journal of Plant Physiology*, 159(7), 664–672.
- Copolovici, L., Kännaste, A., Remmel, T., & Niinemets, Ü. (2014). Volatile organic compound emissions from *Alnus glutinosa* under interacting drought and herbivory stresses. *Environmental and Experimental Botany*, 100, 55–63.
- Copolovici, L., & Niinemets, Ü. (2010). Flooding induced emissions of volatile signalling compounds in three tree species with differing water-logging tolerance. *Plant, Cell & Environment*, 33(9), 1582–1594.
- Devi, M. J., & Reddy, V. R. R. (2018). Transpiration response of cotton to vapor pressure deficit and its relationship with stomatal traits. *Frontiers in Plant Science*, 9, 1572.
- di Ferdinando, M., Brunetti, C., Fini, A., & Tattini, M. (2012). Flavonoids as antioxidants in plants under abiotic stresses. In P. Ahmad & M. N. V. Prasad (Eds.), *Abiotic stress responses in plants* (pp. 159–179). New York, NY: Springer.
- Dicke, M., & Baldwin, I. T. (2010). The evolutionary context for herbivore-induced plant volatiles: Beyond the 'cry for help'. *Trends in Plant Science*, 15(3), 167–175.
- Fan, Y., Ma, C., Huang, Z., Abid, M., Jiang, S., Dai, T., & Han, X. (2018). Heat priming during early reproductive stages enhances thermo-tolerance to post-anthesis heat stress via improving photosynthesis and plant productivity in winter wheat (*Triticum aestivum* L.). *Frontiers in Plant Science*, 9, 805.
- Ferner, E., Rennenberg, H., & Kreuzwieser, J. (2012). Effect of flooding on C metabolism of flood-tolerant (*Quercus robur*) and non-tolerant (*Fagus sylvatica*) tree species. *Tree Physiology*, 32(2), 135–145.
- Feussner, I., & Wasternack, C. (2002). The lipoxygenase pathway. *Annual Review of Plant Biology*, 53(1), 275–297.
- Figueiredo, A. C., & Pais, M. S. S. (1994). Ultrastructural aspects of the glandular cells from the secretory trichomes and from the cell suspension cultures of *Achillea millefolium* L. ssp. *millefolium*. *Annals of Botany*, 74(2), 179–190.
- Forkner, R. E., Marquis, R. J., & Lill, J. T. (2004). Feeny revisited: Condensed tannins as anti-herbivore defences in leaf-chewing herbivore communities of *Quercus*. *Ecological Entomology*, 29(2), 174–187.
- Frost, C. J., Mescher, M. C., Carlson, J. E., & de Moraes, C. M. (2008). Plant defense priming against herbivores: Getting ready for a different battle. *Plant Physiology*, 146(3), 818–824.
- Harding, S. A. (2019). Condensed tannins: Arbiters of abiotic stress tolerance? *Tree Physiology*, 39(3), 341–344.

- Hasanzaman, M., Nahar, K., Alam, M., Roychowdhury, R., & Fujita, M. (2013). Physiological, biochemical, and molecular mechanisms of heat stress tolerance in plants. *International Journal of Molecular Sciences*, 14(5), 9643–9684.
- Havaux, M. (1993). Rapid photosynthetic adaptation to heat stress triggered in potato leaves by moderately elevated temperatures. *Plant, Cell & Environment*, 16(4), 461–467.
- Herrmann, K. M., & Weaver, L. M. (1999). The shikimate pathway. *Annual Review of Plant Biology*, 50(1), 473–503.
- Holopainen, J. K., & Gershenzon, J. (2010). Multiple stress factors and the emission of plant VOCs. *Trends in Plant Science*, 15(3), 176–184.
- Hüve, K., Bichele, I., Kaldmäe, H., Rasulov, B., Valladares, F., & Niinemets, Ü. (2019). Responses of aspen leaves to heatflecks: Both damaging and non-damaging rapid temperature excursions reduce photosynthesis. *Plants*, 8(6), 145.
- Hüve, K., Bichele, I., Rasulov, B., & Niinemets, Ü. (2011). When it is too hot for photosynthesis: Heat-induced instability of photosynthesis in relation to respiratory burst, cell permeability changes and H₂O₂ formation. *Plant, Cell & Environment*, 34(1), 113–126.
- IPCC. (2018). *Global warming of 1.5°C: An IPCC special report on the impacts of global warming of 1.5°C above pre-industrial levels and related global greenhouse gas emission pathways, in the context of strengthening the global response to the threat of climate change, sustainable development, and efforts to eradicate poverty*. Geneva: Intergovernmental Panel on Climate Change.
- Jiang, Y., Ye, J., Li, S., & Niinemets, Ü. (2017). Methyl jasmonate-induced emission of biogenic volatiles is biphasic in cucumber: A high-resolution analysis of dose dependence. *Journal of Experimental Botany*, 68(16), 4679–4694.
- Kanagendran, A., Pazouki, L., Bichele, R., Külheim, C., & Niinemets, Ü. (2018). Temporal regulation of terpene synthase gene expression in *Eucalyptus globulus* leaves upon ozone and wounding stresses: Relationships with stomatal ozone uptake and emission responses. *Environmental and Experimental Botany*, 155, 552–565.
- Kanagendran, A., Pazouki, L., & Niinemets, Ü. (2018). Differential regulation of volatile emission from *Eucalyptus globulus* leaves upon single and combined ozone and wounding treatments through recovery and relationships with ozone uptake. *Environmental and Experimental Botany*, 145, 21–38.
- Kännaste, A., Copolovici, L., & Niinemets, Ü. (2014). Gas chromatography-mass spectrometry method for determination of biogenic volatile organic compounds emitted by plants. In M. Rodríguez-Concepción (Ed.), *Plant isoprenoids: Methods and protocols* (pp. 161–169). New York, NY: Springer Science + Business Media.
- Kask, K., Kännaste, A., Talts, E., Copolovici, L., & Niinemets, Ü. (2016). How specialized volatiles respond to chronic and short-term physiological and shock heat stress in *Brassica nigra*. *Plant, Cell & Environment*, 39(9), 2027–2042.
- Kim, K., & Portis, A. R., Jr. (2005). Temperature dependence of photosynthesis in *Arabidopsis* plants with modifications in Rubisco activase and membrane fluidity. *Plant and Cell Physiology*, 46(3), 522–530.
- Kreuzwieser, J., Graus, M., Wisthaler, A., Hansel, A., Rennenberg, H., & Schnitzler, J. P. (2002). Xylem-transported glucose as an additional carbon source for leaf isoprene formation in *Quercus robur*. *New Phytologist*, 156(2), 171–178.
- Kreuzwieser, J., & Rennenberg, H. (2013). Flooding-driven emissions from trees. In Ü. Niinemets & R. K. Monson (Eds.), *Biology, controls and models of tree volatile organic compound emissions* (Vol. 5, pp. 237–252). Berlin, Germany: Springer.
- Laule, O., Fährholz, A., Chang, H.-S., Zhu, T., Wang, X., Heifetz, P. B., ... Lange, M. (2003). Crosstalk between cytosolic and plastidial pathways of isoprenoid biosynthesis in *Arabidopsis thaliana*. *Proceedings of the National Academy of Sciences*, 100(11), 6866–6871. <https://doi.org/10.1073/pnas.1031755100>
- Lavola, A., Julkunen-Tiitto, R., de la Rosa, T. M., Lehto, T., & Aphalo, P. J. (2000). Allocation of carbon to growth and secondary metabolites in birch seedlings under UV-B radiation and CO₂ exposure. *Physiologia Plantarum*, 109(3), 260–267.
- Lees, G. L., Hinks, C. F., & Suttill, N. H. (1994). Effect of high temperature on condensed tannin accumulation in leaf tissues of big trefoil (*Lotus uliginosus* Schkuhr). *Journal of the Science of Food and Agriculture*, 65(4), 415–421.
- Leuning, R. (1995). A critical appraisal of a combined stomatal-photosynthesis model for C₃ plants. *Plant, Cell & Environment*, 18(4), 339–355.
- Li, S., Harley, P. C., & Niinemets, Ü. (2017). Ozone-induced foliar damage and release of stress volatiles is highly dependent on stomatal openness and priming by low-level ozone exposure in *Phaseolus vulgaris*. *Plant, Cell & Environment*, 40(9), 1984–2003.
- Liu, B., Kaurilind, E., Jiang, Y., & Niinemets, Ü. (2018). Methyl salicylate differently affects benzenoid and terpenoid volatile emissions in *Betula pendula*. *Tree Physiology*, 38(10), 1513–1525.
- Liu, B., Marques dos Santos, B., Kanagendran, A., Neilson, E. H. J., & Niinemets, Ü. (2019). Ozone and wounding stresses differently alter the temporal variation in formylated phenylpropanoids in *Eucalyptus globulus* leaves. *Metabolites*, 9(3), 46.
- Loreto, F., Förster, A., Dürr, M., Ciský, O., & Seufert, G. (1998). On the monoterpene emission under heat stress and on the increased thermotolerance of leaves of *Quercus ilex* L. fumigated with selected monoterpenes. *Plant, Cell & Environment*, 21(1), 101–107.
- Loreto, F., Pinelli, P., Manes, F., & Kollist, H. (2004). Impact of ozone on monoterpene emissions and evidence for an isoprene-like antioxidant action of monoterpenes emitted by *Quercus ilex* leaves. *Tree Physiology*, 24(4), 361–367.
- Loreto, F., & Schnitzler, J.-P. (2010). Abiotic stresses and induced BVOCs. *Trends in Plant Science*, 15(3), 154–166.
- Loreto, F., & Velikova, V. (2001). Isoprene produced by leaves protects the photosynthetic apparatus against ozone damage, quenches ozone products, and reduces lipid peroxidation of cellular membranes. *Plant Physiology*, 127(4), 1781–1787.
- Luo, H.-B., Ma, L., Xi, H.-F., Duan, W., Li, S.-H., Loescher, W., & Wang, L.-J. (2011). Photosynthetic responses to heat treatments at different temperatures and following recovery in grapevine (*Vitis amurensis* L.) leaves. *PLoS One*, 6(8), e23033.
- Magel, E., Mayrhofer, S., Müller, A., Zimmer, I., Hamp, R., & Schnitzler, J.-P. (2006). Photosynthesis and substrate supply for isoprene biosynthesis in poplar leaves. *Atmospheric Environment*, 40, 138–151.
- Marias, D. E., Meinzer, F. C., & Still, C. (2017). Impacts of leaf age and heat stress duration on photosynthetic gas exchange and foliar non-structural carbohydrates in *Coffea arabica*. *Ecology and Evolution*, 7(4), 1297–1310.
- Martínez-Medina, A., Flors, V., Heil, M., Mauch-Mani, B., Pieterse, C. M., Pozo, M. J., ... Conrath, U. (2016). Recognizing plant defense priming. *Trends in Plant Science*, 21(10), 818–822.
- Mauch-Mani, B., Baccelli, I., Luna, E., & Flors, V. (2017). Defense priming: An adaptive part of induced resistance. *Annual Review of Plant Biology*, 68, 485–512.
- Mondolot, L., la Fisca, P., Butois, B., Talansier, E., de Kochko, A., & Campa, C. (2006). Evolution in caffeoylquinic acid content and histolocalization during *Coffea canephora* leaf development. *Annals of Botany*, 98(1), 33–40.
- Nakabayashi, R., Yonekura-Sakakibara, K., Urano, K., Suzuki, M., Yamada, Y., Nishizawa, T., & Shinozaki, K. (2014). Enhancement of oxidative and drought tolerance in *Arabidopsis* by over-accumulation of antioxidant flavonoids. *The Plant Journal*, 77(3), 367–379.
- Niinemets, Ü. (2010). Mild versus severe stress and BVOCs: Thresholds, priming and consequences. *Trends in Plant Science*, 15(3), 145–153.

- Niinemets, Ü. (2018). When leaves go over the thermal edge. *Plant, Cell & Environment*, 41(6), 1247–1250.
- Niinemets, Ü., Kännaste, A., & Copolovic, L. (2013). Quantitative patterns between plant volatile emissions induced by biotic stresses and the degree of damage. *Frontiers in Plant Science*, 4, 262.
- Niinemets, Ü., Kuhn, U., Harley, P. C., Staudt, M., Armeth, A., Cescatti, A., & Peñuelas, J. (2011). Estimations of isoprenoid emission capacity from enclosure studies: Measurements, data processing, quality and standardized measurement protocols. *Biogeosciences*, 8(8), 2209–2246. <https://doi.org/10.5194/bg-8-2209-2011>
- Niinemets, Ü., & Reichstein, M. (2003). Controls on the emission of plant volatiles through stomata: Differential sensitivity of emission rates to stomatal closure explained. *Journal of Geophysical Research: Atmospheres*, 108, 4208.
- Niinemets, Ü., Seufert, G., Steinbrecher, R., & Tenhunen, J. D. (2002). A model coupling foliar monoterpene emission to leaf photosynthetic characteristics in Mediterranean evergreen *Quercus* species. *New Phytologist*, 153(2), 257–275.
- Niinemets, Ü., Tenhunen, J., Harley, P., & Steinbrecher, R. (1999). A model of isoprene emission based on energetic requirements for isoprene synthesis and leaf photosynthetic properties for *Liquidambar* and *Quercus*. *Plant, Cell & Environment*, 22(11), 1319–1335.
- Oh, M.-M., Carey, E. E., & Rajashekar, C. (2009). Environmental stresses induce health-promoting phytochemicals in lettuce. *Plant Physiology and Biochemistry*, 47(7), 578–583.
- Panchuk, I. I., Volkov, R. A., & Schöffl, F. (2002). Heat stress-and heat shock transcription factor-dependent expression and activity of ascorbate peroxidase in *Arabidopsis*. *Plant Physiology*, 129(2), 838–853.
- Pastor, V., Luna, E., Ton, J., Cerezo, M., García-Agustín, P., & Flors, V. (2013). Fine tuning of reactive oxygen species homeostasis regulates primed immune responses in *Arabidopsis*. *Molecular Plant-Microbe Interactions*, 26(11), 1334–1344.
- Pazouki, L., Kanagendran, A., Li, S., Kännaste, A., Memari, H. R., Bichele, R., & Niinemetts, Ü. (2016). Mono- and sesquiterpene release from tomato (*Solanum lycopersicum*) leaves upon mild and severe heat stress and through recovery: From gene expression to emission responses. *Environmental and Experimental Botany*, 132(1–15), 1–15.
- Pazouki, L., Memari, H. R., Kännaste, A., Bichele, R., & Niinemetts, Ü. (2015). Germacrene A synthase in yarrow (*Achillea millefolium*) is an enzyme with mixed substrate specificity: Gene cloning, functional characterization and expression analysis. *Frontiers in Plant Science*, 6, 111.
- Pazouki, L., & Niinemetts, Ü. (2016). Multi-substrate terpene synthases: Their occurrence and physiological significance. *Frontiers in Plant Science*, 7, 1019.
- Peltonen, P. A., Vapaavuori, E., & Julkunen-tiitto, R. (2005). Accumulation of phenolic compounds in birch leaves is changed by elevated carbon dioxide and ozone. *Global Change Biology*, 11(8), 1305–1324.
- Peñuelas, J., & Llusià, J. (2003). BVOCs: Plant defense against climate warming? *Trends in Plant Science*, 8(3), 105–109.
- Perkins, S., Alexander, L., & Nairn, J. (2012). Increasing frequency, intensity and duration of observed global heatwaves and warm spells. *Geophysical Research Letters*, 39, L20714.
- Porta, H., & Rocha-Sosa, M. (2002). Plant lipoxygenases. Physiological and molecular features. *Plant Physiology*, 130(1), 15–21.
- Possell, M., & Loreto, F. (2013). The role of volatile organic compounds in plant resistance to abiotic stresses: Responses and mechanisms. In Ü. Niinemetts & R. K. Monson (Eds.), *Biology, controls and models of tree volatile organic compound emissions* (pp. 209–235). Berlin: Springer.
- Raal, A., Boikova, T., & Püssa, T. (2015). Content and dynamics of polyphenols in *Betula* spp. leaves naturally growing in Estonia. *Records of Natural Products*, 9(1), 41.
- Rasulov, B., Hüve, K., Bichele, I., Laisk, A., & Niinemetts, Ü. (2010). Temperature response of isoprene emission in vivo reflects a combined effect of substrate limitations and isoprene synthase activity: A kinetic analysis. *Plant Physiology*, 154(3), 1558–1570. <https://doi.org/10.1104/pp.110.162081>
- Rasulov, B., Talts, E., Kännaste, A., & Niinemetts, Ü. (2015). Bisphosphonate inhibitors reveal a large elasticity of plastic isoprenoid synthesis pathway in isoprene-emitting hybrid Aspen. *Plant Physiology*, 168(2), 532–548. <https://doi.org/10.1104/pp.15.00470>
- Rasulov, B., Talts, E., & Niinemetts, Ü. (2019). A novel approach for real-time monitoring of leaf wounding responses demonstrates unprecedentedly fast and high emissions of volatiles from cut leaves. *Plant Science*, 283, 256–265.
- Rivero, R. M., Ruiz, J. M., Garcia, P. C., Lopez-Lefebvre, L. R., Sánchez, E., & Romero, L. (2001). Resistance to cold and heat stress: Accumulation of phenolic compounds in tomato and watermelon plants. *Plant Science*, 160(2), 315–321.
- Saeidnia, S., Gohari, A., Mokhber-Dezfuli, N., & Kiuchi, F. (2011). A review on phytochemistry and medicinal properties of the genus *Achillea*. *DARU: Journal of Faculty of Pharmacy, Tehran University of Medical Sciences*, 19(3), 173.
- Salomón, R. L., Rodríguez-Calcerrada, J., & Staudt, M. (2017). Carbon losses from respiration and emission of volatile organic compounds—The overlooked side of tree carbon budgets. In E. Gil-Pelegrin, J. J. Peguero-Pina, & D. Sancho-Knapik (Eds.), *Oaks physiological ecology. Exploring the functional diversity of genus Quercus L.* (pp. 327–359). Cham: Springer International Publishing.
- Sato, F., & Matsui, K. (2012). Engineering the biosynthesis of low molecular weight metabolites for quality traits (essential nutrients, health-promoting phytochemicals, volatiles, and aroma compounds). In P. M. Hasegawa (Ed.), *Plant biotechnology and agriculture* (pp. 443–461). San Diego, CA: Academic Press.
- Schnitzler, J.-P., Graus, M., Kreuzwieser, J., Heizmann, U., Renneberg, H., Wisthaler, A., & Hansel, A. (2004). Contribution of different carbon sources to isoprene biosynthesis in poplar leaves. *Plant Physiology*, 135(1), 152–160.
- Serrano, N., Ling, Y., Bahieldin, A., & Mahfouz, M. M. (2019). Thermopriming reprograms metabolic homeostasis to confer heat tolerance. *Scientific Reports*, 9(1), 1–14.
- Sgarbi, E., Fornasiero, R. B., Lins, A. P., & Bonatti, P. M. (2003). Phenol metabolism is differentially affected by ozone in two cell lines from grape (*Vitis vinifera* L.) leaf. *Plant Science*, 165(5), 951–957.
- Sharkey, T. D. (2005). Effects of moderate heat stress on photosynthesis: Importance of thylakoid reactions, rubisco deactivation, reactive oxygen species, and thermotolerance provided by isoprene. *Plant, Cell & Environment*, 28(3), 269–277.
- Sharkey, T. D., Wiberley, A. E., & Donohue, A. R. (2008). Isoprene emission from plants: Why and how. *Annals of Botany*, 101(1), 5–18.
- Shinohara, T., & Leskovar, D. I. (2014). Effects of ABA, antitranspirants, heat and drought stress on plant growth, physiology and water status of artichoke transplants. *Scientia Horticulturae*, 165, 225–234.
- Silver, G. M., & Fall, R. (1991). Enzymatic synthesis of isoprene from dimethylallyl diphosphate in aspen leaf extracts. *Plant Physiology*, 97(4), 1588–1591.
- Singleton, V. L., & Rossi, J. A. (1965). Colorimetry of total phenolics with phosphomolybdic-phosphotungstic acid reagents. *American Journal of Enology and Viticulture*, 16(3), 144–158.
- Singsaas, E. L., Laporte, M. M., Shi, J.-Z., Monson, R. K., Bowling, D. R., Johnson, K., & Sharkey, T. D. (1999). Kinetics of leaf temperature fluctuation affect isoprene emission from red oak (*Quercus rubra*) leaves. *Tree Physiology*, 19(14), 917–924.
- Stewart-Jones, A., & Poppy, G. M. (2006). Comparison of glass vessels and plastic bags for enclosing living plant parts for headspace analysis. *Journal of Chemical Ecology*, 32(4), 845–864.
- Tattini, M., Galardi, C., Pinelli, P., Massai, R., Remorini, D., & Agati, G. (2004). Differential accumulation of flavonoids and hydroxycinnamates in leaves of *Ligustrum vulgare* under excess light and drought stress. *New Phytologist*, 163(3), 547–561.

- Tombesi, S., Nardini, A., Frioni, T., Soccolini, M., Zadra, C., Farinelli, D., & Palliotti, A. (2015). Stomatal closure is induced by hydraulic signals and maintained by ABA in drought-stressed grapevine. *Scientific Reports*, *5*, 12449.
- Ton, J., Ent, S., van Hulst, M., Pozo, M., Oosten, V. V., van Loon, L., & Pieterse, C. M. (2009). Priming as a mechanism behind induced resistance against pathogens, insects and abiotic stress. *IOBC/wprs Bulletin*, *44*, 3–13.
- Turan, S., Kask, K., Kanagendran, A., Li, S., Anni, R., Talts, E., & Niinemets, Ü. (2019). Lethal heat stress-dependent volatile emissions from tobacco leaves: What happens beyond the thermal edge? *Journal of Experimental Botany*, *70*(18), 5017–5030.
- Urban, J., Ingwers, M., McGuire, M. A., & Teskey, R. O. (2017). Stomatal conductance increases with rising temperature. *Plant Signaling & Behavior*, *12*(8), e1356534.
- Vacca, R. A., de Pinto, M. C., Valenti, D., Passarella, S., Marra, E., & De Gara, L. (2004). Production of reactive oxygen species, alteration of cytosolic ascorbate peroxidase, and impairment of mitochondrial metabolism are early events in heat shock-induced programmed cell death in tobacco Bright-Yellow 2 cells. *Plant Physiology*, *134*(3), 1100–1112.
- Velikova, V., Müller, C., Ghirardo, A., Rock, T. M., Aichler, M., Walch, A., & Schnitzler, J.-P. (2015). Knocking down of isoprene emission modifies the lipid matrix of thylakoid membranes and influences the chloroplast ultrastructure in poplar. *Plant Physiology*, *168*(3), 859–870.
- Velikova, V., Pinelli, P., & Loreto, F. (2005). Consequences of inhibition of isoprene synthesis in *Phragmites australis* leaves exposed to elevated temperatures. *Agriculture, Ecosystems & Environment*, *106*(2–3), 209–217.
- Vitalini, S., Beretta, G., Iriti, M., Orsenigo, S., Basilio, N., Dall'Acqua, S., & Fico, G. (2011). Phenolic compounds from *Achillea millefolium* L. and their bioactivity. *Acta Biochimica Polonica*, *58*, 203–212.
- Vogt, T. (2010). Phenylpropanoid biosynthesis. *Molecular Plant*, *3*(1), 2–20.
- von Caemmerer, S., & Farquhar, G. D. (1981). Some relationships between the biochemistry of photosynthesis and the gas exchange of leaves. *Planta*, *153*(4), 376–387.
- Wang, D., Heckathorn, S. A., Mainali, K., & Tripathee, R. (2016). Timing effects of heat-stress on plant ecophysiological characteristics and growth. *Frontiers in Plant Science*, *7*, 1629.
- Wang, X., Cai, J., Jiang, D., Liu, F., Dai, T., & Cao, W. (2011). Pre-anthesis high-temperature acclimation alleviates damage to the flag leaf caused by post-anthesis heat stress in wheat. *Journal of Plant Physiology*, *168*(6), 585–593.
- Wang, X., Cai, J., Liu, F., Dai, T., Cao, W., Wollenweber, B., & Jiang, D. (2014). Multiple heat priming enhances thermo-tolerance to a later high temperature stress via improving subcellular antioxidant activities in wheat seedlings. *Plant Physiology and Biochemistry*, *74*, 185–192.
- Wang, X., Cai, J., Liu, F., Jin, M., Yu, H., Jiang, D., & Cao, W. (2012). Pre-anthesis high temperature acclimation alleviates the negative effects of post-anthesis heat stress on stem stored carbohydrates remobilization and grain starch accumulation in wheat. *Journal of Cereal Science*, *55*(3), 331–336.
- Wang, X., Liu, F., & Jiang, D. (2017). Priming: A promising strategy for crop production in response to future climate. *Journal of Integrative Agriculture*, *16*(12), 2709–2716.
- Wright, L. P., Rohwer, J. M., Ghirardo, A., Hammerbacher, A., Ortiz-Alcaide, M., Raguschke, B., & Phillips, M. A. (2014). Deoxyxylulose 5-phosphate synthase controls flux through the methylerythritol 4-phosphate pathway in *Arabidopsis*. *Plant Physiology*, *165*(4), 1488–1504.
- Xia, J., Sinelnikov, I. V., Han, B., & Wishart, D. S. (2015). MetaboAnalyst 3.0-making metabolomics more meaningful. *Nucleic Acids Research*, *43*(W1), W251–W257.
- Xia, J., & Wishart, D. S. (2016). Using MetaboAnalyst 3.0 for comprehensive metabolomics data analysis. *Current Protocols in Bioinformatics*, *55*(1), 14.10.11–14.10.91.
- Xu, B., & Chang, K.-C. S. (2007). A comparative study on phenolic profiles and antioxidant activities of legumes as affected by extraction solvents. *Journal of Food Science*, *72*(2), S159–S166. <https://doi.org/10.1111/j.1750-3841.2006.00260.x>
- Yoshikawa, M., Luo, W., Tanaka, G., Konishi, Y., Matsuura, H., & Takahashi, K. (2018). Wounding stress induces phenylalanine ammonia lyases, leading to the accumulation of phenylpropanoids in the model liverwort *Marchantia polymorpha*. *Phytochemistry*, *155*, 30–36.
- Zhu, L., Bloomfield, K. J., Hocart, C. H., Egerton, J. J., O'Sullivan, O. S., Penillard, A., ... Atkin, O. K. (2018). Plasticity of photosynthetic heat tolerance in plants adapted to thermally contrasting biomes. *Plant, Cell & Environment*, *41*(6), 1251–1262.

SUPPORTING INFORMATION

Additional supporting information may be found online in the Supporting Information section at the end of this article.

How to cite this article: Liu B, Zhang L, Rusalepp L, et al. Heat priming improved heat tolerance of photosynthesis, enhanced terpenoid and benzenoid emission and phenolics accumulation in *Achillea millefolium*. *Plant Cell Environ*. 2021;44:2365–2385. <https://doi.org/10.1111/pce.13830>



Sulaiman, HY, Liu, B, Abiola, YO, Kaurilind, E and Niinemets, Ü, 2023. Impact of heat priming on heat shock responses in *Origanum vulgare*: Enhanced foliage photosynthetic tolerance and biphasic emissions of volatiles. *Plant Physiology and Biochemistry* 196: 567-579.



Impact of heat priming on heat shock responses in *Origanum vulgare*: Enhanced foliage photosynthetic tolerance and biphasic emissions of volatiles

Hassan Yusuf Sulaiman^{a,*}, Bin Liu^{a,**}, Yusuph Olawale Abiola^a, Eve Kaurilind^a, Ülo Niinemets^{a,b}

^a Chair of Crop Science and Plant Biology, Estonian University of Life Sciences, Kreutzwaldi 1, 51006, Tartu, Estonia

^b Estonian Academy of Sciences, Kohtu 6, 10130, Tallinn, Estonia

ARTICLE INFO

Keywords:

Benzenoids
Heat acclimation
Heat stress responses
Lipoxygenase volatiles
Monoterpenes
Photosynthesis
Rubisco activity
Sesquiterpenes
Volatile organic compounds

ABSTRACT

Climate change enhances the frequency of heatwaves that negatively affect photosynthesis and can alter constitutive volatile emissions and elicit emissions of stress volatiles, but how pre-exposure to mildly warmer temperatures affects plant physiological responses to subsequent severe heat episodes remains unclear, especially for aromatic plants with high and complex volatile defenses. We studied the impact of heat shock (45 °C/5 min) applied alone and after exposure to moderate heat stress (35 °C/1 h, priming) on foliage photosynthesis and volatile emissions in the aromatic plant *Origanum vulgare* through 72 h recovery period. Heat stress decreased photosynthesis rates and stomatal conductance, whereas the reductions in photosynthesis were primarily due to non-stomatal factors. In non-primed plants, heat shock-induced reductions in photosynthetic activity were the greatest, but photosynthetic activity completely recovered by the end of the experiment. In primed plants, a certain inhibition of photosynthetic activity remained, suggesting a sustained priming effect. Heat shock enhanced the emissions of volatiles including lipoxygenase pathway volatiles, long-chained fatty acid-derived compounds, mono- and sesquiterpenes, geranylgeranyl diphosphate pathway volatiles, and benzenoids, whereas different heat treatments resulted in unique emission blends. In non-primed plants, stress-elicited emissions recovered at 72 h. In primed plants, volatile emissions were multiphasic, the first phase, between 0.5 and 10 h, reflected the primary stress response, whereas the secondary rise, between 24 and 72 h, indicated activations of different defense metabolic pathways. Our results demonstrate that exposure to mild heat leads to a sustained physiological stress memory that enhances plant resistance to subsequent severe heat stress episodes.

1. Introduction

Heat waves are predicted to occur more frequently as global warming progresses (Rahmstorf and Coumou, 2011). High-temperature stress in plants triggers physiological modifications that result in photosynthetic reductions and alterations in constitutive and stress-induced biogenic volatile emissions (Velikova et al., 2005; Copolovici et al., 2012). Exposure to moderate heat stress can induce a series of thermal acclimation responses, including activation of expression of heat shock proteins, accumulation of secondary metabolites, and chromatin remodeling and modification (Sanyal et al., 2018; Hilker and Schmittling, 2019; Niinemets, 2020; Guihur et al., 2022). Moderate

stress-mediated reprogramming of gene activation networks and metabolome leads to a tougher, stress-conditioned phenotype, and such a heat-stress “memory” can remain active for several days to weeks (Sanyal et al., 2018; Hilker and Schmittling, 2019; Khan et al., 2022). Such acquired-stress tolerance prepares plants for subsequent stress exposure, a phenomenon known as defense priming. Priming reduces the direct effect of subsequent severe stress by facilitating maximal functioning and recovery of physiological processes (Wang et al., 2014; Abid et al., 2016; Khan et al., 2022). For instance, in *Triticum aestivum*, heat priming enhanced photosynthetic capacity via increased antioxidant activity (Fan et al., 2018). In *Achillea millefolium*, priming improved photosynthetic recovery and enhanced the synthesis of antioxidative secondary metabolites (Liu et al., 2021).

* Corresponding author.

** Corresponding author.

E-mail addresses: Hassan@emu.ee (H.Y. Sulaiman), Bin.liu@emu.ee (B. Liu).

<https://doi.org/10.1016/j.plaphy.2023.02.013>

Received 9 December 2022; Received in revised form 21 January 2023; Accepted 7 February 2023

Available online 9 February 2023

0981-9428/© 2023 Elsevier Masson SAS. All rights reserved.

Abbreviations

A	net assimilation rate
C_i	intercellular concentrations of CO ₂
DOXP	1-deoxy-D-xylulose 5-phosphate
FAD	long-chained fatty acid-derived compounds
GGDP	geranylgeranyl diphosphate
g_s	stomatal conductance
LOX	lipoxygenase
MEP	2-C-methyl-D-erythritol 4-phosphate
MeSA	methyl salicylate
PPFD	photosynthetic photon flux density
Rubisco	ribulose-1,5-bisphosphate carboxylase oxygenase
V_{max}	Rubisco carboxylase activity
VOC	volatile organic compounds

Photosynthesis is a complex physiological process involving photosynthetic electron transport, photophosphorylation, and carbon assimilation, and the underlying mechanism of heat stress inhibition of photosynthesis is equally complex. Heat stress can reduce photosynthesis by limiting stomatal diffusion, photosynthetic electron transport and photophosphorylation, or the activity of ribulose-1,5-bisphosphate carboxylase-oxygenase (Rubisco), the key enzyme for carbon fixation (Salvucci and Crafts-Brandner, 2004; Moore et al., 2021). At temperatures just above the thermal optimum, both stomatal and biochemical factors may play an important role in limiting photosynthesis and the contribution of either factor is largely species-dependent (Kask et al., 2016; Turan et al., 2019; Okereke et al., 2021). Under extreme temperatures, the mechanism underlying reductions in photosynthesis is less clear, and once the thermal threshold is exceeded, photosynthesis starts to decrease in a time-dependent manner even after returning to lower temperatures (Hüve et al., 2011, 2019; Niinemets, 2018). In several species, the association between net CO₂ assimilation rates (A) and stomatal conductance to water vapor (g_s) is decoupled under severe heat stress (Copolovici et al., 2012; Kask et al., 2016). In such a case, photosynthesis may be directly constrained by inhibition of activities of photosynthetic electron transport and/or Rubisco. Reductions in the activities of biochemical processes can be completely reversible after exposure to moderate heat stress, but lethal stress can involve irreversible damages, and recovery might not occur (Crafts-Brandner and Law, 2000; Haldimann and Feller, 2004; Hüve et al., 2011). Although heat priming can improve heat resistance of photosynthesis and prevent the complete destruction of the photosynthetic machinery, improvements in resistance might be coupled with reduced photosynthetic activity in non-stressed conditions due to the maintenance of primed state (Cen and Sage, 2005; Wahid et al., 2007). However, there is limited information on potential interactions between heat stress priming and the degree of recovery after exposure to severe heat stress.

Typically, lipoxygenase (LOX) pathway volatiles, also called green leaf volatiles, including different C₅–C₆ aldehydes and alcohols are among the earliest volatiles elicited upon heat shock stress (Copolovici et al., 2012; Chatterjee et al., 2020; Sulaiman et al., 2021). Emissions of LOX pathway volatiles are quantitatively associated with the severity of stress and damage sustained (Niinemets, 2010; Copolovici et al., 2011; Niinemets et al., 2013). Shortly after the LOX emission burst, typically in a few hours, stressed plants activate different defense pathways, leading to the emissions of different specialized volatiles including isoprenoids (homo-, mono-, sesquiterpenes and their derivatives) from plastidial 2-C-methyl-D-erythritol 4-phosphate/1-deoxy-D-xylulose 5-phosphate (MEP/DOXP) and cytosolic mevalonate pathways (Dudareva et al., 2005; Sallaud et al., 2009), benzenoid compounds including methyl salicylate (MeSA) and benzaldehyde from plastidial shikimate pathway (Misztal et al., 2015; Sulaiman et al., 2021). In addition, heat stress often

triggers the emissions of carotenoid breakdown products from the geranylgeranyl diphosphate (GGDP) pathway in the plastid (García-Plazaola et al., 2017; Chatterjee et al., 2020; Okereke et al., 2021). The onset of stress-induced volatiles signals the activation of key defense pathways, and the volatile emissions elicited by heat stress often reflect stress severity (Kask et al., 2016; Turan et al., 2019). Furthermore, the emissions of antioxidant volatiles including terpenoids and benzenoids play an important role in heat stress recovery by quenching reactive oxidative species in the plant lipid phase and by activating systemic resistance (Harrison et al., 2013; Faralli et al., 2020). Changes in the activity of volatile emission pathways initiated by historical heat episodes can affect volatile emission responses during subsequent severe heat stress episodes (Bruce et al., 2007; Holopainen and Gershenson, 2010). However, there is limited information on how pre-heat exposure-induced modifications in the magnitude of emissions and emission profiles are associated with plant response to severe heat stress and recovery from severe heat stress.

We investigated the impact of moderate heat stress exposure (35 °C/1 h) on foliage photosynthetic characteristics and volatile organic compound (VOC) emissions in the cosmopolitan aromatic crop plant *Origanum vulgare* L. (Lamiaceae) during subsequent severe heat stress (45 °C/5 min; heat shock). The foliage of *O. vulgare* contains a high amount of terpenoids and phenolic compounds due to the presence of glandular trichomes on the leaf surface (Gutiérrez-Grijalva et al., 2017; Lombrea et al., 2020). Thus *O. vulgare* is a representative model for studying stress-dependent changes in secondary metabolism in species with high constitutive activity of secondary metabolic pathways. Our study provides evidence of strong interactive effects of heat priming and heat shock responses on stress response and recovery of photosynthesis and volatile emissions. In particular, we demonstrate that 1) moderate heat stress (priming) decreases photosynthesis rate and modifies secondary metabolic pathways as reflected in enhanced emissions of LOX compounds and terpenoids; 2) heat stress-induced reductions in photosynthesis are primarily due to non-stomatal factors 3) heat shock-induced photosynthetic reductions are lower and recovery of photosynthesis is faster in primed plants 4) heat shock application induces unique volatile emission blends in primed and non-primed plants.

2. Material and methods

2.1. Plant material

Origanum vulgare plants were grown from seed obtained from Nordic Botanical Ltd (Tartu, Estonia). The seeds were sown in 0.5 l plastic pots filled with a 1:1 mixture of quartz and commercial potting soil containing slow-release micro- and macronutrients (Biolan Oy, Kekkila group, Finland). The plants were cultivated in a growth room with an ambient CO₂ concentration of 380–400 μmol mol⁻¹, day/night temperatures of 25/18 °C, relative humidity of 60–70% and photosynthetic photon flux density (PPFD) of 800 μmol m⁻² s⁻¹ at plant level supplied for 12 h photoperiod. The plants were irrigated to soil field capacity every two days. The experiment was carried out with three-month-old plants. Fully mature upper canopy leaves were used in the experiments. Sampled upper canopies had 8–12 leaves and an average total leaf area of 15.2 ± 1.4 cm² (n = 12).

2.2. Application of moderate heat priming treatment

Priming treatment was applied by enclosing the leaves in a temperature-controlled glass chamber of a customized gas-exchange measurement system (section 2.4 for details of the system and glass chamber) for 1 h, from 08:00 to 09:00. The set atmospheric conditions in the chamber were similar to the plant growth conditions, except that chamber temperature was set at 35 °C (leaf temperature = 35 ± 1 °C). Immediately after the priming application, the chamber temperature was reset to 25 °C. The priming treatment was applied to six plants, and

in three of the treated plants, gas exchange characteristics were measured right after the priming application. The remaining three plants were returned to the growth conditions for 72 h and then subjected to heat shock treatment.

2.3. Heat shock application

Heat shock was applied using the standard procedure described by Kask et al. (2016), Liu et al. (2021), and Sulaiman et al. (2021). In summary, experimental leaves were enclosed in a chemically inert polyester bag (cooking bag), to prevent direct contact with water, and immediately immersed in water kept at a stable temperature of 45 °C in a temperature-controlled water bath (VWR International, Radnor, PA, USA). The experimental leaves were kept in the medium for 5 min, plus additional 30 s to account for the finite thermal conductivity of the polyester bag. The heat shock treatment was applied to three non-primed plants and three primed plants. The leaves were carefully removed from the polyester bag immediately after heat shock treatment, and inserted in the gas exchange measurement chamber for photosynthetic measurements and volatile sampling. Three independent control plants were treated in the same way, except that the water temperature was 25 °C.

2.4. Gas exchange measurement and volatile sampling

Foliage photosynthetic characteristics were measured with a custom-made open gas exchange system (Copolovici and Niinemets, 2010 for details). The system had a 1.2 l temperature-controlled double-glass cylindrical chamber with a stainless steel bottom designed for sampling trace gases. Light was supplied by four 50 W halogen lamps positioned atop the chamber. For temperature control, water with a set temperature was circulated between the chamber's double glass layers. Air temperature in the chamber was monitored by a thermistor (NTC, model ACC-001, RTI Electronics, Inc., St. Anaheim, CA, USA). The chamber was flushed with ambient air drawn from outside the building (air flow rate 0.036 L s⁻¹). The air entering the chamber was purified by passing through a custom-made ozone trap and a charcoal filter and humidified to the desired relative humidity with a custom-made humidifier. After leaf enclosure, standard measurement conditions of leaf temperature of 25 °C, leaf-to-air vapor pressure deficit of 1.7 kPa, PPFD of 800 μmol m⁻² s⁻¹ and CO₂ concentrations of 380–400 μmol mol⁻¹ were established. The leaf temperature was monitored by a thermocouple attached to the lower leaf surface. Concentrations of CO₂ and H₂O at the inlet and outlets of the chamber were measured using a dual-channel infrared gas analyzer (CIRAS III, PP-systems, Amesbury, MA, USA). Gas exchange measurements were conducted immediately after leaf gas exchange rates had attained a steady-state rate, typically in ca. 18–20 min after leaf enclosure. Measurements were conducted at 0.5, 5 h, 10, 24, 48, and 72 h after treatment.

Volatiles were collected simultaneously with gas exchange measurements. A suction pump (210–1003 MTX, SKC Inc., Houston, TX, USA) operated at a constant flow rate of 0.2 L min⁻¹ for 20 min was used to collect volatiles onto a stainless steel adsorbent cartridge filled with three different carbon-based adsorbents designed for maximum adsorption of C₃–C₁₇ volatiles (Kännaste et al., 2014 for a detailed description of the adsorbent cartridges and volatile sampling). Background volatile concentrations from the empty chamber were collected every day before leaf measurements. Measured leaves were photographed and leaf surface area was computed with ImageJ 1.8.0 (NIH, Bethesda, Maryland, USA).

The adsorbent cartridges were analyzed using a combined Shimadzu TD20 automated cartridge desorber and Shimadzu 2010 GC-MS system (Shimadzu Corporation, Kyoto, Japan) as described in Kännaste et al. (2014). Volatile compounds were identified and quantified using pure chemical standards (Sigma-Aldrich, St. Louis, MO, USA) and NIST Mass Spectral Library ver. 0.5. The GC-MS chromatograms were analyzed

using the open-access program OpenChrom ver. 1.2.0 (Alder) (Wenig and Odermatt, 2010). Background volatile concentrations were subtracted from measurements with plants. The detected volatiles were grouped based on their biosynthesis pathways and analyzed as lipoxygenase (LOX) pathway volatiles (short-chained fatty acid-derived compounds; green leaf volatiles), long-chained saturated fatty acid-derived (FAD) compounds, carbohydrate derivatives (furans), terpenoids (isoprene, mono- and sesquiterpene), geranylgeranyl diphosphate pathway (GGDP) volatiles (carotenoid breakdown products) and benzenoids (Table 1 for the list of compounds). The compounds detected under non-stressed conditions were considered constitutive volatiles, whereas compounds detected only after the application of stress treatments were constitutive volatiles (Copolovici and Niinemets, 2016, Table 1).

Foliage net assimilation rate (*A*), intercellular CO₂ concentration (*C_i*), and stomatal conductance to water vapor (*g_s*) were computed according to von Caemmerer and Farquhar (1981), and volatile emission rates according to Niinemets et al. (2010). The maximum Rubisco carboxylase activity (*V_{max}*) was calculated according to De Kauwe et al. (2016) using the Rubisco kinetic characteristics of Galmés et al. (2016). As *C_i* was used as the substitute for chloroplastic CO₂ concentration, the estimates of *V_{max}* provide the apparent Rubisco maximum activity.

2.5. Statistical analyses

For all traits, averages with standard errors (SE) of three biological replicates in each treatment were calculated. The individual and interaction effects of heat priming, heat shock, and recovery time on plant physiological activities were tested using three-way ANOVA. Averages at different heat stress recovery time points were compared using Fisher's least significant difference (LSD) following one-way ANOVA. Where required, the data used for ANOVA were log-transformed to improve the normality of distribution. The relationships of *A* with *V_{max}* and VOC emissions were evaluated using linear regressions. The impacts of stress treatments on VOC emission blends were analyzed using the principal component analysis after mean-scaling of the data. All statistical tests were considered significant at *P* < 0.05. All statistical tests and visualizations were conducted with R ver 4.2.0 statistical software (R Core Team, 2021).

3. Results

3.1. Effects of heat priming and heat shock stress on photosynthetic characteristics

Moderate heat stress (priming) decreased net assimilation rate (*A*) two-fold throughout the recovery period, from 11 to 15 μmol m⁻² s⁻¹ in the control plants to 7–8 μmol m⁻² s⁻¹ (*P* < 0.05 for Priming, Fig. 1A). At 0.5 h after heat shock application, *A* was 23-fold lower in non-primed plants (*P* < 0.001 in comparison to control plants) and 10-fold lower in primed plants (*P* < 0.05 in comparison to control plants, Fig. 1A). In non-primed plants, *A* remained lower (*P* < 0.05) than in primed plants for 24 h after treatment (Fig. 1A). Net assimilation rates in primed plants and primed + heat shock-treated plants were similar (*P* > 0.05) except at 0.5 h after treatment (Fig. 1A). At the end of the experiment, *A* in non-primed plants had recovered fully to the level of control, but in non-primed plants, *A* was similar to the levels observed after priming treatment and somewhat lower than in control (Fig. 1A).

Overall, stomatal conductance to water vapor (*g_s*) was uncoupled from *A* after heat stress applications (Fig. 1A and B). Reductions in *g_s* were only observed at 0.5 h recovery time in plants treated with heat shock alone (*P* < 0.05). Increases in intercellular concentrations of CO₂ were observed parallel to reductions in *A* in all three heat treatments, implying that reductions in *A* were primarily due to non-stomatal factors (Fig. 1A, C). The maximum apparent Rubisco carboxylase activity (*V_{max}*) was reduced in all three heat treatments (Fig. 1A, D), the time-

Table 1Average \pm SE emission rates ($\text{nmol m}^{-2} \text{s}^{-1}$) of volatile organic compounds (VOC) emitted by non-stressed (Control), heat shock-stressed (Heat), moderate heat-stressed (Priming), and heat shock-stressed primed plants (Priming + Heat shock) *Origanum vulgare* leaves at 0.5, 5, 10, 24, 48, 72 h after treatment.

Emission rates ($\mu\text{mol m}^{-2} \text{s}^{-1}$)		0.5 h				5 h				10 h			
Volatiles		Control	Heat	Priming	Priming + Heat	Control	Heat	Priming	Priming + Heat	Control	Heat	Priming	Priming + Heat
Lipoxygenase pathways (LOX) volatiles													
1	2-Ethyl-hexanol ⁺	0.137 \pm 0.064	0.39 \pm 0.13	0.20 \pm 0.20	0.25 \pm 0.19	0.10 \pm 0.05	0.35 \pm 0.10	0.24 \pm 0.04	0.22 \pm 0.02	0.137 \pm 0.064	0.15 \pm 0.027	0.027 \pm 0.010	0.046 \pm 0.046
2	3-Hexen-2-one ⁺⁺	nd	0.0028 \pm 0.0028	0.10 \pm 0.10	nd	nd	nd	0.048 \pm 0.012	nd	nd	nd	0.010 \pm 0.010	0.011 \pm 0.006
3	Hexanal ⁺	0.041 \pm 0.028	0.06 \pm 0.02	nd	0.15 \pm 0.12	0.019 \pm 0.011	0.060 \pm 0.030	nd	0.10 \pm 0.10	0.014 \pm 0.020	nd	nd	nd
Long-chained saturated fatty acid-derived (FAD) compounds													
4	Decanal ⁺	0.068 \pm 0.076	0.21 \pm 0.11	nd	0.45 \pm 0.41	0.068 \pm 0.076	0.024 \pm 0.024	0.206 \pm 0.109	0.27 \pm 0.27	0.15 \pm 0.03	0.74 \pm 0.37	0.024 \pm 0.109	nd
5	Heptanal ⁺	0.057 \pm 0.021	0.041 \pm 0.031	nd	nd	0.066 \pm 0.017	nd	nd	0.0016 \pm 0.0016	0.045 \pm 0.007	nd	0.0014 \pm 0.0013	nd
6	Octanal ⁺	nd	0.097 \pm 0.039	nd	nd	nd	0.022 \pm 0.012	nd	0.127 \pm 0.112	nd	0.059 \pm 0.032	0.00012 \pm 0.00012	nd
7	Nonanal ⁺	0.346 \pm 0.143	0.174 \pm 0.057	nd	0.33 \pm 0.32	0.35 \pm 0.08	0.026 \pm 0.026	0.0143 \pm 0.0143	0.305 \pm 0.305	0.165 \pm 0.085	0.433 \pm 0.433	0.012 \pm 0.012	nd
Carbohydrate-derived volatile													
8	2-Methyl-furan ⁺⁺	nd	0.074 \pm 0.043	nd	nd	nd	0.084 \pm 0.043	nd	nd	nd	nd	nd	nd
9	2-Pentyl-furan ⁺⁺	nd	0.010 \pm 0.010	nd	0.0024 \pm 0.0024	nd	0.018 \pm 0.005	0.0046 \pm 0.0025	0.036 \pm 0.027	nd	0.0009 \pm 0.0009	0.006 \pm 0.006	nd
10	Furaneol ⁺	nd	nd	nd	nd	nd	nd	nd	nd	nd	nd	nd	nd
Isoprene and derivatives													
11	Methacrolein	0.028 \pm 0.028	0.18 \pm 0.09	0.114 \pm 0.066	0.044 \pm 0.044	0.195 \pm 0.141	0.08 \pm 0.08	0.043 \pm 0.043	0.19 \pm 0.09	nd	nd	0.076 \pm 0.076	0.106 \pm 0.106
12	Isoprene ⁺⁺	nd	0.035 \pm 0.031	nd	nd	nd	0.0207 \pm 0.0208	nd	nd	nd	0.0535 \pm 0.0319	nd	nd
Monoterpenes													
13	3-Carene ⁺	0.007 \pm 0.005	0.050 \pm 0.027	nd	0.022 \pm 0.022	0.0013 \pm 0.0006	0.139 \pm 0.071	nd	nd	0.0417 \pm 0.0379	nd	nd	nd
14	Camphene ⁺⁺	nd	0.029 \pm 0.009	0.037 \pm 0.037	nd	nd	nd	nd	nd	nd	nd	nd	nd
15	Limonene ⁺	nd	0.005 \pm 0.005	nd	nd	nd	0.0048 \pm 0.0046	nd	nd	nd	nd	nd	nd
16	β -Myrcene ⁺⁺	nd	0.018 \pm 0.018	0.016 \pm 0.015	0.051 \pm 0.038	nd	0.027 \pm 0.027	nd	nd	nd	0.0139 \pm 0.0139	0.051 \pm 0.038	nd
17	α -Ocimene ⁺⁺	nd	0.029 \pm 0.029	nd	nd	nd	nd	nd	nd	nd	nd	nd	nd
18	α -Pinene ⁺	0.012 \pm 0.007	0.37 \pm 0.11	nd	0.064 \pm 0.064	0.0063 \pm 0.0017	0.52 \pm 0.19	nd	nd	0.011 \pm 0.005	0.0038 \pm 0.0038	0.201 \pm 0.023	0.53 \pm 0.53
19	α -Terpinene ⁺⁺	nd	nd	nd	0.0203 \pm 0.0203	nd	0.006 \pm 0.006	0.0043 \pm 0.0043	nd	nd	nd	0.0009 \pm 0.0009	nd
20	α -Thujene ⁺⁺	nd	0.0012 \pm 0.0008	nd	nd	nd	0.0007 \pm 0.0007	nd	nd	nd	0.069 \pm 0.069	nd	nd
Sesquiterpenes													
21	α -Farnesene ⁺⁺	nd	0.048 \pm 0.048	nd	nd	nd	nd	nd	nd	nd	0.27 \pm 0.27	nd	nd
Geranylgeranyl diphosphate pathways volatiles													
22	6-Methyl-5-hepten-2-one ⁺	0.056 \pm 0.022	0.42 \pm 0.25	nd	1.5 \pm 0.8	0.066 \pm 0.008	0.26 \pm 0.18	0.066 \pm 0.066	nd	0.038 \pm 0.028	0.87 \pm 0.87	0.031 \pm 0.031	nd
23	Geranyl acetone ⁺	0.031 \pm 0.021	0.27 \pm 0.26	nd	0.41 \pm 0.16	0.031 \pm 0.021	0.05 \pm 0.04	0.09 \pm 0.05	0.21 \pm 0.21	0.031 \pm 0.021	0.25 \pm 0.25	0.20 \pm 0.20	nd
Benzoids													

(continued on next page)

Table 1 (continued)

Emission rates ($\mu\text{mol m}^{-2} \text{s}^{-1}$)													
Volatiles	0.5 h				5 h				10 h				
	Control	Heat	Priming	Priming + Heat	Control	Heat	Priming	Priming + Heat	Control	Heat	Priming	Priming + Heat	
24	Benzaldehyde ⁺	0.036 ± 0.008	0.14 ± 0.08	nd	0.13 ± 0.09	0.0343 ± 0.0022	0.15 ± 0.03	nd	0.15 ± 0.07	0.024 ± 0.009	0.55 ± 0.32	0.009 ± 0.009	
25	Benzothiazole ⁺	nd	0.068 ± 0.036	nd	0.061 ± 0.034	nd	nd	nd	nd	nd	nd	nd	
26	Methyl salicylate ⁺⁺	nd	nd	nd	nd	nd	0.038 ± 0.036	nd	nd	nd	nd	0.11 ± 0.11	
Emission rates ($\mu\text{mol m}^{-2} \text{s}^{-1}$)													
Volatiles	24 h				48 h				72 h				
	Control	Heat	Priming	Priming + Heat	Control	Heat	Priming	Priming + Heat	Control	Heat	Priming	Priming + Heat	
Lipoxygenase pathways volatiles													
1	2-Ethyl-hexano ⁺	nd	0.054 ± 0.057	0.108 ± 0.044	nd	nd	0.16 ± 0.16	0.044 ± 0.027	0.302 ± 0.129	nd	nd	0.09 ± 0.09	0.034 ± 0.034
2	3-Hexen-2-one ⁺⁺	nd	nd	nd	0.047 ± 0.026	nd	nd	0.0026 ± 0.0026	0.0019 ± 0.0019	nd	nd	0.026 ± 0.026	0.0058 ± 0.0058
3	Hexanal ⁺	0.0011 ± 0.0011	nd	nd	nd	nd	nd	nd	0.028 ± 0.028	0.123 ± 0.123	nd	nd	0.012 ± 0.012
Long-chained-saturated fatty acid-derived compounds													
4	Heptanal ⁺	0.014 ± 0.007	nd	nd	0.0009 ± 0.0009	0.009 ± 0.009	nd	nd	0.0003 ± 0.0003	0.026 ± 0.007	nd	nd	0.0067 ± 0.0067
5	Decanal ⁺	0.15 ± 0.02	0.068 ± 0.030	0.029 ± 0.027	nd	0.057 ± 0.057	0.49 ± 0.49	0.0024 ± 0.0024	0.092 ± 0.075	0.026 ± 0.026	0.023 ± 0.023	nd	0.14 ± 0.07
6	Octanal ⁺⁺	nd	0.008 ± 0.019	0.0026 ± 0.0026	nd	nd	0.019 ± 0.019	nd	0.039 ± 0.025	nd	nd	nd	0.015 ± 0.015
7	Nonanal ⁺	0.054 ± 0.048	0.023 ± 0.012	0.0068 ± 0.0068	0.057 ± 0.057	0.054 ± 0.048	0.29 ± 0.29	nd	0.10 ± 0.05	0.073 ± 0.073	nd	nd	0.10 ± 0.05
Carbohydrate-derived volatiles													
8	2-Methyl-furan ⁺⁺	nd	0.080 ± 0.020	nd	nd	nd	0.00043 ± 0.00043	nd	0.032 ± 0.032	nd	nd	nd	nd
9	2-Pentyl-furan ⁺⁺	nd	0.0013 ± 0.0013	0.0026 ± 0.0008	0.049 ± 0.021	nd	0.026 ± 0.019	nd	0.005 ± 0.005	nd	nd	nd	0.017 ± 0.001
10	Furaneol ⁺	nd	nd	nd	nd	nd	0.026 ± 0.019	nd	nd	nd	nd	nd	nd
Isoprene and derivatives													
11	Methacrolein ⁺	0.11 ± 0.07	0.17 ± 0.17	nd	0.15 ± 0.05	nd	0.087 ± 0.087	nd	nd	nd	0.065 ± 0.065	nd	0.23 ± 0.23
12	Isoprene ⁺⁺	nd	0.06 ± 0.06	nd	0.06 ± 0.06	nd	nd	0.0041 ± 0.0041	0.036 ± 0.036	nd	nd	nd	nd
Monoterpenes													
13	3-Carene ⁺	0.094 ± 0.094	0.059 ± 0.021	nd	nd	0.0616 ± 0.0417	nd	nd	0.09 ± 0.06	0.011 ± 0.011	nd	nd	0.046 ± 0.046
14	Camphene ⁺⁺	nd	nd	nd	0.010 ± 0.010	nd	0.0125 ± 0.0125	nd	0.0139 ± 0.0139	nd	nd	nd	0.0085 ± 0.0085
15	Limonene ⁺⁺	nd	0.009 ± 0.005	0.0011 ± 0.0011	nd	nd	nd	nd	0.008 ± 0.008	nd	nd	nd	0.005 ± 0.005
16	β-Myrcene ⁺⁺	nd	nd	nd	0.008 ± 0.008	nd	nd	nd	nd	nd	nd	nd	0.010 ± 0.010
17	α-Ocimene ⁺⁺	nd	nd	nd	0.0046 ± 0.0046	nd	0.039 ± 0.039	nd	nd	nd	nd	nd	nd
18	α-Pinene ⁺	nd	0.24 ± 0.14	0.15 ± 0.15	nd	nd	0.094 ± 0.094	0.37 ± 0.19	0.21 ± 0.06	0.099 ± 0.071	nd	nd	0.14 ± 0.14
19	α-Terpinene ⁺⁺	nd	0.018 ± 0.018	0.016 ± 0.016	nd	nd	nd	nd	0.0012 ± 0.0012	nd	nd	nd	nd

(continued on next page)

Table 1 (continued)

Emission rates ($\mu\text{mol m}^{-2} \text{s}^{-1}$)												
Volatiles		0.5 h				5 h				10 h		
		Control	Heat	Priming	Priming + Heat	Control	Heat	Priming	Priming + Heat	Control	Heat	Priming + Heat
20	α -Thujene ⁺⁺	nd	nd	nd	0.0029 ± 0.0029	nd	0.015 ± 0.015	0.036 ± 0.036	nd	nd	nd	nd
Sesquiterpenes												
21	α -Farnesene ⁺⁺	nd	0.0067 ± 0.0067	nd	0.0014 ± 0.0014	nd	nd	nd	nd	nd	0.044 ± 0.044	0.14 ± 0.09
Geranylgeranyl diphosphate pathways volatiles												
22	6-Methyl-5-hepten-2-one ⁺	0.039 ± 0.039	nd	0.049 ± 0.024	0.31 ± 0.16	nd	0.78 ± 0.78	nd	0.25 ± 0.19	0.56 ± 0.56	nd	nd
23	Geranyl acetone ⁺	0.129 ± 0.129	0.21 ± 0.15	0.29 ± 0.16	nd	0.129 ± 0.129	0.33 ± 0.33	0.008 ± 0.008	0.072 ± 0.072	0.054 ± 0.054	nd	0.086 ± 0.043
Benzenoids												
24	Benzaldehyde ⁺	nd	0.069 ± 0.009	0.092 ± 0.059	nd	nd	0.145 ± 0.108	nd	0.087 ± 0.087	0.075 ± 0.075	nd	nd
25	Benzothiazole ⁺	0.023 ± 0.013	nd	0.0041 ± 0.0041	nd	nd	nd	nd	0.011 ± 0.011	nd	nd	0.009 ± 0.009

Constitutive VOC, marked by “+”, refers to VOC emitted from control leaves in pre-stressed conditions. Induced volatiles, marked by “++”, refers to VOC emitted in stressed conditions. nd - not detectable.

dependent changes in V_{max} mirrored changes in A (cf. Fig. 1A and D), and V_{max} scaled positively with A (Fig. 2).

3.2. Elicitation of volatile organic compound emissions by heat priming and heat shock stress

Altogether, emissions of 26 volatile compounds were observed in the emissions from leaves of stressed and non-stressed plants of *O. vulgare* (Table 1 for the list of compounds). The emitted volatiles belonged to five volatile groups: lipoxygenase pathway (LOX) products, long-chained-saturated fatty acid-derived (FAD) compounds, carbohydrate-derived volatiles, geranylgeranyl diphosphate (GGDP) pathway volatiles, monoterpenes, isoprene derivatives (methacrolein) and benzenoids (Table 1). Control leaves of *O. vulgare* were characterized by low-level emissions of 11 volatiles (Table 1). Different heat stress treatments had different impacts on volatile emissions (Table 1, Fig. 3A–G). Priming treatment resulted in rapid emissions of LOX volatiles, and these emissions recovered to the level in control plants at 48 h after treatment (Fig. 3A). Emissions of monoterpenes were increased at 10 and 48 h (Fig. 3D), isoprene and α -farnesene at 48 h (Table 1), and GGDP volatiles at 10 h after priming (Fig. 3E). Albeit the increases in emissions of individual VOC groups that were observed in the priming-treated plants, total emissions of VOC in the priming-treated plants were similar ($P > 0.05$) to that in control plants throughout the recovery period. Heat shock effects on volatile emissions were different in primed and non-primed *O. vulgare* (Fig. 3A–G). In non-primed plants, emissions of LOX compounds, terpenoids (isoprene, mono- and sesquiterpenes), benzenoids, GGDP volatiles, and total VOC emissions were rapidly enhanced upon heat shock treatment (Table 1, Fig. 3A–G). Emissions of carbohydrate derivatives were induced in non-primed plants at 0.5–48 h after heat shock treatment. Emissions of LOX compounds and monoterpenes in non-primed plants were higher than in control, but at 72 h recovery period, the emissions decreased to below the level in control ($P < 0.05$ in comparison to control plants, Fig. 3A, D). Emissions of benzenoids recovered to the control level at 24 h after heat shock treatment (Fig. 3F). GGDP volatile emissions initially recovered at 5 h, but an emission burst was observed at 10 h after treatment (Fig. 3E). In addition, an emission burst of FAD compounds was observed at 10 h after heat shock application. Total VOC emissions recovered to the level in control at the end of the experiment (Fig. 3G).

In heat shock-stressed primed plants, emissions of LOX compounds,

FAD compounds, GGDP volatiles, benzenoids, and total volatiles were rapidly enhanced after the application of heat shock stress; emissions of FAD compounds, GGDP volatiles, benzenoids, and total volatile recovered at 5 h, whereas emissions of LOX compounds recovered at 10 h after treatment (Fig. 3A–G). Emissions of carbohydrate-derived volatiles (furans) were induced in primed plants at 0.5–5 h after the application of heat shock stress. At 0.5 h after heat shock treatment, emissions of carbohydrate derivatives were lower in primed plants than in non-primed plants. The emissions of monoterpenes were enhanced at 10 h after stress application, similar to moderately heat-stressed (priming) plants (Fig. 3D). Secondary emission bursts were observed in the combined priming and heat shock-stressed plants. Emissions of LOX compounds and GGDP volatiles rose again at 24–48 h, monoterpene emissions at 48 h (Fig. 3A, D, E) and isoprene and sesquiterpene emissions (Table 1) at 48–72 h after treatment. Carbohydrate-derived volatiles were induced again at 24–72 h after combined priming and heat stress treatment. Total volatile emissions also increased at 48 h, reflecting the second rise of emissions observed for several volatile groups (Fig. 3G). At the end of the experiment, volatile emissions in heat shock-stressed-primed plants and control plants were quantitatively similar (Fig. 3A–G).

Through the 72 h recovery period, LOX emissions correlated negatively with A in heat shock-stressed plants (Fig. 4A). In primed heat shock-treated plants, A correlated negatively with LOX compound (Fig. 4B) emissions and total volatile emissions (Fig. 4C) through 0.5–10 h recovery period.

Emissions of constitutive volatiles (volatiles present in non-stressed control plants) in non-primed plants were at the highest level at 0.5–10 h after heat shock treatment (Table 1, Fig. 5A). In primed heat-shock-stressed plants, emissions of constitutive volatiles were at the highest level at 0.5 and 48 h recovery times (Table 1, Fig. 5A). At 0.5 h recovery time, in particular, emissions of constitutive volatiles were 5-fold greater in non-primed and 10-fold greater in primed plants than corresponding induced emissions (Table 1, Fig. 5A and B). Emissions of induced volatiles were at the highest level at 10 h in heat shock-treated non-primed plants (Table 1, Fig. 5A). In primed plants, emissions of induced volatiles demonstrated a biphasic pattern, decreasing through 0.5–10 h and increasing through 24–72 h after treatment (Table 1, Fig. 5A). At the end of the experiment, emissions of constitutive volatiles and induced volatiles in primed plants were higher ($P < 0.05$) than in non-primed plants (Table 1, Fig. 5A and B).

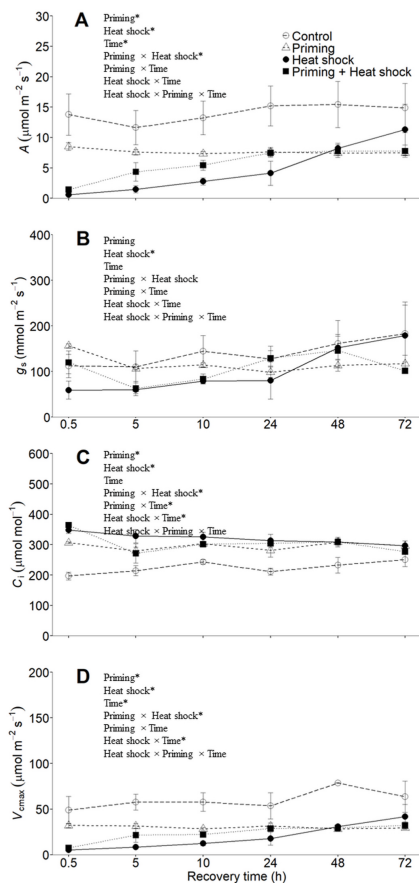


Fig. 1. Changes in net assimilation rate (A), stomatal conductance to water vapor (g_s), intercellular CO_2 concentration (C_i), and maximum carboxylase activity of Rubisco (V_{max}) in non-stressed (control), heat-primed (priming), heat shock-stressed non-primed (Heat shock) and heat shock-stressed primed (Priming + Heat shock) leaves of *Origanum vulgare*. Priming was applied by exposing the leaves to 35°C for 1 h. Heat shock was applied by exposing the leaves to 45°C for 5 min. Experimental leaves were measured at 0.5, 5, 10, 24, 48, and 72 h after treatment application under the following conditions: chamber CO_2 concentration of $400 \mu\text{mol mol}^{-1}$ and vapor pressure deficit between the leaf and the atmosphere of 1.7 kPa , photosynthetic photon flux density of $800 \mu\text{mol m}^{-2} \text{s}^{-1}$, and leaf temperature of 25°C . Data are shown as averages \pm SE of three independent plant replicates. Three-factor ANOVA was used to determine the significance of heat stress treatments and their interactive effects. All statistical effects were considered significant at $P < 0.05$ and are illustrated with asterisks in (A–D).

3.3. Alteration of volatile blends by different heat treatments

Different stress volatiles were induced by different types of stress. The LOX pathway compound, 2-ethyl-hexanol emissions was induced in heat shock-treated plants irrespective of priming. The carbohydrate-derived compounds 2-methyl-furan and furaenol were elicited mainly in non-primed plants and 3-hexen-2-one in primed plants (Table 1). As for benzenoids, emissions of benzaldehyde and benzothiazole were elicited in heat shock-stressed plants regardless of priming, but methyl salicylate (MeSA) emissions were only detected in non-primed plants (Table 1). Emissions of MeSA were also observed after priming applications (Table 1). A similar set of monoterpenes was detected in differently-treated plants (Table 1).

Principal component analysis illustrated that different heat treatments led to unique combinations of VOC blends (Fig. 6A–D). In heat-shock-stressed plants, volatile blends varied for primed and non-primed plants at different recovery times (Table 1, Fig. 6A–D). In particular, at 0.5 h recovery time, non-primed plants were characterized by strong emissions of isoprenoids including isoprene, methacrolein, 3-carene, α -pinene, α -farnesene and camphene, the carbohydrate-derived compounds 2-pentyl-furan and 2-methyl-furan, and the benzenoid benzaldehyde; whereas primed plants were distinguished by emissions of the LOX volatile 2-ethyl-hexanol, the FAD compound nonanal and GGDP volatiles 6-methyl-5-hepten-2-one and geranyl acetone (Fig. 6A and B). At 48 h, higher emissions of 2-ethyl-hexanol, nonanal, decanal, benzaldehyde, 2-pentyl-furan, furaenol and GGDP volatiles distinguished the emissions in non-primed plants, whereas emissions of 3-hexen-2-one, hexanal, 3-carene, limonene, camphen, β -myrcene and benzothiazole characterized emissions in primed plants (Fig. 6C and D).

4. Discussion

4.1. Impacts of moderate heat priming on heat shock responses of photosynthesis

Our results elucidated that exposure to moderate heat stress (35°C) alone resulted in moderate decreases in photosynthetic activities in *O. vulgare* (Fig. 1A). In several previous studies, e.g. in *Achillea millefolium* (Liu et al., 2021) and *Melilotus albus* (Liu et al., 2022), photosynthesis rate was not affected by similar pre-heat treatment. Thus, the priming treatment exerted a stronger stress on *O. vulgare* in our study. This is further supported by changes in volatile emissions observed after the priming stress application (see section 4.2).

Previous studies have shown that heat shock stress can induce transient or permanent photosynthetic reductions and VOC emissions (Pazouki et al., 2016; Urban et al., 2017; Turan et al., 2019) and the degree of changes in these physiological processes can be influenced by previous stress episodes (Teskey et al., 2015; Khan et al., 2022). We demonstrated that heat shock-induced reductions in photosynthesis were smaller in primed *O. vulgare* (Fig. 1A) in agreement with previous studies (e.g. Fan et al., 2018; Liu et al., 2021; Liu et al., 2022). In our study, the reductions in photosynthesis were primarily due to non-stomatal factors, in particular, due to reductions in Rubisco maximum activity (Fig. 1A–D and 2). The temperature sensitivity of maximum Rubisco carboxylase activity varies among species, whereas the carboxylase activity itself typically has a very high optimum temperature of around 50°C ; Rubisco activase is very temperature sensitive (Salvucci and Crafts-Brandner, 2004; Galmés et al., 2016), as the result, heat stress can lead to inhibition of Rubisco activity. For example, moderate heat stress did not reduce photosynthetic capacity in *Nicotiana tabacum* (Rizhsky et al., 2002), but reduced photosynthetic capacity by 16% in *Gossypium hirsutum* (Crafts-Brandner and Law, 2000). In our study, photosynthetic capacity was reduced by 50% in (Fig. 1D), reflecting the high sensitivity of Rubisco enzymatic activity in *O. vulgare*. Photosynthetic capacity in *O. vulgare* recovered upon leaf cooling (Fig. 1D) indicating that the heat stress applications were not lethal and

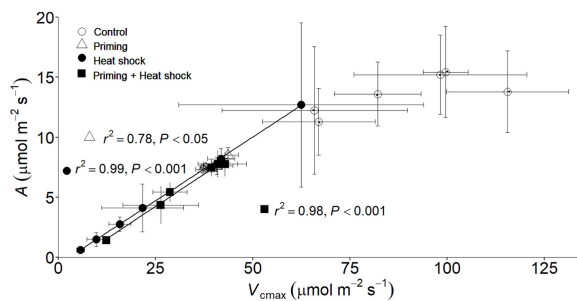


Fig. 2. Correlations between maximum carboxylase activity of Rubisco (V_{cmax}) and net CO_2 assimilation rate (A) in non-stressed (control), moderate heat-treated (priming), heat shock-treated non-primed (heat shock), and heat shock-treated primed (priming + heat shock) *Origanum vulgare* leaves. Each data point represents the average (\pm SE) of three independent replicates measured at 0.5, 5, 10, 24, 48, and 72 h after heat stress treatments.

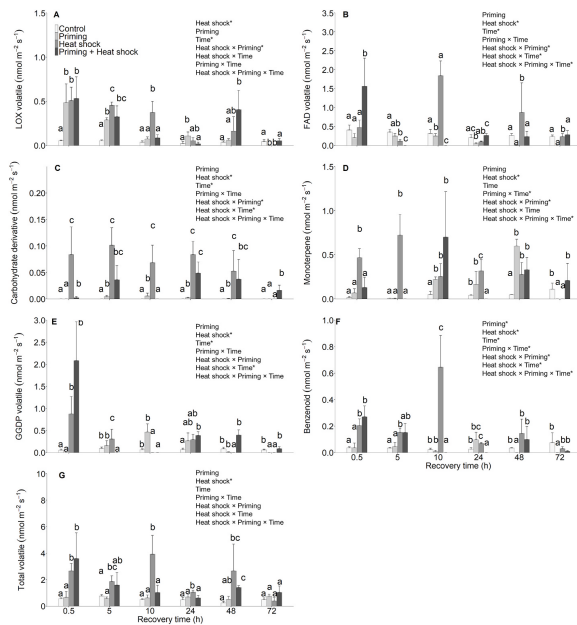


Fig. 3. Emission rates of lipoxygenase (LOX) pathway compounds (A), long-chained fatty acid-derived (FAD) compounds (B), carbohydrate-derived compounds (C), monoterpenes (D), geranylgeranyl (GGDP) pathway compounds (E), benzofuran (F), and total emission of volatile organic compounds (VOC) (G) of control, moderate heat-stressed (Priming), heat shock-stressed non-primed (Heat shock), and heat shock-stressed primed (Priming + Heat shock) *Origanum vulgare* during 72 h recovery period (0 h corresponds to the time heat stress or control treatment was applied). Each bar represents the treatment average \pm SE measured at different recovery times. Averages at each recovery time were compared by the least significant difference (LSD) test following one-way ANOVA. Different lowercase letters denote significant differences ($P < 0.05$) among the treatment groups.

might be attributed to Rubisco inactivation, rather than to direct damage to photosynthetic apparatus or denaturation/aggregation of Rubisco into insoluble complexes (Crafts-Brandner and Law, 2000; Salvucci and Crafts-Brandner, 2004). The relatively lower sensitivity of photosynthetic capacity in priming + heat shock-stressed plants (Fig. 1D) suggested that priming increased the thermal tolerance of Rubisco activity.

Such an improvement can occur by changes in the small subunit composition of Rubisco or by expression of a thermal-stable isoform of Rubisco activase (Law et al., 2001). In addition, pre-heat exposure can improve thermal tolerance and protect photosynthetic processes upon subsequent heat stress by increasing the accumulation of protective chemicals including heat shock proteins, antioxidants, secondary

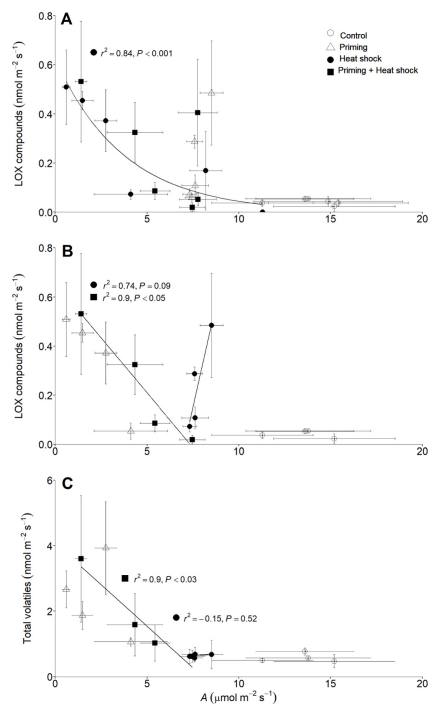


Fig. 4. Correlations between net assimilation rate (A) and emissions of lip-oxygenase (LOX) pathway compounds (A, at 0.5–72 h; B, at 0.5–24 h) and total volatiles (C, at 0.5–24 h recovery period) in non-stressed (control), moderate heat-treated (priming), heat shock-treated non-primed (heat shock), and heat shock-treated primed (priming + heat shock) *Origanum vulgare* leaves. Each data point represents the average (\pm SE) of three independent replicates measured at 0.5, 5, 10, 24, 48, and 72 h (A) and 0.5, 5, 10, and 24 h (B and C) after heat stress treatments.

metabolites, and osmolytes that are otherwise produced in insufficient quantity, if at all, when plants are suddenly confronted with severe heat stress (Wang et al., 2014; Teskey et al., 2015; Abid et al., 2016; Guihur et al., 2022).

When photosynthetic processes recover completely to pre-stress levels, the synthesis of certain protective agents is also slowed down or stopped (Vihervaara et al., 2017). We observed that after the application of priming and combined priming and heat shock treatment, photosynthetic capacity did not recover completely to pre-stress levels (Fig. 1D). Such priming effect indicates sustained phenotypic change that could reflect certain maintenance of the inhibition of Rubisco activity or chloroplastic osmotic medium or overall divergence of resources from primary metabolism (e.g. resorption of N from photosynthetic proteins) to secondary metabolism (Dumschott et al., 2017). Thus, although priming avoids the potentially devastating effect on foliage photosynthetic activity, the trade-off can be reduced photosynthetic activity in non-stressed conditions. Previous studies have

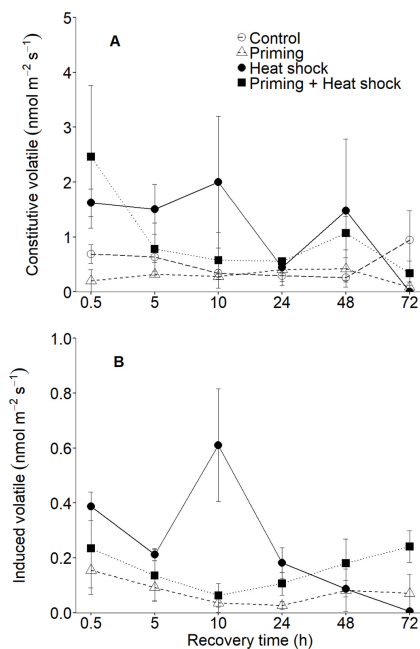


Fig. 5. Changes in average \pm SE ($n = 3$) emission rates of total constitutive (A) and induced volatiles (B) in priming-treated, heat shock-treated, and combined priming and heat shock-treated leaves of *Origanum vulgare* at 0.5, 5, 10, 24, 48, 72 h after heat treatment applications (0 h corresponds to heat treatment application time). Constitutive and induced volatiles as indicated in Table 1.

revealed that heat-stressed plants can avoid complete recovery of photosynthetic activity as a thermal acclimation and energy-saving strategy for subsequent stress encounters (Cen and Sage, 2005; Wahid et al., 2007).

Regarding the impact of heat shock on stomatal conductance (g_s), no universal heat responses of g_s have been observed across studies; at supra-optimal temperatures, g_s can decrease, increase or even be independent of temperature (Rizhsky et al., 2002; Urban et al., 2017). Despite large variation among studies, there is evidence that stomatal closure under supraoptimal temperatures typically occurs in plants with constitutively higher g_s (Marchin et al., 2022). We observed decreases in g_s after applying heat shock in non-primed plants (Fig. 1D), whereas, in the previous experiments (Sulaiman et al., 2021), similar stress resulted in increases in g_s in *O. vulgare*. However, the photosynthesis rates and g_s in control plants were greater in the current study (Fig. 1A and B) than in Sulaiman et al. (2021). This suggests that the plants in the current study might have operated close to the maximum water use capacity as determined by stem hydraulic conductance. Thus, exceeding the physiological capacity upon heat shock might have led to cavitation and sustained reduction in g_s (e.g. Cardoso et al., 2018).

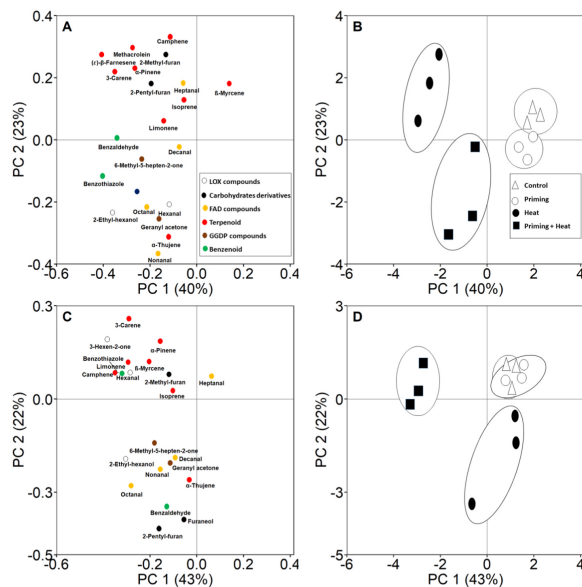


Fig. 6. Principal component analysis (PCA) score plots (A for 0.5 h; C for 48 h treatment recovery time) and loading plots (B for 0.5 h; D for 48 h treatment recovery time) for the volatile emissions of non-stressed (control), heat shock-stressed (heat shock), moderate heat-stressed (priming), and heat shock-stressed primed (priming + heat shock) *O. vulgare* leaves. The percentages of variation explained by the two PCA axes are demonstrated in the axis labels. In the loading plots (B and D), the impact of individual volatile compounds (Table 1 for the emission rates of volatiles) increases with increasing distance from the origin of the coordinate system.

4.2. Impact of heat shock on volatile emissions in primed and non-primed plants

Enhanced emission of lipoxygenase (LOX) volatiles is typically the first stress signal observed upon heat shock stress (Copolovici et al., 2012; Chatterjee et al., 2020; Okereke et al., 2022). Stress-elicited LOX volatiles are rapidly biosynthesized by constitutively active lipoxygenases upon the release of polyunsaturated fatty acids from membrane phospholipids (Stolterfoht et al., 2019; Vincenti et al., 2019). LOX emissions bursts indicate severe stress that results in the formation of reactive oxygen species (ROS) and membrane-level damage (Jansen et al., 2009; Niinemetts et al., 2013). In contrast to previous studies (Liu et al., 2021, 2022), pre-heat application alone resulted in the elicitation of LOX emissions in *O. vulgare* (Fig. 3A), suggesting a certain degree of oxidative stress and activation of defense pathways. LOX emissions can play a vital role in defense priming and triggering subsequent stress responses (Farag and Pare, 2002; Niinemetts et al., 2013). Upon heat shock, the initial emission phase lasted for 10 h in primed plants (Fig. 3A), and we suggest that these emissions reflect the direct effect of heat shock on LOX substrate availability. In the case of non-primed plants (Fig. 3A), such a direct effect of heat shock lasted for 48 h suggesting severer damage. The secondary emission phase observed in the primed plants may indicate the activation of signaling pathways that lead to the expression of a suite of genes coding proteins responsible for the synthesis of protective chemicals as well as for modifications in plant membrane constituents that can confer long-term thermal protection (Jiang et al., 2017; Niu and Xiang, 2018; Guihur et al., 2022; Tsvetkova et al., 2002).

We also observed enhanced emissions of various long-chained-saturated aldehydes (FAD) in heat shock-stressed plants, and that

these emissions occurred earlier in primed plants (Fig. 3B). Although the processes resulting in the formation of FAD compounds is not well-known, heat stress-enhanced release of FAD compounds can reflect stress development and accumulation of ROS in the chloroplast (Niu and Xiang, 2018; Sulaiman et al., 2021; Okereke et al., 2022). Additionally, in this study, heat stress induced the emissions of furans, carbohydrate-derived compounds (Table 1, Fig. 3C). Carbohydrate derivatives have been shown to have hydroxyl radical scavenging properties (Mawlong et al., 2016; Wang et al., 2019). In heat shock-treated plants, emissions of carbohydrate-derived compounds followed a similar kinetic as LOX pathway emissions (cf. Fig. 3A and C), thus emissions of carbohydrate derivatives might reflect a defensive mechanism for alleviating heat stressed-induced oxidative stress (Mawlong et al., 2016).

Terpenoid emissions can play a protective role against extremely high temperatures by scavenging reactive oxygen species and increasing the stability of the thylakoid membrane (Harrison et al., 2013; Faralli et al., 2020). The rapid heat shock induction of mono- and sesquiterpene emissions in the non-primed *O. vulgare* (Fig. 3D) is consistent with previous studies (Sulaiman et al., 2021). We suggest that these emissions reflect *de novo* synthesis of isoprenoids. The *de novo* biosynthesis of isoprene and monoterpenes occur via the plastidial MEP/DOXP pathways, and sesquiterpene biosynthesis occurs via the cytosolic mevalonate pathway, although stress can also elicit *de novo* formation of sesquiterpenes in the plastid (Dudareva et al., 2005; Sallaud et al., 2009; Pazouki and Niinemetts, 2016). In non-primed plants (Table 1), we observed rapid induction of isoprene and its oxidation product methacrolein which might have resulted from non-enzymatic isoprene synthesis or due to the activity of multi-substrate terpene synthases, as the formation of isoprene synthase is unlikely during such rapid heat

application (Velikova et al., 2005; Niinemets et al., 2010).

In primed plants, elicitation of terpenoid release was delayed (Fig. 3D), probably due to a substrate level control; once primed, the plants likely prioritized other chloroplastic metabolic pathways, e.g. carotenoid synthesis in the GGDP pathway over monoterpenes synthesis (Lu and Li, 2008). Enhanced carotenoid turnover was reflected in the emissions of the carotenoid breakdown products geranyl acetone and 6-methyl-5-hepten-2-one (Fig. 3E) and might have played an important role in alleviating oxidative stress and improving thermal acclimation (Havaux, 2014; García-Plazaola et al., 2017). The emissions of mono- and sesquiterpenes during secondary emission bursts (Fig. 3D, Table 1) reflect *de novo* synthesis of isoprenoids that may occur due to substrate accumulation and/or stimulation of the activity of rate-limiting enzymes (Pazouki et al., 2016; Serrano et al., 2019; Liu et al., 2021).

We observed the elicitation of shikimate pathways-derived volatiles, mainly benzothiazole and benzaldehyde upon heat shock stress treatment (Table 1, Fig. 3F). The enzymes responsible for the biosynthesis of these benzenoid compounds remain unclear. However, Huang et al. (2022) demonstrated that in *Petunia* species, the biosynthesis of benzaldehyde occurred in peroxisomes via the β -oxidative or non- β -oxidative pathways. The inductions of both benzothiazole and benzaldehydes have previously been associated with oxidative stress (Okereke et al., 2021; Sulaiman et al., 2023). Thus, the relatively higher emissions of benzenoids (Fig. 3F) in non-primed plants may suggest severer cellular stress. We observed the emissions of methyl salicylate (MeSA) in non-primed plants at 72 h (Table 1) which may reflect the accumulation of salicylic acid (SA). Although we did not detect MeSA after the application of heat shock in primed plants, the MeSA emissions observed after priming treatment (Table 1) may indicate SA accumulation which might have played a role in enhancing the activation of defense pathways and heat stress acclimation (Wang et al., 2010). SA formation under non-lethal heat stress can increase the accumulation of proline and total content of osmotic that can enhance membrane integrity (Cviková et al., 2013; Nguyen et al., 2016; Guihur et al., 2022). Thus, in primed plants, the SA-dependent defenses had already been activated before heat shock stress application, whereas they were likely activated at the end of the experiment at 72 h in non-primed plants.

Stress VOC emission is an indicator of stress and stress-related physiological responses such as the activation of secondary metabolic pathways (Holopainen and Gershenzon, 2010; Hirao et al., 2012). Photosynthetic reductions are also associated with physiological stress (Velikova et al., 2005; Turan et al., 2019; Sulaiman et al., 2023). In primed plants, photosynthesis correlated negatively with LOX compound emissions and total volatile emissions in the primary emission phase, 0.5–10 h after stress application (Fig. 4B and C), indicating that the recovery of volatile emissions in this phase reflects the alleviation of heat stress. In the case of non-primed plants, the alleviation of direct effects of heat shock stress was prolonged (Fig. 1A–D, 3A–G and 4A). In primed plants, the secondary emission phase observed constitutes increases in constitutive volatile emissions and strong induction of volatiles (Fig. 5A and B) indicating increases in the activity of already active defense metabolic pathways and the induction of different defense pathways.

Different heat treatments altered the composition of VOC emissions differently (Table 1). The composition of volatiles emitted at different times during stress recovery indicate the type of stress and the different biochemical pathways activated (Niinemets et al., 2013; Misztal et al., 2015). The richer blend of LOX compounds (Table 1, Fig. 6A–D) induced in non-primed plants suggests much more severe cellular damage. The emissions of carbohydrate derivatives indicate severe stress in non-primed plants. For instance, the emissions of 2-methyl-furan were observed in severely heat-stressed *Nicotiana tabacum* (Turan et al., 2019) and *Brassica nigra* (Kask et al., 2016). The different characteristic isoprenoid emissions (isoprene, mono- and sesquiterpenes) observed upon heat shock stress in non-primed plants (Fig. 6A and B) reflect stress activation of synthesis of different terpenoids. The more diverse blend of

different terpenoid and benzenoid compounds (Fig. 6A–D) in non-primed plants further suggests that the heat stress elicitation of volatile defense pathways was greater in this treatment. Priming abolished much of the constitutive and induced volatile responses (Fig. 6A and B), suggesting that heat resistance was achieved by other physiological modifications, e.g. sustained activation of defense pathways and accumulation of protective secondary metabolites (Niu and Xiang, 2018; Tsvetkova et al., 2002). Further studies are required to investigate the heat shock stress indicators including pool sizes and accumulation of non-volatile secondary metabolites.

5. Conclusion

This study investigated the impact of severe transient heat stress on photosynthetic characteristics and volatile emissions in non-primed and pre-moderate heat-stressed leaves of *O. vulgare* through 72 h stress recovery period. Our results demonstrated that photosynthetic reductions were greater in non-primed plants, in particular, 2-fold greater than in primed plants at 0.5 h after heat shock, indicating that pre-exposure to moderate heat stress increased heat stress tolerance. Overall, photosynthetic reductions were primarily due to non-stomatal factors, including reduced Rubisco activity. Upon return to lower temperatures, photosynthetic activity in non-primed plants fully recovered to that in non-stressed control plants, but the recovery was delayed. In primed plants, photosynthetic recovery was faster, but certain photosynthetic inhibition remained by the end of the experiment, indicating a sustained priming effect that may be indicative of a trade-off between photosynthetic activity and metabolic reprogramming in primed plants to enhance defenses.

Heat shock stress resulted in major emissions of volatile organic compounds including LOX pathway volatiles, and long-chain saturated fatty acid-derived aldehydes, carbohydrate derivatives, monoterpenes, sesquiterpenes, GGDP pathway compounds and benzenoids in primed and non-primed plants, but comparatively, in primed plants, the emissions recovered earlier and rose again, indicating a continuous activation of biochemical defense pathways. Bouquets of volatiles were different for primed and non-primed plants, and in the primed plants, volatile blends varied for primary and secondary emission phases, indicating the activation of varying biosynthesis pathways. Volatile emission data collectively indicated that heat stress resistance was enhanced by heat priming. In nature, high-temperature episodes can last hours to days and the duration of heat stress may influence plant responses. Thus, our findings may not reflect typical heat stress responses in the field, but demonstrate the rapid ability of primed plants to activate acquired thermotolerance and acclimatory responses during subsequent warm days. We argue that knowledge of heat stress history is important in predicting plant physiological responses during subsequent heat stress episodes and developing crop plants with improved heat stress tolerance.

Author contributions

BL and ÜN conceived the original idea of the study. BL and ÜN designed and planned the research. BL, EK, and HYS conducted the experiment. HYS and YOA analyzed the data. HYS wrote the manuscript and all co-authors contributed to writing the manuscript and approved the final version of the manuscript.

Declaration of competing interest

The authors declare that they have no known competing financial interests or personal relationships that could have appeared to influence the work reported in this paper.

Data availability

Data will be made available on request.

Acknowledgments

This research was funded by the European Commission through the European Research Council (advanced grant 322603, SIP-VOL+), the EU Regional Development Fund within the framework of the Centre of Excellence EcoChange (2014–2020.4.01.15-0002), and the Estonian University of Life Sciences (base funding P190252PKTT). The equipment used in the study was partly purchased from funding by the EU Regional Development Fund (AnEE Estonia, 2014–2020.4.01.20-0285, and the project “Plant Biology Infrastructure-TAIM”, 2014–2020.4.01.20-0282) and the Estonian Research Council (TTS, “Plant Biology Infrastructure – TAIM”).

References

- Abid, M., Tian, Z., Ata-Ul-Karim, S.T., Liu, Y., Cui, Y., Zahoor, R., Jiang, D., Dai, T., 2016. Improved tolerance to post-anthesis drought stress by pre-drought priming at vegetative stages in drought-tolerant and -sensitive wheat cultivars. *Plant Physiol. Biochem.* 106, 218–227. <https://doi.org/10.1016/j.plaphy.2016.05.003>.
- Bruce, T.J., Matthes, M.C., Napier, J.A., Pickett, J.A., 2007. Stressful “memories” of plants: evidence and possible mechanisms. *Plant Sci.* 173, 603–608. <https://doi.org/10.1016/j.plantsci.2007.09.002>.
- Cardoso, A.A., Brodrick, T.J., Lucani, C.J., DaMatta, F.M., McAdam, S.A., 2018. Coordinated plasticity maintains hydraulic safety in sunflower leaves. *Plant Cell Environ.* 41, 2567–2576. <https://doi.org/10.1111/pce.13335>.
- Cen, Y.P., Sage, R.F., 2005. The regulation of Rubisco activity in response to variation in temperature and atmospheric CO₂ partial pressure in sweet potato. *Plant Physiol.* 139, 979–990. <https://doi.org/10.1104/pp.105.066233>.
- Chatterjee, P., Kanagendran, A., Samadhar, S., Pazouki, L., Sa, T.M., Niinemets, Ü., 2020. Influence of *Brevibacterium linens* RS16 on foliage photosynthesis and volatile emission characteristics upon heat stress in *Eucalyptus grandis*. *Sci. Total Environ.* 700, 134453. <https://doi.org/10.1016/j.scitotenv.2019.134453>.
- Copolovici, L., Kännaste, A., Pazouki, L., Niinemets, Ü., 2012. Emissions of green leaf volatiles and terpenoids from *Solanum lycopersicum* are quantitatively related to the severity of cold and heat shock treatments. *J. Plant Physiol.* 169, 664–672. <https://doi.org/10.1016/j.jplph.2011.12.019>.
- Copolovici, L., Kännaste, A., Remmel, T., Vislap, V., Niinemets, Ü., 2011. Volatile emissions from *Alnus glutinosa* induced by herbivory are quantitatively related to the extent of damage. *J. Chem. Ecol.* 37, 18–28. <https://doi.org/10.1007/s10886-010-9897-9>.
- Copolovici, L., Niinemets, Ü., 2016. Environmental impacts on plant volatile emission. In: Blande, J., Glinwood, R. (Eds.), *Deciphering Chemical Language of Plant Communication. Signaling and Regulation in Plants*. Springer, Cham. https://doi.org/10.1007/978-3-319-39498-1_2.
- Copolovici, L., Niinemets, Ü., 2010. Flooding induced emissions of volatile signalling compounds in three tree species with differing waterlogging tolerance. *Plant Cell Environ.* 33, 1582–1594. <https://doi.org/10.1111/j.1365-3040.2010.02166.x>.
- Crafts-Brandner, S.J., Law, R.D., 2000. Effect of heat stress on the inhibition and recovery of the ribulose-1,5-bisphosphate carboxylase/oxygenase activation state. *Planta* 212, 67–74. <https://doi.org/10.1007/s004420000364>.
- Cviková, M., Gempelová, L., Martincová, O., Vanková, R., 2013. Effect of drought and combined drought and heat stress on polyamine metabolism in proline-over-producing tobacco plants. *Plant Physiol. Biochem.* 73, 7–15. <https://doi.org/10.1016/j.plaphy.2013.08.005>.
- De Kauwe, M.G., Lin, Y.-S., Wright, I.J., Medlyn, B.E., Crous, K.Y., Ellsworth, D.S., Maire, V., Prentice, I.C., Atkin, O.K., Rogers, A., et al., 2016. A test of the “one-point method” for estimating maximum carboxylation capacity from field-measured, light-saturated photosynthesis. *New Phytol.* 210, 1130–1144. <https://doi.org/10.1111/nph.13815>.
- Dudareva, N., Andersson, S., Orlova, L., Gatto, N., Reichelt, M., Rhodes, D., Boland, W., Gershenzon, J., 2005. The nonmevalonate pathway supports both monoterpene and sesquiterpene formation in snapdragon flowers. *Proc. Natl. Acad. Sci. USA* 102, 932–935. <https://doi.org/10.1073/pnas.0407360102>.
- Dumschott, K., Richter, A., Loescher, W., Merchant, A., 2017. Post photosynthetic carbon partitioning to sugar alcohols and consequences for plant growth. *Phytochemistry* 144, 243–252. <https://doi.org/10.1016/j.phytochem.2017.09.019>.
- Fan, Y., Ma, C., Huang, S., Abid, M., Jiang, S., Dai, T., Zhang, W., Ma, S., Jiang, D., Han, X., 2018. Heat priming during early reproductive stages enhances thermo-tolerance to post-anthesis heat stress via improving photosynthesis and plant productivity in winter wheat (*Triticum aestivum* L.). *Front. Plant Sci.* 9, 805. <https://doi.org/10.3389/fpls.2018.00805>.
- Farag, M.A., Pare, P.W., 2002. C6-Green leaf volatiles trigger local and systemic VOC emissions in tomato. *Phytochemistry* 61, 545–554. [https://doi.org/10.1016/S0031-9422\(02\)00240-6](https://doi.org/10.1016/S0031-9422(02)00240-6).
- Faralli, M., Li, M., Varotto, C., 2020. Shoot characterization of isoprene and ocimene-emitting transgenic arabidopsis plants under contrasting environmental conditions. *Plants* 9, 477. <https://doi.org/10.3390/plants9040477>.
- Galmés, J., Hermida-Carrera, C., Laanisto, L., Niinemets, Ü., 2016. A compendium of temperature responses of Rubisco kinetic traits: variability among and within photosynthetic groups and impacts on photosynthesis modeling. *J. Exp. Bot.* 67, 5067–5091. <https://doi.org/10.1093/jxb/erw267>.
- García-Plazaola, J.I., Portillo-Estrada, M., Fernández-Marín, B., Kännaste, A., Niinemets, Ü., 2017. Emissions of carotenoid cleavage products upon heat shock and mechanical wounding from a foliose lichen. *Environ. Exp. Bot.* 133, 87–97. <https://doi.org/10.1016/j.envexpbot.2016.10.004>.
- Gulthar, A., Rebeaud, M.E., Goloubinoff, P., 2022. How do plants feel the heat and survive? *Trends Biochem. Sci.* <https://doi.org/10.1016/j.tibs.2022.05.004>.
- Gutiérrez-Grijalva, E.P., Picos-Salas, M.A., Leyva-López, N., Criollo-Mendoza, M.S., Vazquez-Olivo, G., Heredia, J.B., 2017. Flavonoids and phenolic acids from oregano: occurrence, biological activity and health benefits. *Plants* 7, 2. <https://doi.org/10.3390/plants7010002>.
- Haldimann, P., Feller, U., 2004. Inhibition of photosynthesis by high temperature in oak (*Quercus pubescens* L.) leaves grown under natural conditions closely correlates with a reversible heat-dependent reduction of the activation state of ribulose-1,5-bisphosphate carboxylase/oxygenase. *Plant Cell Environ.* 27, 1169–1183. <https://doi.org/10.1111/j.1365-3040.2004.01222.x>.
- Harrison, S.P., Mourolopoulos, C., Dani, K.S., Prentice, I.C., Armeth, A., Atwell, B.J., Barkley, M.P., Leishman, M.R., Loreto, F., Medlyn, B.E., Niinemets, Ü., 2013. Volatile isoprenoid emissions from plastid to planet. *New Phytol.* 197, 49–57. <https://doi.org/10.1111/nph.12021>.
- Havaux, M., 2014. Carotenoid oxidation products as stress signals in plants. *Plant J.* 79, 597–606. <https://doi.org/10.1111/tpj.12386>.
- Hilker, M., Schülling, T., 2019. Stress priming, memory, and signalling in plants. *Plant Cell Environ.* 42, 753–761. <https://doi.org/10.1111/pce.13326>.
- Hirao, T., Okazawa, A., Harada, K., Kobayashi, A., Muranaka, T., Hirata, K., 2012. Green leaf volatiles enhance methyl jasmonate response in Arabidopsis. *J. Biosci. Bioeng.* 114, 540–545. <https://doi.org/10.1016/j.jbiosc.2012.06.010>.
- Holopainen, J.K., Gershenzon, J., 2010. Multiple stress factors and the emission of plant VOCs. *Trends Plant Sci.* 15, 176–184. <https://doi.org/10.1016/j.tplants.2010.01.006>.
- Huang, X.-Q., Li, R., Fu, J., Dudareva, N., 2022. A peroxisomal heterodimeric enzyme is involved in benzaldehyde synthesis in plants. *Nat. Commun.* 13, 1352. <https://doi.org/10.1038/s41467-022-28978-2>.
- Hive, K., Bichele, I., Kaldmäe, H., Rasulov, B., Valladares, F., Niinemets, Ü., 2019. Responses of aspen leaves to heatflecks: both damaging and non-damaging rapid temperature excursions reduce photosynthesis. *Plants* 8, 145. <https://doi.org/10.3390/plants8010145>.
- Hive, K., Bichele, I., Rasulov, B., Niinemets, Ü., 2011. When it is too hot for photosynthesis: heat-induced instability of photosynthesis in relation to respiratory burst, cell permeability changes and H₂O₂ formation. *Plant Cell Environ.* 34, 1113–1126. <https://doi.org/10.1111/j.1365-3040.2010.02229.x>.
- Jansen, R.M.C., Miebach, M., Kleist, E., Henten, E.J.V., Wildt, J., 2009. Release of lipoxigenase products and monoterpenes by tomato plants as an indicator of *Borytrichae*-induced stress. *Plant Biol.* 11, 859–868. <https://doi.org/10.1111/j.1438-8677.2008.0183.x>.
- Jiang, Y., Ye, J., Li, S., Niinemets, Ü., 2017. Methyl jasmonate-induced emission of biogenic volatiles is biphasic in cucumber: a high-resolution analysis of dose dependence. *J. Exp. Bot.* 68, 4679–4694. <https://doi.org/10.1093/jxb/erw244>.
- Kännaste, A., Copolovici, L., Niinemets, Ü., 2014. Gas Chromatography–Mass Spectrometry Method for Determination of Biogenic Volatile Organic Compounds Emitted by Plants. In: *Plant Isoprenoids*, vols. 161–169. Humana Press, New York, NY. https://doi.org/10.1007/978-1-4939-0606-2_11.
- Kask, K., Kännaste, A., Talts, E., Copolovici, L., Niinemets, Ü., 2016. How specialized volatiles respond to chronic, and short-term physiological and shock heat stress in *Brassica nigra*. *Plant Cell Environ.* 39, 2027–2042. <https://doi.org/10.1111/pce.12775>.
- Khan, A., Khan, V., Pandey, K., Sopory, S.K., Sanan-Mishra, N., 2022. Thermo-priming mediated cellular networks for abiotic stress management in plants. *Front. Plant Sci.* 13, 866409. <https://doi.org/10.3389/fpls.2022.866409>.
- Law, D.R., Crafts-Brandner, S.J., Salucci, M.E., 2001. Heat stress induces the synthesis of a new form of ribulose-1,5-bisphosphate carboxylase/oxygenase in cotton leaves. *Planta* 214, 117–125. <https://doi.org/10.1007/s004420100392>.
- Liu, B., Zhang, L., Rusalepp, L., Kaurilind, E., Sulaiman, H.Y., Püssa, T., Niinemets, Ü., 2021. Heat priming improved heat tolerance of photosynthesis, enhanced terpenoid and benzenoid emission and phenolics accumulation in *Achillea millefolium*. *Plant Cell Environ.* 44, 2365–2385. <https://doi.org/10.1111/pce.13830>.
- Liu, B., Kaurilind, E., Zhang, L., Okereke, O.C., Remmel, T., Niinemets, Ü., 2022. Improved plant heat shock resistance is introduced differently by heat and insect infestation: the role of volatile emission traits. *Oecologia* 199, 53–68. <https://doi.org/10.1007/s00442-022-05168-x>.
- Lombrea, A., Antal, D., Ardelean, F., Avram, S., Pavel, L.Z., Vlaia, I., Mut, A.M., Diaconescu, Z., Dehelean, C.A., Soica, C., Dancu, C., 2020. A recent insight regarding the phytochemistry and bioactivity of *Origanum vulgare* L. essential oil. *Int. J. Mol. Sci.* 21, 9653. <https://doi.org/10.3390/ijms21249653>.
- Lu, S., Li, L., 2008. Carotenoid metabolism: biosynthesis, regulation, and beyond. *J. Integr. Plant Biol.* 50, 778–785. <https://doi.org/10.1111/j.1744-7909.2008.00708.x>.
- Marchin, R.M., Backes, D., Ossola, A., Leishman, M.R., Tjoelker, M.G., Ellsworth, D.S., 2022. Extreme heat increases stomatal conductance and drought-induced mortality

- risk in vulnerable plant species. *Global Change Biol.* 28, 1133–1146. <https://doi.org/10.1111/gcb.15976>.
- Mawlong, I., Kumar, S., Singh, D., 2016. Furan fatty acids: their role in plant systems. *Phytochemistry Rev.* 15, 121–127. <https://doi.org/10.1007/s11014-014-9388-7>.
- Miszal, P.K., Hewitt, C.N., Wildt, J., Blande, J.D., Eller, A.S., Pares, S., Gentner, D.R., Gilman, J.B., Graus, M., Greenberg, J., Guenther, A.B., 2015. Atmospheric benzene emissions from plants rival those from fossil fuels. *Sci. Rep.* 5, 1–10. <https://doi.org/10.1038/srep12064>.
- Moore, C.E., Meacham-Hensold, K., Lemonnier, P., Slattery, R.A., Benjamin, C., Bernacchi, C.J., Lawson, T., Cavanagh, A.P., 2021. The effect of increasing temperature on crop photosynthesis: from enzymes to ecosystems. *J. Exp. Bot.* 72, 2822–2844. <https://doi.org/10.1093/jxb/erab090>.
- Nguyen, D., Rieu, I., Mariani, C., van Dam, N.M., 2016. How plants handle multiple stresses: hormonal interactions underlying responses to abiotic stress and insect herbivory. *Plant Mol. Biol.* 91, 727–740. <https://doi.org/10.1007/s11103-016-0481-8>.
- Niinemets, Ü., 2010. Mild versus severe stress and BVOCs: thresholds, priming and consequences. *Trends Plant Sci.* 15, 145–153. <https://doi.org/10.1016/j.tplants.2009.11.008>.
- Niinemets, Ü., 2018. When leaves go over the thermal edge. *Plant Cell Environ.* 41, 1247–1250. <https://doi.org/10.1111/pce.13184>.
- Niinemets, Ü., 2020. Leaf trait plasticity and evolution in different plant functional types. *Annual Plant Reviews* 3, 473–522. <https://doi.org/10.1002/9781119312994.sp09714>.
- Niinemets, Ü., Arneith, A., Kuhn, U., Monson, R.K., Peñuelas, J., Staudt, M., 2010. The emission factor of volatile isoprenoids: stress, acclimation, and developmental responses. *Biogeosciences* 7, 2203–2223. <https://doi.org/10.5194/bg-7-2203-2010>.
- Niinemets, Ü., Kännaste, A., Copolovici, L., 2013. Quantitative patterns between plant volatile emissions induced by biotic stresses and the degree of damage. *Front. Plant Sci.* 4, 262. <https://doi.org/10.3389/fpls.2013.00262>.
- Niu, Y., Xiang, Y., 2018. An overview of biomembrane functions in plant responses to high-temperature stress. *Front. Plant Sci.* 9, 915. <https://doi.org/10.3389/fpls.2018.00915>.
- Okerke, C.N., Kaurilind, E., Liu, B., Kanagendran, A., Pazouki, L., Niinemet, Ü., 2022. Impact of heat stress of varying severity on papaya (*Carica papaya*) leaves: major changes in stress volatile signatures, but surprisingly small enhancements of total emissions. *Environ. Exp. Bot.* 195, 104777. <https://doi.org/10.1016/j.envexpbot.2021.104777>.
- Okerke, C.N., Liu, B., Kaurilind, E., Niinemet, Ü., 2021. Heat stress resistance drives coordination of emissions of suites of volatiles after severe heat stress and during recovery in five tropical crops. *Environ. Exp. Bot.* 184, 104375. <https://doi.org/10.1016/j.envexpbot.2021.104375>.
- Pazouki, L., Kanagendran, A., Li, S., Kännaste, A., Memari, H.R., Bichele, R., Niinemet, Ü., 2016. Mono- and sesquiterpene release from tomato (*Solanum lycopersicum*) leaves upon mild and severe heat stress and through recovery: from gene expression to emission responses. *Environ. Exp. Bot.* 132, 1–15. <https://doi.org/10.1016/j.envexpbot.2016.08.003>.
- Pazouki, L., Niinemet, Ü., 2016. Multi-substrate terpenoid synthases: their occurrence and physiological significance. *Front. Plant Sci.* 7. <https://doi.org/10.3389/fpls.2016.01019>, 019.
- R, Core Team, 2021. R: a Language and Environment for Statistical Computing. R Foundation for Statistical Computing, Vienna, Austria. <https://www.R-project.org/>.
- Rahmstorf, S., Coumou, D., 2011. Increase of extreme events in a warming world. *Proc. Natl. Acad. Sci. USA* 108, 17905. <https://doi.org/10.1073/pnas.1101766108>.
- Rizkhy, L., Liang, H., Mittler, R., 2002. The combined effect of drought stress and heat shock on gene expression in tobacco. *Plant Physiol.* 130, 1143–1151. <https://doi.org/10.1104/pp.006858>.
- Sallaud, C., Rontein, D., Onillon, S., Jabès, F., Giacalone, C., Thoraval, S., Escoffier, C., Herbette, G., Leonhardt, N., Gausse, M., 2009. A novel pathway for sesquiterpene biosynthesis from Z, Z-farnesyl pyrophosphate in the wild tomato *Solanum habrochaites*. *Plant Cell* 21, 301–317. <https://doi.org/10.1105/tpc.107.057885>.
- Salvucci, M.E., Crafts-Brandner, S.J., 2004. Inhibition of photosynthesis by heat stress: the activation state of Rubisco as a limiting factor in photosynthesis. *Physiol. plantarum* 120, 179–186. <https://doi.org/10.1111/j.0031-9317.2004.0173.x>.
- Sanyal, R.P., Misra, H.S., Saini, A., 2018. Heat-stress priming and alternative splicing-linked memory. *J. Exp. Bot.* 69, 2431–2434. <https://doi.org/10.1093/jxb/ery111>.
- Serrano, N., Ling, Y., Bahiedin, A., Maifrou, M.M., 2019. Thermopriming reprograms metabolic homeostasis to confer heat tolerance. *Sci. Rep.* 9, 1–14. <https://doi.org/10.1038/s41598-018-36484-z>.
- Stolterfoht, H., Rinnofer, C., Winkler, M., Pichler, H., 2019. Recombinant lipoxygenases and hydroperoxide lyases for the synthesis of green leaf volatiles. *J. Agric. Food Chem.* 67, 13367–13392. <https://doi.org/10.1021/acs.jafc.902690>.
- Sulaiman, H.Y., Liu, B., Kaurilind, E., Niinemet, Ü., 2021. Phloem-feeding insect infestation antagonizes volatile organic compound emissions and enhances heat stress recovery of photosynthesis in *Origanum vulgare*. *Environ. Exp. Bot.* 189, 104551. <https://doi.org/10.1016/j.envexpbot.2021.104551>.
- Sulaiman, H.Y., Runno-Pauson, E., Kaurilind, E., Niinemet, Ü., 2023. Differential impact of crown rust (*Puccinia coronata*) infection on photosynthesis and volatile emissions in the primary host *Avena sativa* and the alternate host *Rhizopus frugalis*. *J. Exp. Bot.* <https://doi.org/10.1093/jxb/era001>.
- Teskey, R., Werten, T., Bauweraerts, I., Aneye, M., McGuire, M.A., Steppe, K., 2015. Responses of tree species to heat waves and extreme heat events. *Plant Cell Environ.* 38, 1699–1712. <https://doi.org/10.1111/pce.12417>.
- Tsvetkova, N.M., Horvath, I., Török, Z., Wolkers, W.F., Balogi, Z., Shigapova, N., Crowe, L.M., Tablin, F., Vieting, E., Crowe, J.H., Vigh, L., 2002. Small heat-shock proteins regulate membrane lipid polyphosphatase. *Proc. Natl. Acad. Sci. USA* 99, 13504–13509. <https://doi.org/10.1073/pnas.192468399>.
- Turan, S., Kask, K., Kanagendran, A., Li, S., Anni, R., Talts, E., Rasulov, B., Kännaste, A., Niinemet, Ü., 2019. Lethal heat stress-dependent volatile emissions from tobacco leaves: what happens beyond the thermal edge? *J. Exp. Bot.* 70, 5017–5030. <https://doi.org/10.1093/jxb/erz255>.
- Urban, J., Ingwers, M.W., McGuire, M.A., Teskey, R.O., 2017. Increase in leaf temperature opens stomata and decouples net photosynthesis from stomatal conductance in *Pinus taeda* and *Populus deltoides* x *nigra*. *J. Exp. Bot.* 68, 1757–1767. <https://doi.org/10.1093/jxb/erx052>.
- Velikova, V., Pinelli, P., Loreto, F., 2005. Consequences of inhibition of isoprene synthesis in *Phragmites australis* leaves exposed to elevated temperatures. *Agric. Ecosyst. Environ.* 106, 209–217. <https://doi.org/10.1016/j.ageec.2004.10.009>.
- Vihervaara, A., Mahat, B.D., Guertin, M.J., Chu, T., Danko, C.G., Lék, J.T., Sistonen, L., 2017. Transcriptional response to stress is pre-wired by promoter and enhancer architecture. *Nat. Commun.* 8, 255. <https://doi.org/10.1038/s41467-017-00151-0>.
- Vincenti, S., Mariani, M., Alberti, J.-C., Jacopini, S., Brunini-Bronzini de Caraffa, V., Berti, L., Maury, J., 2019. Biocatalytic synthesis of natural green leaf volatiles using the lipoxygenase metabolic pathway. *Catalysts* 9, 873. <https://doi.org/10.3390/catal9100873>.
- Von Caemmerer, S., Farquhar, G.D., 1981. Some relationships between the biochemistry of photosynthesis and the gas exchange of leaves. *Planta* 153, 376–387. <https://doi.org/10.1007/BF00384257>.
- Wahid, A., Gelani, S., Ashraf, M., Foolad, M.R., 2007. Heat tolerance in plants: an overview. *Environ. Exp. Bot.* 61, 199–223. <https://doi.org/10.1016/j.envexpbot.2007.05.011>.
- Wang, L.-J., Fan, L., Loescher, W., Duan, W., Liu, G.-J., Cheng, J.-S., Luo, H.-B., Li, S.-H., 2010. Salicylic acid alleviates decreases in photosynthesis under heat stress and accelerates recovery in grapevine leaves. *BMC Plant Biol.* 10, 34. <https://doi.org/10.1186/1471-2229-10-34>.
- Wang, Y., Zhu, M., Mei, J., Luo, S., Leng, T., Chen, Y., Nie, S., Xie, M., 2019. Comparison of furans formation and volatile aldehydes profiles of four different vegetable oils during thermal oxidation. *J. Food Sci.* 84, 1966–1978. <https://doi.org/10.1111/1750-3841.14659>.
- Wang, X., Cai, J., Liu, F., Dai, T., Cao, W., Wollenweber, B., Jiang, D., 2014. Multiple heat priming enhances thermo-tolerance to a later high temperature stress via improving subcellular antioxidant activities in wheat seedlings. *Plant Physiol. Biochem.* 74, 185–192. <https://doi.org/10.1016/j.plaphy.2013.11.014>.
- Wenig, P., Oedermaier, J., 2010. OpenChrom: a cross-platform open source software for the mass spectrometric analysis of chromatographic data. *BMC Bioinf.* 11, 1–9. <https://doi.org/10.1186/1471-2105-11-405>.



Sulaiman, HY, Liu B, Kaurilind E, Niinemets Ü. 2021. Phloem-feeding insect infestation antagonizes volatile organic compound emissions and enhances heat stress recovery of photosynthesis in *Origanum vulgare*. *Environmental and Experimental Botany* 189: 104551.



Contents lists available at ScienceDirect

Environmental and Experimental Botany

journal homepage: www.elsevier.com/locate/envexpbot

Phloem-feeding insect infestation antagonizes volatile organic compound emissions and enhances heat stress recovery of photosynthesis in *Origanum vulgare*

Hassan Y. Sulaiman^{a,*}, Bin Liu^a, Eve Kaurilind^a, Ülo Niinemets^{a,b}^a Chair of Crop Science and Plant Biology, Estonian University of Life Sciences, Kreutzwaldi 5, 51006 Tartu, Estonia^b Estonian Academy of Sciences, Kohtu 6, 10130 Tallinn, Estonia

ARTICLE INFO

Keywords:
Benzenoid
Biotic stress
Lipoxygenase
Monoterpene
Sesquiterpene
Terpene
Heat-shock response

ABSTRACT

Heatwaves are expected to become more frequent and directly exert major stress on plants. Warmer weather can also increase the frequency of biotic infestations. However, how biotic stress alters heat resistance and how interacting heat and biotic stresses alter volatile organic compound (VOC) emissions remain unclear. We studied how heat shock (45 °C for 5 min) and *Trialeurodes vaporariorum* infestation alone and in combination affect foliage photosynthetic characteristics and VOC emissions in *Origanum vulgare*, right after heat stress through 48 h recovery. Heat stress alone decreased photosynthesis rate (*A*) but increased stomatal conductance (*g_s*), emissions of lipoxygenase pathway volatiles (LOX), benzenoids and terpenoids. Neither *A* nor VOC emissions recovered to pre-stress values at 48 h after stress application. Whitefly infestation reduced *A* and increased *g_s*, and resulted in a moderate increase in terpene emissions, but inhibited constitutive LOX and benzenoid emissions. Heat stress applied on whitefly infestation reduced *A* and increased *g_s*, and resulted in a much lower enhancement of LOX and terpene emissions. Photosynthetic characteristics fully recovered at 48 h after stress treatment. Our results suggest that under phloem-feeding insect herbivory, VOC emission responses to extreme temperature are highly desensitized and photosynthetic thermal tolerance is improved.

1. Introduction

Environmental stress can trigger plants to modify physiological characteristics including volatile organic compound (VOC) emission (Blande et al., 2014; Rinnan et al., 2014; Jud et al., 2016). Stress-elicited VOC synthesized via different secondary metabolism pathways can offer direct protection, such as repelling herbivores and serving as non-enzymatic antioxidants, or indirect protections by triggering different defense pathways in plants (Niinemets et al., 2013; Salerno et al., 2017; Brill et al., 2019). Among the earliest volatiles elicited upon stress exposure are lipoxygenase (LOX) pathway volatiles, also called green leaf volatiles, that consist of different C5- and C6-aldehydes and derivatives (Loreto et al., 2006; Niinemets et al., 2010a, b; Scala et al., 2013). Emissions of ubiquitous LOX volatiles start in a time scale of minutes after stress exposure and are usually accompanied by long-term, hours to days, activation of different defense pathways leading to the emissions of various specialized volatiles including isoprenoids (mono-, sesquiterpenes and their derivatives) from plastidial

2-C-methyl-D-erythritol 4-phosphate/1-deoxy-D-xylulose 5-phosphate (MEP/DOXP) and cytosolic mevalonate (MVA) pathways (Dudareva et al., 2004, 2005; Sallaud et al., 2009) to benzenoids primarily originating from the shikimate pathway in the plastid (Rostas et al., 2006; Irti and Faoro, 2009; Misztal et al., 2015). The degree of recovery upon stress-elicited emissions depends on stress severity (Copolovici and Niinemets, 2010; Grote et al., 2019; Niinemets et al., 2013).

Plants in nature often encounter sequential or simultaneous biotic and abiotic stress combinations, such as heat and insect infestation (Holopainen and Gershenzon, 2010; Niinemets, 2010; Pareja and Pinto-Zevallos, 2016). Plant response to one stressor can be suppressed or enhanced by the presence of another stressor, as the hormonal pathways controlling stress and recovery responses function synergistically or antagonistically (Ben Rejeb et al., 2014; Atkinson et al., 2015). In the case of sequential or superimposed stress effects, metabolic changes initiated by the preceding stresses can prime responses to subsequent stressors (Cardoza et al., 2002; Copolovici et al., 2012; Bäurle, 2018; Hilker and Schmittling, 2019). Due to changes in plant

* Corresponding author.

E-mail address: Hassanyusulsulaiman@emu.ee (H.Y. Sulaiman).<https://doi.org/10.1016/j.envexpbot.2021.104551>

Received 8 April 2021; Received in revised form 30 May 2021; Accepted 4 June 2021

Available online 8 June 2021

0098-8472/© 2021 Elsevier B.V. All rights reserved.

physiological activity and oxidative status induced right after the stress and priming/acclimation responses occurring through recovery, the effects of sequential stressors can often be interactive rather than additive, regardless of the time between the occurrence of both stresses (Niinemets, 2010; Atkinson et al., 2015; Hilke and Schmülling, 2019). Moreover, VOC emission responses to combined stresses are species- and stress-specific and cannot be easily predicted based on the activity of stress signaling pathways in response to single stress (Holopainen and Gershenzon, 2010; Niinemets, 2010). For example, ozone stress reduced herbivore inducible emissions in *Brassica napus* (Himanen et al., 2009), whereas in *Solanum lycopersicum*, ozone stress amplified emission responses to *Bemisia tabaci* infestation (Cui et al., 2014). Drought enhanced volatile emissions in *Spodoptera exigua*-fed *Solanum dulcamara* (Dawood et al., 2016), whereas in *Vicia faba*, drought reduced volatile emissions induced by *Trissolcusbasalis* feeding (Salerno et al., 2017). Despite the gain in knowledge, the physiological mechanisms for study-to-study differences in VOC emission responses to frequently co-existing stresses remain largely unclear.

Heat stress in plants results from exposure to supraoptimal temperatures ($T > 35\text{ }^{\circ}\text{C}$), leading to a reduction in net assimilation rate (A) due to damage in the thylakoid membranes of chloroplast and inactivation of Rubisco (Camejo et al., 2005; Demirevska-Kepova et al., 2005; Luo et al., 2011), and with damage of plasma membrane and a burst of reactive oxygen species (ROS), particularly in severe stress case (Wahid et al., 2007; Hueve et al., 2011). Herbivory leads to direct physical damage due to removal of plant parts (chewing herbivores) or piercing specific plant tissues by phloem-feeding herbivores such as aphids and whiteflies, and by xylem-feeding herbivores such as spittlebugs and leafhoppers. Both heat and herbivory stress independently prompt qualitative and quantitative changes in VOC profiles with several converging features including elicitation of LOX and terpene emissions (Niinemets et al., 2013; Turan et al., 2019; Faiola and Taipale, 2020), but their combined effects are poorly understood.

It is further important to mention that different types of herbivores elicit different defense responses in plants. While chewing herbivores elicit LOX pathway and jasmonic acid (JA) dependent defenses, phloem-feeders elicit salicylic acid (SA) dependent defenses (Holopainen and Gershenzon, 2010; Eberl et al., 2018; Zhang et al., 2018). Stress elicitation of either signaling typically antagonizes the other (Kempema et al., 2007; Van der Does et al., 2013). Heat stress, on the other hand, typically elicits JA-dependent signaling pathways (Sharma and Laxmi, 2016; Xu et al., 2016), and heat stress resistance can be enhanced by SA accumulation due to physiological modifications such as enhanced proline content and overall enhanced osmotic content that improve membrane integrity (Chen et al., 2009; Islam et al., 2009; Cvikrova et al., 2013; Nguyen et al., 2016). Membrane-level damage due to heat shock can be further amplified by chewing herbivore-dependent JA accumulation (Balfagón et al., 2019 for review). Conversely, piercing herbivore-dependent SA accumulation can increase the plant resistance to heat stress and antagonize JA-dependent volatile emissions (Thaler et al., 2012; Tsai et al., 2019). The suppression of the JA signaling may result in an overall decrease in VOC emission (Engelberth et al., 2001; Eberl et al., 2018). Thus, different types of herbivory can result in different interactive responses during heat stress.

In this study, we investigated how heat shock and greenhouse whitefly feeding individually and in conjunction alter the kinetic of VOC emissions and foliage photosynthetic characteristics in *Origanum vulgare*. *Origanum vulgare* L. (Lamiaceae) is a cosmopolitan crop plant with highly aromatic foliage due to large glandular trichomes containing high amounts of terpenoids (Chun et al., 2005; Agliassa and Maffei, 2018) and benzenoids toxic to herbivorous insects (Carroll et al., 2017). Greenhouse whitefly (*Trialeurodes vaporariorum* Westwood, hereafter GWF) is a polyphagous phloem-feeder species, notorious for invading and feeding on greenhouse vegetables including *O. vulgare* (Gabarra et al., 2004; McKee et al., 2009). The insect family Aleyrodidae (whitefly) is a good model for studying phloem-feeding insect-plant

interactions, as unlike aphid species that punctures several sites, whitefly confines itself to one site on a minor vein of the phloem and feeds on this site continuously, 21–30 days, and typically does not damage the epidermal or mesophyll cells before piercing the phloem cells (Kempema et al., 2007; Walling, 2008). So far, only a few studies investigated herbivory induced-VOC in *Origanum* spp. and all the previous studies were conducted with chewing herbivores (e.g., Akhtar and Isman, 2004; Carroll et al., 2017; Agliassa and Maffei, 2018). To our knowledge, VOC emissions induced by heat stress applied alone or in combination with insect feeding have not been investigated in *O. vulgare*. We hypothesized that the presence of GWF infestation acts primarily through the SA-dependent pathway and results in foliage benzenoid emissions and minor changes in LOX volatiles and terpenoids, and that GWF infestation reduces volatile responses during heat shock stress and that the two stress effects will exert antagonistic effects on VOC emissions and gas exchange characteristics during the recovery period.

2. Materials and methods

2.1. Plant material and growth

Origanum vulgare seeds purchased from Nordic Botanical Ltd (Tartu, Estonia) were sown in well-drained 0.5 l plastic pots filled with 1:1 mixture of quartz and commercial potting soil that included slow-release essential micro- and macronutrients (Biolan Oy, Kekkila group, Finland). The plants were cultivated in a plant-growth room conditioned at day/night temperature of 24/18 $^{\circ}\text{C}$, an ambient air CO_2 concentration of 380–400 $\mu\text{mol mol}^{-1}$ and relative humidity of 60–70 % and daylight intensity of 600 $\mu\text{mol m}^{-2}\text{ s}^{-1}$ at plant level supplied for 12 h photoperiod. The plants were watered to soil field capacity every two days. Three-month-old plants with fully mature leaves were used in the experiments.

2.2. Insect infestation

Mature *O. vulgare* plants were infested with GWF by placing them in a circular arrangement around the point of intersection of squarely arranged already heavily infested plants in the plant-growth room. To avoid the accumulation of black sooty mold that can be observed when the lower leaf surface covered by insect excreta (honeydew) becomes colonized by fungi, the measurements were conducted after 14 days of infestation. Preceding the measurements there were only a few first instar larvae on the lower leaf surface. Sampled upper canopy leaves of independent plants that hosted a flock of six to eight GWF adults per leaf were used in the experiments. In total 12 independent plants were used in the experiments, six non-infested and six infested plants, in which three infested and three non-infested plants were further subjected to heat shock treatment.

2.3. Heat shock treatment

Heat shock was applied as described previously (Liu et al., 2020) with some modifications here. In summary, upper canopy leaves were firstly enclosed in a polythene bag, to avoid water penetration, and immediately immersed into distilled water set at a stable temperature of 45 $^{\circ}\text{C}$ using a temperature-controlled water bath (VWR International, West Chester, Pennsylvania, USA). The treatment time was 5 min, but the bag was immersed in the medium for 30 s longer to account for the finite thermal conductivity of the polyethylene bag. The control plants (infested and non-infested) were treated in the same way, except that the water bath temperature was 25 $^{\circ}\text{C}$. The plants were carefully removed from the polyethylene bag and inserted in the measurement chamber for foliage gas exchange and volatile measurements in less than 1 min after the treatment. This experimental set-up was carried out in three replicates each for non-infested and infested plants. All the insects were removed from the infested plants, including infested control plants,

before applying the heat shock treatment.

2.4. Gas exchange measurements and volatile sampling

A custom-made open gas exchange system was used to measure the rate of photosynthesis (Copolovici and Niinemets, 2010 for details of the measurement system). The system has a temperature-controlled double-walled cylindrical glass chamber with stainless steel bottom designed for trace gas sampling. The temperature of the chamber was maintained at the desired level by circulating water with the set temperature between the double layers of the chamber. The air temperature inside the chamber was monitored by a thermistor (NTC thermistor, model ACC-001, RTI Electronics, Inc., St. Anaheim, CA, USA). The air was drawn from outside at a constant flow rate of 0.0361 s^{-1} , purified by passing through a custom-made ozone trap and a charcoal filter, and humidified to the desired relative humidity using a custom-made humidifier (Copolovici et al., 2012; Copolovici and Niinemets, 2010). Sampled leaves were enclosed in the glass chamber and a chamber temperature of $25\text{ }^{\circ}\text{C}$ (leaf temperature = $25 \pm 1\text{ }^{\circ}\text{C}$) was established. The enclosed leaves were illuminated by a light intensity of $600\text{ }\mu\text{mol m}^{-2}\text{ s}^{-1}$ supplied to the plants using four 50 W halogen lamps installed right above the chamber. All other environmental variables in the chamber were set to correspond to the plant growth conditions (section 2.1). An infrared dual-channel gas analyzer (CIRAS II, PP-systems, Amesbury, MA, USA) was used to measure the concentrations of H_2O and CO_2 at the chamber inlet and outlet.

Gas exchange measurements were taken immediately after gas flows stabilized and foliar gas-exchange rates attained a stable value, typically in ca. 15–20 min after leaf enclosure. Volatiles were collected concurrently with gas exchange measurements. A suction pump (210–1003 MTX, SKC Inc., Houston, TX, USA) operated at a flow rate of 0.2 L min^{-1} was used to collect 4 L of gas samples onto a stainless steel adsorbent cartridge filled with three different Carbotrap (Supelco, Bellefonte, PA, USA) adsorbents for optimum adsorption of C3–C17 volatiles (Kännaste et al., 2014 for details of cartridges). The measurements were carried out at 0.5 h, 2.5 h, 5 h, 24 h, and 48 h after the treatments. The measurements in independent control plants were carried out analogously. Volatiles were also collected regularly from the empty measurement chamber to estimate background volatile concentrations. Pictures of all the sampled leaves were taken with a digital camera at 1200 dpi and leaf surface area was measured with ImageJ 1.8.0 (NIH, Bethesda, Maryland, USA).

2.5. GS–MS analyses

The adsorbent cartridges were analyzed using a combined Shimadzu TD20 automated cartridge desorber and Shimadzu 2010 GC–MS system (Shimadzu Corporation, Kyoto, Japan) following the procedure described in Kännaste et al. (2014). The compounds were identified and quantified using chemical standards (Sigma-Aldrich, St. Louis, MO, USA) and NIST library ver. 05. Background volatile concentrations in the empty chamber were subtracted from the concentrations reached with leaves enclosed. We grouped volatiles based on their metabolic pathways of synthesis and analyzed qualitative and quantitative changes as LOX pathway volatiles, terpenoids, benzenoids, fatty acid-derived compounds (FAD), and geranylgeranyl diphosphate pathway (GGDP) volatiles (carotenoid breakdown products, Table 1 for the list of compounds). As hexanal can be produced both via LOX pathway and the pathway forming other saturated aldehydes, but under stress, it primarily comes from LOX pathway (Heiden et al., 2003), hexanal was considered as the LOX pathway product and all other aliphatic saturated compounds with more than six carbon atoms as FAD volatiles.

2.6. Data analyses

The A and stomatal conductance to water vapor (g_s) per leaf area

were calculated from gas exchange measurements according to von Caemmerer and Farquhar (1981). The VOC emission rates were calculated according to Niinemets et al. (2011). The effect of heat shock, GWF infestation and recovery time and their interaction on gas exchange characteristics and VOC emission rates were tested by using three-way ANOVA. Means at different time points through stress recovery were statistically compared using Fisher's least square difference following one-way ANOVA. Where necessary, the data used for ANOVA tests were log-transformed to improve the distribution of variances. The relationships among different VOC groups and gas exchange characteristics in different treatments were explored using linear regression. The differences in treatment group volatile blends were explored by principal component analysis (PCA) after mean-centring and logarithmical data transformation. The differences in the volatile blends were also explored by permutational multivariate analysis (PERMANOVA) using the Bray-Curtis dissimilarity statistic. The data were log-transformed before PERMANOVA. All statistical tests were considered significant at $P \leq 0.05$. All statistical computations and visualizations were conducted with R ver. 4.2.0 statistical software (R Core Team, 2020).

3. Results

3.1. Stress effects on photosynthetic characteristics

In the non-infested control plants, A was stable at a level of 7–9 $\mu\text{mol m}^{-2}\text{ s}^{-1}$ throughout the experiment (Fig. 1a). At 2.5 h after heat stress application, the A in the non-infested plants significantly ($P < 0.01$) decreased to a level of $5.2 \pm 0.7\text{ }\mu\text{mol m}^{-2}\text{ s}^{-1}$ and remained at that level throughout the experiment (Fig. 1a). Whitefly effects on A varied among different time points through the recovery period ($P < 0.01$ for Whitefly \times Time; Table 2). GWF infestation applied alone significantly decreased A to a level of $4.9 \pm 1.1\text{ }\mu\text{mol m}^{-2}\text{ s}^{-1}$ ($P < 0.05$ compared to control) through the initial 5 h recovery period (Fig. 1a). Combined heat shock and insect infestation significantly decreased A to a level of $2.8 \pm 0.6\text{ }\mu\text{mol m}^{-2}\text{ s}^{-1}$ ($P < 0.01$ compared to control) through the first 5 h after treatment (Fig. 1a). At 24 h after treatment, all infested plants, regardless of heat stress treatment, had recovered partly, and by the end of the experiment, they had fully recovered (Fig. 1a).

Stomatal conductance (g_s) in the non-infested control plants was at a stable level of 32–40 $\text{mmol m}^{-2}\text{ s}^{-1}$. Upon heat shock treatment, g_s in the non-infested control plants immediately increased ($P < 0.01$) and remained at a high level of 54–72 $\text{mmol m}^{-2}\text{ s}^{-1}$ throughout the experiment (Fig. 1b). Insect infestation alone and combined heat shock and insect infestation treatment respectively increased g_s to an elevated level of $60 \pm 14\text{ }\text{mmol m}^{-2}\text{ s}^{-1}$ and $67 \pm 9\text{ }\text{mmol m}^{-2}\text{ s}^{-1}$ ($P < 0.01$ compared to non-stressed conditions) at 0.5 h after treatment (Fig. 1b). However, between 2.5–5 h after treatment, g_s in all the infested plants, regardless of heat stress treatment, was at the level of g_s in non-stressed control plants (Fig. 1b). The g_s subsequently increased with time of recovery, reaching a level of $70 \pm 23\text{ }\text{mmol m}^{-2}\text{ s}^{-1}$ in infested plants not treated with heat and a level of $101 \pm 8\text{ }\text{mmol m}^{-2}\text{ s}^{-1}$ ($P < 0.01$ compared to control) in heat-treated infested plants (Fig. 1b).

3.2. Emission of lipoxygenase pathway products and long-chained fatty acid-derived volatiles

LOX product emissions were at a very low level of 0.021–0.062 $\text{nmol m}^{-2}\text{ s}^{-1}$ in non-infested control plants (Fig. 2a; Table 1). Upon heat shock, LOX emissions in non-infested plants strongly increased ($P < 0.01$) to a level of $2.66 \pm 0.16\text{ }\text{nmol m}^{-2}\text{ s}^{-1}$ and remained high through the recovery period (Fig. 2a; Table 1). No LOX emissions were detected in plants treated with only GWF feeding (Fig. 2a). The interaction between heat shock and whitefly infestation was significant for LOX emissions ($P < 0.01$, Table 2). LOX emissions in the combined heat and whitefly-stressed plants declined from control level to below the level of detection at 24 h and 48 h after treatment (Fig. 2a). Baseline emissions of

Table 1

Average \pm SE emission rates (nmol m⁻² s⁻¹) of volatile organic compounds emitted by non-stressed (Control, n = 3), heat-stressed (Heat, n = 3), *Trialeurodes vaporariorum*-infested (Whiteflies, n = 3) and heat-stressed *T. vaporariorum*-infested (Whiteflies + Heat, n = 3) *Origanum vulgare* leaves at 0.5 h, 2.5 h, 5 h, 24 h and 48 h recovery interval. N.D refers to not detectable.

		0.5 h				2.5 h				5 h			
		Control	Heat	Whiteflies	Whiteflies + Heat	Control	Heat	Whiteflies	Whiteflies + Heat	Control	Heat	Whiteflies	Whiteflies + Heat
LOX pathway compounds													
1	Pentanal	0.003 \pm 0.003	N. D.	N. D.	N. D.	0.003 \pm 0.003	N. D.	N. D.	N. D.	0.002 \pm 0.001	N. D.	N. D.	N. D.
2	Hexanal	0.01 \pm 0.01	1.15 \pm 0.92	N.D	0.09 \pm 0.09	0.004 \pm 0.004	0.18 \pm 0.18	N.D	0.04 \pm 0.02	0.010 \pm 0.006	0.02 \pm 0.02	N.D	0.0002 \pm 0.0002
3	1-Hexanol	0.008 \pm 0.008	1.71 \pm 1.71	N.D	N.D	0.001 \pm 0.001	3.75 \pm 3.75	N.D	N.D	0.001 \pm 0.001	1.50 \pm \pm 1.50	N.D	N.D
4	(E)-3-Hexen-1-ol	0.0019 \pm 0.0010	N.D	N.D	N.D	0.001 \pm 0.001	0.23 \pm 0.20	N.D	N.D	0.001 \pm 0.001	0.15 \pm 0.15	N.D	N.D
Long-chained fatty acid-derived compounds													
5	Heptanal	0.015 \pm 0.003	0.41 \pm 0.31	N.D	0.069 \pm 0.039	0.007 \pm 0.005	N.D	0.06 \pm 0.06	N.D	0.014 \pm 0.007	N.D	0.10 \pm 0.10	N.D
6	2-Ethyl-hexanol	N.D	0.06 \pm 0.06	N.D	0.27 \pm 0.07	N.D	0.39 \pm 0.30	0.09 \pm 0.05	N.D	N.D	0.35 \pm 0.35	2.35 \pm 1.16	0.52 \pm 0.52
7	1-Octanol	0.020 \pm 0.002	N.D	N.D	N.D	0.011 \pm 0.003	N.D	N.D	N.D	0.01 \pm 0.003	N.D	N.D	N.D
8	1-Nonanol	0.009 \pm 0.009	N.D	N.D	N.D	0.002 \pm 0.002	N.D	N.D	N.D	0.009 \pm 0.009	N.D	N.D	N.D
Terpenoids													
9	Isoprene	N.D	N.D	N.D	0.05 \pm 0.05	N.D	0.35 \pm 0.22	0.17 \pm 0.17	0.13 \pm 0.13	N.D	0.029 \pm 0.029	0.136 \pm 0.136	0.05 \pm 0.05
Monoterpenes													
10	α -Thujene	N.D	0.90 \pm 0.20	0.004 \pm 0.004	N.D	N.D	1.47 \pm 0.75	0.14 \pm 0.04	N.D	N.D	N.D	0.13 \pm 0.02	N.D
11	α -sabinene	N.D	0.47 \pm 0.35	N.D	N.D	N.D	0.59 \pm 0.32	N.D	N.D	N.D	0.52 \pm 0.49	N.D	N.D
12	α -pinene	0.01 \pm 0.004	0.51 \pm 0.01	0.12 \pm 0.01	0.045 \pm 0.004	0.007 \pm 0.001	0.31 \pm 0.09	0.64 \pm 0.07	0.042 \pm 0.03	0.12 \pm 0.003	0.3 \pm 0.08	0.54 \pm 0.06	0.037 \pm 0.006
13	Camphene	N.D	N.D	N.D	N.D	N.D	0.011 \pm 0.006	0.04 \pm 0.02	N.D	N.D	0.03 \pm 0.03	0.038 \pm 0.013	N.D
14	α -Ocimene	N.D	0.16 \pm 0.15	0.002 \pm 0.002	N.D	N.D	0.44 \pm 0.33	N.D	N.D	N.D	1.65 \pm 1.31	0.045 \pm 0.045	N.D
15	(E)- β -Ocimene	N.D	2.69 \pm 1.05	1.51 \pm 0.88	0.07 \pm 0.018	N.D	6.83 \pm 2.67	1.67 \pm 1.19	0.04 \pm 0.002	N.D	11.43 \pm 5.38	1.78 \pm 1.24	0.037 \pm 0.001
16	3-Carene	0.007 \pm 0.004	0.11 \pm 0.07	N.D	0.017 \pm 0.009	0.0005 \pm 0.0002	0.11 \pm 0.07	0.18 \pm 0.09	0.006 \pm 0.006	0.001 \pm 0.006	0.062 \pm 0.02	0.24 \pm 0.098	0.0038 \pm 0.0031
17	4-Carene	N.D	0.54 \pm 0.22	N.D	N.D	N.D	0.62 \pm 0.36	N.D	N.D	N.D	0.55 \pm 0.09	N.D	N.D
18	Limonene	0.0003 \pm 0.0003	0.53 \pm 0.23	N.D	0.015 \pm 0.041	0.001 \pm 0.001	0.46 \pm 0.27	0.032 \pm 0.019	N.D	0.002 \pm 0.002	0.21 \pm 0.21	0.036 \pm 0.019	N.D
19	α -Phellandrene	N.D	0.07 \pm 0.06	N.D	N.D	N.D	0.25 \pm 0.17	0.25 \pm 0.17	N.D	N.D	0.179 \pm 0.13	0.067 \pm 0.067	N.D
20	Carvacrol	N.D	0.37 \pm 0.35	N.D	0.041 \pm 0.041	N.D	0.43 \pm 0.32	0.03 \pm 0.03	0.009 \pm 0.009	N.D	0.014 \pm 0.014	0.0005 \pm 0.00005	N.D
21	Terpinolene	N.D	0.11 \pm 0.11	N.D	N.D	N.D	0.21 \pm 0.21	0.03 \pm 0.03	0.0001 \pm 0.0001	N.D	0.176 \pm 0.176	N.D	N.D
22	α -Terpinene	N.D	0.33 \pm 0.24	N.D	N.D	N.D	0.32 \pm 0.28	0.07 \pm 0.07	N.D	N.D	0.376 \pm 0.20	0.03 \pm 0.03	N.D
23	γ -Terpinene	N.D		N.D	N.D	N.D			N.D	N.D			N.D

(continued on next page)

Table 1 (continued)

	0.5 h				2.5 h				5 h				
	Control	Heat	Whiteflies	Whiteflies + Heat	Control	Heat	Whiteflies	Whiteflies + Heat	Control	Heat	Whiteflies	Whiteflies + Heat	
24	β-Myrcene	N.D.	1.59 ± 0.85	N.D.	N.D.	1.45 ± 0.78	0.17 ± 0.05	N.D.	N.D.	1.44 ± 0.89	0.269 ± 0.09	N.D.	
25	Thymol	N.D.	0.22 ± 0.19	N.D.	N.D.	0.75 ± 0.54	0.12 ± 0.06	N.D.	N.D.	0.868 ± 0.85	N.D.	N.D.	
26	p-Cymene	N.D.	0.03 ± 0.01	0.11 ± 0.09	N.D.	0.06 ± 0.06	N.D.	N.D.	N.D.	N.D.	N.D.	N.D.	
Sesquiterpenes													
27	α-Bisabolene	N.D.	0.18 ± 0.18	N.D.	N.D.	0.05 ± 0.02	N.D.	N.D.	N.D.	0.036 ± 0.019	N.D.	N.D.	
Benzenoids													
28	Benzaldehyde	0.04 ± 0.02	0.02 ± 0.02	N.D.	0.039 ± 0.039	0.02 ± 0.01	N.D.	0.08 ± 0.01	0.082 ± 0.015	0.026 ± 0.009	0.31 ± 0.06	N.D.	N.D.
29	Toluene	0.029 ± 0.029	0.02 ± 0.01	N.D.	0.48 ± 0.36	0.05 ± 0.03	0.74 ± 0.39	N.D.	0.80 ± 0.71	0.01 ± 0.01	1.34 ± 0.84	N.D.	N.D.
Geranylgeranyl diphosphate pathway products													
30	6-Methyl-5-heptene-2-one	0.06 ± 0.01	2.28 ± 1.47	N.D.	0.21 ± 0.10	0.007 ± 0.007	0.30 ± 0.30	0.68 ± 0.34	0.027 ± 0.027	0.045 ± 0.023	0.56 ± 0.56	2.69 ± 2.024	0.159 ± 0.108
31	Geranylacetone	0.20 ± 0.01	0.86 ± 0.47	N.D.	N.D.	0.02 ± 0.01	0.29 ± 0.06	0.43 ± 0.43	N.D.	0.02 ± 0.01	0.215 ± 0.20	0.387 ± 0.14	N.D.
24 h													
		Control	Heat	Whiteflies	Whiteflies + Heat	48 h							
						Control	Heat	Whiteflies	Whiteflies + Heat				
Lipxygenase pathway compounds													
1	Pentanal	0.002 ± 0.001	N.D.	N.D.	N.D.	0.004 ± 0.004	N.D.	N.D.	N.D.	N.D.	N.D.	N.D.	
2	Hexanal	0.001 ± 0.001	1.23 ± 0.62	N.D.	N.D.	0.004 ± 0.004	0.08 ± 0.08	N.D.	N.D.	N.D.	N.D.		
3	1-Hexanol	0.034 ± 0.034	1.18 ± 1.18	N.D.	N.D.	0.001 ± 0.001	1.32 ± 1.32	N.D.	N.D.	N.D.	N.D.		
4	(E)-3-Hexen-1-ol	0.19 ± 0.19	0.018 ± 0.010	N.D.	N.D.	0.0003 ± 0.0003	N.D.	N.D.	N.D.	N.D.	N.D.		
Long-chained fatty acid-derived compounds													
5	Heptanal	0.015 ± 0.007	N.D.	N.D.	N.D.	0.012 ± 0.012	N.D.	N.D.	N.D.	N.D.	N.D.		
6	2-Ethyl-hexanal	N.D.	N.D.	N.D.	N.D.	N.D.	2.33 ± 1.38	N.D.	N.D.	N.D.	N.D.		
7	1-Octanol	0.020 ± 0.003	N.D.	N.D.	N.D.	0.010 ± 0.003	N.D.	N.D.	N.D.	N.D.	N.D.		
8	1-Nonanol	0.009 ± 0.009	N.D.	N.D.	N.D.	0.008 ± 0.008	N.D.	N.D.	N.D.	N.D.	N.D.		
Terpenoids													
9	Isoprene	N.D.	N.D.	N.D.	0.16 ± 0.16	N.D.	N.D.	N.D.	N.D.	N.D.	1.17 ± 0.63		
Monoterpenes													
10	α-Thujene	N.D.	N.D.	0.008 ± 0.008	N.D.	N.D.	N.D.	0.12 ± 0.12	N.D.	N.D.	N.D.		
11	α-sabinene	N.D.	0.14 ± 0.07	N.D.	N.D.	N.D.	N.D.	N.D.	N.D.	N.D.	N.D.		
12	α-Pinene	0.007 ± 0.002	0.026 ± 0.01	0.76 ± 0.22	0.034 ± 0.007	0.03 ± 0.02	0.130 ± 0.015	0.39 ± 0.04	0.097 ± 0.03	N.D.	N.D.		
13	Camphene	N.D.	N.D.	N.D.	N.D.	N.D.	N.D.	N.D.	N.D.	N.D.	N.D.		
14	α-Ocimene	N.D.	0.04 ± 0.04	N.D.	N.D.	N.D.	N.D.	N.D.	N.D.	N.D.	N.D.		
15	(E)-β-Ocimene	N.D.	1.50 ± 0.46	1.50 ± 0.46	0.055 ± 0.015	N.D.	0.51 ± 0.23	N.D.	N.D.	N.D.	N.D.		
16	3-Carene	0.001 ± 0.001	0.019 ± 0.009	N.D.	N.D.	0.001 ± 0.001	0.065 ± 0.058	N.D.	N.D.	0.074 ± 0.043	N.D.		
17	4-Carene	N.D.	0.326 ± 0.27	N.D.	N.D.	N.D.	N.D.	N.D.	N.D.	N.D.	N.D.		
18	Limonene	0.001 ± 0.001	0.017 ± 0.013	N.D.	N.D.	0.001 ± 0.001	N.D.	N.D.	N.D.	N.D.	N.D.		
19	α-Phellandrene	N.D.	N.D.	N.D.	N.D.	N.D.	N.D.	N.D.	N.D.	N.D.	N.D.		
20	Carvacrool	N.D.	0.020 ± 0.014	N.D.	N.D.	N.D.	N.D.	N.D.	N.D.	N.D.	N.D.		
21	Terpinolene	N.D.	N.D.	N.D.	N.D.	N.D.	N.D.	N.D.	N.D.	N.D.	N.D.		
22	α-Terpinene	N.D.	N.D.	N.D.	N.D.	N.D.	N.D.	N.D.	N.D.	N.D.	N.D.		
23	γ-Terpinene	N.D.	0.22 ± 0.10	0.167 ± 0.14	N.D.	N.D.	N.D.	N.D.	N.D.	N.D.	N.D.		

(continued on next page)

Table 1 (continued)

	24 h				48 h			
	Control	Heat	Whiteflies	Whiteflies + Heat	Control	Heat	Whiteflies	Whiteflies + Heat
24						0.067 ± 0.040	0.010 ± 0.005	
25	N.D	0.05 ± 0.02	N.D	N.D	N.D	0.23 ± 0.11	N.D	N.D
26	N.D	N.D	N.D	N.D	N.D	N.D	N.D	N.D
27	N.D	N.D	N.D	N.D	N.D	N.D	N.D	N.D
28								
28	0.007 ± 0.007	N.D	N.D	N.D	0.009 ± 0.006	0.17 ± 0.17	N.D	0.20 ± 0.06
29	0.01 ± 0.01	0.92 ± 0.13	N.D	N.D	0.003 ± 0.003	0.23 ± 0.23	N.D	1.45 ± 0.12
30	0.037 ± 0.027	0.18 ± 0.11	0.139 ± 0.139	N.D	0.039 ± 0.039	1.38 ± 1.05	0.16 ± 0.16	N.D
31	N.D	0.23 ± 0.19	0.68 ± 0.39	N.D	N.D	1.18 ± 0.73	0.14 ± 0.12	N.D

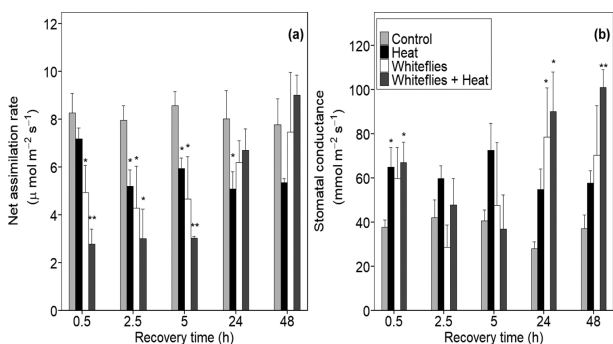


Fig. 1. Changes in net assimilation rate (a) and stomatal conductance to water vapor (b) in mature leaves of *Origanum vulgare* in non-stressed leaves (control), heat shock-stressed leaves (heat), *Trialeurodes vaporariorum* infested leaves (whiteflies) and combined heat shock-treated and *T. vaporariorum*-infested (heat + whiteflies) leaves, from treatment through recovery (0 h corresponds to the application of heat shock or control treatment). Heat shock treatment was applied by immersion the leaves in 45 °C water for 5 min. Both non-heat-stressed control and insect-infested control leaves were treated by immersion in 25 °C water for 5 min. Infested plants were colonized by *T. vaporariorum* for 14 days until measurement and each leaf was colonized by ca. six *T. vaporariorum* adult insects. The insects were removed from all the infested plants before heat application. Each data point is the mean (± SE) of three independent plant replicates measured at different recovery times after heat application. Means were compared by least significant difference test following one-way ANOVA test. Significant differences between control and stress-treated plants at different recovery interval are shown as: **P* < 0.05, ***P* < 0.01, and ****P* < 0.001.

Table 2

Summary of three-way ANOVA for the effects of heat treatment (n = 6), whiteflies infestation, (n = 6), and recovery time (0.5 h, 2.5 h, 5 h, 24 h, 48 h) and their interaction on gas exchange characteristics (net assimilation rate, A; stomatal conductance to water vapor, g_s) and volatile organic compounds (lipoxigenase pathway compounds, LOX; monoterpene, MT; benzenoid, BZ; long-chained fatty-acid derived compounds, FAD; geranylgeranyl diphosphate pathway products, GGDP) emission rates in *Origanum vulgare* leaves. Significant values are shown in bold and italic (*P* ≤ 0.05).

		Heat	Whiteflies	Time	Heat × Whiteflies	Heat × Time	Whitefly × Time	Heat × Whiteflies × Time
1 A	F	10.75	15.92	10.95	3.71	2.31	24.10	2.40
	P	<0.01	<0.01	<0.01	0.05	0.13	<0.01	<0.12
	F	9.68	5.14	5.13	1.26	0.41	10.44	0.84
2 g _s	P	<0.01	0.03	0.03	0.26	0.52	<0.01	0.36
	F	20.37	20.38	0.13	19.15	0.16	0.06	0.08
	P	<0.01	<0.01	0.72	<0.01	0.69	0.80	0.77
3 LOX	F	24.51	15.72	24.46	189.12	4.66	3.37	24.90
	P	<0.01	<0.01	<0.01	<0.01	<0.01	<0.01	<0.01
	F	36.77	2.30	0.06	0.69	0.11	3.70	3.39
5 BZ	P	<0.01	0.13	0.80	0.41	0.74	0.05	0.07
	F	1.40	0.90	0.17	7.93	3.71	6.92	1.23
	P	0.24	0.34	0.67	<0.01	0.05	0.01	0.27
6 FAD	F	0.41	0.00	0.07	23.63	0.14	0.96	0.05
	P	0.52	0.97	0.79	<0.01	0.70	0.33	0.81
	P							

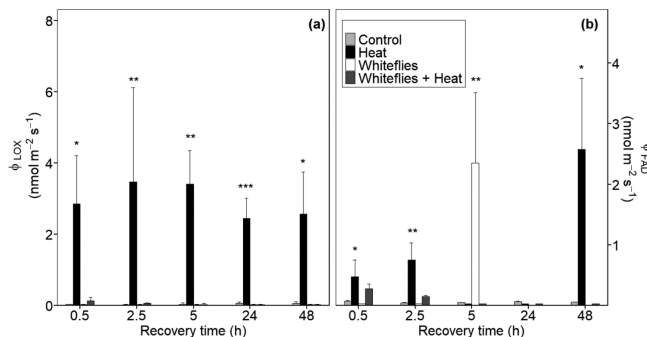


Fig. 2. Emission of total lipoxigenase pathway compounds (LOX, a) and long-chain fatty acid-derived compounds (FAD, b) from leaves of non-treated (control), heat shock-treated (heat), *Trialeurodes vaporariorum*-infested (whiteflies), and combined heat shock-treated and *T. vaporariorum*-infested (whiteflies + heat) plants during recovery (0 h corresponds to the heat shock or control treatment, Fig. 1 for the details of experimental treatment and measurement conditions). Statistical analysis and data presentation as in Fig. 1.

FAD were at the level of $0.06 \pm 0.01 \text{ nmol m}^{-2} \text{ s}^{-1}$ in the non-infested control plants (Fig. 2b). Heat shock applied alone significantly increased ($P < 0.05$) FAD emissions to level of $0.60 \pm 0.14 \text{ nmol m}^{-2} \text{ s}^{-1}$ through 0.5–2.5 h after treatment (Fig. 2b). At 5 h and 24 h after heat shock application, FAD emissions were not detected; however, at 48 h after heat treatment, FAD emissions rose again at a level of $2.32 \pm 1.38 \text{ nmol m}^{-2} \text{ s}^{-1}$. Whitefly infestation applied alone reduced FAD emissions to below the level of detection, although a pronounced emission of FAD at a level of $2.35 \pm 1.16 \text{ nmol m}^{-2} \text{ s}^{-1}$ ($P < 0.01$ compared to non-stressed plants) was observed at 5 h after stress treatment (Fig. 2b). The interaction between heat stress and whitefly infestation was significant ($P < 0.01$, Table 2) for FAD emissions, as the emissions were only detected at 0.5–5 h after combined stress treatment at an elevated level of $0.27 \pm 0.07 \text{ nmol m}^{-2} \text{ s}^{-1}$ ($P < 0.01$ in comparison with control plants, Fig. 2b).

3.3. Emission of terpeneoid

Total monoterpene emission rate was $0.020 \pm 0.008 \text{ nmol m}^{-2} \text{ s}^{-1}$ in non-stressed control plants (Fig. 3a). Both heat stress and whitefly feeding when applied alone increased ($P < 0.01$ for heat stress; $P < 0.05$

for whitefly infestation) monoterpene emissions throughout the recovery period (Fig. 3a). However, combined stress treatment kept monoterpene emissions at control level throughout the recovery period ($P > 0.05$ compared to control level, Fig. 3a). The increase in monoterpene emissions by single stress treatments was more pronounced in the first 5 h after treatment, especially in the heat-stressed non-infested plants where the emission reached the maximum value of $18.4 \pm 9.5 \text{ nmol m}^{-2} \text{ s}^{-1}$ ($P < 0.01$ compared to control plants) at that recovery interval (Fig. 3a; Table 2). Also, stress marker (*E*)- β -ocimene emissions in the heat-treated non-infested plants were elicited to a larger degree in the first 5 h after treatment, whereas elicited to a relatively lower degree subsequently (Fig. 3b). In the first 5 h, (*E*)- β -ocimene emissions in the exclusive whitefly-treated plants were lower than in exclusive heat-treated plants but higher than in heat-treated infested plants (Fig. 3b). However, at the end of the recovery period, (*E*)- β -ocimene emissions were not detected in both heat-treated infested plants and infested plants not treated with heat (Fig. 3b).

In addition to monoterpene, sesquiterpene emissions were observed at an invariable level of $0.040 \pm 0.01 \text{ nmol m}^{-2} \text{ s}^{-1}$ through 0.5–5 h after subjecting non-infested plants to heat shock; thereafter the emissions were not detected (Table 1). Isoprene emissions were also observed

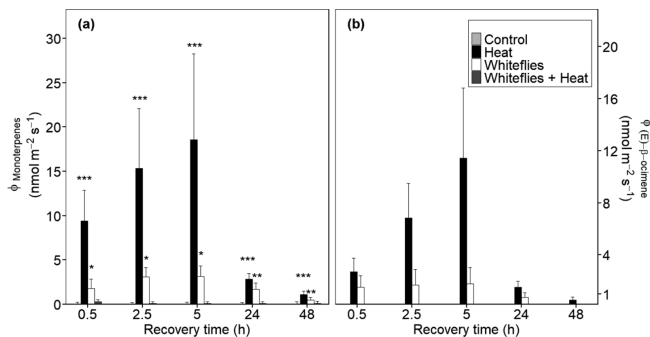


Fig. 3. Total emission of monoterpenes (a) and (*E*)- β -ocimene (b) from leaves of non-treated (control), heat shock-treated (heat), *Trialeurodes vaporariorum*-infested (whiteflies) and combined *T. vaporariorum* feeding- and heat shock-treated (whiteflies + heat) plants during recovery. The heat shock and control treatments were applied at 0 h. Description of experimental treatment and measurement conditions, statistical analysis and data presentation as in Fig. 1.

through the first 5 h after treatment at a level of $0.23 \pm 0.15 \text{ nmol m}^{-2} \text{ s}^{-1}$ in plants treated with heat alone and at a level of $0.19 \pm 0.11 \text{ nmol m}^{-2} \text{ s}^{-1}$ in plants treated with GWF infestation alone (Table 1). In combined-stressed plants, isoprene emissions were observed immediately after treatment at a level of $0.056 \pm 0.056 \text{ nmol m}^{-2} \text{ s}^{-1}$ and remained at that level until at 48 h when the emissions elevated to a level of $1.76 \pm 0.13 \text{ nmol m}^{-2} \text{ s}^{-1}$ (Table 1).

3.4. Benzenoid emissions

Two benzenoid compounds (benzaldehyde and toluene) were detected in the emissions from *O. vulgare*. Benzenoid emission was $0.05 \pm 0.01 \text{ nmol m}^{-2} \text{ s}^{-1}$ in non-stressed plants (Fig. 4). Heat shock increased ($P < 0.01$) benzenoid emissions in non-infested plants throughout the recovery period (Fig. 4). The emission rates reached the highest level ($1.91 \pm 0.6 \text{ nmol m}^{-2} \text{ s}^{-1}$) at 5 h after heat treatment (Fig. 4). Benzenoid emissions were not detected in the plants treated with only whitefly infestation (Table 1). Heat-treated infested plants emitted benzenoid at an elevated level of $0.95 \pm 0.35 \text{ nmol m}^{-2} \text{ s}^{-1}$ ($P < 0.01$ in comparison with control plants) through the first 2.5 h after treatment (Fig. 4). The emission fell below the detection threshold at 5 h and 24 h after the combined treatment but rose again at 48 h at a significant level of $1.66 \pm 0.18 \text{ nmol m}^{-2} \text{ s}^{-1}$ (Fig. 4). Toluene emission rate was positively correlated ($r = 0.78$, $P < 0.01$) with that of benzaldehyde in heat-treated infested plants.

3.5. Emission of geranylgeranyl diphosphate pathway volatiles

Baseline emissions of GGDP compounds ranged between 0.03 – $0.07 \text{ nmol m}^{-2} \text{ s}^{-1}$ (Table 1). Heat shock applied alone rapidly increased ($P < 0.01$) GGDP compounds emissions in non-infested plants throughout the recovery period (Fig. 5). GGDP volatile emissions in the plants subjected to only GWF infestation started at 2.5 h at an elevated level ($P < 0.01$ compared to non-stressed level) and remained high throughout the recovery period (Fig. 5). GGDP volatile emissions in the combined stress-treated plants were somewhat enhanced relative to non-stressed plants between 0.5–5 h, nevertheless much less than single stress-treated plants (Fig. 5).

3.6. Changes in the bouquet of volatiles

The composition of Volatiles in the control plants remained

indistinguishable throughout the experiment (PERMANOVA, $P = 0.65$; Bray-Curtis $R = 0.23$). All the stress treatments influenced the Volatile blends, according to PCA (Fig. 6b) and PERMANOVA ($P < 0.01$ in comparison to control) analyses. Volatile blends in the single-stressed plants were also different for every 24 h interval (PERMANOVA; $P < 0.05$). VOC bouquet in infested plants, regardless of heat treatment, was similar to the VOC blend in non-stressed plants at the later stages of recovery (Fig. 6a, PERMANOVA; $P > 0.05$). LOX and monoterpenes were associated with exclusive heat treatment (Fig. 6b). GGDP compounds were associated with only single-stressed plants (Fig. 6b).

3.7. Correlation among the emissions of different volatile groups and gas-exchange characteristics

Total emissions of monoterpene compounds correlated positively with total emissions of LOX and benzenoid compounds in the plants subjected to only heat stress (Fig. 7a, b). Monoterpene emissions strongly scaled negatively with *A* in the plant subjected to only GWF infestation, however, in the heat-stressed infested plants, the negative correlation was weak (Fig. 7c). GGDP emissions correlated negatively with *A* in the infested plants not treated with heat (2.5–48 h; $r = -0.8$, $P = 0.26$).

4. Discussion

4.1. Heat stress effects on photosynthetic characteristics

Heat stress can affect *A* and *g_s* differently, ranging from inhibition to even stimulation (Hueve et al., 2011; Kerchev et al., 2012; Urban et al., 2017), reflecting the differences in stress severity with mild stress having minor effects and severe heat stress having major negative effects (Kask et al., 2016; Pazouki et al., 2016; Urban et al., 2017). In our study, heat shock applied alone moderately decreased photosynthesis rate and increased stomatal openness in *O. vulgare* (Fig. 1a, b), in agreement with moderately heat-stressed *Pinus taeda* (Urban et al., 2017), *Populus deltoides* (Urban et al., 2017) and *S. lycopersicum* (Pazouki et al., 2016). As *g_s* was enhanced, the decrease in *A* can be primarily attributed to non-stomatal inhibition such as thermal damage of photosynthetic electron transport and Rubisco activity as reported in other studies (Demirevska-Kepova et al., 2005; Salvucci and Crafts-Brandner, 2004). Nevertheless, under extreme heat stress, a progressive decline in photosynthesis can occur during recovery, indicating induction of a

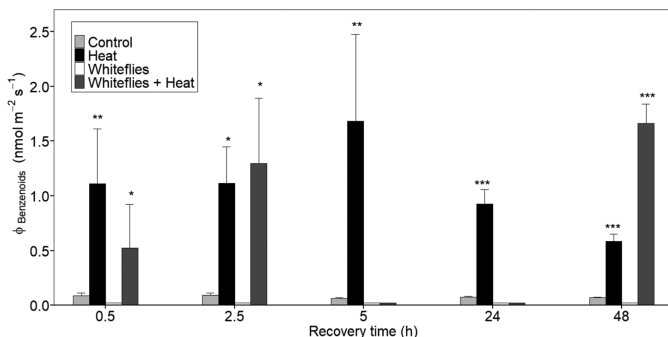


Fig. 4. Total emission of benzenoids from leaves of non-treated (control), heat shock-treated (heat), *Trialeurodes vaporariorum*-infested (whiteflies) and combined *T. vaporariorum* feeding- and heat shock-treated (whiteflies + heat) plants during recovery. The heat and control treatments were applied at 0 h (Fig. 1 for the details of experimental and measurement conditions). Statistical analysis and data presentation as in Fig. 1.

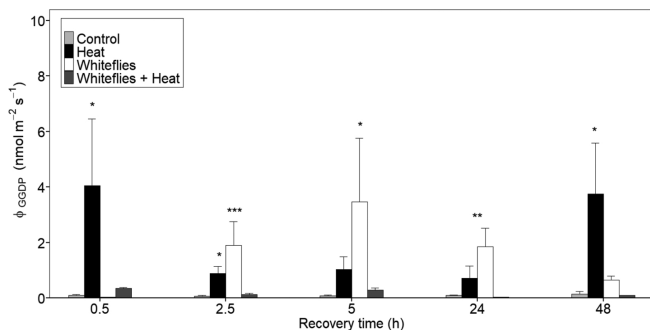


Fig. 5. Total emission of geranylgeranyl diphosphate pathway (GGDP) compounds from leaves of non-treated (control), heat shock-treated (heat), *Trialeurodes vaporariorum*-infested (whiteflies), and combined *T. vaporariorum* feeding- and heat shock-treated (whiteflies + heat) plants during recovery (0 h corresponds to the application of heat shock or control treatment, Fig. 1 for the details of experimental and measurement conditions). Statistical analysis and data presentation as in Fig. 1.

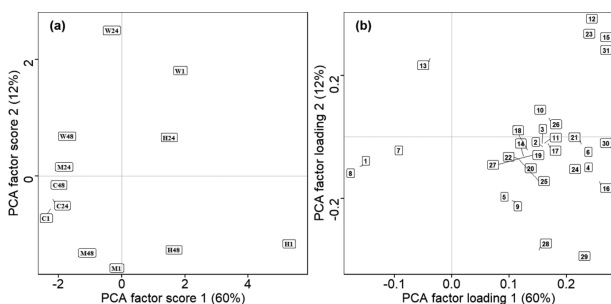


Fig. 6. Loading (b) and score plot (a) derived from principal component analysis (PCA) based on the time-course of emitted volatiles for non-stressed control (C), heat shock-treated (H), *Trialeurodes vaporariorum*-infested (W), and combined *T. vaporariorum* feeding- and heat shock-treated plants. Each symbol in the score plot represents the average of three independent biological replicates. Numbers after the treatment codes in the score plot indicate the different days of volatile measurements as follows: 1: 0.5-5 h (day 1); 24: 24 h (day 2); and 48: 48 h (day 3). In the loading plot, each number represents a unique volatile compound ordered as: 1. pentanal; 2. hexanal; 3. 1-hexanol 4. (E)-3-hexen-1-ol; 5. heptanal; 6. 2-ethylhexanol; 7. 1-octanol; 8. 1-nonanol; 9. isoprene; 9. toluene; 10. α -thujene; 11. α -sabinene; 12. α -pinene; 13. camphene; 14. α -ocimene; 15. (E)- β -ocimene; 16; 3-carene; 17. 4-carene; 18. limonene; 19. α -phellandrene; 20. carvacrol; 21. terpinolene; 22. α -terpinene 23. γ -terpinene; 24. β -myrcene; 25. thymol; 26. p-cymene; 27. α -bisabolene; 28. benzaldehyde; 29. toluene; 30. geranyl acetone; 31. 6-methyl-5-hepten-2-one. The contribution of each emitted compound increases with increasing the distance from the origin of the coordinate system. Experimental condition as described in Fig. 1.

nene; 24. β -myrcene; 25. thymol; 26. p-cymene; 27. α -bisabolene; 28. benzaldehyde; 29. toluene; 30. geranyl acetone; 31. 6-methyl-5-hepten-2-one. The contribution of each emitted compound increases with increasing the distance from the origin of the coordinate system. Experimental condition as described in Fig. 1.

programmed cell death-like process (Hueve et al., 2011; Balfagón et al., 2019). In our study, the photosynthesis rate did not decrease in time, indicating that the applied stress was not lethal and the leaves maintained physiological activity through the experimental period. Maintenance of physiological activity was aided by the increase in g_s that partly compensated for the inhibition of biochemical limitations of photosynthesis (Fig. 1b). Such a positive response of heat stress on g_s can occur in well-watered plants and can play an important role in the field by reducing extreme surface leaf temperature due to enhanced evaporative cooling (Crawford et al., 2012; Urban et al., 2017).

4.2. Insect feeding and combined insect feeding and heat stress treatment effects on photosynthesis

Herbivore feeding on specialized foliar tissues has a profound effect on photosynthetic characteristics (Trumble et al., 1993; Nabity et al., 2009). Our results showed that regardless of heat shock treatment, gas exchange characteristics in infested plants followed a similar trend (Fig. 1a, b). In exclusive GWF-stressed plants, A was reduced and g_s was somewhat enhanced at the beginning of the experiment, followed by a reduction in g_s at 2.5 h and a further increase from 5 h until stabilization

at 24 h (Fig. 1a, b). Thus this suggests that the first 5 h measurement period, together with the time taken to remove to insects and subject the plants to the same treatment as control plants, i.e. submerging in water at 25 °C, while the leaves were enclosed in a bag and did not have direct contact with water, was sufficient to seal the wounds and start the repair of the conductive network. The recovery in A between 5–48 h was paralleled by increases in g_s (Fig. 1a, b), suggesting that the mechanism is plausible. However, there was a mismatch between high g_s and low A at 0.5 and 2.5 h (Fig. 1a, b). The high g_s values at these measurement intervals might be indicative of evaporation from the damaged leaf locations rather than transpiration through stomata. Such an artificial increase in g_s is often the case in leaf herbivory and mechanical damage, although turgor loss in cells surrounding the stomata can also cause enhanced stomatal water loss (Rasulov et al., 2019; Jiang et al., 2020).

Initially, A was strongly reduced in heat-treated infested plants (Fig. 1a). This indicates an additive effect of the interaction of the already low photosynthesis rate due to the GWF feeding and the superimposed heat stress. However, differently from photosynthesis in exclusively heat-stressed plants, plants subjected to combined GWF infestation and heat stress recovered to a greater degree (Fig. 1a). This suggests that the GWF treatment enhanced the plant recovery capacity,

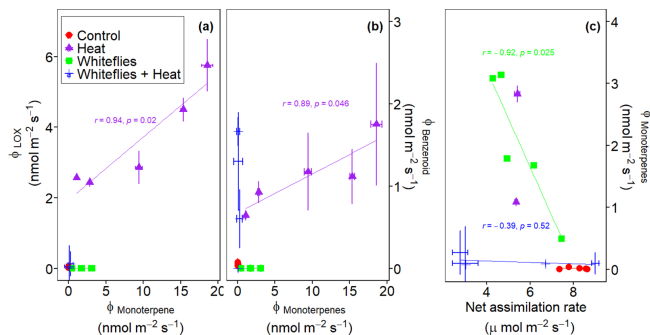


Fig. 7. Correlation between total monoterpenes emission and LOX compounds emission (a), benzenoids emission (b) and changes in net assimilation rate (c) in leaves of non-treated (control), heat shock-treated (heat), *Trialeurodes vaporariorum*-infested (whiteflies), and combined *T. vaporariorum*-infested- and heat shock-treated (whiteflies + heat) plants during recovery (Fig. 1 for the details of experimental and measurement conditions). Each geometric symbol corresponds to the mean (\pm SE) of three independent replicates at each recovery time point. The data were fitted by linear regression with the regression equations $y = 2.4 + 0.006x$ (a, heat-stressed non-infested plants), $y = 0.67 + 0.047x$ (b, heat-stressed non-infested plants), $y = 6.3 - 0.7x$ (c, infested plants not treated with heat shock) and $y = 0.18 - 0.011x$ (c, combined heat-stressed and insect-infested plants).

possibly reflecting a certain convergence in stress response pathways (Raja et al., 2017). Also, volatile emission responses further suggested that insect feeding rendered the plants more tolerant to heat stress (Section 4.2–4.3). As with the infested plants not treated with heat, the recovery was partly associated with increases in g_s and improved CO₂ availability for Rubisco. Nevertheless, the improved capacity was associated also with the elimination of heat stress-caused non-stomatal limitations, which were not completely overcome in the case of non-infested heat-stressed plants.

4.3. Insect feeding inhibits heat stress-inducible emissions of lipoxygenase pathway products and long-chained fatty acid-derived compounds

The lipoxygenases are constitutively active in the foliage of plants and provided there is the substrate, i.e. polyunsaturated fatty acid, these enzymes quickly up-regulate LOX emissions upon any severe stress that results in membrane-level damages (Feussner and Wasternack, 2002; Heiden et al., 2003; Andreou and Feussner, 2009). The released LOX compounds signal the presence of severe stress in affected plants (Jansen et al., 2009; Maccarrone et al., 1992; Niinemets et al., 2013). The rapid heat-enhanced LOX emission in *O. vulgare* (Fig. 2a) is consistent with previous observations (e.g., Joo et al., 2011; Copolovici et al., 2012; Kask et al., 2016). Heat stress-induced LOX emission is considered an indicator of cellular damage and generation of an oxidative burst (Copolovici et al., 2011; Niinemets et al., 2013; Kanagendran et al., 2018; Turan et al., 2019). If so, the persistent release of LOX volatiles at a high level from the heat-stressed *O. vulgare* suggested that heat shock resulted in a sustained increase in the level of ROS. Severe abiotic stress response often leads to a multiphasic LOX emission response, with a rapid emission burst, between 0.5–5 h, directly associated with the applied stress and with one or several long-term components, between 12–48 h, possibly reflecting an endogenous rise of ROS due to increased membrane permeability (Hueve et al., 2011; Jiang et al., 2017; Li et al., 2017; Jiang et al., 2020). Due to the time resolution of the experiment, we cannot discriminate between these different emission bursts, but it is plausible the high LOX emission responses reflect these later-developing emission bursts.

Unlike leaf-chewers or even aphid that punctures several feeding sites (Copolovici et al., 2011, 2014; Li et al., 2014). GWF feeding exerts very localized damage on plants (Walling, 2008) such that responses are specific to the damaged/infested sites, thus overall defense response including LOX emission would remain low (Holopainen, 2011; Appel

and Crocroft, 2014). However, in the current study, constitutive level LOX emissions were suppressed in the infested plants (Fig. 2a). Investigations on gene expression levels may elucidate how GWF suppressed LOX emissions in *O. vulgare*. Thus, we suggest that LOX emissions may not reflect stress severity in GWF-stressed *O. vulgare*.

In the infested plants subjected to heat shock, LOX emissions were at a very low level between 0.5–5 h (Fig. 2a), this indicates that the impact of heat stress on the infested plants was less, and the boosted recovery suggests that GWF feeding improved innate thermal resistance. It is unclear how whitefly infestation improved resilience to heat stress. Nevertheless, exposure to biotic stress can induce the accumulation of certain signaling protein or transcription factors (Bruce et al., 2007; Bäurle, 2018) that can protect cells during subsequent oxidative stress (Galís et al., 2009; Sasidharan et al., 2011; Brilli et al., 2019), thereby improving resistance and enhancing recovery (Vacca et al., 2004; Suzuki and Mittler, 2006; Velikova et al., 2011).

The emissions of FAD compounds above basal level have been linked to the activation of LOX pathway activities (Hu et al., 2009, 2011). Stress can induce the accumulation of saturated aldehydes/alcohols, formed from the reaction of ROS with protein and lipid (Sunkar et al., 2003; Mano et al., 2019). The accumulation of FAD can escalate ROS damage in the chloroplast (Sunkar et al., 2003; Stiti et al., 2011). The release of these compounds is thought of as a detoxification mechanism that stressed plants use to lessen the excessive accumulation of FAD toxicity and the resulting oxidative stress (Sunkar et al., 2003; Mano et al., 2019). Thus, the release of FAD compounds in the current study (Fig. 2b), may reflect this phenomenon.

4.4. Insect infestation decreases heat stress-inducible emissions of terpenoids, including stress marker β -ocimene

Origanum vulgare accumulates monoterpenes and sesquiterpenes in glandular trichomes (Carroll et al., 2017; Agliassa and Maffei, 2018; Baraldi et al., 2019), but when the leaves are not damaged, it is a low-level constitutive monoterpene emitter (Baraldi et al., 2019) as supported by our results (Fig. 3a), and in our study, it only emitted sesquiterpenes when heat treatment was applied alone (Table 1). The rapid high emissions of terpenoids and the positive scaling of monoterpenes with LOX emissions in heat shock-treated non-infested plants (Fig. 7a) reflect rapid *de novo* synthesis of isoprenoids, thus suggesting the quick channelling of MEP/DOXP pathway metabolites from essential isoprenoid synthesis towards volatile isoprenoid synthesis (Owen and

Peñuelas, 2005 for review). Rapid induction of terpenoid (mono- and sesquiterpenes) emission by extreme temperature is consistent with previous studies (e.g., Copolovici et al., 2012; Kask et al., 2016; Liu et al., 2020) and can play a protective role against thermal stress by quenching ROS in the mesophyll and increasing the thermostability of the thylakoid membrane (Loreto et al., 1998; Harrison et al., 2013; Faralli et al., 2020), thus providing certain protection to photosynthetic processes (Foyer, 2018). Both monoterpene and sesquiterpenes emissions can emanate from either the storage pool or *de novo* synthesis. In the case of *de novo* synthesis, the biosynthesis for sesquiterpenes occurs via MVA pathway in the cytosol and via MEP/DOXP pathway in plastids for monoterpenes (Memari et al., 2013; Niinemets et al., 2013; Tholl, 2015), although stress-elicited sesquiterpenes emission can also occur in plastids (Dudareva et al., 2005; Sallaud et al., 2009).

Terpenoid synthase is regulated at the upstream by JA signaling pathway (Eberl et al., 2018; Xu et al., 2016). Whitefly-feeding triggers less accumulation of JA-dependent defenses (Moran and Thompson, 2001; Zarate et al., 2007), which may explain the moderate enhancement of monoterpene emissions in the exclusive GWF-stressed plants in our study. The negative scaling of A with monoterpenes emissions in the infested plants (Fig. 7c) suggests that monoterpenes likely mediated in the repair of network conductivity by eliminating herbivore wounding-generated oxidative stress. On the other hand, the low terpenoid emissions in heat-stressed infested plants, at least compared to that in heat-stressed non-infested plants, reflects low stress-related demand for essential isoprenoids (Fig. 3a). Biotic stresses that primarily elicit SA-dependent responses can reduce abiotic stress-inducible terpenoid emissions by reducing the induction of transcriptional terpene synthases (Eberl et al., 2018).

The emission of β -ocimene is common in stressed plants, particularly in herbivory and heat-stressed plants, and is quantitatively associated with stress severity (Jansen et al., 2009; Copolovici et al., 2011, 2012; Liu et al., 2020; Staudt et al., 2010). In our study, the elicitation of (*E*)- β -ocimene was in comparison high in heat-stressed plants, moderate in GWF-stressed plants, and very low in combined heat and whitefly-stressed plants (Fig. 3b). This indicates that plants exposed to heat shock alone were more stressed followed by the plants exposed to GWF feeding alone. Nevertheless, (*E*)- β -ocimene is the primary monoterpene compound elicited by all the stress treatments (Fig. 3a, b). Several experiments have shown that (*E*)- β -ocimene dominates phloem-feeding-induced monoterpene emissions (e.g., Kigathi et al., 2019; Staudt et al., 2010) and have been demonstrated to be more toxic to herbivores than SA-regulated emissions (Zhang et al., 2009, 2013). The elicitation of isoprene emission can also reflect stress severity (Niinemets et al., 2010a,b, 2013; Sharkey et al., 2008). However, we observed very low isoprene emissions (Table 1) compared to other emitter species (Vickers et al., 2011, 2009; Monson et al., 2013), thus not related to the degree of stress. Such emission can reflect either non-enzymatic formation of isoprene due to rapid fluctuations in the pH of the chloroplast (Brilli et al., 2011; Turan et al., 2019) or multi-substrate terpene synthases, i.e., isoprene was formed as a side product of induced- monoterpene synthases (Pazouki and Niinemets, 2016). Nevertheless, enhanced terpene emissions in plants have been linked to elevation in terpene synthase gene expressions (Navia-Giné et al., 2009; Eberl et al., 2018). Thus collectively, our data suggest that heat stress and GWF feeding applied separately induced higher expressions of terpene synthase genes and other proteins in the MEP/DOXP and MVA pathways resulting in significant *de novo* emissions of isoprenoids.

4.5. Heat stress induction of benzenoid emissions in infested plants is multiphasic

We detected two benzenoid compounds, toluene and benzaldehydes, in the volatile blend of *O. vulgare*. The emission of benzaldehyde initiates upon enzymatic oxidation of less volatile benzyl alcohol in the shikimate

pathway located in the plastid (Dudareva et al., 2004). Although toluene was noted in the emission blend of both stressed and non-stressed plants (e.g., Misztal et al., 2015; Liu et al., 2018) and was shown to be ^{13}C labeled (Heiden et al., 2003) and thus *de novo* synthesized, the exact pathway for its biosynthesis is still unclear. However, our data showed a positive association in the emission pattern of toluene and benzaldehyde, indicating that toluene possibly emanated from the same shikimate pathway. The activity of the shikimate pathway is regulated by SA signaling pathway (Chen et al., 2009; Vogt, 2010).

Previous studies have shown that mere sensing of phloem-feeders can trigger the emissions of benzenoid, including methyl salicylate (MeSA), the most frequent phloem-feeding insect-induced compound (Arimura et al., 2011; War et al., 2011; Misztal et al., 2015). However, contrary to our hypothesis, we did not detect benzenoid emissions in the GWF-stressed plants in the current study. Nevertheless, the emission of MeSA per se can sometimes prove difficult to infested plants (Misztal et al., 2015). For example, MeSA was not detected in *Rhopalosiphum padi*-infested *Festuca pratensis* (Li et al., 2014), and *B. tabaci*/*Tetranychus urticae*-infested lima bean (Zhang et al., 2009). Stress-induced emissions from the shikimate pathway are typically periodic (War et al., 2011; Misztal et al., 2015). Moreover, plants hormonal responses to phloem-feeding insects may differ depending on the insect colonization stage (Wasternack and Hause, 2013; Aartsma et al., 2017). Thus, we cannot exclude the possibility of benzenoid emissions earlier than our volatile measurement. We suspect that the GWF-stressed plants might have channeled aromatic precursors toward phenolic accumulation, such as anthocyanin and condensed tannin that can prevent cell death and lipid peroxidation, rather than volatile production (Kumar and Pandey, 2013; Cheng et al., 2018). However, future investigation on the plant secondary metabolite profile including phenolic accumulation might extend this explanation.

Both shikimate and MEX/DOXP pathways use the same early intermediate (phosphoenolpyruvate) in the plastid, suggesting the possibility of competition or cooperation at substrate level between the two pathways (Niinemets et al., 2013). Thus, the strong association (Fig. 7b) and the similarity in the emission kinetics (Figs. 3a and 4) of benzenoids and monoterpenes in the heat-stressed non-infested plants possibly suggest coordination at substrate level in the biosynthesis of the two volatile compound classes. Benzenoid emissions in the combined heat and whitefly-stressed plants, showed a multiphasic induction response while monoterpenes were more or less not enhanced (Figs. 3a and 4). Stress-induced changes in enzymes activity can result in the preferential activation of one pathway leading to a reduction in the synthesis of the end product of the other pathway (Liu et al., 2018; Niinemets et al., 2013). Therefore, the enhanced benzenoid emissions in the interacting heat and herbivory-stressed plants might suggest preferential activation of the shikimate pathway over the MEX/DOXP pathways in the plant. Whereas the induction of monoterpenes emissions upon herbivory may also partly explain the inhibition of benzenoids in exclusive herbivore-stressed plants. However, further investigation is required to explore the activity of the shikimate pathways and the multiphasic nature of heat-inducible benzenoid emissions in GWF-infested plants.

4.6. High emissions of geranylgeranyl diphosphate pathway compounds in whitefly-stressed plants

In the current study, all the stress treatments increased the emission of GGDP-derived volatiles (Fig. 5), which is an unsaturated by-product of fatty acids breakdown resulting from the oxidation of carotenoids in plastids, the same compartments where monoterpene precursor (geranyl diphosphate) is produced (Aharoni et al., 2005; Owen and Peñuelas, 2005; Memari et al., 2013). Interestingly, different from other volatile groups, GGDP volatiles in the GWF-stressed plants were quite high, at least temporarily (Fig. 5). Thus that may reflect the reduction of chlorophyll and carotenoids contents, consistent with the variegated leaf phenotype observed in infested plants (Josse et al., 2000; Nisar

et al., 2015) and may partly explain the negative correlation between GGDP and photosynthesis rate

4.7. Heat stress can affect the quality of volatile response to insect herbivory

Both heat stress and whitefly feeding applied alone and in combination affected the quality of VOC emissions in *O. vulgare*. However, VOC emission blends in all the stress-treated plants, except in plants treated with heat alone, recovered to control quality at the end of the experiment (Fig. 6b). Heat shock-induced qualitative changes in plants often persist for several days after exposure (Kleist et al., 2012; Kask et al., 2016; Liu et al., 2020). The volatile blend emitted by GWF-stressed *O. vulgare* may act as defensive semiochemicals, e.g., 6-methyl-5-hepten-2-one and β -ocimene can attract herbivore parasitoid (Yu et al., 2018; Farré-Armengol et al., 2017), β -ocimene can also directly repel herbivore (Farré-Armengol et al., 2017). Therefore, changes in volatile blend elicited by superimposing heat shock on GWF infestation might affect volatile-mediated multitrophic interaction. Further investigations including tritrophic analysis and plant attractiveness are required.

Altogether, our data showed that VOC emissions under heat stress were lower in GWF-infested plants compared to non-infested plants, thus consistent with aphid-infested *Picea abies* (Jóó et al., 2011), *Pinus sylvestris* (Jóó et al., 2011) and *Pseudotsuga menziesii* (Kleist et al., 2012) under heat stress.

5. Conclusions

The current study shows that the physiological and volatile emission responses of the aromatic herb *O. vulgare* to the joint effect of severe transient heat stress and phloem-feeding by GWF differ from responses to the individual effects of both stresses. In essence, infested heat-stressed plants exhibited a relatively greater initial decrease in A, than non-infested heat-stressed plants, but the infested plants recovered to a much greater degree. This indicates either a greater heat tolerance or a greater recovery capacity in the infested plants. Heat stress applied alone led to major enhancements of emissions of LOX pathway volatiles, and mono- and sesquiterpenes, benzenoid, FAD compounds and GGDP pathway volatiles, and most of the emissions had not reached pre-stress levels even at 48 h after stress application. Under combined heat stress and GWF infestation, volatile emissions, particularly LOX, terpene and benzenoid emissions were much lower than under heat stress applied alone. This evidence again supported the enhanced heat resistance of whitefly-infested plants. Collectively, the data suggest that herbivory can strongly antagonize VOC emission responses to thermal stress and improve the acclimation of photosynthetic thermo-tolerance. The priming effect of biotic stress on thermal tolerance might in nature contribute to plant productivity and fecundity during extreme climate events. We argue that the quantitative and qualitative data on volatile emissions provide illuminative insight into the development of heat stress response and heat stress sensitivity even under complex interactive stresses.

Author statements

HYS – Conception and design, execution of experiment, analysis and interpretation of data, drafting and critical revision of the article for important intellectual content.

BL – Conception and design, execution of experiment and critical revision of the article for important intellectual content

EK – Conception and design, Execution of experiment, critical revision of the article for important intellectual content.

ÜN – Conception and design, interpretation of data, drafting the article and critical revision of the article for important intellectual content.

Declaration of Competing Interest

The authors report no declarations of interest.

Acknowledgements

This study was funded by the European Commission through the European Research Council (advanced grant 322603, SIP-VOL+) and the European Regional Development Fund (Centre of Excellence Ecol-Change). HYS was supported by the Dora Plus scholarship (Archimedes Foundation); BL was supported by the Estonian University of Life Sciences (baseline-funded project P190252PKTT) and the Estonian Research Council (team grant project PRG947). We thank Lauri Laanisto for providing the oregano seed.

References

- Aartsma, Y., Bianchi, F.J., van der Werf, W., Poelman, E.H., Dicke, M., 2017. Herbivore-induced plant volatiles and tritrophic interactions across spatial scales. *New Phytol.* 216, 1054–1063. <https://doi.org/10.1111/nph.14475>.
- Agliassa, C., Maffei, M.E., 2018. *Origanum vulgare* terpenoids induce oxidative stress and reduce the feeding activity of *Spodoptera littoralis*. *Int. J. Mol. Sci.* 19, 2805. <https://doi.org/10.3390/ijms19092805>.
- Aharoni, A., Jongsma, M.A., Bouwmeester, H.J., 2005. Volatile science? Metabolic engineering of terpenoids in plants. *Trends Plant Sci.* 10, 594–602. <https://doi.org/10.1016/j.plants.2005.10.005>.
- Akhtar, Y., Isman, M.B., 2004. Feeding responses of specialist herbivores to plant extracts and pure allelochemicals: effects of prolonged exposure. *Entomol. Exp. Appl.* 111, 201–208. <https://doi.org/10.1111/j.0013-8703.2004.00169.x>.
- Andreou, A., Feussner, I., 2009. Lipxygenases—structure and reaction mechanism. *Phytochemistry* 70, 1504–1510. <https://doi.org/10.1016/j.phytochem.2009.05.008>.
- Appel, H.M., Cocroft, R.B., 2014. Plants respond to leaf vibrations caused by insect herbivore chewing. *Oecologia* 175, 1257–1266. <https://doi.org/10.1007/s00489-014-0495-9>.
- Arimura, A., Ozawa, R., Maffei, M.E., 2011. Recent advances in plant early signaling in response to herbivory. *Int. J. Mol. Sci.* 12, 3723–3739. <https://doi.org/10.3390/ijms12063723>.
- Atkinson, N.J., Jain, R., Urwin, P.E., 2015. The response of plants to simultaneous biotic and abiotic stress. *Combined Stresses in Plants*. Springer International Publishing, Cham, pp. 181–201. https://doi.org/10.1007/978-3-319-07899-1_9.
- Balfagón, D., Sengupta, S., Gómez-Cadenas, A., Fritsch, F.B., Azad, R.K., Mittler, R., Zandalinas, S.I., 2019. Jasmonic acid is required for plant acclimation to a combination of high light and heat stress. *Plant Physiol.* 18, 1668–1682. <https://doi.org/10.1104/pp.19.00956>.
- Baraldi, R., Neri, L., Costa, F., Facini, O., Rappardini, F., Carriero, G., 2019. Ecophysiological and micromorphological characterization of green roof vegetation for urban mitigation. *Urban For. Urban Green.* 37, 24–32. <https://doi.org/10.1016/j.ufug.2018.03.002>.
- Bäurle, I., 2018. Can't remember to forget you: chromatin-based priming of somatic stress responses. In: *Academic Press Seminars in Cell & Developmental Biology*, Vol. 83, pp. 133–139. <https://doi.org/10.1016/j.semcbi.2017.09.032>.
- Blanco, J.D., Holopainen, J.K., Niinemets, Ü., 2014. Plant volatiles in polluted atmospheres: stress responses and signal degradation. *Plant Cell Environ.* 37, 1892–1904. <https://doi.org/10.1111/pce.12352>.
- Brilli, F., Ruuskanen, T.M., Schnitzhofer, R., Müller, M., Breitenlechner, M., Bittner, V., et al., 2011. Detection of plant volatiles after leaf wounding and darkening by proton transfer reaction “time-of-flight” mass spectrometry (PTR-TOF). *PLoS One* 6, e20419. <https://doi.org/10.1371/journal.pone.0020419>.
- Brilli, F., Loreto, F., Baccelli, L., 2019. Exploiting plant volatile organic compounds (VOCs) in agriculture to improve sustainable defense strategies and productivity of crops. *Front. Plant Sci.* 10, 264. <https://doi.org/10.3389/fpls.2019.00264>.
- Bruce, T.J., Matthes, M.C., Nagler, J.A., Pickett, J.A., 2007. Stressful “memories” of plants: evidence and possible mechanisms. *Plant Sci.* 173, 603–608. <https://doi.org/10.1016/j.plantsci.2007.09.002>.
- Camejo, D., Rodríguez, P., Morales, M.A., Dell'Amico, J.M., Torrecillas, A., Alarcón, J.J., 2005. High temperature effects on photosynthetic activity of two tomato cultivars with different heat susceptibility. *J. Plant Physiol.* 162, 281–289. <https://doi.org/10.1016/j.jplph.2004.07.014>.
- Cardozo, Y.J., Albani, H.T., Tumlinson, J.H., 2002. In vivo volatile emissions from peanut plants induced by simultaneous fungal infection and insect damage. *J. Chem. Ecol.* 28, 161–174. <https://doi.org/10.1023/A:1013523104853>.
- Carroll, J.F., Demirci, B., Kramer, M., Bernier, U.R., Agramon, N.M., Baser, K.H.C., Tabanca, N., 2017. Repellency of the *Origanum onites* L. Essential oil and constituents to the lone star tick and yellow fever mosquito. *Nat. Prod. Res.* 31, 2192–2197. <https://doi.org/10.1080/14786419.2017.1289485>.
- Chen, Z., Zheng, Z., Huang, J., Lai, Z., Fan, B., 2009. Biosynthesis of salicylic acid in plants. *Plant Signal. Behav.* 4, 493–496. <https://doi.org/10.4161/psb.4.6.8392>.
- Cheng, G.X., Li, R.J., Wang, M., Huang, L.J., Khan, A., Ali, M., Gong, Z.H., 2018. Variation in leaf color and combine effect of pigments on physiology and resistance

- to whiteness of pepper (*Capsicum annum* L.). *Sci. Hortic.* 229, 215–225. <https://doi.org/10.1016/j.scienta.2017.11.014>.
- Chun, S.S., Vatter, D.A., Lin, Y.T., Shetty, K., 2005. Phenolic antioxidants from clonal oregano (*Origanum vulgare*) with antimicrobial activity against *Helicobacter pylori*. *Process. Biochem.* 40, 809–816. <https://doi.org/10.1016/j.procbio.2004.02.018>.
- Copolovici, L., Kännaste, A., Remmel, T., Ninimets, Ü., 2014. Volatile organic compound Emissions from *Alnus glutinosa* under interacting drought and herbivory stresses. *Environ. Exp. Bot.* 100, 55–63. <https://doi.org/10.1016/j.envexpbot.2013.12.011>.
- Copolovici, L., Kännaste, A., Remmel, T., Vislap, V., Ninimets, Ü., 2011. Volatile emissions from *Alnus glutinosa* induced by herbivory are quantitatively related to the extent of damage. *J. Chem. Ecol.* 37, 18–28. <https://doi.org/10.1007/s10886-010-9897-9>.
- Copolovici, L., Kännaste, A., Pazuoli, L., Ninimets, Ü., 2012. Emissions of green leaf volatiles and terpenoids from *Solanum lycopersicum* are quantitatively related to the severity of cold and heat shock treatments. *J. Plant Physiol.* 169, 664–672. <https://doi.org/10.1016/j.jplph.2011.12.013>.
- Copolovici, L., Ninimets, Ü., 2010. Flooding induced emissions of volatile signalling compounds in three tree species with differing waterlogging tolerance. *Plant Cell Environ.* 33, 1582–1594. <https://doi.org/10.1111/j.1365-3040.2010.02166.x>.
- Crawford, A.H., McLachlan, D.H., Hetherington, A.M., Franklin, K.A., 2012. High temperature exposure increases plant cooling capacity. *Curr. Biol.* 22, R396–R397. <https://doi.org/10.1016/j.cub.2012.03.044>.
- Cui, H., Su, J., Wei, J., Hu, Y., Ge, F., 2014. Elevated O₂ enhances the attraction of whitefly-infested tomato plants to *Encarsia formosa*. *Sci. Rep.* 4, 1–6. <https://doi.org/10.1038/srep05350>.
- Cvikrová, M., Gemperlová, L., Martinčová, O., Vanková, R., 2013. Effect of drought and combined drought and heat stress on polyamine metabolism in proline-over-producing tobacco plants. *Plant Physiol. Biochem. J.* 7, 1–15. <https://doi.org/10.1016/j.plaphy.2013.08.005>.
- Dawood, T., Yang, X., Visser, E.J., Te Beck, T.A., Kensch, P.R., Cristescu, S.M., et al., 2016. A co-opted hormonal cascade activates dormant adventitious root primordia upon flooding in *Solanum dulcamara*. *Plant Physiol.* 170, 2351–2364. <https://doi.org/10.1104/pp.15.00773>.
- Dudareva, N., Pichersky, E., Gershenzon, J., 2004. Biochemistry of plant volatiles. *Plant Physiol.* 135, 1893–1902. <https://doi.org/10.1104/pp.104.04.1893>.
- Demirciova-Kepova, K., Holzer, R., Simova-Stolova, L., Feller, U., 2005. Heat stress effects on ribulose-1,5-bisphosphate carboxylase/oxygenase, Rubisco binding protein and Rubisco activase in wheat leaves. *Biol. Plant.* 49 (4), 521–525. <https://doi.org/10.1007/s10535-005-0045-2>.
- Dudareva, N., Andersson, S., Orlova, I., Gatto, N., Reichelt, M., Rhodes, D., et al., 2005. The nonmevalonate pathway supports both monoterpene and sesquiterpene formation in snapdragon flowers. *Proc. Natl. Acad. Sci.* 102, 933–938. <https://doi.org/10.1073/pnas.0407360102>.
- Eberl, F., Hammerbacher, A., Gershenzon, J., Unsicker, S.B., 2018. Leaf rust infection reduces herbivore-induced volatile emission in black poplar and attracts a generalist herbivore. *New Phytol.* 220, 760–772. <https://doi.org/10.1111/nph.14565>.
- Engelberth, J., Koch, T., Schüller, G., Bachmann, N., Rechenbach, J., Boland, W., 2001. Ion channel-forming alamethicin is a potent elicitor of volatile biosynthesis and tendrillar curling. Cross talk between jasmonate and salicylate signaling in lima bean. *Plant Physiol.* 125, 369–377. <https://doi.org/10.1104/pp.125.1.369>.
- Faioła, C., Taipale, D., 2020. Impact of insect herbivory on plant stress volatile emissions from trees: A synthesis of quantitative measurements and recommendations for future research. *Atmospheric Environment: X* 5, 1000660. <https://doi.org/10.1016/j.aesox.2019.100060>.
- Faralli, M., Li, M., Varotto, C., 2020. Shoot characterization of isoprene and ocimene-emitting transgenic *Arabidopsis* plants under contrasting environmental conditions. *Plants* 9, 477. <https://doi.org/10.3390/plants9040477>.
- Farré-Armengol, G., Filella, L., Llusà, J., Peñaflor, J., 2017. *p*-Ocimene, a key floral and foliar volatile involved in multiple interactions between plants and other organisms. *Molecules* 22, 1148. <https://doi.org/10.3390/molecules22071148>.
- Feussner, I., Wasternack, C., 2002. The lipoxygenase pathway. *Annu. Rev. Plant Biol.* 53, 275–297. <https://doi.org/10.1146/annurev.arplant.53.100301.135248>.
- Foyer, C.H., 2018. Reactive oxygen species, oxidative signaling and the regulation of photosynthesis. *Environ. Exp. Bot.* 154, 134–142. <https://doi.org/10.1016/j.envexpbot.2018.05.003>.
- Gabarra, R., Alomar, O., Castañé, C., Goulia, M., Albajes, R., 2004. Movement of greenhouse whitefly and its predators between in- and outside of Mediterranean greenhouses. *Agric. Ecosyst. Environ.* 102, 341–348. <https://doi.org/10.1016/j.agee.2003.08.012>.
- Galís, I., Gaquerel, E., Pandey, S.P., Baldwin, I.T., 2009. Molecular mechanisms underlying plant memory in JA-mediated defence responses. *Plant Cell Environ.* 32, 617–627. <https://doi.org/10.1111/j.1365-3040.2008.01862.x>.
- Grote, R., Sharma, M., Ghirardo, A., Schmitzler, J.P., 2019. A new approach for estimating abiotic and biotic stress-induced de novo emissions of biogenic volatile organic compounds from plants. *Frontiers in Forests and Global Change* 2, 26. <https://doi.org/10.3389/ffgc.2019.00026>.
- Harrison, S.P., Morfopoulos, C., Dani, K.S., Prentice, I.C., Arnett, A., Attwell, B.J., et al., 2013. Volatile isoprenoid emissions from plastic to planar. *New Phytol.* 197, 49–57. <https://doi.org/10.1111/nph.12021>.
- Heiden, A.C., Kobel, K., Langebartels, C., Schub-Thomas, G., Wildt, J., 2003. Emissions of oxygenated volatile organic compounds from plants Part I: emissions from lipoxygenase activity. *J. Atmos. Chem.* 45, 143–172. <https://doi.org/10.1023/A:1024069605420>.
- Hilker, M., Schmülling, T., 2019. Stress priming, memory, and signalling in plants. *Plant Cell Environ.* 42, 753–761. <https://doi.org/10.1111/pce.13526>.
- Himanan, S.J., Nerg, A.M., Nissinen, A., Pinto, D.M., Stewart Jr, C.N., Poppy, G.M., Holopainen, J.K., 2009. Effects of elevated carbon dioxide and ozone on volatile terpene emissions and multitrophic communication of transgenic insecticidal oilseed rape (*Brassica napus*). *New Phytol.* 181, 174–186. <https://doi.org/10.1111/j.1469-8137.2008.02643.x>.
- Holopainen, J.K., 2011. Can forest trees compensate for stress-generated growth losses by induced production of volatile compounds? *Tree Physiol.* 31, 1356–1377. <https://doi.org/10.1093/treephys/tpq111>.
- Holopainen, J.K., Gershenzon, J., 2010. Multiple stress factors and the emission of plant VOCs. *Trends Plant Sci.* 15, 176–184. <https://doi.org/10.1016/j.pst.2010.01.006>.
- Hu, Z.H., Shen, Y.B., Su, X.H., 2009. Saturated aldehydes C₆–C10 emitted from ashleaf maple (*Acer negundo* L.) leaves at different levels of light intensity, O₂, and CO₂. *J. Plant Biol.* 52, 289–297. <https://doi.org/10.1007/s12374-009-9035-9>.
- Hu, Z.H., Leng, P.S., Shen, Y.B., Wang, W.H., 2011. Emissions of saturated C₆–C10 aldehydes from poplar (*Populus simonii* P. *Pyramidalis* Opera 8277) cuttings at different levels of light intensity. *J. For. Res.* 22, 233. <https://doi.org/10.1007/s11676-011-0155-9>.
- Hueve, K., Bichele, I., Rasulov, B., Ninimets, Ü.L.O., 2011. When it is too hot for photosynthesis: heat-induced instability of photosynthesis in relation to respiratory burst, cell permeability changes and H₂O₂ formation. *Plant Cell Environ.* 34, 113–126. <https://doi.org/10.1111/j.1365-3040.2010.02229.x>.
- Iriti, M., Faoro, P., 2009. Chemical diversity and defence metabolism: how plants cope with pathogens and ozone pollution. *Int. J. Mol. Sci.* 10, 3371–3399. <https://doi.org/10.3390/ijms10083371>.
- Islam, M.M., Hoque, M.A., Okuma, E., Banu, M.N.A., Shimoishi, Y., Nakamura, Y., Murata, Y., 2009. Exogenous proline and glycinebetaine increase antioxidant enzyme activities and confer tolerance to cadmium stress in cultured tobacco cells. *J. Plant Physiol.* 166, 1587–1597. <https://doi.org/10.1016/j.jplph.2009.04.002>.
- Janzen, R.M.C., Michbach, M., Kleist, E., Van Henten, E.J., Wildt, J., 2009. Release of lipoxygenase products and monoterpenes by tomato plants as an indicator of *Botrytis cinerea*-induced stress. *Plant Biol.* 11, 859–868. <https://doi.org/10.1111/j.1438-8677.2008.00183.x>.
- Jiang, Y., Ye, J., Li, S., Ninimets, Ü., 2017. Methyl jasmonate-induced emission of biogenic volatiles is biphasic in cucumber: a high-resolution analysis of dose dependence. *J. Exp. Bot.* 68, 4679–4694. <https://doi.org/10.1093/jxb/erz244>.
- Jiang, Y., Ye, J., Rasulov, B., Ninimets, Ü., 2020. Role of stomatal conductance in modifying the dose response of stress-volatile emissions in methyl jasmonate treated leaves of cucumber (*Cucumis sativa*). *Int. J. Mol. Sci.* 21, 1018. <https://doi.org/10.3390/ijms21031018>.
- Joo, É., Dewulf, J., Ameylnck, C., Schoon, N., Pokorska, O., Šimpraga, M., et al., 2011. Constitutive versus heat and biotic stress induced BVOC emissions in *Pseudeucoia menziesii*. *Atmos. Environ.* 45, 3655–3662. <https://doi.org/10.1016/j.atmosenv.2011.04.048>.
- Josse, E.M., Simkin, A.J., Gaffe, J., Labouré, A.M., Kuntz, M., Carol, P., 2000. A plastid terminal oxidase associated with carotenoid desaturation during chromoplast differentiation. *Plant Physiol.* 123, 1427–1436. <https://doi.org/10.1104/pp.123.4.1427>.
- Jud, W., Vanzo, E., Li, Z., Ghirardo, A., Zimmer, J., Sharkey, T.D., et al., 2016. Effects of heat and drought stress on post-illuminated bursts of volatile organic compounds in isoprene-emitting and non-emitting poplar. *Plant Cell Environ.* 39, 1204–1215. <https://doi.org/10.1111/pce.12643>.
- Kanagendran, A., Pazuoli, L., Ninimets, Ü., 2018. Differential regulation of volatile emission from *Eucalyptus globulus* leaves upon single and combined ozone and wounding treatments through recovery and relationships with ozone uptake. *Environ. Exp. Bot.* 145, 21–38. <https://doi.org/10.1016/j.envexpbot.2017.10.012>.
- Kännaste, A., Copolovici, L., Ninimets, Ü., 2014. Gas chromatography–mass spectrometry method for determination of biogenic volatile organic compounds emitted by plants. *Plant Isoprenoids*. Humana Press, New York, NY, pp. 161–169. https://doi.org/10.1007/978-1-4939-0606-2_11.
- Kask, K., Kännaste, A., Tals, E., Copolovici, L., Ninimets, Ü., 2016. How specialized volatiles respond to chronic and short-term physiological and shock heat stress in *Brassica nigra*. *Plant Cell Environ.* 39, 2027–2042. <https://doi.org/10.1111/pce.12775>.
- Kempema, L.A., Cui, X., Holzer, F.M., Walling, L.L., 2007. Arabidopsis transcriptome changes in response to phloem-feding silverleaf whitefly nymphs. Similarities and distinctions in responses to aphids. *Plant Physiol.* 143, 849–865. <https://doi.org/10.1104/pp.106.090602>.
- Kerchev, P.I., Fenton, B., Foyer, C.H., Hancock, R.D., 2012. Plant responses to insect herbivory: interactions between photosynthesis, reactive oxygen species and hormonal signalling pathways. *Plant Cell Environ.* 35, 441–453. <https://doi.org/10.1111/j.1365-3040.2011.02399.x>.
- Rigathi, R.N., Weisser, W.W., Reichelt, M., Gershenzon, J., Unsicker, S.B., 2019. Plant volatile emission depends on the species composition of the neighboring plant community. *BMC Plant Biol.* 19, 58. <https://doi.org/10.1186/s12870-018-1541-9>.
- Kleist, E., Mentel, T.F., Andres, S., Bohne, A., Follers, A., Kiendler-Scharr, A., et al., 2012. Irreversible impacts of heat on the emissions of monoterpenes, sesquiterpenes, phenolic BVOC and green leaf volatiles from several tree species. *Biogeosciences* 9, 5111. <https://doi.org/10.5194/bg-9-5111-2012>.
- Kumar, S., Pandey, A.K., 2013. Chemistry and biological activities of flavonoids: an overview. *The scientific world journal*. <https://doi.org/10.1155/2013/162759>.
- Li, T., Blande, J.D., Gundel, P.E., Helander, M., Saikonen, K., et al., 2014. *Epilochloa* endophytes alter inducible indirect defences in host grasses. *PLoS One* 9, e101331. <https://doi.org/10.1371/journal.pone.0101331>.

- Liu, B., Kaurilind, E., Jiang, Y., Ninemets, Ü., 2018. Methyl salicylate differently affects benzenoid and terpenoid volatile emissions in *Betula pendula*. *Tree Physiol.* **38**, 1513–1525. <https://doi.org/10.1093/treephys/tpy050>.
- Liu, B., Zhang, L., Rusaletpe, L., Kaurilind, E., Sulaiman, H.Y., Püssa, T., Ninemets, Ü., 2020. Heat priming improved heat tolerance of photosynthesis, enhanced terpenoid and benzenoid emission and phenolic accumulation in *Achillea millefolium*. *Plant Cell Environ.* <https://doi.org/10.1111/pce.13830>.
- Loreto, F., Förster, A., Dür, M., Csiky, Ö., Seufert, G., 1998. On the monoterpene emission under heat stress and on the increased thermotolerance of leaves of *Quercus ilex* L. fumigated with selected monoterpenes. *Plant Cell Environ.* **21**, 101–107. <https://doi.org/10.1046/j.1365-3040.1998.00268.x>.
- Loreto, F., Barra, C., Brilli, F., Nogues, L., 2006. On the induction of volatile organic compound emissions by plants as consequence of wounding or fluctuations of light and temperature. *Plant Cell Environ.* **29**, 1820–1828. <https://doi.org/10.1111/j.1365-3040.2006.01561.x>.
- Luo, H.B., Ma, L., Xi, H.F., Duan, W., Li, S.H., Loeschner, M., et al., 2011. Photosynthetic responses to heat treatments at different temperatures and following recovery in grapevine (*Vitis amurensis* L.) leaves. *PLoS One* **6**, e23003. <https://doi.org/10.1371/journal.pone.0023003>.
- Maccarrone, M., Veldink, G.A., Vliegengaart, J.F., 1992. Thermal injury and ozone stress affects soybean lipoxygenases expression. *FEBS Lett.* **309** (3), 225–230. [https://doi.org/10.1016/00145793\(92\)80778-f](https://doi.org/10.1016/00145793(92)80778-f).
- Mano, J.J., Kanameda, S., Kuramitsu, R., Matsura, N., Yamauchi, Y., 2019. Detoxification of reactive carbonyl species by glutathione transferase Tau isozymes. *Front. Plant Sci.* **10**, 487. <https://doi.org/10.3389/fpls.2019.00487>.
- McKee, G.J., Goodhue, R.E., Zalom, F.G., Carter, C.A., Chalfant, J.A., 2009. Population dynamics and the economics of invasive species management: the greenhouse whitefly in California-grown strawberries. *J. Environ. Manage.* **90**, 561–570. <https://doi.org/10.1016/j.jenvman.2007.12.011>.
- Memari, H.R., Pazouki, L., Ninemets, Ü., 2013. The biochemistry and molecular biology of volatile messengers in trees. *Biology, Controls and Models of Tree Volatile Organic Compound Emissions*. Springer, Dordrecht, pp. 47–93. https://doi.org/10.1007/978-94-007-6606-8_3.
- Miszal, P.K., Hewitt, C.N., Wildt, J., Blande, J.D., Eller, A.S., Fares, S., et al., 2015. Atmospheric benzenoid emissions from plants rival those from fossil fuels. *Sci. Rep.* **5**, 12864. <https://doi.org/10.1038/srep12864>.
- Monson, R.K., Jones, R.T., Rosenfield, T.N., Schitzler, J.P., 2013. Why only some plants emit isoprene. *Plant Cell Environ.* **36**, 503–516. <https://doi.org/10.1111/pce.12015>.
- Moran, P.J., Thompson, G.A., 2001. Molecular responses to aphid feeding in Arabidopsis in relation to plant defense pathways. *Plant Physiol.* **125**, 1074–1085. <https://doi.org/10.1104/pp.125.2.1074>.
- Nabity, P.D., Zavala, J.A., DeLuca, E.H., 2009. Indirect suppression of photosynthesis on individual leaves by arthropod herbivory. *Ann. Bot.* **103**, 655–663. <https://doi.org/10.1093/aob/mcn127>.
- Navia-Giné, W.G., Gomez, S.K., Yuan, J., Chen, F., Korth, K.L., 2009. Insect-induced gene expression at the core of volatile terpene release in *Medicago truncatula*. *Plant Signal. Behav.* **4**, 636–638. <https://doi.org/10.4161/psb.4.7.8971>.
- Nguyen, D., Rieu, I., Mariani, C., van Dam, N.M., 2016. How plants handle multiple stresses: hormonal interactions underlying responses to abiotic stress and insect herbivory. *Plant Mol. Biol.* **91**, 727–740. <https://doi.org/10.1007/s11103-016-0481-8>.
- Ninemets, Ü., 2010. Mild versus severe stress and BVOCs: thresholds, priming and consequences. *Trends Plant Sci.* **15**, 145–153. <https://doi.org/10.1016/j.tplants.2009.11.008>.
- Ninemets, Ü., Copolović, L., Hivice, K., 2010a. High within-canopy variation in isoprene emission potentials in temperate trees: implications for predicting canopy-scale isoprene fluxes. *J. Geophys. Res. Biogeosci.* **115**. <https://doi.org/10.1029/2010JG001436>.
- Ninemets, Ü., Monson, R.K., Arneith, A., Ciccioli, P., Kesselmeier, J., Kuhn, U., et al., 2010b. The leaf-level emission factor of volatile isoprenoids: caveats, model algorithms, response shapes and scaling. *Biogeosciences* **7**, <https://doi.org/10.5194/bg-7-1809-2010>.
- Ninemets, Ü., Kuhn, U., Harley, P.C., Staudt, M., Arneith, A., Cesatti, A., et al., 2011. Estimations of isoprenoid emission capacity from enclosure studies: measurements, data processing, quality and standardized measurement protocols. *Biogeosciences* **8**, 2209–2246. <https://doi.org/10.5194/bg-8-2209-2011>.
- Ninemets, Ü., Kännaste, A., Popolović, L., 2013. Quantitative patterns between plant volatile emissions induced by biotic stresses and the degree of damage. *Front. Plant Sci.* **4**, 262. <https://doi.org/10.3389/fpls.2013.00262>.
- Nisar, N., Li, L., Lu, S., Khin, N.C., Pogson, B.J., 2015. Carotenoid metabolism in plants. *Mol. Plant* **8**, 68–82. <https://doi.org/10.1016/j.molp.2014.12.007>.
- Owen, S.M., Peñuelas, J., 2005. Opportunistic emissions of volatile isoprenoids. *Trends Plant Sci.* **10**, 420–426. <https://doi.org/10.1016/j.tplants.2005.07.010>.
- Parejo, M., Pinto-Zevallos, D.M., 2016. Impacts of induction of plant volatiles by individual and multiple stresses across trophic levels. *Deciphering Chemical Language of Plant Communication*. Springer International Publishing, Cham, pp. 61–93. https://doi.org/10.1007/978-3-319-33498-1_3.
- Pazouki, L., Ninemets, Ü., 2016. Multi-substrate terpene synthases: their occurrence and physiological significance. *Front. Plant Sci.* **7**, 1019. <https://doi.org/10.3389/fpls.2016.01019>.
- Pazouki, L., Kanagendran, A., Li, S., Kännaste, A., Memari, H.R., Bicheler, R., Ninemets, Ü., 2016. Mono- and sesquiterpene release from tomato (*Solanum lycopersicum*) leaves upon mild and severe heat stress and through recovery: from gene expression to emission responses. *Environ. Exp. Bot.* **132**, 1–15. <https://doi.org/10.1016/j.envexpbot.2016.08.003>.
- R Core Team, 2020. R: A Language and Environment for Statistical Computing. R Foundation for Statistical Computing 2020, Vienna, Austria. <http://www.R-project.org/>.
- Raja, V., Majeed, U., Kang, H., Andrabhi, K.I., John, R., 2017. Abiotic stress: interplay between ROS, hormones and MAPKs. *Environ. Exp. Bot.* **137**, 142–157. <https://doi.org/10.1016/j.envexpbot.2017.02.010>.
- Rasulov, B., Talts, E., Ninemets, Ü., 2019. A novel approach for real-time monitoring of leaf wounding responses demonstrates unprecedentedly fast and high emissions of volatiles from cut leaves. *Plant Sci.* **283**, 256–265. <https://doi.org/10.1016/j.envexpbot.2017.02.010>.
- Rejeh, I.B., Pastor, V., Mouch-Mani, B., 2014. Plant responses to simultaneous biotic and abiotic stress: molecular mechanisms. *Plants* **3**, 458–475. <https://doi.org/10.3390/plants3040458>.
- Rinnan, R., Steinke, M., McGenity, T., Loreto, F., 2014. Plant volatiles in extreme terrestrial and marine environments. *Plant Cell Environ.* **37**, 1776–1789. <https://doi.org/10.1111/pce.12320>.
- Rostás, M., Ton, J., Mouch-Mani, B., Turlings, T.C., 2006. Fungal infection reduces herbivore-induced plant volatiles of maize but does not affect naive parasitoids. *J. Chem. Ecol.* **32**, 1897. <https://doi.org/10.1111/pce.12320>.
- Salerno, G., Frati, F., Marino, G., Ederli, L., Pasqualini, S., Loreto, F., et al., 2017. Effects of water stress on emission of volatile organic compounds by *Vicia faba*, and consequences for attraction of the egg parasitoid *Trissolcus basalis*. *J. Pest Sci.* (2004) **90**, 635–647. <https://doi.org/10.1007/s10340-016-0830-z>.
- Sallaud, C., Rontein, D., Ouilhon, S., Jabès, F., Duffé, P., Giacalone, C., Thoraval, S., Ecoffier, C., Herbet, G., Leonhardt, N., Cousse, M., Tissier, A., 2009. A novel pathway for sesquiterpene biosynthesis from Z,Z-farnesyl pyrophosphate in the wild tomato *Solanum habrochaites*. *Plant Cell* **21** (1), 301–317. <https://doi.org/10.1105/tpc.107.057885>.
- Salvucci, M.E., Crafts-Brandner, S.J., 2004. Mechanism for deactivation of Rubisco under moderate heat stress. *Physiol. Plant.* **122** (4), 513–519.
- Sasidharan, R., Voosenek, L.A., Pierik, R., 2011. Cell wall modifying proteins mediate plant acclimatization to biotic and abiotic stresses. *Crit. Rev. Plant Sci.* **30**, 548–562. <https://doi.org/10.1080/07352689.2011.615706>.
- Scala, A., Allmann, S., Mirabella, R., Haring, M.A., Schuurink, R.C., 2013. Green leaf volatiles: a plant's multifunctional weapon against herbivores and pathogens. *Int. J. Mol. Sci.* **14**, 17781–17811. <https://doi.org/10.3390/ijms140917781>.
- Sharkey, T.D., Wiberley, A.F., Donohue, A.R., 2008. Isoprene emission from plants: Why and how. *Ann. Bot.* **101** (1), 5–18. <https://doi.org/10.1093/aob/mcn240>.
- Sharma, M., Laxmi, A., 2016. Jasmonates: emerging players in controlling temperature stress tolerance. *Front. Plant Sci.* **6**, 1129. <https://doi.org/10.3389/fpls.2015.01129>.
- Staudt, M., Jackson, B., El-aouhi, H., Buaotis, B., Lacroze, J.-P., Poëssel, J.-L., Sauge, M.-H., Ninemets, Ü., 2010. Volatile organic compound emissions induced by the aphid *Myzus persicae* differ among resistant and susceptible peach cultivars and a wild relative. *Tree Physiol.* **30** (10), 1320–1334. <https://doi.org/10.1093/treephys/tpq072>.
- Sitti, N., Missihoun, T.D., Kotchohi, S., Kirch, H.H., Bartels, D., 2011. Aldehyde dehydrogenases in *Arabidopsis thaliana*: biochemical requirements, metabolic pathways, and functional analysis. *Front. Plant Sci.* **2**, 65. <https://doi.org/10.3389/fpls.2011.00065>.
- Sunkar, R., Bartels, D., Kirch, H.H., 2003. Overexpression of a stress-inducible aldehyde dehydrogenase gene from *Arabidopsis thaliana* in transgenic plants improves stress tolerance. *Plant J.* **35**, 452–464. <https://doi.org/10.1046/j.1365-3113.2003.01819.x>.
- Suzuki, N., Mittler, R., 2006. Reactive oxygen species and temperature stresses: a delicate balance between signaling and destruction. *Physiol. Plant.* **126**, 45–51. <https://doi.org/10.1111/j.0031-9317.2005.00582.x>.
- Thaler, J.S., Humphrey, P.T., Whiteman, N.K., 2012. Evolution of jasmonate and salicylate signal crosstalk. *Trends Plant Sci.* **17** (5), 260–270. <https://doi.org/10.1016/j.tplants.2012.02.010>.
- Tholl, D., 2015. Biosynthesis and biological functions of terpenoids in plants. *Biotechnology of Isoprenoids*. Springer International Publishing, Cham, pp. 63–106. <https://doi.org/10.1007/978-10-10-210-295>.
- Trumble, J.T., Kolodny-Hirsch, D.M., Ting, I.P., 1993. Plant compensation for arthropod herbivory. *Annu. Rev. Entomol.* **38**, 93–119. <https://doi.org/10.1146/annurev.en.38.010193.000521>.
- Tsai, W.A., Weng, S.H., Chen, M.C., Lin, J.S., Tsai, W.S., 2019. Priming of plant resistance to heat stress and tomato yellow leaf curl Thailand virus with plant-derived materials. *Front. Plant Sci.* **10**, 906. <https://doi.org/10.3389/fpls.2019.00906>.
- Turan, S., Kask, K., Kanagendran, A., Li, S., Anni, R., Talts, E., Rasulov, B., Kännaste, A., Ninemets, Ü., 2019. Lethal heat stress-dependent volatile emissions from tobacco leaves: what happens beyond the thermal edge? *J. Exp. Bot.* **70**, 5017–5030. <https://doi.org/10.1093/jxb/erz255>.
- Urban, J., Ingwers, M.W., McGuire, M.A., Teskey, R.O., 2017. Increase in leaf temperature opens stomata and decouples net photosynthesis from stomatal conductance in *Pinus taeda* and *Populus deltoides* x *nigra*. *J. Exp. Bot.* **68**, 1757–1767. <https://doi.org/10.1093/jxb/erx052>.
- Vacca, R.A., de Pinto, M.C., Valenti, D., Passarella, S., Marra, E., De Gara, L., 2004. Production of reactive oxygen species, alteration of cytosolic ascorbate peroxidase, and impairment of mitochondrial metabolism are early events in heat shock-induced programmed cell death in tobacco Bright-yellow 2 cells. *Plant Physiol.* **134**, 1100–1112. <https://doi.org/10.1104/pp.103.035956>.
- Van der Does, D., Leon-Reyes, A., Koornneef, A., Van Verk, M.C., Rodenburg, N., Pauwels, L., et al., 2013. Salicylic acid suppresses jasmonic acid signaling downstream of SCFOI1-JAZ by targeting GCC promoter motifs via transcription factor ORA59. *Plant Cell* **25**, 744–761. <https://doi.org/10.1105/tpc.112.108548>.

- Velikova, V., Várkonyi, Z., Szabó, M., Maslenkova, L., Nogués, I., Kovács, L., et al., 2011. Increased thermostability of thylakoid membranes in isoprene-emitting leaves probed with three biophysical techniques. *Plant Physiol.* 157, 905–916. <https://doi.org/10.1104/pp.111.182519>.
- Vickers, C.E., Possell, M., Cojocariu, C.I., Velikova, V.B., Laohawornkitkul, J., Ryan, A., et al., 2009. Isoprene synthesis protects transgenic tobacco plants from oxidative stress. *Plant Cell Environ.* 32, 520–531. <https://doi.org/10.1111/j.1365-3040.2009.01946.x>.
- Vickers, C.E., Possell, M., Laohawornkitkul, J., Ryan, A.C., Hewitt, C.N., Mullineaux, P. M., 2011. Isoprene synthesis in plants: lessons from a transgenic tobacco model. *Plant Cell Environ.* 34, 1043–1053. <https://doi.org/10.1111/j.1365-3040.2011.02303.x>.
- Vogt, T., 2010. Phenylpropanoid Biosynthesis. *Mol. Plant* 3 (1), 2–20. <https://doi.org/10.1093/mp/ssp106>.
- Von Caemmerer, S.V., Farquhar, G.D., 1981. Some relationships between the biochemistry of photosynthesis and the gas exchange of leaves. *Planta* 153, 376–387. <https://doi.org/10.1007/BF00384257>.
- Wahid, A., Gelani, S., Ashraf, M., Foolad, M.R., 2007. Heat tolerance in plants: an overview. *Environ. Exp. Bot.* 61, 199–223.
- Walling, L.L., 2008. Avoiding effective defenses: strategies employed by phloem-feeding insects. *Plant Physiol.* 146, 859–866. <https://doi.org/10.1104/pp.107.113142>.
- War, A.R., Sharma, H.C., Paulraj, M.G., War, M.Y., Ignacimuthu, S., 2011. Herbivore induced plant volatiles: their role in plant defense for pest management. *Plant Signal. Behav.* 6, 1973–1978. <https://doi.org/10.4161/psb.6.12.18053>.
- Wasternack, C., Hause, B., 2013. Jasmonates: biosynthesis, perception, signal transduction and action in plant stress response, growth and development. An update to the 2007 review in *Annals of Botany*. *Ann. Bot.* 111, 1021–1058. <https://doi.org/10.1093/aob/mct0467>.
- Xu, Y.H., Liao, Y.C., Zhang, Z., Liu, J., Sun, P.W., Gao, Z.H., et al., 2016. Jasmonic acid is a crucial signal transducer in heat shock induced sesquiterpene formation in *Aquilaria sinensis*. *Sci. Rep.* 6, 21843. <https://doi.org/10.1038/srep21843>.
- Yu, H., Zhang, Y., Li, Y., Lu, Z., Li, X., 2018. Herbivore-and MeJA-induced volatile emissions from the redroot pigweed *Amaranthus retroflexus* Linnaeus: their roles in attracting *Micropylis* mediator (Haliiday) parasitoids. *Arthropod. Interact.* 12, 575–589. <https://doi.org/10.1007/s13293-018-9606-0>.
- Zarate, S.I., Kempema, L.A., Walling, L.L., 2007. Silverleaf whitefly induces salicylic acid defenses and suppresses effectual jasmonic acid defenses. *Plant Physiol.* 143, 866–875. <https://doi.org/10.1104/pp.106.090035>.
- Zhang, P.J., Zheng, S.J., van Loon, J.J., Boland, W., David, A., Mumm, R., Dicke, M., 2009. Whiteflies interfere with indirect plant defense against spider mites in Lima bean. *Proc. Natl. Acad. Sci.* 106, 21202–21207. <https://doi.org/10.1073/pnas.0907890106>.
- Zhang, P.J., He, Y.C., Zhao, C., Ye, Z.H., Yu, X.P., 2018. Jasmonic acid-dependent defenses play a key role in defending tomato against *Bemisia tabaci* nymphs, but not adults. *Front. Plant Sci.* 9, 1065. <https://doi.org/10.1104/pp.106.090035>.
- Zhang, P.J., Xu, C.X., Zhang, J.M., Lu, Y.B., Wei, J.N., Liu, Y.Q., et al., 2013. Phloem-feeding whiteflies can fool their host plants, but not their parasitoids. *Funct. Ecol.* 27, 1304–1312. <https://doi.org/10.1111/1365-2435.12132>.



Sulaiman, HY, Runno-Paurson, E, Kaurilind, E and Niinemets, Ü. 2023. Differential impact of crown rust (*Puccinia coronata*) infection on photosynthesis and volatile emissions in the primary host *Avena sativa* and the alternate host *Rhamnus frangula*. *Journal of Experimental Botany* 74: 2029-2046.

RESEARCH PAPER

Differential impact of crown rust (*Puccinia coronata*) infection on photosynthesis and volatile emissions in the primary host *Avena sativa* and the alternate host *Rhamnus frangula*

Hassan Y. Sulaiman^{1,*,}, Eve Runno-Paurson^{1,2,}, Eve Kaurilind^{1,2,} and Ülo Niinemets^{1,2,}

¹ Chair of Crop Science and Plant Biology, Estonian University of Life Sciences, Kreutzwaldi 5, 51006 Tartu, Estonia

² Estonian Academy of Sciences, Kohtu 6, 10130 Tallinn, Estonia

* Correspondence: Hassan@emu.ee

Received 16 May 2022; Editorial decision 2 January 2023; Accepted 3 January 2023

Editor: John Lunn, Max Planck Institute of Molecular Plant Physiology, Germany

Abstract

Rust infection results in decreases in photosynthesis and stress volatile emissions, but how these changes vary among host species has not been studied. We demonstrated that the impact of the obligate biotrophic fungus, *Puccinia coronata* f. sp. *avenae*, on foliage physiological processes is stronger in the primary host, *Avena sativa* (cultivated oat), than in the alternate host, *Rhamnus frangula* (alder buckthorn). Photosynthesis decreased with increasing percentage of damaged leaf area (D_A) in both species, but reductions were greater in *A. sativa*. In *A. sativa*, photosynthetic reductions resulted from reductions in stomatal conductance and photosynthetic capacity; in *R. frangula*, reductions were due to reduced capacity. Infection reduced photosynthetic biomass and key nutrients in *A. sativa*, but not in *R. frangula*. In *A. sativa*, stress-elicited emissions (methyl jasmonate, green leaf volatiles, long-chain saturated aldehydes, mono- and sesquiterpenes, benzenoids, and carotenoid breakdown products) increased with increasing D_A from 0% to 40%, but decreased with further increases in D_A . In *R. frangula*, volatile emissions were slightly elicited but, surprisingly, constitutive isoprene emissions were enhanced. Different hosts had characteristic volatile fingerprints, indicating differential activation of biochemical pathways. Fungal-elicited reductions in photosynthesis scale uniformly with stress severity. In the sensitive host, biphasic scaling of volatiles indicates that heavy spread of chlorosis/necrosis leads to an overall cessation of physiological functioning.

Keywords: Biotic stress, fungal infection, isoprene, jasmonate emission, lipoxygenase pathway volatiles, pathogen attack, photosynthesis, species differences, terpenoids, volatile organic compounds.

Abbreviations: A_A , net assimilation rate per leaf area; A_M , net assimilation rate per dry mass; C_i , intercellular concentration of CO_2 ; C_M , carbon content per unit dry mass; D_A , percentage of damaged leaf area; DOXP, 1-deoxy-D-xylulose 5-phosphate; FAD, long-chain fatty acid-derived; GGDP, geranylgeranyl diphosphate; g_s , stomatal conductance; LMA, dry mass per unit area; LOX, lipoxygenase; MeJA, methyl jasmonate; MEP, 2-C-methyl-D-erythritol 4-phosphate; MeSA, methyl salicylate; MVA, mevalonate; N_M , nitrogen content per dry mass; P_M , phosphorus content per dry mass; PPF, photosynthetic photon flux density; VOC, volatile organic compound.

© The Author(s) 2023. Published by Oxford University Press on behalf of the Society for Experimental Biology. All rights reserved. For permissions, please email: journals.permissions@oup.com

Introduction

Oat crown rust is a devastating plant disease that primarily infects oats (*Avena* spp.), in particular the key crop common oat (*Avena sativa* L.), and also several other wild grasses. In *A. sativa*, the disease is caused by the obligate biotrophic rust fungus *Puccinia coronata* f. sp. *avenae* P. Syd. and Syd (Chong and Zegeye 2004; Liu and Hambleton, 2013). The sexual reproduction is completed in alder buckthorn (*Rhamnus frangula*, L., syn. *Frangula alnus* P. Mill., *Rhamnaceae*), as the fertilization happens in *R. frangula*, but the main phases, karyogamy and meiosis, occur in oat leaves (see Nazareno *et al.*, 2018 for details of the *P. coronata* life cycle).

Due to the complex life history of *P. coronata*, prediction of the impact of the pathogen is difficult. In general, plant responses to a given pathogen depend on host compatibility and resistance, including host vigor and presence of constitutive defenses, and capacity to induce defenses (Ponzio *et al.*, 2016; Dracatos *et al.*, 2018). Virulence of multi-host pathogens could vary for the primary and alternate host(s) (Rigaud *et al.*, 2010; Bettgenhaeuser *et al.*, 2014; Lorrain *et al.*, 2018). Multi-host pathogens with heteroecious life cycles tend to be less virulent for their alternate hosts than for their primary host, as the alternate hosts are mainly required for transit (Bettgenhaeuser *et al.*, 2014). Additionally, alternate hosts usually have several resistance genes that reduce the efficacy of pathogens (Lorrain *et al.*, 2018). Moreover, for *P. coronata*, the primary host, *A. sativa*, is a monocot, while the alternate host, *R. frangula*, is a dicot, and the response to fungal infection is known to differ for monocots and dicots (see Kouzai *et al.*, 2018). Thus, a detailed quantitative understanding of the responses of host plants to infection by *P. coronata*, whose virulence has remarkably increased in recent years (Menzies *et al.*, 2019; Sowa and Paczós-Grządca, 2021), is essential in predicting potential yield loss and developing interventions to cope with the infection.

Generally, rust infections cause nutrient depletion, increases in rates of water loss due to stomatal rupture, and reductions in photosynthetic activity and biomass of the host plant (Major *et al.*, 2010; Gortari *et al.*, 2018). In cereal grasses, loss of leaf biomass due to rust infections can result in declines in the production and economic value of the grains (Lorrain *et al.*, 2019; Nazareno *et al.*, 2018). As plant response to a given biotic agent varies with stress severity (Niinemets, 2010; Niinemets *et al.*, 2013; Kännaste *et al.*, 2023), predicting the responses to fungal infection requires a clear understanding of the relationships between different physiological processes and stress severity. In the case of necrotrophic fungal infections that primarily result in cell death, the spread of dead tissue can explicitly explain the loss of photosynthetic capacity (Greenberg and Yao 2004; Berger *et al.*, 2007). However, the quantitative relationships between changes in leaf photosynthetic activity and the spread of biotrophic infections are much less understood. For biotrophic pathogen infections, decreases in photosynthetic activity have also been demonstrated to scale with the percentage of

the total chlorotic and necrotic area of the leaf (Copolovici *et al.*, 2014; Jiang *et al.*, 2016). Yet, the complexity of loss of photosynthetic function in biotrophic pathogen infection is beyond the spread of dead tissue, as it involves changes in stomatal control, key nutrient contents, and leaf sink-source relationships (Araya *et al.*, 2006; Berger *et al.*, 2007; Veresoglou *et al.*, 2013). The reduction of photosynthetic activity is often associated with decreases in leaf dry mass per unit area, a key morphological trait that together with nutrient contents characterizes the accumulation of photosynthetic biomass per unit area (Niinemets, 1999; Poorter *et al.*, 2009). Scholes and Rolfe (1996) studied localized decreases of photosynthesis in *A. sativa* infected with *P. coronata* and demonstrated that photosynthetic activity decreases from inoculation with *P. coronata* to sporulation, but whether the loss of photosynthetic activity scaled with the severity of infection or was associated with changes in stomatal conductance (g_s), nutrient status (C, N, and P), and biomass was not studied. To our knowledge, for multi-host pathogens, including *P. coronata*, there is currently no information on how different life stages of the given biotrophic pathogen affect the photosynthetic functioning of its primary and alternate hosts and to what extent different factors contribute to decreases in photosynthesis in different hosts.

Apart from decreasing photosynthesis, pathogen infection activates defense signaling pathways triggering various stress and signaling volatile organic compound (VOC) emissions (Huber and Bauerle, 2016; Liu *et al.*, 2016). Responses to biotic stress occur through jasmonic acid (JA) or/and salicylic acid (SA) signaling pathways; activation of either of the two pathways is typically associated with the release of the volatile hormone derivatives of methyl jasmonate (MeJA) or methyl salicylate (MeSA) (Chauvin *et al.*, 2013; Liu *et al.*, 2016). However, there is certain crosstalk between these two signal transduction pathways that can be either antagonistic or synergistic, and activation of one of the two pathways can trigger activation of the other (Attaran *et al.*, 2009; Patt *et al.*, 2018). Prioritization between the two pathways often depends on the behavior of the pathogen (Gális *et al.*, 2009; Savatin *et al.*, 2014). Typically, biotrophic and hemibiotrophic pathogens preferentially elicit SA signaling while necrotrophic pathogens trigger JA responses (Savatin *et al.*, 2014; Gortari *et al.*, 2018). Similar to herbivore-dependent wounding, pathogen-dependent development of lesions and necrosis results in emissions of short-chain fatty acid-derived compounds (green leaf volatiles) from the lipoxygenase (LOX) pathway (Arneith and Niinemets, 2010; Copolovici *et al.*, 2011). However, in contrast to herbivores, which usually elicit the emissions of LOX compounds as a direct transient response to wounding, fungal infections induce sustained LOX emissions, reflecting a chronic stress impact (Vuorinen *et al.*, 2007; Copolovici *et al.*, 2011; Jiang *et al.*, 2016). Pathogen attacks also induce emissions of volatile terpenoids including mono- and sesquiterpenes and their derivatives (Vuorinen *et al.*,

2007; Armeth and Niinemets, 2010) synthesized in the plastidial 2-C-methyl-D-erythritol 4-phosphate/1-deoxy-D-xylulose 5-phosphate (MEP/DOXP) pathway and the cytosolic mevalonate (MVA) pathway, and a variety of volatile phenolics/benzenoids emanating from the shikimate pathway (Dudareva et al., 2013; Junker and Tholl, 2013).

Emerging evidence indicates that fungal-elicited VOC emissions depend quantitatively on the severity of infection as characterized by the spread of lesions (Niinemets et al., 2013; Copolovici et al., 2014; Jiang et al., 2016). For example, the emissions of LOX compounds, monoterpenes, and benzenoids quantitatively scaled with the severity of *Melampsora larici-populina* (poplar leaf rust) in *Populus balsamifera* (balsam poplar) (Jiang et al., 2016) and with the severity of *Erysiphe althoides* (oak powdery mildew) infections in *Quercus robur* (common oak) (Copolovici et al., 2014). However, biotic stress responses often depend on the physiological and genotypic characteristics of the host species. For instance, *Triaenodes vipanariorum* infestation induced LOX emissions in *Solanum melongena* (Darshane et al., 2017), whereas a similar infestation inhibited constitutive LOX emissions in *S. lycopersicum* (Darshane et al., 2017) and *Origanum vulgare* (Sulaiman et al., 2021). Therefore, similar pathogens can elicit variant physiological responses in primary hosts and alternate hosts with potentially different pathogen resistance and, accordingly, with different severity of stress sustained at the given level of pathogen pressure. Volatile emission responses are especially likely to differ significantly between distantly related species (Dracotos et al., 2018) such as *A. sativa* and *R. frangula*. So far, VOC responses to *P. coronata* infection have not been investigated either in the primary or in the alternate host(s).

Furthermore, different hosts can differ in the level of constitutive volatile emissions (emissions under non-stressed conditions) and that can further impact the degree of elicitation of induced emissions (Brilli et al., 2009; Dani et al., 2014). In the case of constitutive isoprene emitters, constitutive isoprene emissions are characteristically negatively associated with induced isoprenoid emissions (Toome et al., 2010; Copolovici et al., 2014; Jiang et al., 2016), but how a given pathogen affects different hosts with varying degrees of constitutive isoprene emissions has not been investigated. This is particularly relevant for *P. coronata*, as it infects the primary host *A. sativa*, a weak constitutive emitter, and the alternate host *R. frangula*, a moderately strong constitutive isoprene emitter. VOCs are major precursors in ozone and secondary aerosol formation. Understanding the relationships between leaf VOC emissions and environmental stresses provides important data for scaling up biogenic emissions from leaves to the ecosystem level and assessing biogenic VOC contributions to shaping tropospheric chemistry.

We investigated how *P. coronata*-induced changes in foliage photosynthesis and VOC emissions scale with the severity of infection in *A. sativa* and *R. frangula*. We hypothesized that (i) *P. coronata* infection results in quantitative decreases in pho-

tosynthesis rates and increases in stress volatile emissions with increasing severity of infection in both species; (ii) the impact of *P. coronata* on photosynthesis and VOC emissions at the given level of infection is stronger in the primary host *A. sativa* than in the alternate host *R. frangula*; (iii) emissions of constitutive isoprene scale negatively with induced emissions; and (iv) *P. coronata*-induced volatile blends differ among species. Our study demonstrates major differences among hosts in the degree of VOC induction, and similar photosynthetic reductions, but due to changes in different underlying traits.

Materials and methods

Study site and plant material

The study was conducted in Põlva County, Estonia (58.6°N, 26.5°E, elevation 61 m) in summer 2018. The summer was warm with a monthly average (±SE) air temperature of 19.5 ± 1.4 °C, precipitation of 56 ± 17 mm, and relative air humidity of 68.2 ± 2.8% for June–August (data of the Laboratory of Environmental Physics, Institute of Physics, University of Tartu, <http://meteo.physic.ut.ee>). In particular, air temperature substantially exceeded the corresponding long-term average (16.7 °C), whereas precipitation (56 mm), and relative humidity (68%) were similar to the long-term averages (1991–2020), the Estonian Environment Agency, <http://www.emhi.ee>). Warm and humid weather favors the growth and dispersal of *P. coronata* and the early formation of teliospores (Liu and Hambleton, 2013; Nazareno et al., 2018).

Rhamnus frangula was sampled in the mixed Norway spruce (*Picea abies* L.) and Scots pine (*Pinus sylvestris* L.) forest near Veski village, Põlva County, Estonia (58.6°N, 26.48°E, elevation 61 m) in mid-June. By the inception of this study, nearly all *R. frangula* shrubs were infected with basidiospores developed from telia in *A. sativa* leaves and >90% of the leaves on each infected shrub had manifested rust lesions. Analogously, by the end of July, almost all *A. sativa* plants growing in a nearby oat field (58.65°N, 26.47°E, elevation 61 m) were infected and had developed visible uredinia and telia spots.

To investigate the quantitative relationship between the severity of *P. coronata* infections and physiological characteristics in *R. frangula*, leaves with varying degrees of visible symptoms of infection and leaves with no visible signs of infections were collected from seven infected shrubs and three non-infected shrubs (~3 m tall with a stem diameter of ~4 cm). Twigs with multiple leaves, ~20 cm long, were cut under water, the cut end was held in water, and the twigs were immediately transported to the laboratory where representative leaves were selected for the measurements. Altogether, 15 leaves (three non-infected control and 12 infected leaves) with varying degrees of infection were measured (see Fig. 1B for representative images of leaves).

In early August, ~2-month-old *A. sativa* cv. 'Kalle' plants with leaves with varying degrees of infection were collected from the organic oat field at Veski village. The plants were collected by excavating whole plants with the whole root ball and attached soil without damaging the root zone. Individual plants were immediately placed in 1 liter plastic pots. The pots were filled with the field soil at the site, gently watered, and transported to a growth room with day/night temperatures of 25/18 °C, relative humidity of 60–70%, photosynthetic photon flux density (PPFD) of 800 μmol m⁻² s⁻¹, and CO₂ concentration of 380–400 μmol per mol of air (hereafter μmol mol⁻¹) at plant level provided for 12 h a day. The pots were kept in the growth room for 4 d until the plants acclimatized to the condition in the pot. The plants were irrigated to field capacity every 48 h. Sampled *A. sativa* plants were ~90 cm tall, and in the vegetative state. Three non-infected control and 20 infected leaves with different degrees of infections from independent plants were measured. The severity of infection was quantified as

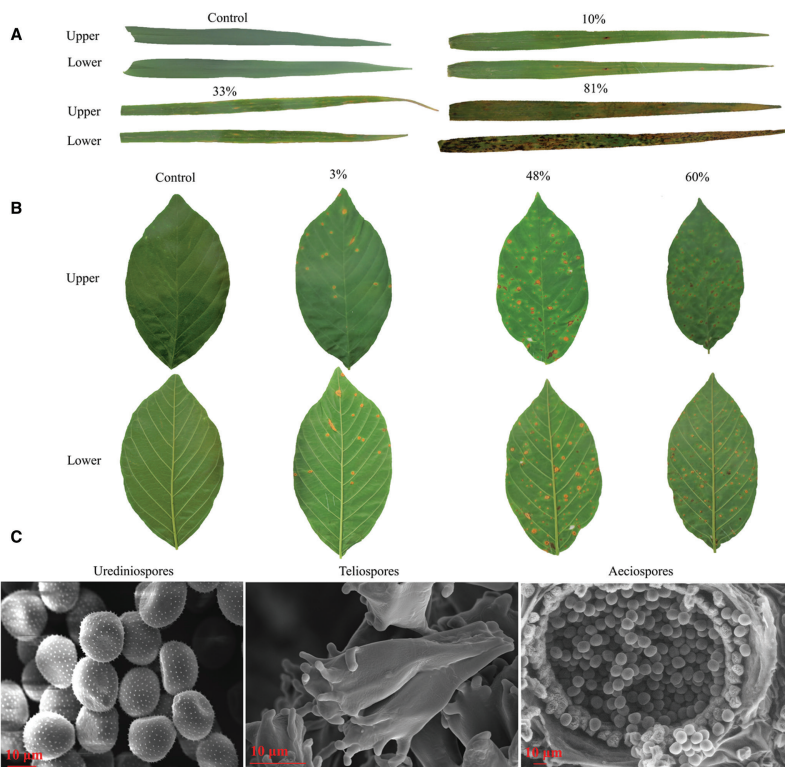


Fig. 1. Characteristic images of upper and lower leaf surfaces of the leaves of the annual grain crop *Avena sativa* (A) and the deciduous shrub *Rhamnus frangula* (B) exhibiting different severities of crown rust fungus (*Puccinia coronata* f. sp. *avenae*) infection, and SEM micrographs of the urediniospores, teliospores, and aeciospores (from left to right) of *P. coronata* (C). *Avena sativa* is the primary host and *R. frangula* is the alternate host of *P. coronata*.

the percentage of the total leaf area covered by visible chlorotic and necrotic regions (total damaged leaf area, D_d). Based on the severity of infection, infected *A. sativa* leaves were divided into five infection categories: non-infected control (0% D_d), mildly infected (~10% D_d), moderately infected (~40% D_d), severely infected (~60% D_d), and extremely infected (~80% D_d). Mature topmost leaves of the same age were selected for physiological measurements (see Fig. 1A for images of representative leaves).

Identification of *Puccinia coronata* f. sp. *avenae*

SEM (Zeiss LS15, Carl Zeiss AG, Jena, Germany) was used to examine the morphology of the aeciospores, urediniospores, and teliospores in

P. coronata-infected leaves. The spores were imaged with the detector SE1 at a working distance (WD) of 8.5–9 mm between the sample surfaces and the lens, and with extra high tension voltages of 14.27, 15.0, or 17.6 kV. The surface characteristics of the inocula were distinctly recognized in the images (Fig. 1C). *Puccinia coronata* can be identified based on morphological features, but the forma specialis, f. sp. *avenae*, is identified based on the host species, *A. sativa* (Liu and Hambleton, 2013; Dracatos et al., 2018). There is a relatively large genetic variability among and within the populations of *P. coronata*, both in aecial and in uredinal hosts (Liu and Hambleton, 2013; Berlin et al., 2018; Sowa and Paczos-Grzęda, 2021), but for our physiological analysis, population diversity was not determined.

Gas exchange measurements and volatile sampling

A customized open gas exchange system was used to measure rates of foliage photosynthetic characteristics (see Copolovici and Niinemets, 2010 for details). The system is equipped with a temperature-controlled double-glass cylindrical 1.2 liter chamber with a stainless steel bottom devised for trace gas sampling. Water with set temperature was circulating between the double layers of the chamber. Air temperature was monitored by a thermistor (NTC, model ACC-001, RTI Electronics, Inc., St. Anaheim, CA, USA). The chamber was flushed with ambient air at a constant flow rate of 0.036 l s^{-1} . Before entering the chamber, the air passed through a custom-made ozone trap and a charcoal filter, and was humidified to the desired relative humidity with a custom-made humidifier (Copolovici and Niinemets 2010; Copolovici *et al.*, 2012). After leaf enclosure, standard measurement conditions of leaf temperature of 25°C , PPFD of $800 \mu\text{mol m}^{-2} \text{ s}^{-1}$, CO_2 concentration of $400 \mu\text{mol mol}^{-1}$, and leaf to air vapor pressure deficit of 1.7 kPa were established. The light was supplied by four 50 W halogen lamps. The leaf temperature was measured by a thermocouple affixed to the lower leaf surface. Concentrations of H_2O and CO_2 at chamber inlets and outlets were measured using a dual-channel infrared gas analyzer (CIRAS II, PP-systems, Amesbury, MA, USA). Steady-state net assimilation rates and stomatal conductance to water vapor (g_w) were measured immediately after gas exchange rates had stabilized, typically in ~ 15 min after leaf enclosure.

Volatiles were collected during gas exchange measurements. A suction pump (210-1003 MTX, SKC Inc., Houston, TX, USA) operated at a flow rate of 0.21 min^{-1} was used to pass 4 liters of air onto a stainless steel cartridge filled with three different Carbotrap adsorbents (Supelco, Bellefonte, PA, USA) optimized for adsorbing C_3 – C_{17} volatiles (see Kännaste *et al.*, 2014 for details). Volatiles were also collected regularly from empty chambers to determine the background concentrations of volatiles. The cartridges were analyzed using a Shimadzu TD20 automated cartridge desorber and Shimadzu 2010 GC-MS system (Shimadzu Corporation, Kyoto, Japan) as in Kännaste *et al.* (2014). Pure chemical standards (Sigma-Aldrich, St. Louis, MO, USA), NIST library ver. 2.2 (2014), and the open-access program OpenChrom ver. 1.2.0 (Alder) (Wenig and Odermatt, 2010) were used to identify and quantify the volatiles (see Tables 1 and 2 for detected compounds in *A. sativa* and *R. frangula*). Background volatile concentrations were subtracted from the measurements of leaves. Foliage photosynthetic characteristics were calculated according to von Caemmerer and Farquhar (1981) and volatile emission rates according to Niinemets *et al.* (2011).

Determination of leaf dry mass per area, and carbon, nitrogen, and phosphorus contents per dry mass

In *R. frangula* leaves, aeciospores emerge on the lower surface, and pycniospores lodge on the upper surface, whereas in *A. sativa*, urediniospores germinate on both leaf surfaces. These spores colonize mesophyll spaces and absorb nutrients through haustoria, and constitute the characteristic sign of infection that is manifested as bright orange-yellow oblong pustules (Nazareno *et al.*, 2018). Chlorotic and necrotic areas were evident on both leaf surfaces of infected leaves in this study. After volatile collection, photographs were taken from both leaf sides. The leaves were oven-dried at 70°C for 72 h and then weighed. For each leaf, the total leaf area and infected leaf area on both sides were computed from the pictures using ImageJ 1.8.0 (NIH, Bethesda, MD, USA), and D_A values for both leaf surfaces were calculated. Dry mass per unit area (LMA) was computed by dividing leaf dry mass by leaf area. Dried leaves of an approximately similar degree of infection were ground together, and nitrogen (N_M) and carbon (C_M) contents per unit dry mass were determined by the dry combustion method using a Vario MAX CNS analyzer (Elementar, Langensfeld, Germany). Phosphorus content per dry mass (P_M) was determined using an Agilent 4200 microwave plasma-atomic emission spectrometer (Agilent Technologies, Inc., Santa Clara, CA, USA) after digesting the sample in sulfuric acid.

Data analyses

A paired-samples *t*-test was used to test the significance of differences in degrees of infection of lower and upper leaf surfaces. The quantitative relationships between the severity of infections and photosynthetic characteristics, LMA, N_M , P_M , C_M , and volatile emission rates were explored using linear and non-linear regressions. Differences in trait averages among leaves with different levels of infection were tested using Fisher's least significant difference following single-factor ANOVA. An independent-samples *t*-test was used to test the significance of differences in emissions of volatile classes between species at different levels of infection severity. Where required, the data used for ANOVA and *t*-test were log-transformed to satisfy the assumption of homoscedasticity. The differences in the volatile composition of infected leaves of host species were explored by principal component analysis (PCA) after mean scaling of the data. The differences in the volatile blends were also explored by permutational multivariate analysis (PERMANOVA) using the Bray-Curtis dissimilarity statistic. All statistical tests and data visualization were conducted with R ver 4.2.0 statistical software (R Core Team, 2021), and were considered significant at $P < 0.05$.

Results

Variations in the severity of infection on leaf surfaces

Percentages of the damaged area (D_A) of upper and lower surfaces of infected *A. sativa* leaves were similar ($P = 0.26$), and all statistical analyses returned similar results when the D_A of either leaf surface was used (data not shown); thus, we report only the statistical relationships with the D_A of the lower surface. In *R. frangula*, visual leaf damage was greater for the upper leaf surface than for the lower surface (average \pm SE of upper surface versus lower surface = $29 \pm 7\%$ versus $1.24 \pm 0.16\%$, $P < 0.001$; see Fig. 1B for a representative of sampled leaves). The correlation between the D_A of the two leaf surfaces of *R. frangula* was positive but weak ($r^2 = 0.37$, $P < 0.03$). The quantitative dependencies between damaged area and leaf physiological characteristics were somewhat stronger with D_A for the upper leaf surface than with D_A for the lower surface or with the average D_A of both leaf surfaces (data not shown). For this species, in the following, we present only the analyses conducted with the D_A for the upper leaf surface.

Effects of crown rust fungus on the photosynthetic characteristics of *A. sativa* leaves

Across the entire range of infection, there was a negative non-linear relationship between CO_2 net assimilation rate per leaf area (A_A) and the severity of *P. coronata* infection (Fig. 2A). In comparison with control leaves ($4.5 \pm 0.6 \mu\text{mol CO}_2 \text{ m}^{-2} \text{ s}^{-1}$, hereafter $\mu\text{mol m}^{-2} \text{ s}^{-1}$), the infection resulted in a 3.5-fold decrease in A_A in moderately infected leaves, but in extremely infected leaves, A_A decreased by two orders of magnitude to almost zero level ($0.042 \pm 0.020 \mu\text{mol m}^{-2} \text{ s}^{-1}$; Fig. 2A; see Supplementary Fig. S1 for comparison with control leaves of *A. sativa* grown in a controlled environment). Although the reductions in A_A due to the severity of infection were paralleled by reductions in g_w , decreased less; in extremely infected leaves,

Table 1. Average \pm SE emission rates of volatile organic compounds emitted by non-infected (control) and *P. coronata*-infected *A. sativa* leaves with different degrees of infection.

Volatile compounds	Emissions rates (pmol m ⁻² s ⁻¹)				
	Control	Mildly infected	Moderately infected	Severely infected	Extremely infected
LOX pathway compounds and derivatives					
2-Pentanone	11.3 \pm 0.3	8.8 \pm 8.8	nd	nd	nd
2-Ethyl-hexanol	9 \pm 6	454 \pm 180* a	1240 \pm 590*** b	435 \pm 170*** a	81 \pm 46*
Hexan-1-ol	6 \pm 3	30 \pm 23	nd	23.8 \pm 2.7	2.4 \pm 2.0
(E)-2-Hexenal	nd	8.6 \pm 4.8	21.7 \pm 11.8*	13 \pm 7	nd
(Z)-3-Hexen-1-ol	33 \pm 12	15 \pm 15	18 \pm 18	nd	8 \pm 8
Methyl jasmonate	nd	13.7 \pm 7.8 a	65 \pm 48 b	43 \pm 29 c	nd
Total LOX compounds	60 \pm 11	530 \pm 113* a	1344 \pm 638** a	514 \pm 209* a	92 \pm 39
Long-chain fatty acid-derived (FAD) compounds					
1-Octanol	11 \pm 6	24 \pm 24	14 \pm 14	31 \pm 14	nd
1-Nonanol	14 \pm 8 ab	28 \pm 14 a	9 \pm 9 ab	nd	1.37 \pm 1.37 b
2-Dodecanol	nd	nd	18 \pm 17	6.8 \pm 1.0	12 \pm 6
Dodecanol	15 \pm 12	29 \pm 8	98 \pm 66	71.4 \pm 28.6	nd
Undecanol	nd	35 \pm 35	685 \pm 320 a	232 \pm 93	222 \pm 68
Total FAD compounds	41 \pm 14	117 \pm 26**	824 \pm 306*** a	342 \pm 75**	311 \pm 115**
Isoprene and derivatives					
Isoprene	211 \pm 113	176 \pm 11	154 \pm 45	428 \pm 167	210 \pm 124
Methacrolein	103 \pm 11	nd	nd	nd	nd
Monoterpenes					
3-Carene	nd	nd	387 \pm 78	167 \pm 41	187 \pm 77
Eucalyptol	6 \pm 1	14 \pm 11	3 \pm 3	nd	4 \pm 2
Linalool	3.8 \pm 2.0	nd	nd	nd	nd
β -Myrcene	7 \pm 7	6.3 \pm 5.5	3 \pm 1	8 \pm 5	0.52 \pm 0.52
β -Phellandrene	7.5 \pm 2.3	nd	27.8 \pm 26.8	15 \pm 10	nd
β -Pinene	nd	50 \pm 25	17 \pm 2	17 \pm 6	nd
Total monoterpenes	24 \pm 3	70 \pm 34	438 \pm 75*** a	207 \pm 56* b	232 \pm 105* b
Sesquiterpenes					
(E)- β -Farnesene	nd	nd	60 \pm 16	14 \pm 11	nd
Longifolene	9.5 \pm 0.7	nd	nd	2.6 \pm 1.1	0.20 \pm 0.20
Total sesquiterpenes	9.5 \pm 0.7	nd	60 \pm 17* b	19 \pm 12	0.20 \pm 0.20
GGDP compounds					
6-Methyl-5-hepten-2-one	23.4 \pm 9.6	164 \pm 149	350 \pm 155*	292 \pm 68*	201 \pm 95*
Geranyl acetone	40 \pm 22	190 \pm 113	1182 \pm 171*** a	343 \pm 38*	375 \pm 95*
Total GGDP compounds	63 \pm 12	353 \pm 110*	1532 \pm 196*** b	636 \pm 74** b	577 \pm 188***
Benzenoids					
Benzaldehyde	120 \pm 46	220 \pm 110 b	272 \pm 67 b	397 \pm 94* b	120 \pm 66
Benzyl alcohol	195 \pm 55	118 \pm 60	331 \pm 112* b	159 \pm 36	19 \pm 19
Benzothiazole	27 \pm 5	71 \pm 41	87 \pm 52	44 \pm 8	nd
Total benzenoids	343 \pm 36	411 \pm 98b	691 \pm 131* b	601 \pm 59* b	139 \pm 50
Total volatiles	1140 \pm 138	1715 \pm 233* a	5695 \pm 631*** c	2984 \pm 83*** b	1748 \pm 281* a

Infection severity classes are: -10%, mildly infected; -40%, moderately infected; -60%, severely infected; -80%, extremely infected (n=3 for all infection groups). nd, not detectable.

Means were compared by the least significant difference test following one-way ANOVA. Significant differences between control and infected leaves with different degrees of infection are shown as: * P <0.05, ** P <0.01, and *** P <0.001. Different lowercase letters indicate significant differences among means of infected leaves with varying degrees of infection. In addition to the compounds reported in the table, emissions of acetaldehyde were observed from control and infected leaves, but the emission rates were not statistically different among the groups (P =0.38).

g_s was only reduced by 3.2-fold (Fig. 2B). Thus, decreases in g_s can only partly explain the reduction in A_A in the infected leaves. The infection reduced the intercellular concentration of CO₂ (C_i) in all cases, but the degree of reduction was greater at the initial stages of infection (Fig. 2C).

Photosynthetic characteristics in *P. coronata*-infected *R. frangula* leaves

In *R. frangula* leaves, A_A correlated negatively with the severity of *P. coronata* infection (Fig. 2A). A_A was reduced by 1.3-fold (in

Table 2. Average \pm SE emission rates of volatile organic compounds emitted by non-infected (control) and mildly (~10%) and severely (~60%) *P. coronata*-infected leaves of *Rhamnus frangula* ($n=3$ for all groups).

Volatile compounds	Emission rates ($\mu\text{mol m}^{-2} \text{s}^{-1}$)		
	Control	Mildly infected	Severely infected
LOX pathway compounds and derivatives			
2-Pentanone	21 \pm 20	1.0 \pm 0.5	10 \pm 7
2-Ethyl-hexanol	12 \pm 7	170 \pm 46*	47 \pm 29
Hexanal	48 \pm 5	52 \pm 18	30 \pm 17
Hexan-1-ol	4.4 \pm 4.0	40 \pm 1.0	2.6 \pm 1.0
(Z)-3-Hexen-1-ol	42 \pm 27	38 \pm 30	139 \pm 120
3-Hexen-2-one	9.0 \pm 2.8	4.3 \pm 1.8	3.8 \pm 2.3
(Z)-3-Hexen-1-ol acetate	116 \pm 32	169 \pm 140	107 \pm 70
Methyl jasmonate	2.7 \pm 0.9	2.6 \pm 0.8	0.43 \pm 0.10
Total LOX compounds	255 \pm 25	440 \pm 91	341 \pm 143
Long-chain fatty acid-derived (FAD) compounds			
1-Octanal	9 \pm 7	7 \pm 2	12 \pm 4.0
Dodecanal	22 \pm 8	14 \pm 12	9 \pm 5
Total FAD compounds	31 \pm 10	21 \pm 14	19.7 \pm 2.6
Isoprene and derivatives			
Isoprene	2100 \pm 1100	5700 \pm 2100	15 600 \pm 4500**
Methacrolein	nd	24 \pm 3	12 \pm 8
Monoterpenes			
Limonene	9 \pm 3	13 \pm 6	13 \pm 7
Camphene	1.0 \pm 0.5	1.0 \pm 0.5	3 \pm 1
Eucalyptol	3 \pm 1	22 \pm 19	1.4 \pm 0.8
Total monoterpenes	12 \pm 4	36 \pm 21	18 \pm 6
Sesquiterpenes			
Longifolene	1.5 \pm 1.1	0.42 \pm 0.08	0.13 \pm 0.08
GGDP compounds			
6-Methyl-5-hepten-2-one	109 \pm 46	67 \pm 38	82 \pm 44
Geranyl acetone	35 \pm 13	158 \pm 83	59 \pm 24
Total GGDP compounds	143 \pm 46	224 \pm 46	141 \pm 58
Benzenoids			
Benzothiazole	30 \pm 22	91 \pm 40	18 \pm 10
Benzaldehyde	52 \pm 11	55 \pm 29	135 \pm 90
Total benzenoids	70 \pm 40	126 \pm 42	153 \pm 10
Total volatiles	2758 \pm 980	6778 \pm 2290	17 092 \pm 4393

nd, not detectable. Means were compared by the least significant difference test following one-way ANOVA. Significant differences between control and infected leaves with different degrees of infection are shown as: * $P<0.05$, ** $P<0.01$, and *** $P<0.001$. In addition to the compounds reported in the table, emissions of acetaldehyde were observed from control and infected leaves, but the emission rates were not statistically different among the groups ($P>0.05$).

comparison with $6.67 \pm 0.2 \mu\text{mol m}^{-2} \text{s}^{-1}$ in control, $P<0.05$) in leaves with ~60% damaged area. g_s did not change, but C_i changed slightly with infection (Fig. 2B, C).

Leaf dry mass per unit area and implication for changes in net assimilation rates

In *A. sativa*, LMA did not decrease in mildly infected leaves ($48 \pm 6 \text{ g m}^{-2}$ in control versus $37 \pm 4 \text{ g m}^{-2}$ in mildly infected leaves, $P=0.07$), but decreased by 1.6-fold (in comparison with control, $P<0.01$) in infected leaves with moderate to extreme infection (Fig. 3). Net assimilation rate per dry mass ($A_M=A_A/LMA$) was negatively correlated with the severity of infection ($r^2=0.76$, $P<0.001$). A_M decreased by 54-fold, from 92 ± 16

$\text{nmol g}^{-1} \text{s}^{-1}$ in control leaves to $1.7 \pm 1.4 \text{ nmol g}^{-1} \text{s}^{-1}$ in extremely infected leaves. Thus, the contribution of the infection-dependent reduction in LMA to the decrease in A_A was relatively small compared with the total reduction in A_A (107-fold), implying that net assimilation rates primarily decreased due to reductions in A_M . In *R. frangula*, LMA was similar for control and infected leaves ($30 \pm 2 \text{ g m}^{-2}$ in control versus $29 \pm 1 \text{ g m}^{-2}$ in infected leaves, $P=0.85$).

Dependencies of leaf C, N, and P on the severity of infection

In *A. sativa* leaves, C_M increased in infected leaves (Fig. 4A), N_M decreased with increasing severity of infection (Fig. 4B),

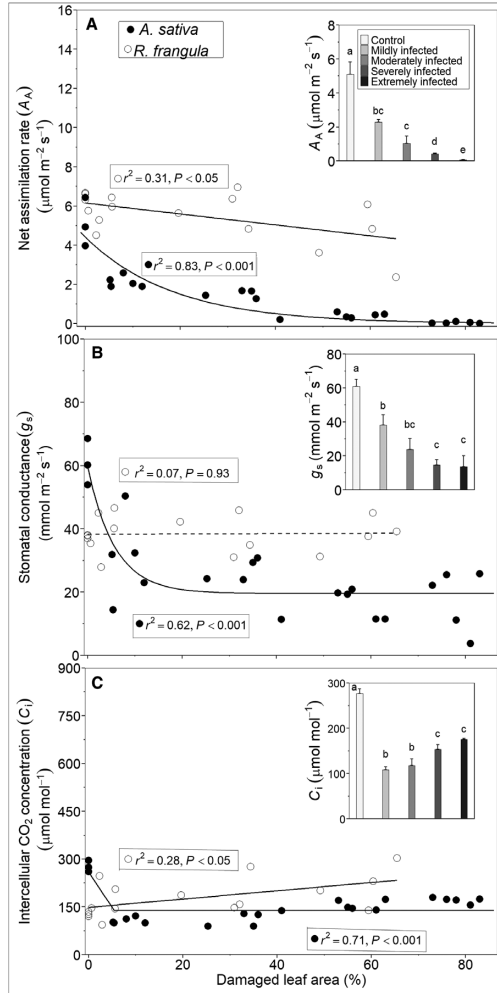


Fig. 2. Relationships of leaf net assimilation rate (A_A , A), stomatal conductance to water vapor (g_s , B), and intercellular CO_2 concentration (C_i , C) with the severity of crown rust (*P. coronata*) infection in the primary host *A. sativa* (filled circles) and the alternate host *R. frangula* (open circles). The degree of leaf infection was characterized by the percentage of the infected area (D_A) of the lower leaf surface for *A. sativa* and upper surface for *R. frangula*. Data were fitted by non-linear regressions in the form: $y=4.41(e^{-0.054x})$ (A), $y=19.6 + 40.1(0.84^x)$ (B), $y=117 \times (x-5.4) \times (x-5.4)$ (C) for *A. sativa*, and by linear regressions

in the form: $y=6.15-0.028x$ (A), $y=38.3+0.005x$ (B), $y=149+1.3x$ (C) for *R. frangula*. Altogether, 23 *A. sativa* leaves (three non-infected control leaves and 20 infected leaves) and 15 *R. frangula* leaves (three non-infected control leaves and 12 infected leaves) with different degrees of crown rust infection were measured (see Fig. 1A, B for photos of sampled leaves with different degrees of infection). The measurements were conducted at an ambient CO₂ concentration of 400 $\mu\text{mol mol}^{-1}$ of air, a leaf temperature of 25 °C, a PPFD of 800 $\mu\text{mol m}^{-2} \text{s}^{-1}$, and a vapor pressure deficit between the leaf and the atmosphere of 1.7 kPa. The insets in (A–C) show the average \pm SE ($n=3$ for each group) of A_n , g_n , and C_n in non-infected control (0% D_A), mildly infected (~10% D_A), moderately infected (~40% D_A), severely infected (~60% D_A), and extremely infected (~80% D_A) *A. sativa* leaves. For each group, data points that were nearest to the level of infection were selected. Averages were pairwise compared by least significant difference tests following one-way ANOVA. Different lowercase letters indicate significant differences among infected leaves with different degrees of infection.

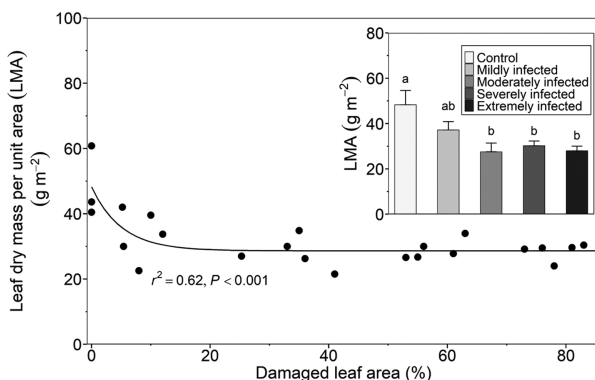


Fig. 3. Leaf dry mass per unit area (LMA) in relation to the severity of *P. coronata* infection in *A. sativa* (see Fig. 1A for images of representative infected leaves). The severity of leaf infection was quantified by the percentage of the infected area (D_A) of the lower leaf surface. Data were fitted by a non-linear regression: $y=28.64+19.6(0.9)^x$. The inset shows the average \pm SE of LMA of non-infected control, mildly infected (~10% D_A), moderately infected (~40% D_A), severely infected (~60% D_A), and extremely infected (~80% D_A) *A. sativa* leaves. Statistical analysis and data presentation are as in Fig. 2 inset.

and D_M decreased in the infected *A. sativa* leaves (Fig. 4C). In *R. frangula* leaves, C_M (average \pm SE of control versus severely infected leaves of $44.16 \pm 0.04\%$ versus $44.5 \pm 1.0\%$, $P=0.71$ for the difference between means), N_M ($3.50 \pm 0.44\%$ versus $3.95 \pm 0.03\%$, $P=0.36$), and P_M ($0.27 \pm 0.01\%$ versus $0.38 \pm 0.06\%$, $P=0.20$) were not affected by *P. coronata* infection.

Changes in volatile emissions in leaves infected with *P. coronata*

Non-infected leaves of *A. sativa* (Table 1) and *R. frangula* (Table 2) each emitted 20 volatile compounds belonging to different volatile classes including LOX pathway compounds, long-chain saturated fatty acid-derived (FAD) compounds, terpenoids (isoprene, mono- and sesquiterpenes), benzenoids, and carotenoid breakdown products [geranylgeranyl diphosphate pathway (GGDP) volatiles]. In control leaves, the emission rates of most volatiles were close to the level of detection (Tables 1, 2) except for moderately high emissions of benzaldehyde and

benzyl alcohol in *A. sativa* (Table 1), and constitutive isoprene emissions in *R. frangula* (Table 2).

Puccinia coronata infection had a strong impact on volatile emissions of *A. sativa* (Table 1); the response of emissions to *P. coronata* infection differed for mild to moderate infection (0–40% D_A) and moderate to severe infection (40–80% D_A). The elicitation of LOX compounds, FAD compounds, GGDP volatiles, and benzenoids started during mild infection, but the elicitation of mono- and sesquiterpenes began during moderate infection (Table 1). Overall, the induced emissions reached the highest level during moderate infection. Compared with control leaves, LOX emissions increased by 16-fold, FAD compounds by 22-fold, monoterpenes by 20-fold, and GGDP by 25-fold during moderate infection (Table 1; Fig. 5). LOX pathway products were quantitatively the largest volatile class emitted during moderate infection (Table 1). For 0–40% severity of infection, emissions of all the detected volatile classes correlated positively with the severity of infection (Fig. 6A–F). With increasing severity of infection, for 40–80% D_A , emissions of all detected volatile classes correlated negatively with

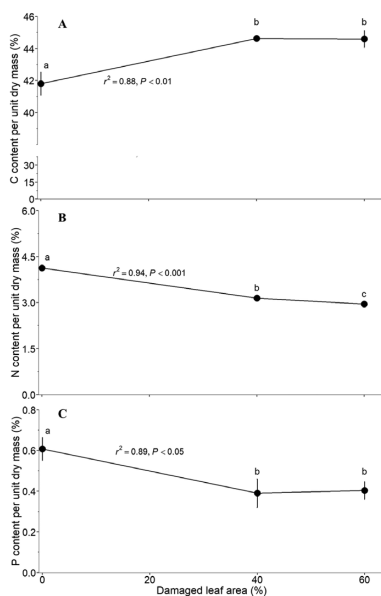


Fig. 4. Changes in carbon (A), nitrogen (B), and phosphorus (C) contents per dry mass in non-infected control, moderately infected (~40% damaged leaf area, D_A), and severely infected (~60% D_A) *A. sativa* leaves. Leaves with an approximately similar severity of infection were pooled for chemical analyses (see Fig. 1A for images of sampled leaves with varying degrees of infection). Each data point is the average \pm SE of three independent replicates. Statistical analysis and data presentation are as in Fig. 2 inset.

D_A (Fig. 6A–F). Once the severity of infection reached ~80%, the emissions of LOX pathway compounds and benzenoids decreased to the level in control leaves, whereas sesquiterpene emissions decreased to below the level of detection (Table 1). The emission rates of GGDP pathway compounds, FAD compounds, and monoterpenes were still significantly higher in extremely infected *A. sativa* leaves than in control leaves (Table 1). The constitutive emissions of methacrolein were below the level of detection in all the infected *A. sativa* leaves with different degrees of damage (Table 1).

Puccinia coronata infection had moderate effects on the volatile emissions in *R. frangula*. The most conspicuous response was the major enhancement of emissions of isoprene in leaves with an ~60% degree of infection, and the induction of methacrolein in all the infected leaves with different degrees of infection (Table 2). In addition, the emissions of the LOX

compound, 2-ethyl-hexanol, were elicited in *R. frangula* leaves with 5–20% D_A (Table 2).

The species comparisons demonstrated that at the given level of infection, emissions of most volatiles responded much more strongly to the infection in *A. sativa* than in *R. frangula* (Fig. 6). Only LOX emissions at the highest infection level were similar among species (Fig. 6A), reflecting the reduction in LOX emissions at the most severe infection level in *A. sativa* (Fig. 5A). In addition, isoprene emissions were much higher in the constitutive isoprene emitter *R. frangula* (cf. Tables 1, 2).

PCA demonstrated that volatile blends in infected *A. sativa* leaves were separated from volatile blends in non-infected *A. sativa* and *R. frangula* leaves irrespective of infection (Fig. 7; PERMANOVA, $P < 0.001$; Bray–Curtis $R = 0.86$). Emissions of MeJA, (*E*)-2-hexenal, 2-ethyl-hexanol, dodecanal, undecanal, β -pinene, 3-carene, (*E*)- β -farnesene, GGDP compounds, benzaldehyde, and benzothiazole distinguished emissions in infected *A. sativa* leaves (Fig. 7). Infected *R. frangula* leaves were not separated from non-infected *R. frangula* leaves (Fig. 7; PERMANOVA, $P = 0.10$; Bray–Curtis $R = 0.36$) and were characterized by emissions of hexanal, (*Z*)-3-hexen-1-ol-acetate, isoprene, limonene, and camphene.

Discussion

Variations in the severity of infection on leaf surfaces of *R. frangula*

In *R. frangula*, D_A was greater for upper leaf surfaces, and the D_A of the two leaf surfaces was weakly correlated. Pycniospores are formed at the spermatial stage, whereas aeciospores germinate subsequently after plasmogamy (Nazareno et al., 2018). Thus, it is probable that at the given severity of infection, aeciospores have not germinated enough to quantitatively compare with pycniospores.

Patterns of reductions of photosynthesis in infected leaves

Puccinia coronata biotrophy (Scholes and Rolfe, 1996) results in independent localized areas of lesions that can expand and invoke heterogeneous changes in photosynthetic characteristics. We observed that *P. coronata* infection resulted in reductions in A_A with increasing severity of infection (Fig. 2A). A reduction in A_A is a general physiological response to biotrophic fungal infection (e.g. Toome et al., 2010; Gortari et al., 2018). Often, the pathogen-dependent decrease in A_A is commensurate with the loss of leaf photosynthetic capacity in the infected region, reflecting hypersensitive responses including programmed cell death and necrosis (Kolmer, 2013; Jorgensen et al., 2017), whereas A_A remains stable in the non-infected area (Zhao et al., 2011; Niinemets et al., 2013). Thus, the severity of infection can exhibit a strong relationship with reductions in A_A (Niinemets et al., 2013). Cellular-level

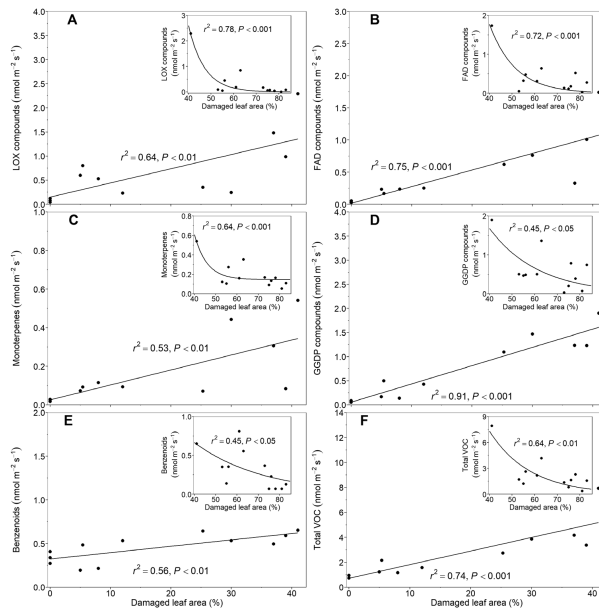


Fig. 5. Relationships between the severity of crown rust infection and emissions of lipoxygenase pathway (LOX) compounds (A), long-chain fatty acid-derived (FAD) compounds (B), monoterpenes (C), geranylgeranyl diphosphate (GGDP) pathway compounds (carotenoid breakdown products, D), benzenoids (E), and total VOCs (F) in *A. sativa* leaves. The degree of leaf infection was determined by the percentage of the infected area (D_A) of the lower leaf surface. The main panels demonstrate the relationships for the infection severity range of 0–40% ($n=12$) and the insets for the infection severity range of 40–80% ($n=12$, see Fig. 1A, B for representative images of leaves with different degrees of infection). Data were fitted by linear and non-linear regressions and the corresponding regression equations are: $y=0.15 + 0.029x$ (A), $y=741.6(e^{-1.14x})$ (inset in A), $y=0.018 + 0.026x$ (B), $y=59.3(e^{-0.039x})$ (inset in B), $y=0.026 + 0.06x$ (C), $y=0.15 + 402.45(e^{-0.17x})$ (inset in C), $y=0.056 + 0.038x$ (D), $y=10.9(e^{-0.048x})$ (inset in D), $y=0.32 + 0.007x$ (E), $y=2.28(e^{-0.031x})$ (inset in E), $y=0.73 + 0.11x$ (F), and $y=68.15(e^{-0.056x})$ (inset in F).

experiments have demonstrated that *P. coronata* infection initiates reductions in A_A by reducing the efficiency of photosynthesis (Φ_{II}) exclusively in the infected area; but, as the lesions expand, photosynthetic activity is reduced throughout the leaf (Scholes and Rolfe, 1996; Gortari *et al.*, 2018) due to stomatal limitations, nutrient resorption, biomass loss, and alteration of sink–source relationships as discussed below. As our study demonstrates, the host species strongly vary in the extent of decrease of photosynthetic activity at the given level of infection (Fig. 2A). In particular, the primary host *A. sativa* responded much more strongly to *P. coronata* infection than the alternate host *R. frangula* due to multiple differences in physiological, structural, and chemical responses to the pathogen.

Impact of rust infections on stomatal limitations of photosynthesis

Reductions in photosynthetic activity of fungal-infected leaves can be due to diffusive and biochemical inhibitions linked to reductions in mesophyll conductance, and activities of Rubisco and the photosynthetic electron transport rate (Toome *et al.*, 2010; Nogueira Júnior *et al.*, 2017; Kännaste *et al.*, 2023). Similar to *Populus deltoides* infected with *Melampsora medusa* (Gortari *et al.*, 2018), *Salix burjatica* × *S. dasyclados* infected with *Melampsora epitea* (Toome *et al.*, 2010), and *Saccharum* spp. hybrids infected with *Puccinia kuehni* (Zhao *et al.*, 2011), the reductions in A_A in *A. sativa* were associated with reductions in g_s (Fig. 2B).

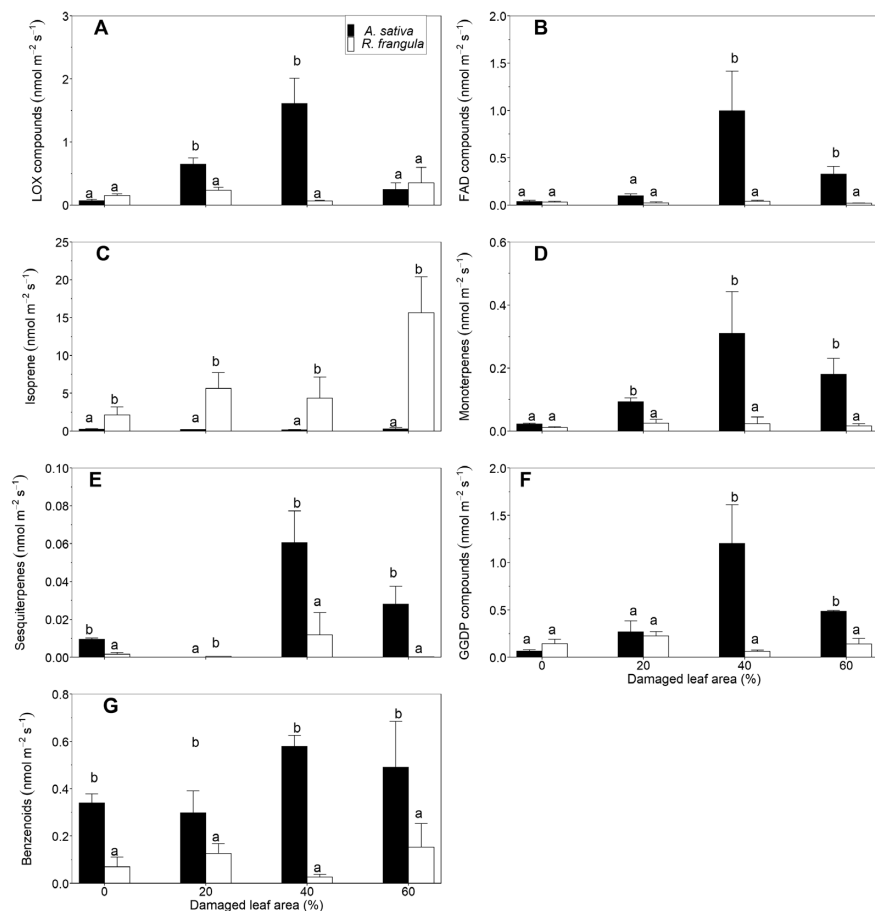


Fig. 6. Species comparisons of total emission rates of lipoxygenase pathway (LOX) compounds (A), long-chain fatty acid-derived (FAD) compounds (B), isoprene (C), monoterpenes (D), sesquiterpenes (E), geranylgeranyl diphosphate (GGDP) pathway compounds (carotenoid breakdown products, F), and benzenoids (G) in non-infected control, mildly infected (~10% damaged area, D_1), moderately infected (~40% D_2), and severely infected (~60% D_3) leaves of *A. sativa* (open bar) and *R. frangula* (filled bar). The severity of leaf infection was characterized by the D_n of lower leaf surface for *A. sativa* and upper surface for *R. frangula* (see Fig. 1A, B for photos of sampled leaves with different degrees of infection). Each data point is the average \pm SE of three independent replicates. Averages at each level of infection severity were compared by an independent-samples *t*-test. Different lowercase letters indicate significant differences between species.

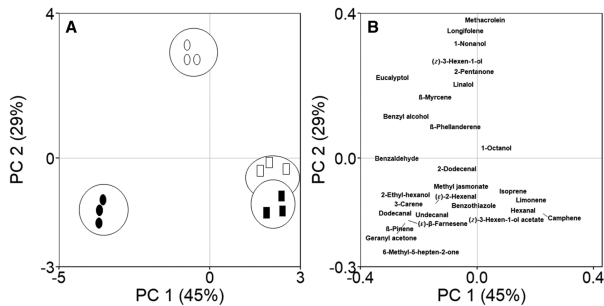


Fig. 7. Score plot (A) and loading plot (B) derived from principal component analysis (PCA) based on the emissions of volatiles (see Tables 1 and 2 for the emission rates) in non-infected and infected leaves (40% severity of infection) of *A. sativa* and *R. frangula*. The severity of leaf infection was characterized by the percentage of the infected area of the lower leaf surface for *A. sativa* and the upper surface for *R. frangula*. Symbols in the score plot represent individual leaves of non-infected *A. sativa* (open circles), infected *A. sativa* (filled circles), non-infected *R. frangula* (open squares), and infected *R. frangula* (filled squares). The impact of the individual compounds shown in the loading plot increases with increasing distance from the origin of the coordinate system. The axis labels show the variation explained by the principal components (PC1 and PC2).

Given that, in general, g_s scales positively with leaf photosynthetic activity (Wong *et al.*, 1979), the negative relationship between g_s and the severity of infection (Fig. 2B) might indicate an overall reduction in leaf physiological activity. However, the decrease in g_s was also associated with reductions in C_i across infected *A. sativa* leaves (Fig. 2C), indicating that the decrease in g_s indeed partly suppressed A_A (Song *et al.*, 2014). This might reflect the disruption of water flow through leaf veins to the outer surfaces of substomatal cavities due to fungal hyphae (Herre *et al.*, 2005). Alternatively, infected plants often close stomata to further reduce the entry of pathogen propagules through stomata (Niks and Rubiales 2002; Grimmer *et al.*, 2012), especially in monocot grass species which have subsidiary cells adjacent to the guard of cells that facilitate stomatal closure (Pitaloka *et al.*, 2021). Such interruptions can ultimately suppress photosynthesis at both infected and non-infected sites (Nogueira Júnior *et al.*, 2017; Ding *et al.*, 2018; Gortari *et al.*, 2018).

Differently from moderately severe infection, increases in C_i in heavily infected leaves with strongly reduced A_A (Fig. 2C) indicate that the impact of the decrease of photosynthetic capacity on A_A was greater than the reduction in g_s (Zhao *et al.*, 2011; Niinemets, 2016). In addition, in the alternate host *R. frangula*, g_s was not correlated with infection severity and C_i tended to increase with increasing infection severity (Fig. 2C). These responses indicate a loss of coupling between stomatal conductance and photosynthesis, and a decrease in leaf water use efficiency as observed with plants infected by different rusts and several other pathogens (Grimmer *et al.*, 2012; Jiang *et al.*, 2016).

We did not quantify the effect of transplantation shock on gas exchange characteristics. We are aware that some sensitive

species can respond to transplantation by partially closing stomata; however, in our experiment, transplanted control plants had similar gas exchange values to control plants grown under controlled conditions (cf. Fig. 2 and Supplementary Fig. S1). Nevertheless, the stomatal closure we observed is systematic and may not influence our conclusions.

Reductions of photosynthesis and relationship with decreases in nutrients and biomass

Localized cellular suicide and necrosis can lead to the resorption of nutrients and soluble carbon from damaged leaf regions, analogous to changes occurring during leaf senescence (Munné-Bosch and Alegre 2004; Tavernier *et al.*, 2007). Additionally, biotrophic fungi absorb nutrients from the mesophyll of infected leaves via haustoria (Staples, 2001). The decrease in N_M and P_M in infected leaves of *A. sativa* (Fig. 4B, C) is consistent with the resorption of nutrients. Reductions in nitrogen concentration indicate decreases in photosynthetic capacity more than reductions in other macronutrients (He *et al.*, 2015; Lei *et al.*, 2021). Decreases in nitrogen concentrations can lead to a rapid fall in maximum Rubisco activity, particularly in C_3 plants, as Rubisco is the principal enzyme for CO_2 fixation and contains a large fraction of leaf N (Makino, 2013; Veresoglou *et al.*, 2013).

Increases in C_M in infected *A. sativa* leaves (Fig. 4A) suggested the accumulation of secondary compounds with high carbon content such as phenolics, such as the lignin in cell walls that enhances leaf robustness (Kovacic *et al.*, 2007; Denness *et al.*, 2011). In addition, increases in carbon can be associated with fungal consumption of cell wall polysaccharides and non-structural carbohydrates that have a lower C content

than the leaves on average (Niinemets *et al.*, 2007). Fungal consumption of cell wall components can further lead to reductions in LMA (Niinemets, 1999; Poorter *et al.*, 2009) as was observed in rust-infected *A. sativa* leaves (Fig. 3). Indeed, infection severity-dependent reduction in photosynthetic biomass significantly contributed to the reduction in A_A in *A. sativa*, although the contribution of A_M was greater ($A_A = A_M/LMA$).

Differently from *A. sativa*, N, P and C contents and LMA were unaffected by rust infection in *R. frangula*, further suggesting that this species was more sensitive to the infection than the primary host *A. sativa*. Overall, the deciduous temperate broad-leaved species form foliage at the beginning of the season, and foliage nutrient contents and LMA are stable throughout the season until the onset of leaf senescence (Niinemets *et al.*, 2004). As our study demonstrates, even major rust infections did not result in the elicitation of nutrient resorption and loss of biomass in *R. frangula*.

Puccinia coronata-induced emissions of lipoxygenase-derived compounds: green leaf volatiles and methyl jasmonate

The biosynthesis of jasmonates and green leaf volatiles utilizes α -linolenic acid derived from the LOX pathway upon photosynthesis (Feussner and Wasternack, 2002; Wasternack and Hause, 2013). The release of jasmonates can indicate the activation of defense signaling pathways leading to systemic defense responses including hypersensitive responses, and elicitation of LOX pathway products and terpenoids (Hirao *et al.*, 2012; Li *et al.*, 2019). The emission of LOX pathway-derived products is a universal response to stresses (Toome *et al.*, 2010; Liu *et al.*, 2021; Sulaiman *et al.*, 2021). Several LOXs are constitutively active in the foliage of plants and, contingent on the availability of substrate, these enzymes rapidly elicit LOX compound emissions upon any stress exposure that is associated with cellular damage or oxidative burst (Feussner and Wasternack, 2002; Arneith and Niinemets, 2010; Copolovici *et al.*, 2011). In *A. sativa*, *P. coronata*-elicited LOX pathway emissions scaled during mild to moderate infection (Fig. 5A; Table 1), suggesting the accumulation of oxidative stress, whereas, in *R. frangula*, LOX product emissions were only elicited to a minor degree (Table 2), indicating less oxidative damage in the alternate host. Furthermore, LOX compound emissions in infected *A. sativa* leaves were accompanied by the release of FAD compounds (Fig. 5A, B), emissions of which have been associated with oxidative stress (Hu *et al.*, 2009, 2011; Kännaste *et al.*, 2023).

Inductions of terpenoid emissions by crown rust infection

Consistent with previous reports (Karl *et al.*, 2009), our results showed that *A. sativa* is a low isoprene emitter (Table 1). We also observed low emissions of constitutive isoprene in *R. frangula* (Table 2), similar to other emitter species from the family

Rhamnaceae, such as *Ziziphium nummularia* (Singh *et al.*, 2008) and *Ziziphium jujuba* (Varshney and Singh 2003). The biosynthesis of isoprene and monoterpenes occurs via the MEP/DOXP pathway utilizing geranyl diphosphate as a precursor, whereas sesquiterpenes are synthesized in main part via the MVA pathway (Niinemets *et al.*, 2002; Nogués *et al.*, 2006). Enhanced mono- and sesquiterpene emissions are ubiquitous responses to pathogen infection (Arneith and Niinemets, 2010; Niinemets *et al.*, 2013).

Differently from mono- and sesquiterpenes, isoprene emission is mostly associated with abiotic stresses (Niinemets *et al.*, 2013). Biotic stresses often decrease constitutive isoprene emissions. For example, in *Populus balsamifera* infected with the rust fungus *Melampsora larici-populina* (Jiang *et al.*, 2016) and in *Quercus robur* infected with oak powdery mildew (*Erysiphe alphitoides*) (Copolovici *et al.*, 2014), terpenoid emissions were elicited, but constitutive isoprene emissions were reduced. In the current study, *P. coronata* infection suppressed the emissions of the isoprene derivative methacrolein, and enhanced the emissions of mono- and sesquiterpenes in *A. sativa* (Table 1); but, surprisingly, in *R. frangula* leaves, it enhanced the emissions of constitutive isoprene emissions and induced the emissions of methacrolein (Table 2), which may suggest differential expression of terpenoid pathway genes (Arimura *et al.*, 2004). This is plausible given that isoprene and monoterpenes rely on the same substrate pool, but the substrate affinity of monoterpene synthase is much greater (Rasulov *et al.*, 2014; Niinemets *et al.*, 2021). This suggests that monoterpene synthesis was elicited much more weakly than isoprene synthesis in rust-infected *R. frangula* leaves.

Crown rust infection induced the emissions of benzenoids and carotenoid breakdown products in *A. sativa* leaves

Pathogen infection can trigger the emissions of various benzenoids from the shikimate pathway (Dudareva *et al.*, 2013). MeSA is the quintessential benzenoid compound elicited by biotrophic pathogen attack (Niinemets *et al.*, 2013). In *A. sativa*, *P. coronata* infection elicited the emissions of benzyl alcohol, benzaldehyde, and benzothiazole, but not of MeSA (Table 1). Different fungal infections can elicit emission of different benzenoids; for example, in *Q. robur*, *E. alphitoides* infection elicited benzaldehyde and MeSA emissions (Copolovici *et al.*, 2014), whereas infection by *Neovotenus* spp. and *Cynips* spp. elicited benzaldehyde and benzothiazole emissions (Jiang *et al.*, 2018). Moreover, the biosynthesis of MeSA in plants involves strenuous processes (Li *et al.*, 2019).

The emissions of chloroplast-synthesized GGDP compounds can reflect carotenoid turnover (Aharoni *et al.*, 2005). Thus, the scaling of GGDP compound emissions during mild to moderate infection in *A. sativa* (Fig. 5D) indicates increases in chlorophyll loss and carotenoid breakdown, consistent with the spread of the characteristic variegated appearance of surfaces of infected leaves (Josse *et al.*, 2000; Nisar *et al.*, 2015).

Reductions of stress volatile emissions in severely infected *A. sativa* leaves

Stress and signaling VOC emissions scaled positively with the degree of infection in *A. sativa*; however, in contrast to previous studies (Copolovici *et al.*, 2014; Jiang *et al.*, 2016, 2018), the emissions leveled down during severe infections and were no longer quantitatively dependent on infection severity (Fig. 5A–F), reflecting substrate limitations due to reduced photosynthesis and a decline in overall physiological activity resulting from the spread of dead tissue (Jiang *et al.*, 2017).

Differences in physiological responses to *P. coronata* infection in the primary and alternate host

The physiological responses of host species are determined by the complex interaction between the fungus and the host species (Ponzio *et al.*, 2016). The degree of impact on physiological processes in a given host species can reflect the pressure exerted by the parasite (Kännaste *et al.*, 2023). We hypothesized that fungal stress-elicited changes in physiological processes are particularly more pronounced in the primary host. Our gas exchange, carbon and nutrient, and biomass data collectively showed the relative photosynthetic tolerance of *R. frangula* leaf upon *P. coronata* infection. Furthermore, emissions of most stress volatiles were much higher in *A. sativa* leaves (Fig. 6A–G; cf. Tables 1 and 2), and scaled positively with the severity of infection (Fig. 5A–F), indicating severe fungal stress. In *R. frangula*, isoprene was the distinctive elicited volatile, whereas a much richer blend of stress volatiles was elicited in *A. sativa* (Fig. 7), reflecting stress-dependent activation of different volatile biosynthesis pathways (Niinemets, 2010). Most of the characteristic volatiles in infected *A. sativa* (Fig. 7) have been associated with severe stress. For example, severe fungal stress resulted in the elicitation of 3-carene, β -pinene, geranyl acetone, benzaldehyde, and benzothiazole in *Q. robur* (Copolovici *et al.*, 2014; Jiang *et al.*, 2016, 2018). Stress-elicited emissions of (*E*)- β -farnesene, 2-ethyl-hexanol, and (*E*)-2-hexenal have been demonstrated to be sensitive indicators of oxidative damage (Sobhy *et al.*, 2017; Bison *et al.*, 2018). Altogether, our VOC data suggest that *P. coronata* infection resulted in much higher emissions of stress volatiles in *A. sativa* than in *R. frangula*.

Previous studies have shown that alternate hosts are equipped with certain resistance genes providing partial resistance to rust pathogen (Bettgenhauser *et al.*, 2014; Lorrain *et al.*, 2018). Evolutionarily, an obligate biotrophic fungus requires continuous interaction with a host species for survival, thus, as expected, exerting a lower stress pressure than necrotrophic or hemibiotrophic pathogens (Bettgenhauser *et al.*, 2014; Lorrain *et al.*, 2019). However, changes in physiological processes and loss of nutrients and leaf biomass in *P. coronata*-infected *A. sativa* leaves quantitatively resemble those induced by hemibiotrophic pathogens, while the impact on the alternate host *R. frangula* is consistent with the biotrophic behavior of the pathogen.

Conclusions

We quantified the impact of *P. coronata* on leaf photosynthetic characteristics and VOC responses in the primary host *A. sativa* and the alternate host *R. frangula* at different levels of infection severity and demonstrated how different physiological parameters (g, carbon and nutrients contents, and biomass) associated with reductions in photosynthesis quantitatively change with the severity of infection. Our results demonstrated that foliage photosynthesis in *A. sativa* decreased with increasing severity of infection, >100-fold at the highest infection severity, and the reduction was primarily due to non-stomatal factors. Comparatively, in *R. frangula*, *P. coronata* affected photosynthetic capacity less, indicating a greater photosynthetic tolerance of *R. frangula*. In *A. sativa*, *P. coronata* infection induced the emission of a rich blend of stress volatiles that initially scaled positively with infection severity, but the emissions decreased when infection became severe, indicating an overall reduction in leaf physiological activity. In *R. frangula*, the infection also induced stress volatile release, but to a much lower degree than in *A. sativa*. However, the infection strongly enhanced constitutive isoprene emissions. Thus, the pathogen elicited varying biochemical responses in the two hosts.

We argue that the quantitative relationship between physiological processes and the severity of infection, as observed in the current study, provides a basis for the analytical understanding of pathogen stress responses. Our volatile results provide viable information for diagnosing crown rust infection using characteristic volatile fingerprints. From an atmospheric viewpoint, stress VOCs, such as benzenoids and isoprenoids that are highly reactive, may contribute to the formation of secondary organic aerosols capable of affecting climatic processes and overall air quality. Thus, the results of leaf-level pathogen-elicited VOC responses can further be incorporated as key input characteristics for regional and global trace gas and reactive carbon emission models.

Supplementary data

The following supplementary data are available at [JXB online](#).

Fig. S1. Data of gas exchange characteristics for non-infected *A. sativa* grown in a controlled environment.

Author contributions

ER-P and ÜN: conceptualization; EK, ER-P, HYS, and ÜN: planning and design; ER-P and HYS: conducting the field work; EK, ER-P, HYS, and ÜN: performing the experiment; HYS: data analysis and writing. All co-authors read, edited, and approved the final manuscript.

Conflict of interest

The authors declare no conflict of interest.

Funding

This research was funded by the European Commission through the European Research Council (advanced grant 322603, SIP-VOL+), the European Union Regional Development Fund within the framework of the Centre of Excellence EcolChange (2014–2020.4.01.15-0002), and the Estonian University of Life Sciences (base funding P190259PKTT). The equipment used in the study was partly purchased from funding by the European Union Regional Development Fund (AnaEE Estonia, 2014–2020.4.01.20-0285 and the project 'Plant Biology Infrastructure-TAIM', 2014–2020.4.01.20-0282).

Data availability

The dataset used in this study is available from the corresponding author on reasonable request.

References

- Aharoni A, Jones MA, Bouwmeester HJ. 2005. Volatile science? Metabolic engineering of terpenoids in plants. *Trends in Plant Science* **10**, 594–602.
- Araya T, Noguchi K, Terashima I. 2006. Effects of carbohydrate accumulation on photosynthesis differ between sink and source leaves of *Phaseolus vulgaris* L. *Plant and Cell Physiology* **47**, 644–652.
- Arimura G, Huber DPW, Bohlmann J. 2004. Forest tent caterpillars (*Malacosoma disstria*) induce local and systemic diurnal emissions of terpenoid volatiles in hybrid poplar (*Populus trichocarpa* x *deltooides*): cDNA cloning, functional characterization, and patterns of gene expression of (-)-germacrene α synthase, PtDTPS1. *The Plant Journal* **37**, 603–616.
- Arneth A, Niinemets Ü. 2010. Induced BVOCs: how to bug our models? *Trends in Plant Science* **15**, 118–125.
- Attaran E, Zeier TE, Griebel T, Zeier J. 2009. Methyl salicylate production and jasmonate signaling are not essential for systemic acquired resistance in *Arabidopsis*. *The Plant Cell* **21**, 954–971.
- Berger S, Sinha AK, Roitsch T. 2007. Plant physiology meets phytopathology: plant primary metabolism and plant–pathogen interactions. *Journal of Experimental Botany* **58**, 4019–4026.
- Berlin A, Wallenhammar AC, Andersson B. 2018. Population differentiation of *Puccinia coronata* between hosts—implications for the epidemiology of oat crown rust. *European Journal of Plant Pathology* **152**, 901–907.
- Bettgenhauser J, Gilbert B, Ayliffe M, Moscou MJ. 2014. Nonhost resistance to rust pathogens—a continuation of continua. *Frontiers in Plant Science* **5**, 664.
- Bison JV, Cardoso-Gustavson P, de Moraes RM, da Silva Pedrosa G, Cruz LS, Freschi L, de Souza SR. 2018. Volatile organic compounds and nitric oxide as responses of a Brazilian tropical species to ozone: the emission profile of young and mature leaves. *Environmental Science and Pollution Research* **25**, 3840–3848.
- Brilli F, Ciccioli P, Frattoni M, Prestinini M, Spanedda AF, Loreto F. 2009. Constitutive and herbivore-induced monoterpenes emitted by *Populus x euroamericana* leaves are key volatiles that orient *Chrysomela populi* beetles. *Plant, Cell & Environment* **32**, 542–552.
- Chauvin A, Caldelari D, Wolfender JL, Farmer EE. 2013. Four 13-lipoxygenases contribute to rapid jasmonate synthesis in wounded *Arabidopsis thaliana* leaves: a role for lipoxygenase 6 in responses to long-distance wound signals. *New Phytologist* **197**, 566–575.
- Chong J, Zegzey T. 2004. Physiologic specialization of *Puccinia coronata* f. sp. *avenae*, the cause of oat crown rust, in Canada from 1999 to 2001. *Canadian Journal of Plant Pathology* **26**, 97–108.
- Copolovici L, Kännaste A, Pazouki L, Niinemets Ü. 2012. Emissions of green leaf volatiles and terpenoids from *Solanum lycopersicum* are quantitatively related to the severity of cold and heat shock treatments. *Journal of Plant Physiology* **169**, 664–672.
- Copolovici L, Kännaste A, Remmel T, Vislap V, Niinemets Ü. 2011. Volatile emissions from *Alnus glutinosa* induced by herbivory are quantitatively related to the extent of damage. *Journal of Chemical Ecology* **37**, 18–28.
- Copolovici L, Niinemets Ü. 2010. Flooding induced emissions of volatile signalling compounds in three tree species with differing waterlogging tolerance. *Plant, Cell & Environment* **33**, 1562–1594.
- Copolovici L, Väärtnou F, Estrada MP, Niinemets Ü. 2014. Oak powdery mildew (*Erysiphe alphitoides*)-induced volatile emissions scale with the degree of infection in *Quercus robur*. *Tree Physiology* **34**, 1399–1410.
- Dani KS, Jamie IM, Prentice IC, Atwell BJ. 2014. Evolution of isoprene emission capacity in plants. *Trends in Plant Science* **19**, 439–446.
- Darshane HLC, Ren H, Ahmed N, Zhang Z-F, Liu YH, Liu TX. 2017. Volatile-mediated attraction of greenhouse whitefly *Trialeurodes vaporariorum* to tomato and eggplant. *Frontiers in Plant Science* **8**, 1285.
- Denness L, McKenna JF, Segonzac C, et al. 2011. Cell wall damage-induced lignin biosynthesis is regulated by a reactive oxygen species- and jasmonic acid-dependent process in *Arabidopsis*. *Plant Physiology* **158**, 1364–1374.
- Ding L, Lu Z, Gao L, Guo S, Shen Q. 2018. Is nitrogen a key determinant of water transport and photosynthesis in higher plants upon drought stress? *Frontiers in Plant Science* **9**, 1143.
- Dracatos PM, Haghdoust R, Singh D, Park RF. 2018. Exploring and exploiting the boundaries of host specificity using the cereal rust and mildew models. *New Phytologist* **218**, 453–462.
- Dudareva N, Klempien A, Muhlemann JK, Kaplan I. 2013. Biosynthesis, function and metabolic engineering of plant volatile organic compounds. *New Phytologist* **199**, 16–32.
- Feussner I, Wasternack C. 2002. The lipoxygenase pathway. *Annual Review of Plant Biology* **53**, 285–297.
- Gális I, Gaquerel E, Pandey SP, Baldwin IT. 2009. Molecular mechanisms underlying plant memory in JA-mediated defence responses. *Plant, Cell & Environment* **32**, 617–627.
- Gortari F, Guiamet JJ, Graciano C. 2018. Plant–pathogen interactions: leaf physiology alterations in poplars infected with rust (*Melampsora medusae*). *Tree Physiology* **38**, 925–935.
- Greenberg JT, Yao N. 2004. The role and regulation of programmed cell death in plant–pathogen interactions. *Cellular Microbiology* **6**, 201–211.
- Grimmer MK, John FM, Paveley ND. 2012. Foliar pathogenesis and plant water relations: a review. *Journal of Experimental Botany* **63**, 4321–4331.
- He M, Zhang K, Tan H, Hu R, Su J, Wang J, Huang L, Zhang Y, Li X. 2015. Nutrient levels within leaves, stems, and roots of the xeric species *Reaumuria songorica* in relation to geographical, climatic, and soil conditions. *Ecology and Evolution* **5**, 1494–1503.
- Herre EA, van Bael SA, Maynard Z, Robbins N, Bischoff J, Arnold AE. 2005. Tropical plants as chimera: some implications of foliar endophytic fungi for the study of host-plant defence, physiology and genetics. In: Burslem DFRP, Pinard MA, Hartley SE, eds. *Biotic interactions in the tropics: their role in the maintenance of species diversity*. Cambridge: Cambridge University Press, 226–237.
- Hirao T, Okazawa A, Harada K, Kobayashi A, Muranaka T, Hirata K. 2012. Green leaf volatiles enhance methyl jasmonate response in *Arabidopsis*. *Journal of Bioscience and Bioengineering* **114**, 540–545.
- Hu Z, Leng P, Shen Y, Wang W. 2011. Emissions of saturated C6–C10 aldehydes from poplar (*Populus simonii* x *pyramidalis* 'Opera 8277') cuttings at different levels of light intensity. *Journal of Forestry Research* **22**, 233–238.
- Hu Z, Shen Y, Su X. 2009. Saturated aldehydes C6–C10 emitted from ashleaf maple (*Acer negundo* L.) leaves at different levels of light intensity, O₂, and CO₂. *Journal of Plant Biology* **52**, 289–297.
- Huber AE, Bauerle TL. 2016. Long-distance plant signaling pathways in response to multiple stressors: the gap in knowledge. *Journal of Experimental Botany* **67**, 2063–2079.

- Jiang Y, Veromann-Jürgenson LL, Ye J, Niinemets Ü. 2018. Oak gall wasp infections of *Quercus robur* leaves lead to profound modifications in foliage photosynthetic and volatile emission characteristics. *Plant, Cell & Environment* **41**, 160–175.
- Jiang Y, Ye J, Li S, Niinemets Ü. 2017. Methyl jasmonate-induced emission of biogenic volatiles is biphasic in cucumber: a high-resolution analysis of dose dependence. *Journal of Experimental Botany* **68**, 4679–4694.
- Jiang Y, Ye J, Veromann L-L, Niinemets Ü. 2016. Scaling of photosynthesis and constitutive and induced volatile emissions with severity of leaf infection by rust fungus (*Melampsora larici-populina*) in *Populus balsamifera* var. *suaveolens*. *Tree Physiology* **36**, 856–872.
- Jorgensen I, Rayamajhi M, Miao EA. 2017. Programmed cell death as a defence against infection. *Nature Reviews. Immunology* **17**, 151–164.
- Josse E-M, Simkin AJ, Gaffé J, Labouré A-M, Kuntz M, Carol P. 2000. A plastid terminal oxidase associated with carotenoid desaturation during chromoplast differentiation. *Plant Physiology* **123**, 1427–1436.
- Junker RR, Tholl D. 2013. Volatile organic compound mediated interactions at the plant-microbe interface. *Journal of Chemical Ecology* **39**, 810–825.
- Kännaste A, Copolovici L, Niinemets Ü. 2014. Gas chromatography-mass spectrometry method for determination of biogenic volatile organic compounds emitted by plants. In: Rodríguez-Concepción M, ed. *Plant isoprenoids*. New York: Humana Press, 161–169.
- Kännaste A, Jürisoo L, Runno-Paurson E, Kask K, Talts E, Pärlist P, Dreñkhan R, Niinemets Ü. 2023. Impacts of Dutch elm disease-causing fungi on foliage photosynthetic characteristics and volatiles in *Ulmus* species with different pathogen resistance. *Tree Physiology* **43**, 57–74.
- Karl M, Guenther A, Köble R, Leip A, Seufert G. 2009. A new European plant-specific emission inventory of biogenic volatile organic compounds for use in atmospheric transport models. *Biogeosciences* **6**, 1059–1087.
- Kolmer J. 2013. Leaf rust of wheat: pathogen biology, variation and host resistance. *Forests* **4**, 70–84.
- Kouzai Y, Noutoshi Y, Inoue K, Shimizu M, Onda Y, Mochida K. 2018. Benzothiadiazole, a plant defense inducer, negatively regulates sheath blight resistance in *Brachypodium distachyon*. *Scientific Reports* **8**, 17358.
- Kovacik J, Klejdus B, Backor M, Repcak M. 2007. Phenylalanine ammonia-lyase activity and phenolic compounds accumulation in nitrogen-deficient *Matricaria chamomilla* leaf rosettes. *Plant Science* **172**, 393–399.
- Lei ZY, Wang H, Wright IJ, et al. 2021. Enhanced photosynthetic nitrogen use efficiency and increased nitrogen allocation to photosynthetic machinery under cotton domestication. *Photosynthesis Research* **150**, 239–250.
- Li N, Han X, Feng D, Yuan D, Huang LJ. 2019. Signaling crosstalk between salicylic acid and ethylene/jasmonate in plant defense: do we understand what they are whispering? *International Journal of Molecular Sciences* **20**, 671.
- Liu B, Zhang L, Rusalapp L, Kaurilind E, Sulaiman HY, Püssa T, Niinemets Ü. 2021. Heat priming improved heat tolerance of photosynthesis, enhanced terpenoid and benzenoid emission and phenolics accumulation in *Achillea millefolium*. *Plant, Cell & Environment* **44**, 2365–2385.
- Liu L, Sonbol F-M, Huot B, Gu Y, Withers J, Mwimba M, Yao J, He SY, Dong X. 2016. Salicylic acid receptors activate jasmonic acid signalling through a non-canonical pathway to promote effector-triggered immunity. *Nature Communications* **7**, 13099.
- Liu M, Hambleton S. 2013. Laying the foundation for a taxonomic review of *Puccinia coronata* s.l. in a phylogenetic context. *Mycological Progress* **12**, 63–89.
- Lorrain C, Gonçalves dos Santos KC, Germain H, Hecker A, Duplessis S. 2019. Advances in understanding obligate biotrophy in rust fungi. *New Phytologist* **222**, 1190–1206.
- Lorrain C, Marchal C, Hacquard S, Delaruelle C, Pétrowski J, Petre B, Hecker A, Frey P, Duplessis S. 2018. The rust fungus *Melampsora larici-populina* expresses a conserved genetic program and distinct sets of secreted protein genes during infection of its two host plants, larch and poplar. *Molecular Plant-Microbe Interactions* **31**, 695–706.
- Major IT, Nicole M-C, Duplessis S, Séguin A. 2010. Photosynthetic and respiratory changes in leaves of poplar elicited by rust infection. *Photosynthesis Research* **104**, 41–48.
- Makino A. 2013. Rubisco and nitrogen relationships in rice: leaf photosynthesis and plant growth. *Soil Science and Plant Nutrition* **49**, 319–327.
- Menzies JG, Xue A, Gruenke J, Dueck R, Deceuninck S, Chen Y. 2019. Virulence of *Puccinia coronata* var. *avenae* f. sp. *avenae* (oat crown rust) in Canada during 2010 to 2015. *Canadian Journal of Plant Pathology* **41**, 379–391.
- Munné-Bosch S, Alegre L. 2004. Die and let live: leaf senescence contributes to plant survival under drought stress. *Functional Plant Biology* **31**, 203–216.
- Nazareno ES, Li F, Smith M, Park RF, Kianian SF, Figueroa M. 2018. *Puccinia coronata* f. sp. *avenae*: a threat to global oat production. *Molecular Plant Pathology* **19**, 1047–1060.
- Niinemets Ü. 1999. Components of leaf dry mass per area—thickness and density—alter photosynthetic capacity in reverse directions in woody plants. *New Phytologist* **144**, 35–47.
- Niinemets Ü. 2010. Mild versus severe stress and BVOCs: thresholds, priming and consequences. *Trends in Plant Science* **15**, 145–153.
- Niinemets Ü. 2016. Uncovering the hidden facets of drought stress: secondary metabolites make the difference. *Tree Physiology* **36**, 129–132.
- Niinemets Ü, Hauff K, Bertin N, Tenhunen JD, Steinbrecher R, Seufert G. 2002. Monoterpene emissions in relation to foliar photosynthetic and structural variables in Mediterranean evergreen *Quercus* species. *New Phytologist* **153**, 243–256.
- Niinemets Ü, Kännaste A, Copolovici L. 2013. Quantitative patterns between plant volatile emissions induced by biotic stresses and the degree of damage. *Frontiers in Plant Science* **4**, 262.
- Niinemets Ü, Kuhn U, Harley PC, et al. 2011. Estimations of isoprenoid emission capacity from enclosure studies: measurements, data processing, quality and standardized measurement protocols. *Biogeosciences* **8**, 2209–2246.
- Niinemets Ü, Kull O, Tenhunen JD. 2004. Within-canopy variation in the rate of development of photosynthetic capacity is proportional to integrated quantum flux density in temperate deciduous trees. *Plant, Cell & Environment* **27**, 293–313.
- Niinemets Ü, Portsmuth A, Tena D, Tobias M, Matesanz S, Valladares F. 2007. Do we underestimate the importance of leaf size in plant economics? Disproportional scaling of support costs within the spectrum of leaf physiognomy. *Annals of Botany* **100**, 283–303.
- Niinemets Ü, Rasulov B, Talts E. 2021. CO₂ responsiveness of leaf isoprene emission: why do species differ? *Plant, Cell & Environment* **44**, 3049–3063.
- Niks RE, Rubiales D. 2002. Potentially durable resistance mechanisms in plants to specialised fungal pathogens. *Euphytica* **124**, 201–216.
- Nisar N, Li L, Lu S, Khin NC, Pogson BJ. 2015. Carotenoid metabolism in plants. *Molecular Plant* **8**, 68–82.
- Nogueira Júnior AF, Ribeiro RV, Appezzato-da-Glória B, Soares MKM, Rasera JB, Amorim L. 2017. *Phakopsora evittis* causes unusual damage to leaves and modifies carbohydrate metabolism in grapevine. *Frontiers in Plant Science* **8**, 1675.
- Nogués I, Brilli F, Loreto F. 2006. Dimethylallyl diphosphate and geranyl diphosphate pools of plant species characterized by different isoprenoid emissions. *Plant Physiology* **141**, 721–730.
- Patt JM, Robbins PS, Niedz R, McCollum G, Alessandro R. 2018. Exogenous application of the plant signalers methyl jasmonate and salicylic acid induces changes in volatile emissions from citrus foliage and influences the aggregation behavior of Asian citrus psyllid (*Diaphorina citri*), vector of Huanglongbing. *PLoS One* **13**, e0193724.
- Pitaloka MK, Harrison EL, Hepworth C, et al. 2021. Rice stomatal mega-papillae restrict water loss and pathogen entry. *Frontiers in Plant Science* **12**, 677839.
- Ponzio C, Weldegergis BT, Dicke M, Gols R. 2016. Compatible and incompatible pathogen-plant interactions differentially affect plant volatile

- emissions and the attraction of parasitoid wasps. *Functional Ecology* **30**, 1779–1789.
- Poorter H, Niinemets Ü, Poorter L, Wright IJ, Villar R.** 2009. Causes and consequences of variation in leaf mass per area (LMA): a meta-analysis. *New Phytologist* **182**, 565–588.
- Rasulov B, Bichele I, Laisk A, Niinemets Ü.** 2014. Competition between isoprene emission and pigment synthesis during leaf development in aspen. *Plant, Cell & Environment* **37**, 724–741.
- R Core Team. 2021. R: a language and environment for statistical computing. Vienna, Austria: R Foundation for Statistical Computing.
- Rigaud T, Perrot-Minnot MJ, Brown MJF.** 2010. Parasite and host assemblages: embracing the reality will improve our knowledge of parasite transmission and virulence. *Proceedings of the Royal Society B: Biological Sciences* **277**, 3693–3702.
- Savatin DV, Gramegna G, Modesti V, Cervone F.** 2014. Wounding in the plant tissue: the defense of a dangerous passage. *Frontiers in Plant Science* **5**, 470.
- Scholes JD, Rolfe SA.** 1996. Photosynthesis in localised regions of oat leaves infected with crown rust (*Puccinia coronata*): quantitative imaging of chlorophyll fluorescence. *Planta* **199**, 573–582.
- Singh R, Singh AP, Singh MP, Kumar A, Varshney CK.** 2008. Emission of isoprene from common Indian plant species and its implications for regional air quality. *Environmental Monitoring and Assessment* **144**, 43–51.
- Sobhy IS, Woodcock CM, Powers SJ, Caulfield JC, Pickett JA, Birkett MA.** 2017. cis-Jasmone elicits aphid-induced stress signalling in potatoes. *Journal of Chemical Ecology* **43**, 39–52.
- Song Y, Miao Y, Song C-P.** 2014. Behind the scenes: the roles of reactive oxygen species in guard cells. *New Phytologist* **201**, 1121–1140.
- Sowa S, Paczos-Grzęda E.** 2021. Virulence structure of *Puccinia coronata* f. sp. *avenae* and effectiveness of pc resistance genes in Poland during 2017–2019. *Phytopathology* **111**, 1158–1165.
- Staples RC.** 2001. Nutrients for a rust fungus: the role of haustoria. *Trends in Plant Science* **6**, 496–498.
- Sulaiman HY, Liu B, Kaurilind E, Niinemets Ü.** 2021. Phloem-feeding insect infestation antagonizes volatile organic compound emissions and enhances heat stress recovery of photosynthesis in *Origanum vulgare*. *Environmental and Experimental Botany* **189**, 104551.
- Tavernier V, Cadiou S, Pageau K, Laugé R, Reisdorf-Cren M, Langin T, Masclaux-Daubresse C.** 2007. The plant nitrogen mobilization promoted by *Colletotrichum lindemuthianum* in *Phaseolus* leaves depends on fungus pathogenicity. *Journal of Experimental Botany* **58**, 3351–3360.
- Toome M, Randjäär P, Copolovici L, Niinemets Ü, Heinsoo K, Luik A, Noe SM.** 2010. Leaf rust induced volatile organic compounds signalling in willow during the infection. *Planta* **232**, 235–243.
- Varshney CK, Singh AP.** 2003. Isoprene emission from Indian trees. *Journal of Geophysical Research: Atmospheres* **108**, 4803.
- Veresoglou SD, Barto EK, Menexes G, Rillig MC.** 2013. Fertilization affects severity of disease caused by fungal plant pathogens. *Plant Pathology* **62**, 961–969.
- von Caemmerer SV, Farquhar GD.** 1981. Some relationships between the biochemistry of photosynthesis and the gas exchange of leaves. *Plant* **153**, 376–387.
- Vuorinen T, Nerg AM, Syrjälä L, Peltonen P, Holopainen J.** 2007. *Epirrita autumnata* induced VOC emission of silver birch differ from emission induced by leaf fungal pathogen. *Arthropod-Plant Interactions* **1**, 159–165.
- Wasternack C, Hause B.** 2013. Jasmonates: biosynthesis, perception, signal transduction and action in plant stress response, growth and development. An update to the 2007 review in *Annals of Botany*. *Annals of Botany* **111**, 1021–1058.
- Wenig P, Odermatt J.** 2010. OpenChrom: a cross-platform open source software for the mass spectrometric analysis of chromatographic data. *BMC Bioinformatics* **11**, 405.
- Wong SC, Cowan IR, Farquhar GD.** 1979. Stomatal conductance correlates with photosynthetic capacity. *Nature* **282**, 424–426.
- Zhao D, Glynn NC, Glaz B, Comstock JC, Sood S.** 2011. Orange rust effects on leaf photosynthesis and related characters of sugarcane. *Plant Disease* **95**, 640–647.



Sulaiman, HY, Runno-Paurson, E, Kaurilind, E and Niinemets, Ü.
2023. The same boat, different storm: stress volatile emissions in
response to biotrophic fungal infections in primary and alternate hosts.
Plant Signaling and Behavior 2217030-2217030.



The same boat, different storm: stress volatile emissions in response to biotrophic fungal infections in primary and alternate hosts

Hassan Yusuf Sulaiman, Eve Runno-Paurson & Ülo Niinemets

To cite this article: Hassan Yusuf Sulaiman, Eve Runno-Paurson & Ülo Niinemets (2023): The same boat, different storm: stress volatile emissions in response to biotrophic fungal infections in primary and alternate hosts, *Plant Signaling & Behavior*, DOI: [10.1080/15592324.2023.2217030](https://doi.org/10.1080/15592324.2023.2217030)

To link to this article: <https://doi.org/10.1080/15592324.2023.2217030>



© 2023 The Author(s). Published with license by Taylor & Francis Group, LLC.



Published online: 26 May 2023.



Submit your article to this journal [↗](#)



Article views: 130



View related articles [↗](#)



View Crossmark data [↗](#)

Full Terms & Conditions of access and use can be found at
<https://www.tandfonline.com/action/journalInformation?journalCode=kpsb20>

The same boat, different storm: stress volatile emissions in response to biotrophic fungal infections in primary and alternate hosts

Hassan Yusuf Sulaiman^a, Eve Runno-Paurson^a, and Ülo Niinemets^{a,b}

^aChair of Crop Science and Plant Biology, Estonian University of Life Sciences, Tartu, Estonia; ^bEstonian Academy of Sciences, Tallinn, Estonia

ABSTRACT

Rust infection results in stress volatile emissions, but due to the complexity of host-pathogen interaction and variations in innate defense and capacity to induce defense, biochemical responses can vary among host species. Fungal-dependent modifications in volatile emissions have been well documented in numerous host species, but how emission responses vary among host species is poorly understood. Our recent experiments demonstrated that the obligate biotrophic crown rust fungus (*P. coronata*) differently activated primary and secondary metabolic pathways in its primary host *Avena sativa* and alternate host *Rhamnus frangula*. In *A. sativa*, emissions of methyl jasmonate, short-chained lipoxigenase products, long-chained saturated fatty acid derivatives, mono- and sesquiterpenes, carotenoid breakdown products, and benzenoids were initially elicited in an infection severity-dependent manner, but the emissions decreased under severe infection and photosynthesis was almost completely inhibited. In *R. frangula*, infection resulted in low-level induction of stress volatile emissions, but surprisingly, in enhanced constitutive isoprene emissions, and even severely-infected leaves maintained a certain photosynthesis rate. Thus, the same pathogen elicited a much stronger response in the primary than in the alternate host. We argue that future work should focus on resolving mechanisms of different fungal tolerance and resilience among primary and secondary hosts.

ARTICLE HISTORY

Received 16 March 2023
Revised 16 May 2023
Accepted 17 May 2023

KEYWORDS

defense signaling pathways;
host-pathogen interaction;
isoprene; infection severity;
limiting nutrient; pathogen
stress; photosynthesis;
volatile organic compounds

Introduction

Numerous studies have demonstrated that pathogen attacks negatively impact photosynthesis and activate different hormonal pathways including jasmonic acid (JA) and/or salicylic acid (SA) signaling and alteration of the activity of different secondary metabolic pathways^{1,2}. This results in enhanced emissions of various stress marker compounds and defensive metabolites such as short-chained lipoxigenase (LOX) pathway volatiles (also called 'green leaf volatiles')^{3,4}, mono- and sesquiterpenes⁵⁻⁷, benzenoids⁸, and carotenoid breakdown products from the geranylgeranyl diphosphate (GGDP) pathway^{3,9}.



Many widespread fungal pathogens such as *Melampsora* spp. and *Puccinia* spp. are multi-host (heterecious) pathogens requiring two phylogenetically different hosts, primary and secondary host to complete their life cycle¹⁰⁻¹². Most studies looking at quantitative relationships between infection severity by multi-host pathogens and stress volatile emissions have focused on single hosts (Toome *et al.*,^{13,14}). However, physiological and biochemical responses can vary among host species of multi-host pathogens at different parts of their life cycle. Such variations might result from differences in adaptive responses in different hosts, interspecific differences in host-pathogen interactions and different pathogen pressures on different hosts^{15,16}. In addition, host differences in the expression of constitutive defenses and capacity to induce defense responses can result in divergent elicitation of volatile emissions in

different host species². Regarding volatiles, variations in the degree of constitutive isoprene emissions can give rise to differences in the induction of emissions of stress-elicited isoprenoids in different hosts^{5,7,14,17}.

Phylogenetically different hosts also have different ecological requirements, implying that heterecious fungal infections can impact a range of ecosystems¹⁸. Furthermore, many primary hosts are widespread crops, and thus, information on fungal stress responses of different host species is important in developing rust fungus-resistant crops^{19,20}. This is especially relevant given that heterecious biotrophic fungi are suggested to exert more severe stress on primary hosts than on alternate hosts, as the pathogens only transit the alternate host²¹. This evidence collectively suggests that potential differences in the physiological responses of primary hosts and alternate hosts of fungal pathogens need to be carefully scrutinized.

Puccinia coronata infection as a model to study fungal-induced physiological changes in different hosts

We conducted experiments to investigate how a heterecious obligate biotrophic fungus, crown rust (*P. coronata*) modifies volatile organic compound (VOC) emission profiles at different levels of infection severity in its primary and secondary hosts²². Its primary host, where the asexual reproduction of the fungus takes place, is the annual grass, cultivated oat (*Avena*

CONTACT Hassan Yusuf Sulaiman  Hassan@emu.ee  Chair of Crop Science and Plant Biology, Estonian University of Life Sciences, Kreutzwaldi 5, Tartu 51006, Estonia

© 2023 The Author(s). Published with license by Taylor & Francis Group, LLC

This is an Open Access article distributed under the terms of the Creative Commons Attribution License (<http://creativecommons.org/licenses/by/4.0/>), which permits unrestricted use, distribution, and reproduction in any medium, provided the original work is properly cited. The terms on which this article has been published allow the posting of the Accepted Manuscript in a repository by the author(s) or with their consent.

sativa L., Gramineae), and the alternate host, where the karyogamy and meiosis of the fungus occur, is the shrub to small tree alder buckthorn (*Rhamnus frangula* L., syn. *Frangula alnus* P. Mill., *Rhamnaceae*). We used *P. coronata* as the fungal model organism as it is highly virulent with a considerable rise in virulence reported recently^{23,24} Sowa and Paczos-Grzęda, 2021). Also, the host species of *P. coronata* have varying degrees of constitutive emissions of isoprene; *A. sativa* is a weak emitter, whereas *R. frangula* is a moderately strong emitter²².

We measured photosynthetic characteristics (light-saturated stomatal conductance, g_s , and net assimilation rate, A) and emissions of VOC simultaneously in leaves with varying severity of *P. coronata* infections using a custom-made gas exchange system designed for trace gas sampling, and identified different volatile compounds using gas-chromatography mass-spectrometry²². Additionally, we quantified mineral nutrients (nitrogen and phosphorous) and carbon contents per leaf dry mass, and leaf dry mass per area (LMA) in the different host species as these variables define the structural and chemical controls on photosynthesis, carbon sink and structural investment²². In these experiments, the severity of the infection, measured by the total leaf area covered by the classical rust symptoms, chlorosis, and necrosis (total visible damaged leaf area, D_A), ranged from 0 (non-infected) to ~80% in *A. sativa* and from 0 to ~60% in *R. frangula* (Fig. 1 and 2 for images of representative infected leaves). In total, 15 leaves of *R. frangula* (three non-infected control and 12 infected leaves) and 23 leaves of *A. sativa* cv. 'Kalle' (three non-infected control and 20 infected leaves) with varying degrees of infection were measured²².

In *R. frangula*, A decreased with increasing severity of the infection and the reductions were primarily due to limitations of photosynthetic capacity (Fig. 1A and 2). In *A. sativa*, fungal-induced stomatal limitations resulted in decreases in photosynthetic activity at all levels of infections (Figures 1A and 2). However, under severe infection, g_s relative to A increased, indicating a certain reduction of photosynthetic capacity²². We observed that in *A. sativa*, but not in *R. frangula*, the reduction in photosynthetic activity was associated with decreases in rate limiting nutrients (N and P) and loss of photosynthetic biomass (Fig. 2), reflecting fungal consumption of leaf nutrient. Given that a large fraction of leaf nitrogen is invested in Rubisco, a decrease in nitrogen content typically results in a drastic reduction in photosynthetic capacity²⁵. In addition, in *A. sativa*, the infection resulted in increases in the C contents of leaves (Fig. 2), suggesting the accumulation of the shikimic acid pathway-produced carbon-rich compounds such as lignin that promote defense against pathogens²⁶.

Differences in fungal activation of volatile synthesis pathways in different host species

Pathogens induce hypersensitive responses that trigger the activation of different hormonal signaling pathways, particularly SA and JA pathways that regulate local and systemic defense/stress responses^{27,28}. Often, the hormonal pathway activated during pathogen infection depends on the pathogen type and its interaction with the hosts²⁹. Typically, biotrophic

fungi activate the SA pathway, whereas the JA pathway is activated by necrotrophic pathogens^{29,30,31}. Research over the past decades has established that these pathways interact antagonistically in response to certain pathogens, in such a way that the activation of one pathway suppresses the other³² (Kunkel and Brooks 2022). However, recent evidence has also demonstrated synergistic interactions between SA and JA pathways in response to different pathogen attacks^{33,34,35}. In particular, rust infection is associated with enhanced SA and JA accumulation due to the positive interaction of JA and SA signaling^{34,35}. In this study, fungal infections induced the emissions of methyl jasmonate (MeJA) in *A. sativa* (Fig. 1B). Given that *A. sativa* emitted benzenoids (Fig. 1B), synthesis of which via the shikimate pathway is regulated by SA accumulation^{2,8}, simultaneous emissions of MeJA and benzenoids reflect the synergistic activities of JA and SA pathways. In *R. frangula*, low-level MeJA emissions were constitutive²², suggesting constitutive expression of JA-dependent systemic responses that improve stress tolerance^{27,36}.

In *A. sativa*, the induction of MeJA emission was accompanied by bursts of different LOX pathway volatiles (Figure 1B). Emissions of LOX pathway derivatives indicate cellular damage and generation of an oxidative burst^{37,38,39}. In the case of *R. frangula*, emissions of LOX volatiles were only enhanced to a minor degree (Figure 1B), suggesting much lower oxidative stress. In *A. sativa*, emissions of LOX volatiles were accompanied by emissions of long-chain saturated fatty acid (FAD) derivatives (Fig. 1A), further indicating a stronger loss of membrane integrity in the primary host.

Terpenoid emissions were also differently enhanced in the primary and alternate hosts (Figures 1B and 2), further underscoring the differences in stress severity experienced by plants as well as the differential regulation of terpenoid pathway genes. In *A. sativa*, *P. coronata* enhanced the emissions of mono- and sesquiterpenes, but suppressed the emission of the oxygenated isoprene derivative methacrolein (Figures 1B and 2). In general, biotic stresses induce mono- and sesquiterpene emissions but decrease constitutive emissions of isoprene as observed in primary isoprene-emitting hosts infected by *Melampsora* spp.^{13,14,40}. Surprisingly, in *R. frangula*, the impact of *P. coronata* on mono- and sesquiterpenes was minor, but the emissions of isoprene were enhanced (Figure 1B). This might indicate both the overall upregulation of the chloroplastic methyl-D-erythritol phosphate (MEP) pathway for isoprenoid synthesis or isoprene synthase activity^{7,17,41,42}. Apparently, the stress threshold for elicitation of terpene synthesis was not exceeded in the alternate host, or *R. frangula* has an overall low capacity for induction of terpene emissions. Although emissions of specialized metabolites can enhance local and systemic defense responses, in some cases, low emissions of these volatiles can reflect enhanced defense^{3,38,43,44}, as observed in *R. frangula* (Figures 1B and 2).

Altogether the different responsiveness of volatile formation pathways in the two hosts led to distinguished volatile fingerprints (Figures 1B and 2). In particular, in the primary host, the bouquet of volatile emissions was much richer (Figure 1B), including indicators of oxidative damage such as 2-ethyl-hexanol and (*E*)-2-hexenal, indicators of enhanced activation of terpenoid synthesis pathways⁴ Kannasta *et al.*,³

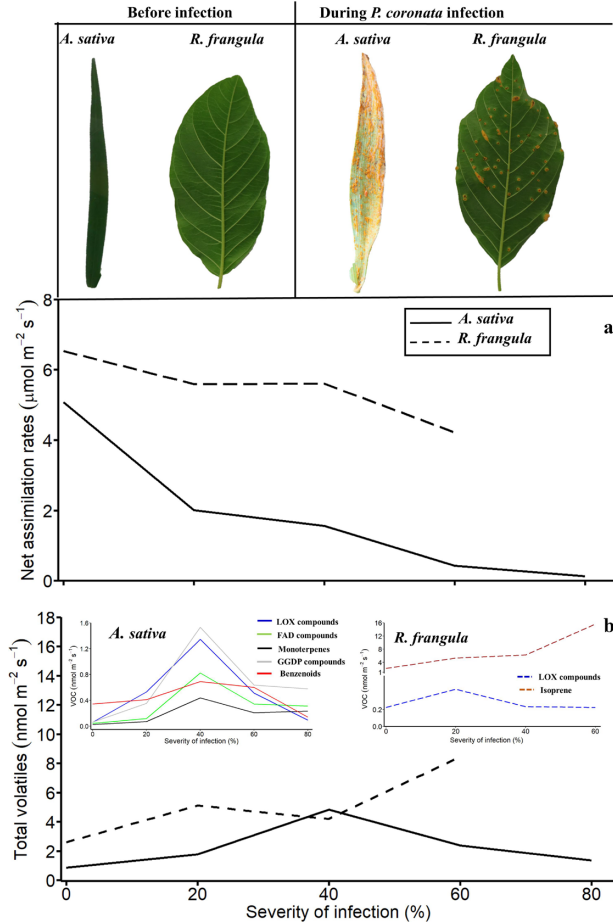


Figure 1. Changes in leaf light-saturated net assimilation rate (A) and total volatile emission (B) in the primary host, the annual grass *Avena sativa*, and the alternate host, the shrub *R. frangula*, under different severity of the crown rust *Puccinia coronata* infection. The insets in (B) show the severity-dependent emissions of different volatile groups including short-chained lipoxygenase (LOX) pathway compounds, methyl jasmonate (MeJA), long-chained saturated fatty acid-derived (FAD) compounds, monoterpenes, geranylgeranyl diphosphate pathway (GGDP) compounds and benzenoids in *A. sativa* and *R. frangula*. The severity of infection was quantified as the percentage of the total chlorotic and necrotic area of the leaf.

and shikimic acid pathways such as β -pinene, β -farnesene, benzaldehyde, and benzothiazole^{1,8}, and indicators of carotenoid breakdown such as geranyl acetone^{3,9}. As other studies of volatile emission responses upon infection of heterocious fungi have looked at primary hosts, whether the observation of lower complexity of volatile profiles in infected alternate hosts is a general pattern requires further investigation.

Scaling of volatile emissions with the severity of *P. coronata* infection

In *A. sativa*, emissions of stress volatiles increased with the severity of infection from 0 to 40% (Figures 1B and 2), suggesting stress severity-dependent elicitation of volatiles. Several previous studies have demonstrated that fungal-dependent

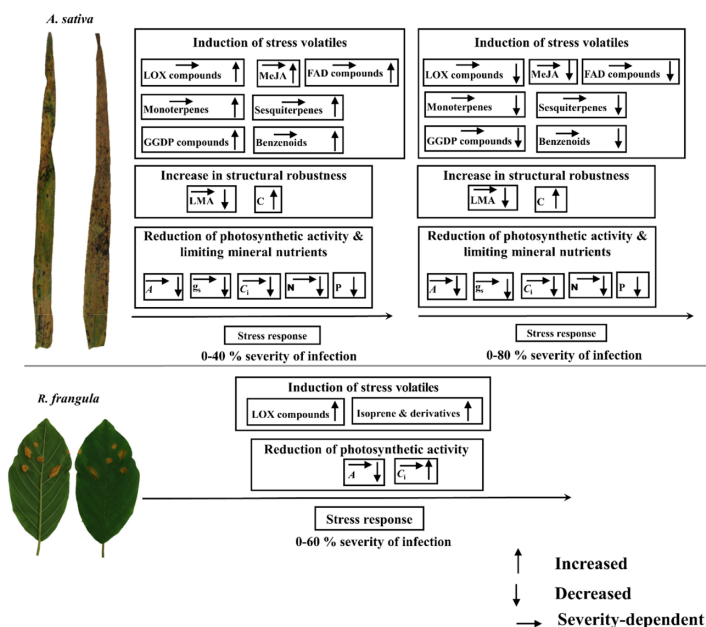


Figure 2. A generalized model of *P. coronata* infection severity-dependent responses of photosynthetic traits and stress volatile emissions in the primary host *A. sativa* and alternate host *R. frangula*. This model shows that the rate of photosynthesis (A) in the primary host is reduced due to stomatal limitations (decreases in stomatal conductance, g_s , and intercellular concentrations of CO_2 , C_i). Reductions in photosynthetic activity are escalated by fungal absorption of limiting mineral nutrients and loss of photosynthetic biomass, indicated by decreases in leaf dry mass per unit area (LMA), due to fungal consumption of leaf biomass. Loss of photosynthetic function is accompanied by accumulation of carbon-rich secondary metabolites e.g. phenolics such as lignin in cell walls that enhances leaf mechanical robustness and reduces cell wall diffusion conductance for CO_2 . In the alternate host, decreases in photosynthesis are due to reductions in photosynthetic capacity. In the primary host, fungal-induced damages and hypersensitive responses trigger a burst of lipoxygenase (LOX) volatiles and the activation of defense signaling associated with jasmonic acid (JA) accumulation. This leads to the induction of emissions of stress volatiles including mono- and sesquiterpenes from chloroplastic and cytosolic terpene synthesis pathways and benzenoids from the shikimate pathway. Additionally, fungal-induced oxidative stress enhances the release of long-chained saturated fatty acid (FAD) derivatives and geranylgeranyl diphosphate (GGDP) pathway volatiles (carotenoid breakdown products). The emissions of volatiles increase with increasing severity of fungal infection, however, under severe infections, the induction of stress volatiles decreases due to substrate limitation that occurs as a result of inhibition of photosynthesis and cessations of physiological activities in necrotic leaf regions. In the resistant alternate host, due to low oxidative stress, LOX emissions are only elicited to a minor degree. Differently from the enhancement of terpene emissions in *A. sativa*, in *R. frangula*, constitutive emissions of isoprene are enhanced upon rust infection, differently from pathogen responses observed in other constitutive isoprene emitters.

emissions scale with the severity of infection^{13,40}, implying that stress volatiles are increasingly elicited with increasing tissue damage. However, the late stages of *P. coronata* infection were characterized by expansions of necrosis, resembling hemibiotrophy, that can lead to the inhibition of photosynthesis and overall physiological activities including volatile emissions^{22,45}. We could not discriminate emissions from infected and non-infected regions of the leaf, however, it has been noted that for chronic infection, scaling of stress VOC with the severity of infection reflects emissions from damaged areas and immediate impact sites^{2,5}. We observed that in severely infected *A. sativa*, photosynthesis was almost completely inhibited due to both stomatal limitation and inhibition of Rubisco activity (Figures 1A and 2). In addition to the spread of necrotic surface area, decreased photosynthesis of still

functional leaf parts might have resulted in a shortage of substrates for volatile synthesis^{46,22}. Correspondingly, in *A. sativa*, the elicitation of volatile emissions declined under severe infections, from 40 to ~80% severity of infection (Figures 1B and 2). Previously, such abolishing of volatile emissions has only been observed for necrotrophic infections^{1,47,48}.

Conclusion

It has been suggested that heterocious biotrophic fungi exert more severe stress on primary hosts than on alternate hosts, as the pathogens mainly require the alternate host for transit before infecting the primary host²¹, but the experimental evidence has been limited. We demonstrated that *P. coronata* infection impacted photosynthesis and activated

biochemical pathways differently in the primary host and the alternate host. The difference in the physiological responses of the different host species demonstrates differences in the fungal stress sensitivity of the different host species. In the sensitive host, *A. sativa*, photosynthesis was almost completely inhibited under extreme infection, resulting in a major decline in the biosynthesis of volatiles²². The scaling of defense responses with increasing severity of infection in the primary host was characterized by an optimum, indicating that above a certain infection threshold, the defenses of the host were exhausted, resulting in escalated tissue damage and cell death.

We found a surprising increase in isoprene emissions in the infected alternate host *R. frangula*. This is different from other studies with constitutive isoprene emitters infected by heterocercous fungal pathogens^{5,14,40}, but in these studies, the constitutive emitters were the primary hosts. Overall, the fungal-dependent changes in photosynthetic traits and volatile emissions were greater in the primary host than in the alternate host, reflecting variations in the sensitivity of the physiological activities of the different hosts. A profound understanding of how different host species respond to heterocercous biotrophic pathogens is relevant to predict fungal spread in both natural ecosystems and crops. We suggest that future assessments of the severity of infections of heterocercous fungi should consider both primary and alternate hosts. Furthermore, comparisons of responses of different host species to the same pathogen can help identify promising plant molecular responses to pathogen infection as a breeding strategy for the enhancement of disease resilience in crop species and cultivars^{49,50,51}.

Acknowledgments

This research was funded by the European Commission through the European Research Council (advanced grant 322603, SIP-VOL+), the EU Regional Development Fund within the framework of the Centre of Excellence EcolChange (2014-2020.4.01.15-0002), and the Estonian University of Life Sciences (base funding P190259PKTT). The equipment used in the study was partly purchased from funding by the EU Regional Development Fund (AnaEE Estonia, 2014-2020.4.01.20-0285, and the project "Plant Biology Infrastructure-TAIM", 2014-2020.4.01.20-0282) and Estonian Research Council ("Plant Biology Infrastructure - TAIM", TT5).

Disclosure statement

No potential conflict of interest was reported by the authors.

Funding

The work was supported by the European Commission through the European Research Council (advanced grant 322603, SIP-VOL+), the EU Regional Development Fund within the framework of the Centre of Excellence EcolChange (2014-2020.4.01.15-0002), and the Estonian University of Life Sciences (base funding P190259PKTT). The equipment used in the study was partly purchased from funding by the EU Regional Development Fund (AnaEE Estonia, 2014-2020.4.01.20-0285, and the project "Plant Biology Infrastructure-TAIM", 2014-2020.4.01.20-0282) and Estonian Research Council ("Plant Biology Infrastructure - TAIM", TT5).

References

- Huang J, Cardoza YJ, Schmelz EA, Raina R, Engelberth J, Tumlinson JH. Differential volatile emissions and salicylic acid levels from tobacco plants in response to different strains of *Pseudomonas syringae*. *Planta*. 2003;217(5):767-775. doi:10.1007/s00425-003-1039-y.
- Niinemets Ü, Kännaste A, Copolovici L. Quantitative patterns between plant volatile emissions induced by biotic stresses and the degree of damage. *Front Plant Sci*. 2013;4. doi:10.3389/fpls.2013.00262.
- Kännaste A, Jürisoo L, Runno-Paurson E, Kask K, Talts E, Pärlist P, Drenkhan R, Niinemets Ü. Impacts of Dutch elm disease-causing fungi on foliage photosynthetic characteristics and volatiles in *Ulmus* species with different pathogen resistance. *Tree Physiol*. 2023;43(1):57-74. doi:10.1093/treephys/tpac108.
- Matsui K, Engelberth J. Green leaf volatiles—the forefront of plant responses against biotic attack. *Plant Cell Physiol*. 2022;63(10):1378-1390. doi:10.1093/pcp/pcac117.
- Jiang Y, Ye J, Li S, Niinemets Ü. Methyl jasmonate-induced emission of biogenic volatiles is biphasic in cucumber: a high-resolution analysis of dose dependence. *J Exp Bot*. 2017;68(16):4679-4694. doi:10.1093/jxb/erx244.
- Niinemets Ü, Hauff K, Bertin N, Tenhunen JD, Steinbrecher R, Seufert G. Monoterpene emissions in relation to foliar photosynthetic and structural variables in Mediterranean evergreen *Quercus* species. *New Phytol*. 2002;153(2):243-256. doi:10.1046/j.0028-646X.2001.00323.x.
- Niinemets Ü, Rasulov B, Talts E. CO₂-responsiveness of leaf isoprene emission: why do species differ? *Plant, Cell & Environment*. 2021;44(9):3049-3063. doi:10.1111/pce.14131.
- Misztal P, Hewitt C, Wildt J, Blande JD, Eller ASD, Fares S, Gentner DR, Gilman JB, Graus M, Greenberg J, et al. Atmospheric benzenoid emissions from plants rival those from fossil fuels. *null*. 2015;5(1):1-10. doi:10.1038/srep12064.
- Zhang J, He L, Dong J, Zhao C, Wang Y, Tang R, Wang W, Ji Z, Cao Q, Xie H, et al. Integrated metabolic and transcriptional analysis reveals the role of carotenoid cleavage dioxygenase 4 (IbCCD4) in carotenoid accumulation in sweetpotato tuberos roots. *Biotechnol Biofuels*. 2023;16(1):1645. doi:10.1186/s13068-023-02299-y.
- Barrett LG, Thrall PH, Burdon JJ, Nicotra AB, Linde CC. Population structure and diversity in sexual and asexual populations of the pathogenic fungus *Melampsora lini*. *Mol Ecol*. 2008;17(14):3401-3415. doi:10.1111/j.1365-294X.2008.03843.x.
- Bayon C, Pei MH, Ruiz C, Hunter T, Karp A, Tubby I. Genetic structure and population dynamics of a heterocercous plant pathogen *Melampsora larici-epitea* in short-rotation coppice willow plantations. *Mol Ecol*. 2009;18(14):3006-3019. doi:10.1111/j.1365-294X.2009.04255.x.
- Huang S, Zuo S, Zheng D, Liu Y, Du Z, Kang Z, Zhao J. Three formae speciales of *Puccinia striiformis* were identified as heterocercous rusts based on completion of sexual cycle on *Berberis* spp. under artificial inoculation. *Phytopathology Research*. 2019;1(1):1-9. doi:10.1186/s42483-019-0021-y.
- Jiang Y, Ye J, Veromann LL, Niinemets Ü, Schnitzler J-P. Scaling of photosynthesis and constitutive and induced volatile emissions with severity of leaf infection by rust fungus (*Melampsora larici-populina*) in *Populus balsamifera* var. *suaevolens*. *Tree Physiol*. 2016;36(7):856-872. doi:10.1093/treephys/tpw035.
- Toome M, Randjävär P, Copolovici L, Niinemets Ü, Heinsoo K, Luik A, Steffen, MN. Leaf rust induced volatile organic compounds signalling in willow during the infection. *Planta*. 2010;232(1):235-243. doi:10.1007/s00425-010-1169-y.
- Eberl F, Hammerbacher A, Gershenson J, Unsicker SB. Leaf rust infection reduces herbivore-induced volatile emission in black poplar and attracts a generalist herbivore. *New Phytol*. 2018;220(3):760-772. doi:10.1111/nph.14565.

16. Grimmer MK, John Foulkes M, Pavley ND. Foliar pathogenesis and plant water relations: a review. *J Exp Bot.* 2012;63(12):4321–4331. doi:10.1093/jxb/er5143.
17. Sharkey TD, Wiberley AE, Donohue AR. Isoprene emission from plants: why and how. *Annal Of Botany.* 2008;101(1):5–18. doi:10.1093/aob/mcm240.
18. Liu M, Hambleton S. Laying the foundation for a taxonomic review of *Puccinia coronata* s.L. in a phylogenetic context. *Mycol Progress.* 2013;12(1):63–89. doi:10.1007/s11557-012-0814-1.
19. Fei W, Liu Y. Biotrophic fungal pathogens: a critical overview. *Appl Biochem Biotechnol.* 2023;195(1):1–16. doi:10.1007/s12010-022-04087-0.
20. Jain A, Sarsaiya S, Wu Q, Lu Y, Shi J. A review of plant leaf fungal diseases and its environment speciation. *Bioengineered.* 2019;10(1):409–424. doi:10.1080/21655979.2019.1649520.
21. Bettgenhauser J, Gilbert B, Ayliffe M, Moscou MJ. Nonhost resistance to rust pathogens – a continuation of continua. *Frontiers Of Plant Science.* 2014;5:664. doi:10.3389/fpls.2014.00664.
22. Sulaiman HY, Runno-Paurson E, Kaurilind E, Niinemets Ü, Lunn J. Differential impact of crown rust (*Puccinia coronata*) infection on photosynthesis and volatile emissions in the primary host *Avena sativa* and the alternate host *Rhamnus frangula*. *J Exp Bot.* 2023;74(6):2029–2046. doi:10.1093/jxb/era001.
23. Menzies JG, Xue A, Gruenke J, Dueck R, Decuening S, Chen Y. Virulence of *Puccinia coronata* var *avenae* f. sp. *avenae* (oat crown rust) in Canada during 2010 to 2015. *Canadian Journal Of Plant Pathology.* 2019;41(3):379–391. doi:10.1080/07060661.2019.1577300.
24. Sowa S and Paczos-Grzędz E. (2021). Virulence Structure of *Puccinia coronata* f. sp. *avenae* and Effectiveness of Pc Resistance Genes in Poland During 2017–2019. *Phytopathology**, 111(7), 1158–1165. doi:10.1094/PHYTO-10-20-0457-R
25. Luo X, Keenan TF, Chen JM, Croft H, Colin Prentice I, Smith NG, Walker AP, Wang H, Wang R, Xu C. et al. Global variation in the fraction of leaf nitrogen allocated to photosynthesis. *null.* 2021;12(1):4866. doi:10.1038/s41467-021-25163-9.
26. Rajashekar CB. Elevated CO₂ levels affect phytochemicals and nutritional quality of food crops. *American Journal Of Plant Sciences.* 2018;9(2):150–162. doi:10.4236/ajps.2018.92013.
27. Turner JG, Ellis C, Devoto A. The Jasmonate Signal Pathway. *Plant Cell.* 2002;14(suppl 1):s153–64. doi:10.1105/tpc.000679.
28. Zeilinger S, Gupta VK, Dahms TES, Silva RN, Singh HB, Upadhyay RS, Gomes EV, Tsui C-M, Nayak SC, van der Meer JR. Friends or foes? Emerging insights from fungal interactions with plants. *FEMS Microbiol Rev.* 2016;40(2):182–207. doi:10.1093/femsre/fuv045.
29. Bruinsma M, Posthumus MA, Mumm R, Mueller MJ, van Loon JJA, Dicke M. Jasmonic acid-induced volatiles of *Brassica oleracea* attract parasitoids: effects of time and dose, and comparison with induction by herbivores. *J Exp Bot.* 2009;60(9):2575–2587. doi:10.1093/jxb/erp101.
30. Crampton BG, Hein I, Berger DK. Salicylic acid confers resistance to a biotrophic rust pathogen, *Puccinia striatata*, in pearl millet (*Pennisetum glaucum*). *Mol Plant Pathol.* 2009;10(2):291–304. doi:10.1111/j.1364-3703.2008.00532.x.
31. Li N, Han X, Feng D, Yuan D, Huang LJ. Signaling crosstalk between salicylic acid and ethylene/jasmonate in plant defense: do we understand what they are whispering? *International Journal Of Molecular Science.* 2019;20(3):E671. doi:10.3390/ijms20030671.
32. Kunkel B N and Brooks D M. (2002). Cross talk between signaling pathways in pathogen defense. *Current Opinion in Plant Biology*, 5(4), 325–331. doi:10.1016/S1369-5266(02)00275-3
33. Mur LA, Kenton P, Atzorn R, Miersch O, Wasternack C. The outcomes of concentration-specific interactions between salicylate and jasmonate signaling include synergy, antagonism, and oxidative stress leading to cell death. *Plant Physiol.* 2006;140(1):249–262. doi:10.1104/pp.105.072348.
34. Tamaoki D, Seo S, Yamada S, Kano A, Miyamoto A, Shishido H, Miyoshi S, Taniguchi S, Akimitsu K, Gomi K. Jasmonic acid and salicylic acid activate a common defense system in rice. *Plant Signal Behav.* 2013;8(6):e24260. doi:10.4161/psb.24260.
35. Ullah C, Schmidt A, Reichelt M, Tsai CJ, Gershenzon J. Lack of antagonism between salicylic acid and jasmonate signalling pathways in poplar. *New Phytol.* 2022;235(2):701–717. doi:10.1111/nph.18148.
36. Mahmud S, Ullah C, Kortz A, Bhattacharyya S, Yu P, Gershenzon J, Vothknecht UC. Constitutive expression of JASMONATE RESISTANT 1 induces molecular changes that prime the plants to better withstand drought. *Plant, Cell And Environment.* 2022;45(10):2906–2922. doi:10.1111/pce.14402.
37. Liu B, Zhang L, Rusalopp L, Kaurilind E, Sulaiman HY, Püssa T, Niinemets Ü. Heat priming improved heat tolerance of photosynthesis, enhanced terpenoid and benzenoid emission and phenolics accumulation in *Achillea millefolium*. *Plant, Cell & Environment.* 2021;44(7):2365–2385. doi:10.1111/pce.13830.
38. Sulaiman HY, Liu B, Kaurilind E, Niinemets Ü. Ploem-feeding insect infestation antagonizes volatile organic compound emissions and enhances heat stress recovery of photosynthesis in *Origanum vulgare*. *Environ Exp Bot.* 2021;189:104551. doi:10.1016/j.envexpbot.2021.104551.
39. Zurbriggen MD, Carrillo N, Hajirezaei MR. ROS signaling in the hypersensitive response. *Plant Signal Behav.* 2010;5(4):393–396. doi:10.4161/psb.5.4.10793.
40. Copolovici L, Väärtnõu F, Estrada MP, Niinemets Ü. Oak powdery mildew (*Erysiphe alphitoides*) induced volatile emissions scale with the degree of infection in *Quercus robur*. *Tree Physiology.* 2014;34(12):1399. doi:10.1093/treephys/tpu091.
41. Magel E, Mayrhofer S, Müller A, Zimmer I, Hamp R, Schnitzler JP. Photosynthesis and substrate supply for isoprene biosynthesis in poplar leaves. *Atmos Environ.* 2006;40:138–151. doi:10.1016/j.atmosenv.2005.09.091.
42. Rasulov B, Bichele I, Laisk A, Niinemets Ü. Competition between isoprene emission and pigment synthesis during leaf development in aspen. *Plant, Cell And Environment.* 2014;37(3):724–741. doi:10.1111/pce.12190.
43. Erb M. Volatiles as inducers and suppressors of plant defense and immunity—origins, specificity, perception and signaling. *Curr Opin Plant Biol.* 2018;44:117–121. doi:10.1016/j.pbi.2018.03.008.
44. Niinemets Ü. Mild versus severe stress and BVOCs: thresholds, priming and consequences. *Trends Plant Sci.* 2010;15(3):145–153. doi:10.1016/j.tplants.2009.11.008.
45. Divon HH, Fluhr R. Nutrition acquisition strategies during fungal infection of plants. *FEMS Microbiol Lett.* 2007;266(1):65–74. doi:10.1111/j.1574-6968.2006.00504.x.
46. Aldea M, Hamilton JG, Resti JP, Zangerl AR, Berenbaum MR, Frank TD, DeLucia EH. Comparison of photosynthetic damage from arthropod herbivory and pathogen infection in understory hardwood saplings. *Oecologia.* 2010;149(2):221–232. doi:10.1007/s00442-006-0444-x.
47. Hammond-Kosack KE, Rudd JJ. Plant resistance signalling hijacked by a necrotrophic fungal pathogen. *Plant Signaling And Behavior.* 2008;3(11):993–995. doi:10.4161/psb.6292.
48. Vandendriessche T, Keulemans J, Geeraerd A, Nicolai BM, Hertog ML. Evaluation of fast volatile analysis for detection of *Botrytis cinerea* infections in strawberry. *Food Microbiol.* 2012;32:406–414.
49. Berger S, Sinha AK, Roitsch T. Plant physiology meets phytopathology: plant primary metabolism and plant–pathogen interactions. *J Exp Bot.* 2007;58(15–16):4019–4026. doi:10.1093/jxb/erm298.
50. Castelyn HD, Appelgrün JJ, Mafa MS, Pretorius ZA, Visser B. Volatiles emitted by leaf rust infected wheat induce a defence response in exposed uninfected wheat seedlings. *Australasian Plant Pathol.* 2015;44(2):245–254. doi:10.1007/s13313-014-0336-1.
51. Kunkel BN, Brooks DM. Cross talk between signaling pathways in pathogen defense. *Curr Opin Plant Biol.* 2002;5(4):325–331. doi:10.1016/S1369-5266(02)00275-3.

CURRICULUM VITAE

First name: Hassan Yusuf
Surname: Sulaiman
Email: Hassan@emu.ee
Academic degree: Master's degree (2016)

Education:

11.2017–08.2023 **PhD studies**, Institute of Agricultural and Environmental Sciences, Estonian University of Life Sciences, Tartu, Estonia
09.2014–03.2016 **MSc in Environmental Sciences**, Cyprus International University, Mersin 10, Turkey
12.2006–01.2011 **BSc in Geography**, Faculty of Science, Bayero University Kano, Nigeria

Professional Employment:

01.2018–10.2022 Estonian University of Life Sciences, Institute of Agricultural and Environmental Sciences, Junior Researcher
11.2021–08.2023 Estonian University of Life Sciences, Institute of Agricultural and Environmental Sciences, Specialist
02.2013-2017 Yusuf Maitama Sule University, Kano, Nigeria, Lecturer

Grants and projects:

- Centre of Excellence in Environmental Adaptation (F11100PKTF)
- Ecology of Global Change: natural and managed ecosystems (8F160018PKTF (TK131))
- Ecology of Global Change: natural and managed ecosystems Analysis and Experimentation on Ecosystems (F200127PKTT (11.7-4/1076)).

ELULOOKIRJELDUS

Nimi: Hassan Yusuf
Perekonnanimi: Sulaiman
e-mail: Hassan@emu.ee
Teaduskraad: Magistrikraad (Msc), 2016

Hariduskäik:

11.2017–08.2023 **PhD** õpe, Eesti Maaülikool, Põllumajandus-ja keskkonnainstituut, Tartu, Eesti.
09.2014–03.2016 **MSc Keskonnateadused**, Cyprus International University, Mersin 10, Turkey
12.2006–01.2011 **BSc Geografia**, Faculty of Science, Bayero University Kano, Nigeria

Teenistuskäik:

01.2018–10.2022 Põllumajandus- ja keskkonnainstituut, Eesti Maaülikool, Nooremteadur
11.2021–08.2023 Põllumajandus- ja keskkonnainstituut, Eesti Maaülikool, Spetsialist
02.2013-2017 Yusuf Maitama Sule University, Kano, Nigeria, õppejõud

Projektid:

- Keskkonnamuutustele Kohanemise tippkeskus (F11100PKTF)
- Globaalmuutuste ökoloogia looduslikes ja põllumajanduskooslustes (8F160018PKTF (TK131))
- Ökosüsteemide analüüs ja eksperimentaaluuringud (F200127PKTT (11.7-4/1076))

LIST OF PUBLICATIONS

1. **Sulaiman, HY**, Runno-Paurson, E, Kaurilind, E and Niinemets, Ü. 2023. The same boat, different storm: stress volatile emissions in response to biotrophic fungal infections in primary and alternate hosts. *Plant Signaling and Behavior* 2217030-2217030. DOI: 10.1080/15592324.2023.2217030.
2. **Sulaiman, HY**, Runno-Paurson, E, Kaurilind, E and Niinemets, Ü. 2023. Differential impact of crown rust (*Puccinia coronata*) infection on photosynthesis and volatile emissions in the primary host *Avena sativa* and the alternate host *Rhamnus frangula*. *Journal of Experimental Botany* **74**: 2029-2046.
3. **Sulaiman, HY**, Liu, B, Abiola, YO, Kaurilind, E and Niinemets, Ü, 2023. Impact of heat priming on heat shock responses in *Origanum vulgare*: Enhanced foliage photosynthetic tolerance and biphasic emissions of volatiles. *Plant Physiology and Biochemistry* **196**: 567-579.
4. **Sulaiman, HY**, Liu B, Kaurilind E, Niinemets Ü. 2021. Phloem-feeding insect infestation antagonizes volatile organic compound emissions and enhances heat stress recovery of photosynthesis in *Origanum vulgare*. *Environmental and Experimental Botany* **189**: 104551.
5. Liu B, Zhang L, Rusalepp L, Kaurilind E, **Sulaiman HY**, Püssa T, Niinemets Ü. 2021. Heat priming improved heat tolerance of photosynthesis, enhanced terpenoid and benzenoid emission and phenolics accumulation in *Achillea millefolium*. *Plant, Cell & Environment*, **44**: 2365-2385.
6. **Sulaiman HY**, Çakir S. 2017. Monitoring the contribution of desert dust intrusion to PM₁₀ concentration in Northern Cyprus. *Clean Air Journal*. 27:53.

CONFERENCE ABSTRACTS

1. **Sulaiman, HY**, Runno-Paurson, E, Kaurilind, E and Niinemets, Ü. 2022. Foliage photosynthesis and volatile emissions in relation to the severity of crown rust infection in host species. Plant Biology Conference, Portland, Oregon.
2. **Sulaiman, HY**, Runno-Paurson, E, Kaurilind, E and Niinemets, Ü. 2022. Crown rust infection is more virulent in the primary host than in the alternate host. New Phytologist Next Generation Scientist Conference, Tartu, Estonia.
3. **Sulaiman, HY**, Runno-Paurson, E, Kaurilind, E and Niinemets, Ü. 2021. Scaling reductions in photosynthesis with the severity of crown rust fungus infection. PhD Student Conference, Aurel Vlaicu University of Arad, Romania.
4. **Sulaiman HY**, Çakir S. 2017. Assessment of the contribution of background emissions and desert dust sources to PM₁₀ concentration. Annual Conference of Nigerian Association of Geographers, Nassarawa State University.

VIIS VIIMAST KAITSMIST

MARGE LANNO

BIOJÄÄTMETE KOMPOSTIMINE RINGMAJANDUSE TINGIMUSTES
BIO-WASTE COMPOSTING IN THE FRAMEWORK OF CIRCULAR ECONOMY

Kaasprofessor Merrit Shanskiy, professor Mait Kriipsalu, teadur Anu Kisand

28. aprill 2023

KEYVAN ESMAEILZADEH SALESTANI

MULLA MIKROBIOOM JA ODRA TRANSKRIPTOOM ERI VILJELUSVIISIDES
IMPACT OF CROPPING SYSTEMS ON SOIL MICROBIOME AND BARLEY
TRANSCRIPTOME

Dotsent Evelin Loit

16. juuni 2023

MERLE VALDMANN

TSÜTOLOOGILINE ENDOMETRIIT PIIMALEHMADEL: DIAGNOOSIMINE, MÕJU
SIGIVUSELE JA PRAAKIMISELE NING SEOSD METABOOLSE STRESSIGA
CYTOLOGICAL ENDOMETRITIS IN DAIRY COWS: DIAGNOSTICS, EFFECTS ON
FERTILITY AND CULLING, AND ASSOCIATIONS WITH METABOLIC STRESS

Professor Andres Valdmann

22. august 2023

HANNES TAMME

PUIDU KUIVATUSE KONTROLLI JA OPTIMEERIMISE MEETODITE
ARENDAAMINE
DEVELOPMENT OF CONTROL AND OPTIMIZATION METHODS FOR WOOD
DRYING

Professor Emeritus Peeter Muiste, PhD, teadur Valdek Tamme

30. august 2023

RAUL SAMPAIO DE LIMA

MEHITAMATA ÕHUSÓIDUKITE UUDSED RAKENDUSED
TULEOHJESÜSTEEMIDE TÄIUSTAMISEL
NOVEL APPROACHES IN MULTI-SENSOR UNMANNED AERIAL VEHICLES AS
BASIS FOR ENHANCING FIRE MANAGEMENT FRAMEWORKS

Professor Kalev Sepp, professor Mait Lang, PhD Ants Vain

2. november 2023

ISSN 2382-7076

ISBN 978-9916-719-38-1 (trükis)

ISBN 978-9916-719-39-8 (pdf)